



CARBON MOLECULAR SIEVE MEMBRANES FOR GAS SEPARATION

Kelly Cristina Briceño Mejías

Dipòsit Legal: T 1057-2014

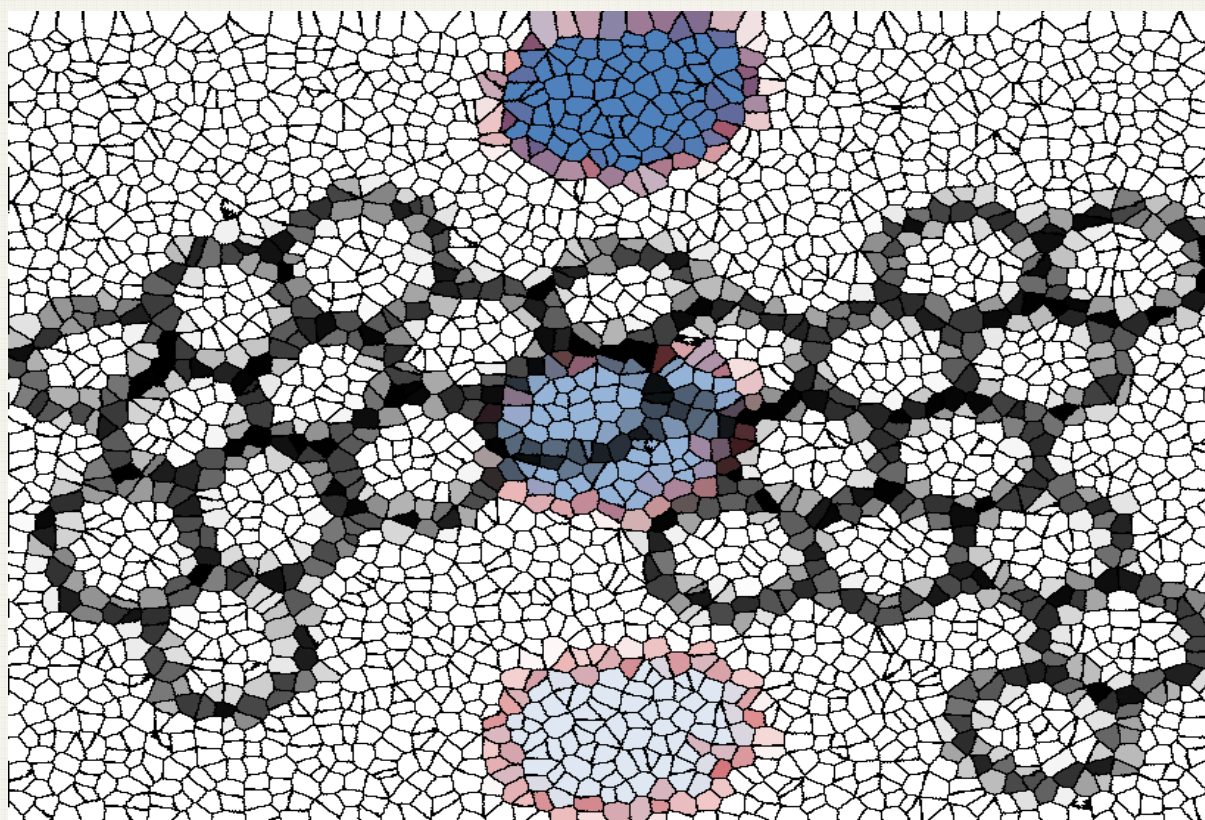
ADVERTIMENT. L'accés als continguts d'aquesta tesi doctoral i la seva utilització ha de respectar els drets de la persona autora. Pot ser utilitzada per a consulta o estudi personal, així com en activitats o materials d'investigació i docència en els termes establerts a l'art. 32 del Text Refós de la Llei de Propietat Intel·lectual (RDL 1/1996). Per altres utilitzacions es requereix l'autorització prèvia i expressa de la persona autora. En qualsevol cas, en la utilització dels seus continguts caldrà indicar de forma clara el nom i cognoms de la persona autora i el títol de la tesi doctoral. No s'autoritza la seva reproducció o altres formes d'explotació efectuades amb finalitats de lucre ni la seva comunicació pública des d'un lloc aliè al servei TDX. Tampoc s'autoritza la presentació del seu contingut en una finestra o marc aliè a TDX (framing). Aquesta reserva de drets afecta tant als continguts de la tesi com als seus resums i índexs.

ADVERTENCIA. El acceso a los contenidos de esta tesis doctoral y su utilización debe respetar los derechos de la persona autora. Puede ser utilizada para consulta o estudio personal, así como en actividades o materiales de investigación y docencia en los términos establecidos en el art. 32 del Texto Refundido de la Ley de Propiedad Intelectual (RDL 1/1996). Para otros usos se requiere la autorización previa y expresa de la persona autora. En cualquier caso, en la utilización de sus contenidos se deberá indicar de forma clara el nombre y apellidos de la persona autora y el título de la tesis doctoral. No se autoriza su reproducción u otras formas de explotación efectuadas con fines lucrativos ni su comunicación pública desde un sitio ajeno al servicio TDR. Tampoco se autoriza la presentación de su contenido en una ventana o marco ajeno a TDR (framing). Esta reserva de derechos afecta tanto al contenido de la tesis como a sus resúmenes e índices.

WARNING. Access to the contents of this doctoral thesis and its use must respect the rights of the author. It can be used for reference or private study, as well as research and learning activities or materials in the terms established by the 32nd article of the Spanish Consolidated Copyright Act (RDL 1/1996). Express and previous authorization of the author is required for any other uses. In any case, when using its content, full name of the author and title of the thesis must be clearly indicated. Reproduction or other forms of for profit use or public communication from outside TDX service is not allowed. Presentation of its content in a window or frame external to TDX (framing) is not authorized either. These rights affect both the content of the thesis and its abstracts and indexes.

DOCTORAL THESIS

CARBON MOLECULAR SIEVE MEMBRANES FOR GAS SEPARATION



Kelly Cristina Briceño Mejías

Università Rovira i Virgili



Kelly Cristina Briceño Mejías

Carbon Molecular Sieve Membranes for Gas Separation

DOCTORAL THESIS

Supervised by:

Dr. Ricard Garcia Valls & Dr. Daniel Montané i Calaf

Department of Chemical Engineering



Tarragona

2012



**Department of Chemical Engineering
University of Rovira I Virgili,
Avinguda Països Catalans, 26
43007, Tarragona, Spain.
Tel: +34-977-558506
Fax: +34-977-558544**

CERTIFICO:

Que el present treball, titulat “Carbon Molecular Sieve Membranes for gas Separation”, que presenta Kelly Cristina Briceño Mejías per a l’obtenció del títol de Doctor, ha estat realitzat sota la meva direcció al Departament Enginyeria Química d’aquesta universitat.

Tarragona,

Dr. Ricard Garcia Valls

Dr. Daniel Montané i Calaf



**Department of Chemical Engineering
University of Rovira I Virgili,
Avinguda Països Catalans, 26
43007, Tarragona, Spain.
Tel: +34-977-558506
Fax: +34-977-558544**

Certify that:

The present work entitled with “Carbon Molecular Sieve Membranes for Gas Separation”, presented by Kelly Cristina Briceño Mejías to obtain the degree of doctor by the University Rovira i Virgili, has been carried out under my supervision at the Chemical Engineering Departament.

Tarragona,

Dr. Ricard Garcia Valls

Dr. Daniel Montané i Calaf

Agradecimientos

Este doctorado ha sido una prueba de superación a nivel educativo, profesional y emocional. Las veces en las que el camino no fue fácil han estado llenas de esas personas en las que se reflejo la palabra POSIBLE. Por esta razón agradezco a instituciones y personas que me ayudaron a que aquello que un día planifique en una hoja de papel este plasmado en más de doscientas páginas de libro:

En primer lloc agraeixo a la Universitat Rovira i Virgili, i en especial al Departament d'Enginyeria Química de la mateixa universitat, l'oportunitat d'haver-me seleccionat per al programa de doctorat. Especialment agraeixo al Dr. Josep Font i a la Comissió de Doctorat per haver-me donat l'oportunitat de reorientar les veles i portar el vaixell a bon port. Gràcies Nuria Juanpere per tot el teu suport durant aquests anys.

Seguidament agraeixo al grup Systemic i Meteor haver-me fet costat durant el procés d'investigació d'aquesta tesis.

Agraeixo al meu supervisor Dr. Ricard Garcia per haver-me donat el timó sense dubtar-ho, i per haver confiat en mi amb una confiança immensa. Crec que se'n diu Fe, i tot i que algunes vegades a mi mateixa se m'escapolia entre les mans, aquesta confiança dipositada sense pors sempre em va fer mirar endavant. Gràcies pel suport econòmic, educatiu i científic.

Agraeixo al meu co-supervisor Dr. Daniel Montané i Calaf per, senzillament, parlar poc i ensenyar-me tant. Gràcies per ensenyar-me com es treballa al laboratori, com s'escriu, com s'exerceix una professió amb honestedat, per la seva paciència al respondre les meves preguntes, pel seu recolzament econòmic, moral i científic. Pel suport incondicional en tot moment.

A mis compañeros de grupo, con la incomparable Pepa a la cabeza de la flota, organizando el avispero: Cinta, Hany, Diana, Albert, Alberto, Jose, Bartek, Asta, Sema, Claudia, Nuria, Cisco.

A los de mas allá de la cafetería, mis compañeros de café y *phding*, Bruno, Jennifer, Sergi, Isabel, Marlene, Vivi, Pablo, Carmen, Nagore, Ivone, Asta, Srujan, Paula, Rukan. Amigos y compañeros inolvidables todos.

A los profesores Marta Giamberini por sus "minuticos" de sabiduría, a Tania Gumi, Jose Antonio Reina, por ser tan cercanos y accesibles, especialmente a Angels Serra, por hacer que la universidad y lo que contiene es de toda la comunidad científica.

Mucho del trabajo aquí plasmado no hubiese sido posible sin el apoyo de esos soldados del taller, como el Ernest y el Josep, gracias a Francesc Ferrando por su gran apoyo. A la maravillosa gente del SRCT como Merce Moncusí, Mariana, Nuria, Lucas, Rita, y el siempre excelente Francesc Girado.

A mis amigos: Maretva Baricot porque me enseñaste que cuando uno el punta de lanza, las piedrecitas son solo el primer premio, y no hay nada mas gratificante que ser pionero en algo y dejar el camino para que otros sigan adelante. A Albert Gasull, por ser el agua fresca de cada medio día, tu apoyo siempre ha estado ahí y te lo agradezco. A Sergio Rios por ser la palabra afilada, la sonrisa sincera de mi triunfo,

por ser mi apoyo, mi roca donde he podido descansar. A vosotros les agradezco cada palabra de aliento.

Agradezco al Dr. Francisco Rodríguez Reinoso por aceptar hacer el primer contacto y por aceptarme en su grupo para la realización de la estancia. Agradezco al Dr. Joaquín Silvestre Alberó por sus inmensos consejos, su paciencia y la ayuda incondicional, única y brillante en todo momento. A Ana María Silvestre por su inmensa ayuda, y su gran paciencia. A la maravillosa gente toda del lab. de Materiales Avanzados de la Universidad de Alicante, si por mi hubiese sido me quedaba un año de estancia.

Especiales gracias al Dr. Jose Ignacio Calvo y al Dr. Antonio Hernández del Departamento de Física Aplicada, Facultad Ciencias, Universidad de Valladolid por aceptar la colaboración con mi grupo. Gracias por la infinita paciencia, después de casi tres años intentando hacer la medición.

Vielen dank zu Nadine, dass sie mir die Möglichkeit, ersten Kontakt mit IKTS haben; zu Dr. Ingolf für alle Ihr Interesse an meinem Projekt, ihre Unterstützung und Ermutigung. Dank der wunderbaren Arbeitsausrüstung, exzellente Leute im Labo, sie bewillkommen mich dort wie in ein Familienmitglied, Ich werde euch nie vergessen. Dank von mein ganzem Herzen

Ringrazio di cuore il Dr. Angelo Basile e il Dr. Adolfo Iulianelli per avermi aperto le porte del ITM-CNR in Calabria. In laboratorio ho passato tre mesi pieni di allegria. Non posso lamentarmi di niente, neanche del caldo torrido di Agosto, perchè la temperatura aiutò alla riuscita della festa con la membrana. Ho di tutti voi, Tiziana, Simona, Massimo, Adele e Daniela, il migliore dei ricordi. Dopo tutto abbiamo ottenuto sia la membrana che la festa.

Gracias a todos los colegas del BBG y NBG por que gracias a ellos aprendí cuál era mi camino.

Al mio migliore amico, al collega, al professore, alla mia luce, alla mia casa e mio sole: Valerio Beni. Grazie per la tua pazienza, appoggio, il tuo amore e solo per stare nella mia vita. Sei stato una benedizione durante questa tesi e spero che insieme, nel futuro, potremo raccontare un sacco di belle storie.

Ellos no estuvieron acompañándome físicamente en la Universidad pero sencillamente han tenido la fe ciega en mi, y he llevado en el corazón cada día: Dr. Feliz Llovel, Christina Guldagher, Laura, Wicher ter Veld, Oliver Conradi, Pedro Delvasto, Carmen Angarita. A toda mi familia, mis padres mis fans numero uno, Teresita Mejías y Francisco Briceño y a mis tesoros Eduardo y Francisco Briceño. A mi viejita Giselita Bello, Virginia Briceño, Primitiva Briceño. A ellos mi agradecimiento e infinitas ¡gracias!

¡A Dios todopoderoso y a la fuerza incomparable de mi Orinoco!

Kelly Briceño.-

SUMMARY

Membrane separations are simple, energy efficient processes, which can be economically competitive with traditional separation technologies. In the case of gas separation both dense and porous materials have been developed for different application where hydrogen production is one of the most important niches of development. Hydrogen is being one of the most important vectors to develop alternative clean power generation sources. Nowadays, a lot of processes require the fabrication of pure hydrogen for efficiency and better performance. Different materials have been reported as gas separation membranes but still numerous problems related to stability, cost and fabrication must be overcome. The actual goal is to achieve materials that report good separation properties in new type of configuration facing industrial applications.

Carbon molecular sieve membranes (CMSM) achieve high separation factors and permeance values than polymeric membranes. During the last 30 years they have gained importance due to their excellent performance as gas separation membranes. However, most research work has been focused on flat or hollow fiber configurations and minor attention has been done to supported CMSM. The main reason is due the difficulties associated to fabricate a defect free membrane using a highly reproducible fabrication method that allow to obtain a carbon layer after one polymer precursor coating step. In tubular configuration, these hybrid membranes are suitable for scaling up towards industrial applications, being more competitive than commercial unsupported hollow fiber membranes and films, especially under high pressure and temperature.

The main objective of this work was to explore alternative fabrication methods for the fabrication of supported CMSM. In order to achieve this objective polyimide was coated over inorganic supports using two different approaches. The two methods reported in this thesis were spinning-coating and dip-coating. The idea of spinning-coating was adapted from fabrication of supported carbon planar film. In this work it was developed the same idea coating TiO₂ tubular supports under rotation with polyimide (Matrimid®). The thickness of the carbon membranes was controlled adjusting the viscosity of the polymeric solution, and after an exhaustive solvent

elimination it was possible to obtain a defect free carbon membrane. The influence of methanol washing, pyrolysis temperature (550-700°C), and presence of the support allowed to extracting conclusions about the characteristics of the carbon material. Single gas permeance of H₂, CO, CO₂, N₂, CH₄ were obtained and ideal selectivity computed from this measurements indicated the presence of pinholes on the carbon membrane. However, the characterization of this carbon obtained after 550° and 700° C by adsorption-desorption analysis allowed to confirm the microporosity of the carbon layer. As an important contribution of this work the influence of the support as pore modifier of the carbon structure is presented after analysis of supported and unsupported samples. Different characterization techniques are presented and integrated in this work to analyze the microporous character of the carbon layer (immersion calorimetry, AFM) and to evaluate the mesoporous characteristics of the asymmetric membrane (liquid-liquid displacement porosimetry). An additional coating procedure with polydimethylsiloxane (PDMS) was performed to decrease the influence of pinholes which caused a permeance decrease but increase on ideal selectivity values over Knudsen theoretical index.

As a second fabrication technique, the modification of Al₂O₃ inorganic support allowed to achieve microporosity in the support that allowed the fabrication of CMSM by dip-coating procedure. Similarly to the dip-coating method, viscosity and polymer concentration were optimized in order to achieve high ideal separation factors for hydrogen pairs. For the type of membranes obtained by this method single gas permeance of H₂, He, CO₂, O₂, N₂, CH₄, Propane, n-butane, 1-butene, SF₆ was performed. Influence of pyrolysis temperature, aging, non-solvent immersion, and support were also studied as pore modifier of the carbon membrane. However, for these membranes the characterization was focused on the effect on permeance and selectivity more than in the characterization of the material.

The findings described in this PhD thesis open new perspectives for alternative fabrication techniques of CMSM. This work reports not only the permeance and selective properties of CMSM as the traditional approaches rule. Moreover, brings how each fabrication variable could affect the final properties of the membrane. Integration of structure and properties are presented as an alternative strategy to design new pore architecture on CMSM.

LIST OF CONTENTS

| | Pages |
|---|-------|
| Summary | i |
| List of Figures | iv |
| List of Tables | xi |
| List of Acronyms | xiii |
| Chapter 1: Scope and Thesis objectives | 1 |
| Chapter 2: State of the Art of Carbon Molecular Sieves Supported on Tubular Ceramics for Gas Separation Applications | 9 |
| Chapter 3: Carbon Based Membrane Reactors | 31 |
| Chapter 4: Fabrication Variables Affecting the Structure and Properties of Supported Carbon Molecular Sieve Membranes for Hydrogen Separation | 69 |
| Chapter 5: Characterization of Carbon Molecular Sieve Membranes Supported on Ceramic Tubes | 104 |
| Chapter 6: Carbon molecular sieve membranes supported on non-modified ceramic tubes for hydrogen separation in membrane reactors | 126 |
| Chapter 7: Exploring New Variables in the Fabrication of Supported Carbon Molecular Sieves Membranes for Gas Separation | 151 |
| Chapter 8: General conclusions and Future work | 176 |

LIST OF FIGURES

| | Pag |
|--|------------|
| Chapter 1 | |
| Figure 1. Comparative search for different membrane materials used in gas separation. | 3 |
| Figure 2. Schematic view of membrane reactor concept. | 4 |
| Figure 3 Stationary hydrogen station | 4 |
| Chapter 2 | |
| Figure 1. Schematic concept of a bimodal catalytic membrane (microporous top layer coated on a bimodal catalytic support). | 12 |
| Figure 2. Schematic diagram of methanol reforming– MR configurations: a methanol reforming– mesoporous MR combined with water–gas shift reaction | 13 |
| Figure 3. Carbon deposition on pores | 18 |
| Figure 4. Schematic representation of (a) a thin polymer film supported on an asymmetric support and an (b) asymmetric membrane infiltrated by a polymer solution | 21 |
| Figure 5. Permeation mechanisms of gas mixtures through finely microporous-membranes | 23 |
| Chapter 3 | |
| Figure 1 Common carbon allotropes used as carbon membrane materials. a, graphite and b, amorphous carbon | 36 |
| Figure 2 Robeson´s plot: O ₂ /N ₂ selectivity vs O ₂ permeability for polymeric (AP) and carbon (PM) membranes. | 38 |

| | |
|---|----|
| Figure 3. Classification of carbon membranes based on their configurations. | 40 |
| Figure 4 Schematic concept of a bimodal catalytic membrane (microporous top layer coated on a bimodal catalytic support). | 43 |
| Figure 5. Schematic of folded graphite-like layers | 44 |
| Figure 6 Crack formation on supported carbon membrane | 48 |
| Figure 7 PFR and CMRs conversions as a function of feed flow at 773K; the simulated counter-current-mode behavior is also included | 50 |
| Figure 8. SEM cross-section of porous membrane reactor | 61 |
| Figure 9. Schematic describing the preparation of a glassy carbon microstructure using a PDMS mold. | 62 |
| Figure 10. Close up of glassy carbon surface | 62 |

Chapter 4

| | |
|---|----|
| Figure 1 Experimental setup for gas permeation experiments | 77 |
| Figure 2 Transversal photomicrography of the polymer films deposited on the ceramic support at different polymer concentrations (A untreated ceramic; B 3 wt%, C 13 wt%, and D 20 wt%) | 80 |
| Figure 3 Surface photomicrography of the polymer films deposited on the ceramic support at different polymer concentrations (A = 3 wt%, B = 13 wt%, and C = 20 wt%) | 81 |
| Figure 4 Progressive formation of cracks with pyrolysis temperature increasing at a heating rate of 2.5°C/min. (A: 100°C, B: 220°C, C: 420°C, D: 580°C) | 82 |
| Figure 5 Thermogravimetric analysis curves of a Matrimid powder (Original), cast membrane after 110 °C, and a casted membrane after 110 °C and methanol bath (110 °C + methanol) | 83 |

| | |
|---|----|
| Figure 6 On-line ESEM imaging of the pyrolysis of a supported polymer film after ethanol washing (A: 100 °C, B: 220 °C, C: 420 °C, D: 580 °C) | 84 |
| Figure 7 Back scattering images of the ceramic support and a supported carbon membrane obtained at a heating rate of 1 °C/min and a final temperature. | 86 |
| Figure 8 AFM images of the ceramic support (left), the supported carbon membrane (center) and a non-supported carbon membrane (right). | 88 |
| Figure 9 WXRd for carbon supported (C-S) and non-supported (C-NS) carbon membranes obtained at 550 °C | 89 |
| Figure 10 WXRd for carbon supported (C-S) and non-supported (C-NS) carbon membranes obtained at 850 °C | 89 |
| Figure 11. Permeance values for supported carbon membranes at different pyrolysis temperatures | 91 |
| Figure 12 Adsorption-desorption isotherms for supported carbon membranes at different pyrolysis temperatures | 92 |
| Figure 13 Ideal selectivity values for supported carbon membranes at different pyrolysis temperatures | 93 |

Chapter 5

| | |
|---|-----|
| Figure 1 Unsupported carbon obtained at 550°C (A) and 700°C (B) | 110 |
| Figure 2 Supported carbon obtained at 550°C (A) and 700°C (B) | 111 |
| Figure 3 CH ₄ and CO ₂ adsorption–desorption isotherms for the different carbon non-supported membranes obtained at 550°C and 700 °C pyrolysis temperatures. | 114 |

- Figure 4** CH₄ and CO₂ adsorption–desorption isotherms for the different carbon supported membranes obtained at 550°C and 700°C pyrolysis temperature. 115
- Figure. 5** Enthalpy of immersion (J/g) for the different supported and unsupported samples into liquids of different molecular dimensions (dichloromethane (DCM), benzene (BZN), n-hexane (N-HEX), 2,2-dimethyl-butane(DMB)) 117
- Figure 6** Permeability distribution for a Tami Support non coated (S_NC) coated with polymer (S_P300), coated with carbon pyrolyzed at 550° (S_C550) and 700°C (S_C700). 120
- Figure 7** Molecular cut-off for TiO₂ support (S_NC), polymer supported membrane (S_P300), carbon supported membrane obtained at 550 and 700 °C (S_C550, S_C700). 121
- Figure 8** CO₂ and CH₄ permeance (bars) and ideal selectivity factors (▲) for supported carbon samples obtained at 550°C 600°C and 700°C. * denotes samples with an additional PDMS coating. Values measured at 23°C and 1 bar. 122

Chaper 6

- Figure. 1.** Schematic view of carbon supported membrane in the permeation module 132
- Figure 2** Permeance vs pressure difference for a carbon supported membrane (150 °C). 135
- Figure 3** Gas permeance vs 1/sqrt(Mw) for carbon supported membrane at different permeation temperatures ($\Delta P= 1$ bar). 136
- Figure 4** Gas permeance vs 1/sqrt(T) for a carbon membrane for different gases ($\Delta P= 1$ bar) 136

| | |
|--|-----|
| Figure. 5 Ideal selectivity factor vs permeation temperature for different pair of gases at $\Delta P= 0.5$ bar (empty symbols= Ideal Knudsen theoretical values) | 139 |
| Figure 6 Ideal selectivity factor vs permeation temperature for different couples of gases at $\Delta P= 2.5$ bar (empty symbols= Ideal Knudsen theoretical values) | 139 |
| Figure. 7 Permeance versus pressure difference in carbon supported membrane with and without PDMS coating | 141 |
| Figure. 8 Permeance versus kinetic diameter for carbon supported membrane after PDMS coating evaluated at room temperature ($\Delta P = 2$ bar) | 142 |
| Figure. 9 Ideal selectivity for different pair of gases for carbon supported membrane after PDMS evaluated at room temperature. ($\Delta P = 2$ bar) | 143 |
| Figure 10. Yield versus temperature of a TR and a carbon membrane reactor for SRM | 145 |
| Figure 11 Methanol conversion versus temperature of a TR and a carbon membrane reactor. | 145 |

Chapter 7

| | |
|--|-----|
| Figure 1 Permeance of membranes pyrolyzed at 650°C. | 158 |
| Figure 2 Single gas permeance performed at 150°C for Matrimid carbon supported membranes. | 160 |
| Figure 3 Single gas permeance performed at 150°C for carbon supported membranes pyrolyzed at 550°C. | 161 |
| Figure 4 Ideal selectivity for carbon supported membranes pyrolyzed at 550°C | 162 |

| | |
|--|-----|
| Figure 5 Permeance values for CMSM vs kinetic diameter obtained for samples with the same thermal history before (polymer) and after (carbon) pyrolysis at 650°C. | 162 |
| Figure 6 Permeance values for CMSM vs kinetic diameter obtained for samples with different thermal history (pre-treatment at 250°, 300°, 350°C) before (polymer) and after (carbon) pyrolysis at 650°C. | 163 |
| Figure 7. Ideal selectivity values for CMSM vs kinetic diameter obtained for samples with the same and different thermal history after pyrolysis at 650°C. | 163 |
| Figure 8 Permeance values of carbon membranes obtained on TiO ₂ and Al ₂ O ₃ supports at 550°C. | 164 |
| Figure 9 Permeance values for CMSM vs kinetic diameter obtained at different pyrolysis temperatures. | 167 |
| Figure 10 Ideal selectivity values for CMSM vs kinetic diameter obtained at different pyrolysis temperatures.. | 167 |
| Figure 11 Permeance vs. Kinetic diameter of carbon molecular sieve membrane obtained at 650°C pyrolysis temperature after oxidation treatment at 350°C at 0.5 hrs | 169 |
| Figure 12 Permeance vs. Kinetic diameter of carbon molecular sieve membrane obtained at 650°C pyrolysis temperature after oxidation treatment at 350°C at 6hrs. | 169 |
| Figure 13 Ideal selectivity factors of carbon molecular sieve membrane obtained at 650°C pyrolysis temperature after oxidation treatment at 350°C at 0.5 and 6hrs. | 170 |
| Figure 14 Permeance vs Kinetic diameter of carbon molecular sieve membrane obtained at 650°C pyrolysis temperature at 250°C and low pressure | 171 |
| Figure 15 Ideal selectivity of carbon molecular sieve membrane | 171 |

obtained at 650°C pyrolysis temperature at 250°C and low pressure

Figure 16 Permeance vs. Kinetic diameter of carbon molecular sieve membrane CA_1 obtained at 650°C pyrolysis temperature after autoclave tests at 180°C, 30 bar and 24 hr (one exposure and repetition). 172

Figure 17 Ideal selectivity of carbon molecular sieve membrane CA_1 obtained at 650°C pyrolysis temperature after autoclave tests (one exposure and repetition). 172

LIST OF TABLES

| Chapter 2 | Pag. |
|--|-------------|
| Table 1. Supported tubular CMSMs | 16 |
| Table 2. Studies that report fabrication parameters on CMS-supported membranes. | 17 |
| Chapter 3 | |
| Table 1. Methods for the preparation of supported CMSM | 47 |
| Table 2. Simulated conversion results at various temperatures and operation modes | 50 |
| Table 3. H ₂ yield and methanol conversion versus temperature in both TR and CMR for steam reforming of methanol | 57 |
| Chapter 4 | |
| Table 1. Viscosity Matrimid/NMP polymeric solutions | 78 |
| Table 2. <i>I_d/I_g</i> values for carbon samples obtained after different treatments | 85 |
| Table 3. Glass transition temperature (<i>T_g</i>) of supported and non-supported Matrimid samples | 87 |
| Table 4. References reported in the fabrication of asymmetric/supported carbon membranes. | 94 |
| Chapter 5 | |
| Table 1 Area and pore volume of carbon samples determined by immersion calorimetry. | 118 |

Chapter 6

| | |
|---|-----|
| Table 1. Parameters of the TiO ₂ ceramic support | 131 |
| Table 2. Arrhenius coefficient for a supported carbon membrane at $\Delta P=$ 1 bar | 137 |
| Table 3. Hydrogen purity in a carbon membrane reactor | 146 |

Chapter 7

| | |
|--|-----|
| Table 1. Polymer solutions used on coating of ceramic supports. | 155 |
| Table 2. Permeance and Ideal selectivity of CMSM obtained at the same conditions. | 158 |
| Table 3. Ideal selectivity of carbon membranes tested at 150°C at different polymer concentrations. | 160 |
| Table 4. Ideal selectivity values of carbon membranes obtained over TiO ₂ and Al ₂ O ₃ supports at 550°C. | 165 |

LIST OF ACRONYMS

- LCA: Life cycle analysis
- CMSM: Carbon molecular sieve membrane
- CMS: Carbon molecular sieves
- MR: membrane reactor
- WGS: wáter gas shift
- HAMR: hybrid adsorbed membrane reactor
- PPO: poly(2,6-dimethyl-1,4-phenylene oxide)
- CVD: Chemical vapour deposition
- PFA: polyfurfuryl alcohol
- AFM: atomic force microscopy
- STM: scanning probe microscopy
- NMP: 1-methyl-2- pyrrolidone
- THF: Tetrahydrofuran
- ESEM: Environmental Scanning Electronic Microscope
- TGA: Thermogravimetric analysis
- PDMS: polydimethylsiloxane
- WXRd: Wide angle X-Ray Diffraction
- GPC: Gel permeation chromatography
- BPDA-ODA: 3,3',4,4'-biphenyltetracarboxylic dianhidride- 4,4'-oxydianiline
- DCM: dichloromethane
- BZN: benzene
- N-HEX: n-hexane
- DMB: 2,2-dimethyl-butane
- MWCO: molecular weight cut-off
- LLDP: Liquid-liquid displacement porosimetry
- AAM: Alumina asymmetric membrane
- ASCM: Adsorption selective carbon membranes

CAM: coated alumina membrane
C-MEMS: Carbon microelectromechanical systems
CMR: carbon membrane reactor
CMS: carbon molecular sieves
CVD: Chemical vapor deposition
FAME: fatty acid methyl esters
FBR: fixed bead reactor
HAMR: Hybrid adsorbent-membrane reactor
MIMIC: Micro molding in capillaries
MRs: Membrane reactors
MSCM: Carbon molecular sieves membranes
LDH: Layered double hydroxides
PA: Polyamic acid
PEMFC: Proton exchange membrane fuel cells
PSA: Pressure swing adsorption
Pd: Palladium
PDMS: Polydimethylsiloxane
PFR: plug flow reactor
PTFE: polytetrafluoroethylene
SRM: Steam reforming of methanol
XRD: X-ray diffraction
YSZ: Yttria-stabilized zirconia
 μ TM: Micro transfer molding

CHAPTER 1

Scope and Thesis Objectives

Scope and Thesis Objectives

During the last two centuries human being have increased their quality life to levels not experienced before. Nowadays, a technological advance brings a comfortable level of life that will not probably go back. The advances in technological developments was not always in parallel with the impact it had on the resources consumed. Climate change problems, increase on fuel's price and contamination or depletion of water sources to mention a few, imply to make effort in producing more sustainable technologies and to decrease the impact of those existing in the near future. Nowadays, it is not possible to think in technology development without including the life cycles analysis (LCA) and also considering the economic impact cost associated to them. In this context membrane material bring an alternative answer to deal with different problems associated with environmental impact and production by using more efficient processes. Gas separation membranes is an example of those materials that emerged from laboratory to adapt rapidly on industrial applications, being an attractive alternative to conventional, expensive and contaminant methods for gas separation. The broad range of applications includes nitrogen generation, refinery hydrogen recovery, syngas ratio adjustment, landfill gas upgrading, pollution control to noun few of them. Depending on the application both dense and porous membranes include a large variety of materials where polymers are the most widely reported. Figure 1 shows a comparative view of different materials used on for gas separation. A review on available literature regarding gas separation material available during the last 35 years is it clear that polymeric materials have been predominant for gas separation. Other available materials like molecular sieving include zeolites, ceramics and carbon. Even zeolites are most dominant, carbon molecular sieve membranes (CMSM) have gained attractive attention during the last years and they are the object of study in this thesis. The main reasons why carbon membranes have been scarcely developed up today are their brittleness, high price and low hydrothermal stability. Moreover, there are still a lot of issues related to understand the relationship between structure and properties that have been scarcely reported. This relationship has been being approach on flat membranes. Although this can be widely found in the literature, most of them cannot be applied on industrial applications.

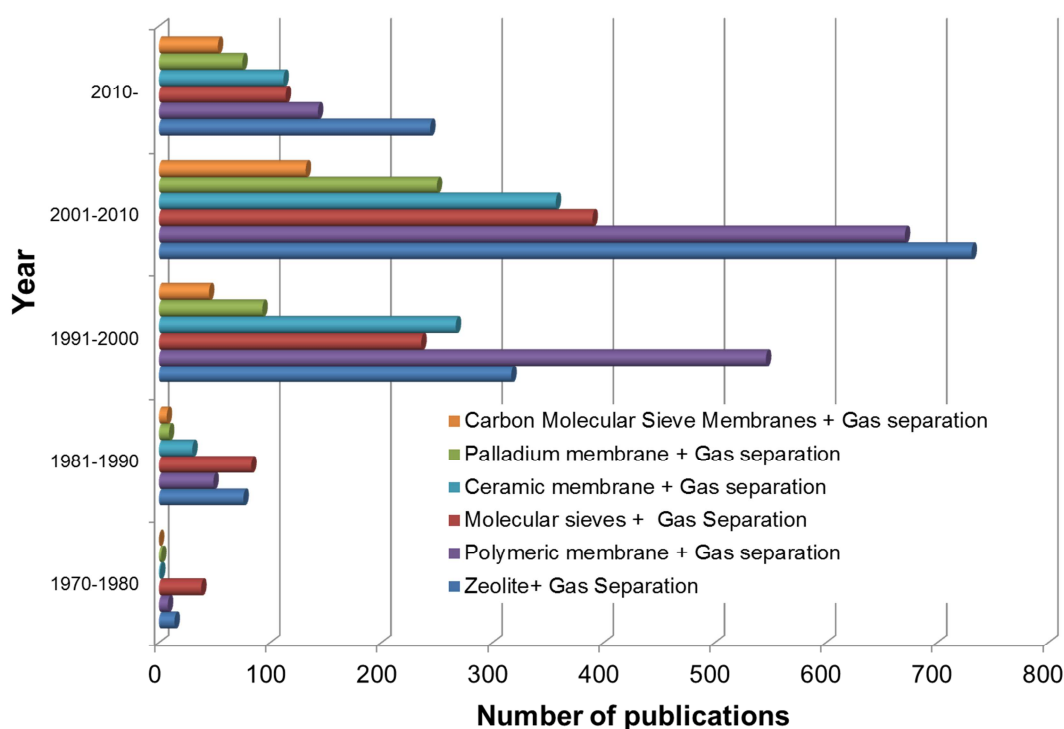


Figure 1. Comparative search for different membrane materials used in gas separation

Membranes made from metals, zeolites and ceramics has successfully overcome the gap between laboratory and industrial application. However, carbonaceous membrane has still to solve issues like thermal stability in order to be considered as alternative materials. In addition, depending on application the fabrication method can be a limiting factor for application of these membranes. In the manufacturing of CMSM is common to need controlled clean room facilities or to have repetitive coating steps to decrease defects and to achieve mechanically stable membranes. These aspects could represent an economical drawback for their study and further application. Based on what has been previously exposed, efforts should be made to develop a manufacturing process that solve the main drawbacks related to obtain competitive carbon membranes for gas separation.

The thesis presented was part of an Opentok Marie Curie European Project devoted to design, characterize and apply porous materials for novel applications. The final objective of the European project was to obtain materials for hydrogen purification. For

this reason, it was proposed the study of carbon molecular sieve membranes for on board hydrogen production. This implied the fabrication of membranes that could be suitable for membrane reactors applications. On the other hand, it was required to obtain a material with high permeance and separation factors in a compact structure that would allow the integration of catalyst. Figure 2 shows the schematic view of a membrane reactor where reaction and separation are integrated in order to promote shift of the products from the equilibrium.

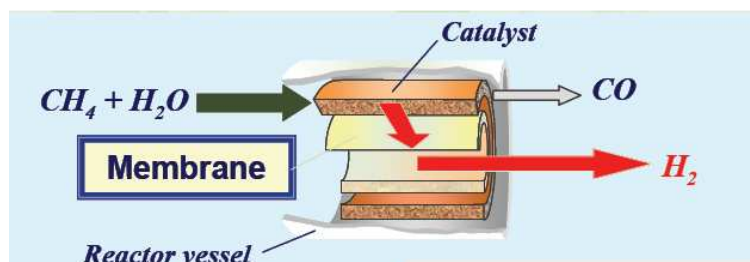


Figure 2. Schematic view of membrane reactor concept

The idea to integrate high separation membranes in membrane reactors has been considered for both on-board production of hydrogen and deliver of hydrogen as fuel on stationary sources using palladium membranes (Fig 3). However, the price and low permeance values of hydrogen membranes push the interest to find alternative materials.



Figure 3. Stationary hydrogen station

In the frame of the European project this thesis was conceived to fabricate membranes for possible application in membrane reactors. The focus of this research was to explore an alternative fabrication method without the need to modify a mesoporous

support. The main hypothesis is that it is possible to create a carbon membrane with a microporous and mesoporous part integrated in the same membrane using a shorter route of manufacturing than reported in the literature. This layer must be carefully deposited on a porous support in order to guaranty:

- To use a mesoporous support without previous modification of its porosity.
- To obtain a carbon membrane after one coating step of the polymer precursor
- In order to achieve maximum permeance values, it is important to minimize the immersion of the polymer precursor on the porous structure of the support
- The final membrane must be free of cracks.

In order to achieve these requirements, it was proposed a fabrication method than allow the control of the thickness at the deposition stage given by the concentration of the polymer solution. This method was though to eliminate the following problems:

- Time and costs related to support modification.
- Need of clean room.
- To avoid repetitive coating procedures of polymer precursor towards to achieve a defect free membrane.
- To achieve separation of smaller kinetic diameter gases comparable to hydrogen
- Do not use post-treatment for to increase or decrease pore size of carbon membranes.

After the above explanations the main objectives of the present PhD thesis were:

- To propose a new fabrication method fast, simple and suitable to be performed out of clean room.
- To obtain a carbon molecular sieve membrane over a mesoporous support without the need to modify the support and avoiding repetitive polymeric coating.
- To identify the transport mechanisms of the carbon membranes obtained and allow their evaluation as candidate materials for membrane reactors.

- To determine the influence of the fabrication steps on the final structure of the carbon membrane obtained in order to allow tailoring the pore size of the carbonaceous structure.
- To develop alternative characterization techniques of the carbon material in order to establish relationship structure-properties of carbon membranes obtained.
- To overcome the problems associated to the fabrication method obtained to achieve high selectivity and permeance of the carbon membrane.

In this sense, the research work was divided into:

Chapter 1: outline the thesis scope. This chapter includes the main motivation and thesis objectives.

Chapter 2: introduce the challenges of gas separation membranes and address the carbon membranes on the competitive field of gas separation. Some important concepts are revised considering the point of view of fabrication of supported carbon membranes. In this chapter, it is also revised the problem of lack of techniques for a detailed characterization of the supported carbon membrane.

Chapter 3: This is a general view of the potential applications of porous carbon membranes in different research fields. The main approach is to apply them on membrane reactors, for this reason a revision of their properties is done for this application. The author brings a connection between the common properties of porous carbon membranes and how they can be used in macro and micro membrane reactors.

Chapter 4: refers to the first part of the experimental work. An alternative fabrication method to those reported in the literature was achieved. The fabrication variables are fully analyzed towards defect free membrane. For this reason a characterization of the influence of methanol immersion is presented. This chapter introduces questions about the influence of new variables on the carbon structure that has not been usually reported in the literature.

Chapter 5: integration of multi-characterization techniques for the membrane morphology. Detailed analysis of carbon membrane allows concluding the

importance of support and pyrolysis temperature. Moreover, the application of these membranes in gas separation requires an additional characterization than microporosity. For this reason, Mesoporosity is characterized by Liquid Liquid Displacement Porosimetry (LLDP) in order to set parameters that determine the mesoporous modification. This chapter allows a textural characterization of the carbon and confirms that alternative variables to those reported in the literature, must be considered for pore design.

Chapter 6: the transport mechanism analysis ere determined for membranes reported in chapter 2. Permeance of different gases (H_2 , CO_2 , N_2 , CH_4 , CO) was performed at room temperature and at $150\text{ }^\circ\text{C}$. This analysis allowed to compare the membrane obtained with other inorganic membranes reported in the literature for membrane reactor applications. For this reason, a first attempt of carbon membranes applications obtained in this work is reported for methanol steam reforming.

Chapter 7: An alternative fabrication method is considered in order to validate the results obtained before. This method implied the modification of the inorganic support (which is a protected patent). The high reproducibility of this method allowed to confirm the results exposed before and also allowed to explore questions related to the new variables suggested to influence the carbon structure. It allowed us to rise conclusions about the importance of other fabrication variables non-reported up to now.

CHAPTER 2:
**State of the Art of Carbon Molecular Sieves Supported on Tubular
Ceramics for Gas Separation Applications**
(Art.1)

Published on: Special issue: Special theme: Membrane Reactors Part II. Asia-Pac. J. Chem.
Eng. Vol 5, Issue 1, pp 169-178, (2010).

State of the Art of Carbon Molecular Sieves Supported on Tubular Ceramics for Gas Separation Applications

Kelly Briceño^a, Ricard Garcia-Valls^a, Daniel Montane^b

^aDepartment of Chemical Engineering, Rovira i Virgili University, Av. Països Catalans, 26, 43007, Tarragona (Catalunya), Spain

^bCatalonia Institute for Energy Research (IREC). Bioenergy and Biofuels Area. C/ Marcel·lí Domingo 2, Building N5, Universitat Rovira i Virgili. 43007, Tarragona, Spain

ABSTRACT

During recent years, research into alternative power generation and less polluting vehicles has been directed towards the fabrication of compact and efficient devices using hydrogen fuel cells. As a compact viable proposal, membrane reactors (MR) have been studied as means of providing a fuel cell with an on-board supply device for pure hydrogen streams obtained by reforming hydrocarbons. However, the development of MRs is strongly dependant on the membrane having high permeation flux and high selectivity ratios towards H₂ in a mixture of gases. To meet this need, carbon membranes are proposed materials, which have pores that are the same size as the kinetic diameters of syngases. These would provide an alternative to polymers, metals and ceramics in MR applications. Moreover, a tubular shape is a highly recommended configuration for achieving a compact and large reaction surface area. However, it is not easy to obtain a supported and amorphous carbon layer from polymer pyrolysis because the fabrication methods, the type of precursor material, characteristics of the support and pyrolysis conditions are all closely connected. The combination of all these factors and the stability problems of carbon membranes have limited the use of carbon molecular sieves (CMS) in large-scale applications. This review attempts to provide an overview of the use of carbon membranes in MRs for gas separation. It also reviews the advances in the materials, fabrication methods and characterisation techniques of specific supported carbon molecular sieve membranes that have been supported on tubular carriers so they can take advantage of the high permeation and selectivity values previously reported for unsupported CMS.

KEYWORDS: carbon molecular sieves (CMSs); carbon molecular sieve membranes (CMSMs); hydrogen separation; gas separation; membrane reactor materials

SCOPE OF MEMBRANE REACTORS

Hydrogen can be considered to be one of the most important fuel sources that helps in satisfying the current and future energy needs of the world. In addition, it could play a big role in reducing greenhouse gas emissions, especially considering the current environmental regulations. A promising approach to feeding polymer electrolyte fuel cells (PEMFCs) is to produce hydrogen by steam reforming hydrocarbons followed by a water gas shift (WGS) reaction. Such systems would be able to generate cleaner power than an internal combustion engine^[1]. In hydrogen-based automotive technology, reforming hydrocarbons in an on-site reforming reactor would create a valuable alternative to an external reforming and refuelling infrastructure. It is thus highly attractive to carry liquid fuels suitable for conversion into hydrogen-rich gas. However, there are problems with this approach because the hydrogen produced by reforming hydrocarbons contains gases such as CO and CO₂ that poison the anode catalyst and thus reduce the performance of the fuel cell.^[1-4] For this reason, the production of high-purity hydrogen fuel is fundamental to the development of the on-board feeding of fuel cells.

The WGS reaction has been identified as an additional step for obtaining the highest yield of H₂ in the hydrocarbon-reforming process, according to the reaction shown in Eqn 1^[4]:



In addition, it has been reported that the configuration of the membrane reactor (MR) has improved the WGS reaction's effectiveness in producing hydrogen^[4,5] MRs are not new^[6-8] and can be used in compact and on-board applications. This type of device is designed to selectively remove products from a mixture in equilibrium-limited reactions. The changes produced in the equilibrium composition increase the reaction yield.^[9] In fact, MRs have shown better efficiency than conventional tubular reactors. For this reason, the new developments in MRs could further improve the overall

efficiency of processes in H_2 production technology. For example, Tsuru *et al.* configured an MR so that it used steam methane reforming with $\alpha\text{-Al}_2\text{O}_3$ membranes covered in an Ni-doped layer to produce hydrogen. In this case, the separation layer was located on the outer surface of the cylindrical support, giving an H_2/N_2 permeance ratio between 25 and 502 (Fig. 1).^[10]

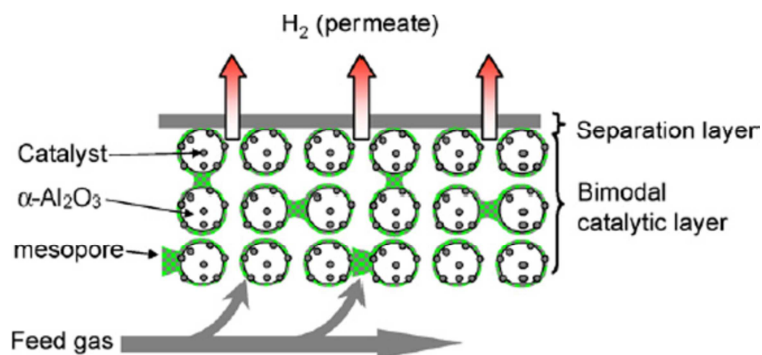


Figure 1. Schematic concept of a bimodal catalytic membrane (microporous top layer coated on a bimodal catalytic support).[10].

THE IMPORTANCE OF MEMBRANE MATERIALS AND SHAPE IN A MR

In a MR, the membrane plays the role of the integrated separation element; for this reason the permeation and selectivity of the membranes are crucial to the total reactor performance. Polymers are good candidates among the possible membrane materials, but they are limited by the trade-off trend between gas permeability and selectivity and they often lose performance at high temperatures.^[11,12] In high temperature gas separation applications, two different types of membranes have been used: microporous (zeolites, silica and carbon) and dense membranes (ceramic or metals).^[13]

Extensive research has been done on applying inorganic materials to MRs;^[6,7,10,14 – 16] however, there are still matters of cost and stability when applying these materials in large-scale industrial applications.^[7,17,18]

Developments of new materials, optimal and reproducible fabrication techniques and new configurations are needed in order to achieve stable MRs with good thermal and mechanical properties. For more information on this subject, the reader should refer to the several studies that have analysed different inorganic materials for this purpose.^[19]

Many studies have dealt with membranes supported on an asymmetric structure. Lee *et al.*^[20] reported permeation values and high hydrogen recovery in inorganic membrane materials. They studied different configurations of asymmetric membranes and noticed that the final performance was significantly affected by the materials of which the asymmetric membrane was made. Figure 2 shows a diagram of a methanol mesoporous MR combined with WGS.

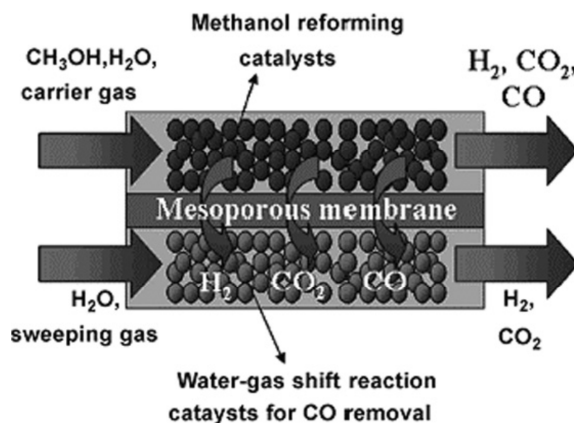


Figure 2. Schematic diagram of methanol reforming– MR configurations: a methanol reforming–mesoporous MR combined with water–gas shift reaction.^[20]

An optimal asymmetric hybrid configuration of the membrane could provide high hydrogen recovery and good flow of gases to the permeate side, but would also require the development of new materials for highly permselective membranes suitable for MR applications. This would mean considering the contribution of each separation mechanism for each component layer in order to determine the overall yield and separation values. These transport mechanisms have been reviewed for inorganic materials such as ceramics, zeolites and carbon.^[12]

Another important aspect of the MR is the shape of the supported membrane, which can be planar or tubular. The tubular configuration has been considered preferable from the standpoint of large-scale applications, including MR applications. This is because of its high packing density and high surface reaction area.^[19,21]

The use of hydrogen selective materials in a tubular shape for permeation testing has been reported for carbon membranes from pyrolysed polymer hollow fibres. However, even though these membranes have been reported in commercial applications, they

suffer from low mechanical stability and fabrication problems such as macrovoid formation or alterations to the final membrane properties depending on the spinning conditions in the dough.^[22–24] Also, the fabrication of polymer hollow fibres is a very complicated process that depends on many variables.^[25–27] Supported tubular membranes are an alternative that would have more mechanical stability and would reduce the polymeric materials needed for their fabrication, thus significantly lowering the cost.

THE SELECTIVE MEMBRANE: CARBON MOLECULAR SIEVES (CMS)

A highly selective membrane for gas separation has to allow separation between small molecules with similar sizes. Examples of materials with these properties are molecular sieves made of silica, zeolites and carbon. Compared to polymeric materials, they push the upper boundary of the permeability vs selectivity tradeoff.^[28,29] Carbogenic materials have been used in different applications since the last 20 years because of their sieving properties,^[30] with gas separation being one of the most common applications.^[31–34] As with zeolites, these materials separate molecules based on the size and shape differences. In the case of carbon molecular sieves (CMSs), their chaotic structure can be controlled by the chemical composition of the precursor and the fabrication conditions during polymer pyrolysis. Moreover, CMSs are thermally more stable and are resistant to reactions with acids, and these qualities make these materials very useful for processes where separation is done in aggressive environments.^[35] The crystalline structure of zeolites is not easily controlled, especially in high-scale applications, and these materials are still under research.^[36] Finally, silica is the most competitive membrane material for gas separation;^[12] however, the industrial application of silica membranes is still limited by problems such as poor reproducibility.^[37]

In the field of MRs, there is a very small number of reports about nanoporous carbon membranes. Itoh and Haraya have been pioneers in the field of carbon MRs.^[21] They fabricated an MR in a hybrid configuration with a selective carbon hollow fibre membrane for dehydrogenating cyclohexane.^[21] They showed that the permeation rates of hydrogen, argon and cyclohexane in the MR were controlled by molecular sieving and diffusion mechanisms. Lapkin *et al* also reported the use of carbon membranes in a

contractor for the hydration of propane.^[38] However, very few studies can be found regarding hydrogen separation using WGS reaction.^[39] Harale *et al.*^[40] reported the hybrid adsorbed membrane reactor (HAMR) where the reaction and membrane separation processes are coupled with adsorption. They used the nanoporous CMS membrane for hydrogen separation and double hydroxide materials as adsorbents.

The use of carbon materials in MR applications is limited because of their low oxidation resistance under severe conditions. Nonetheless, the excellent permeation and selectivity properties, and the relative ease with which preparation and shape are controlled, make nanoporous carbon membranes competitive with other materials for high-performance gas separation. Harale *et al.*^[40] provide one of the few examples of the use of these membranes in this type of application when they used carbon membranes for WGS reaction at 250 °C. On the other hand, the stability problems of carbon membranes are still being studied. Lagorsse *et al.*^[41] looked at hollow fibre carbon molecular sieve membranes CMSMs that were treated 1 year after fabrication to remove the oxygen surface groups that cause the loss of stability in these membranes. Passivation and regeneration (treatment in an H₂ atmosphere at 893 K) are alternative treatments for recovering membrane stability. Most of the limitations of carbon membranes arise from the membrane fabrication. Sometimes CMSMs do not behave as expected because of the limited control over thickness, especially when several coating steps are required. Therefore, improving and developing CMSM fabrication are key areas in making these membranes more competitive with other materials.

FABRICATION METHODS IN CMSMS

The most commonly used method for obtaining CMSMs is polymer pyrolysis. After the pyrolysis of most polymeric precursors, a carbon material is obtained that has improved permeability and selectivity compared to the polymer precursor.^[42] Accordingly, a lot of emphasis has been laid on selecting the polymer. In the case of supported membranes, there is a close relationship between the pyrolysis conditions and the methods used to form a defect-free film of the polymer used as carbon precursor.^[43 - 45] The pore size distribution and the adsorption capacity, which control the selectivity for gas separation, can be tailored during fabrication by controlling parameters such as the pyrolysis

temperature, time and flow rate of the sweep gas present during the pyrolysis.^[46–51] For supported samples, it is important to consider the subsequent thickness of the polymer, and the presence of cracks during pyrolysis resulting from differences in thermal coefficients of precursors and supports. Several methods are reported in Table 1 for tubular supported CMSMs in large-scale and compact applications.

Table 1. Supported tubular CMSMs
(Kinetic diameter: H₂ (2.89 Å) CO₂ (3.3Å) O₂ (3.46Å) CH₄ (3.8Å)[52]).

| Carbon Layer thickness | Type of support | Method | Permeance ($\times 10^{-8}$ mol/m ² ·s·Pa) | Selectivity | Ref |
|-------------------------------|---|-----------------------------------|---|--|------------|
| 30 μ m | Porous Carbon disk | Spin-coating | He:0.8 | O ₂ /N ₂ ~10 CO ₂ /N ₂ =45 CO ₂ /CH ₄ =160 | [46] |
| 6 μ m | Porous α -alumina support | Coating+ Vapour deposition | CO ₂ : 2 O ₂ : 0.3 | He/CO ₂ : 8 CO ₂ /N ₂ : 73 O ₂ /N ₂ :14 | [53] |
| Non reported | glass/ α -Al ₂ O ₃ | Vapour deposition | H ₂ :0.93 CO ₂ :0.29 CH ₄ :0.017 | CO ₂ /CH ₄ =25 | [52] |

To fabricate supported CMSMs, it is important to consider the research done for unsupported materials. The packaging of polymer molecules is related to the permeation properties of the final carbon membrane, and is affected by the polymer structure, the solubility of the polymer in the solvent and the temperature at which the polymer is placed over the support.^[42,48]

Variables related to polymers

The structure of a polymer precursor precursor polymer and the pyrolysis temperature are key factors that determine the properties of the carbon membrane. However, there are other variables that can influence the final structure of the material. Table 2 gives a summary of the most important parameters considered for CMSMs supported on tubular ceramic carriers, which is the shape that this study focuses on. For unsupported membranes, Saufi and Ismail *et al* .^[45] provide an in-depth report on the main fabrication parameters to be considered.

Table 2. Studies that report fabrication parameters on CMS-supported membranes.

| Material | Type of support | Variable that affect permeation | Ref |
|--|---------------------------|---|------|
| poly(2,6-dimethyl-1,4-phenylene oxide) (PPO) polymer | Alumina tubular support | Polymer concentration. Pyrolysis temperature | [60] |
| BPDA-pp'-ODA | α -alumina support | Additional treatment of vapour deposition | [53] |
| Novolak-type phenolic resin | γ -alumina support | Deposition of inorganic layers. Polymer solution concentration | [44] |
| BPDA-pp'-ODA | α -alumina support | Carbonization temperature. | [51] |

As has been mentioned, the pore structure of CMSMs is closely related to the pyrolysis conditions, especially the carbonisation temperature.^[61] The thermal decomposition of polymer precursors such as polyimides produces gases such as He, CO₂, O₂ and N₂. Different types of products in each step of pyrolysis can either favour shrinkage or the production of new micropores in the material. A detailed fractional factorial design of experiments showed that the carbonisation temperature had the strongest influence on gas permeation in the carbon membrane, whereas the heating rate did not have big

influence on the development of the membrane structure during the carbonisation process. Sua and Lua outlined that a nitrogen atmosphere coupled with lower final temperature gave the highest permeabilities for the four gases studied.^[62]

ALTERNATIVE FABRICATION METHODS FOR CMSMS

As has been described, pyrolysis of deposited polymers is one of the most common methods for CMS preparation. Coating of inorganic porous materials with a polymer layer as carbon precursor has been presented as the main fabrication method, but critical thickness and the difference in thermal expansion coefficients between the polymer and support has to be considered in order to avoid crack formation. For this reason, alternatives methods, such as vapour deposition have been extensively reported in literature.^[63] In this approach, carbon coating is done with a hydrocarbon as a precursor gas introduced in porous materials at elevated temperatures (800–1000 °C). The gas is then cracked, which leads to the deposition of carbon on the surface of porous material. Some researchers report carbon deposition as a technique for increasing the selectivity of porous materials. Wan *et al.*^[64] deposited carbon by cracking benzene. The molecular sieves obtained showed kinetic selectivities of 16.0 and 7.06 for CO₂/CH₄ and O₂/N₂ respectively. Similarly, David *et al.*^[65] modified a carbon support by cracking benzene at 650–800 °C, which led to coke being deposited on the pore walls. The pore sizes comparable to those suitable for diffusing Ar and O₂ were on the order of 4–25 Å. Figure 3 shows a picture of the coke formation in the pore mouth of a carbon support.

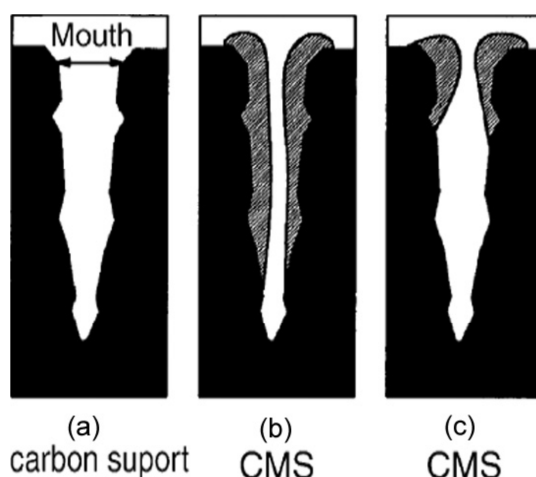


Figure 3. Carbon deposition on pores.^[65]

Li *et al* .^[66] fabricated a tubular carbon-coated membrane by chemical vapour deposition (CVD) of methane on a multi-layered porous ceramic substrate at a temperature of 1000 °C. They also reported that CVD allowed good control of film thickness. Hou *et al* .^[67] explored the concept of depositing carbon materials in an inorganic framework. They impregnated zeolites-Y with PFA, which was then polymerized inside the zeolite channels. This composite material was then heated at 600°C under acetylene CVD and yielded a carbon material. They concluded that PFA impregnation is the least efficient and longest step for microporous-carbon production and highlighted the advantages of obtaining ordered microporous-materials by CVD.

Overall, vapour deposition and its variations provide better control of the thickness of the deposited carbon layer, although they also require the use of high pressures at high temperature. In addition, the structure of the material obtained by carbon deposition and the relationship between the material's structure and the final permeation and selectivity properties have not been fully reported. As with polymer pyrolysis, understanding how fabrication variables and the characteristics of the precursors in the pore architecture influence the final structure of the carbon layer would help us understand the final properties of the membranes and design specific pore architecture for a given mixture of gases.

FABRICATION ISSUES IN CMSMS ON TUBULAR SUPPORTS

Coating polymeric materials over an inorganic support prior to pyrolysis bring mechanical stability to carbon membrane materials. The deposition of the polymer is a key step in the fabrication of supported CMS. This process must be controlled in order to produce consistent continuous films. Shiflett and Foley^[68] deposited PFA onto porous stainless steel tubes by ultrasonic deposition. After pyrolysis, a supported nanoporous carbon membrane without cracks was obtained. This approach had the advantage of controlling the catastrophic cracking formation when the film's thickness was close to 20 µm.^[24]

The effect of the different pyrolysis parameters on CMSMs^[68] has been extensively reported, but very little work has focused on understanding the technical, physical and mechanical issues of membrane fabrication, especially for tubular-shaped supported membranes. The influence of the thickness of the polymer precursor, the differences in the expansion thermal coefficients and the pyrolysis conditions needed for a defect free membrane have not been fully reported.^[69] This is because different parameters have to be considered from those that are usually reported.^[70,71] Both the coating method and the choice of support can determine the performance and stability of the resulting membrane.^[72] In fact, the challenges encountered in developing polymer films on inorganic supports are very similar to those that appear when depositing inorganic films. One of the most important problems is the lack of thickness reproducibility during the gelification of some polymers. This is usually solved by repetitive coating in order to avoid pinholes, cracks or defects in the membranes, which is time consuming and has a high energy cost.^[73]

In order to have an energy-saving process, the membrane must have a limited number of coating steps. Moreover, depositing a crack-free polymer membrane is strongly dependent on the nature of the polymer. For example, the thermoplastic character of some polymers can cause melting during heating and pyrolysis, which would change the membrane shape and thickness and lead to a redistribution of the polymer layer. Wei *et al.*^[72] obtained a successful carbon membrane after one coating step by depositing novolac phenol-formaldehyde-based resins modified with hexamine. This gave the resin a thermosetting character that favoured optimal polymer localisation over the support and a defect-free and mechanically stable CMSM. In addition to chemically modifying the polymer, the film deposited is influenced by the surface of the porous support, as Huang and Dittmeyer^[73] reported when they prepared thin palladium supports. In fact, Sedigh *et al.*^[74] showed that the polymer's penetration into the support can be controlled by a thin layer of γ -alumina (average pore diameter of 5 nm). The characteristics, the concentration and the viscosity of the filler material (polymer) over a support with a variable grade of porosity determine the formation of a stable layer of material or the infiltration of the precursor in the support, and this means differences in membrane thickness and final performance (Figure 4).

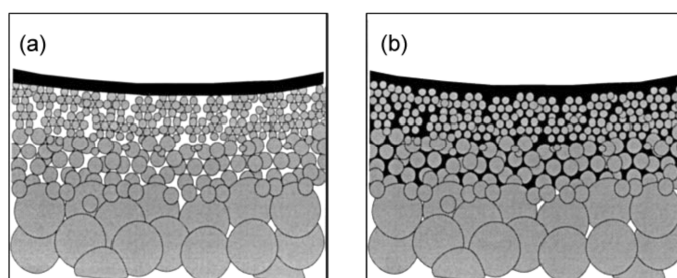


Figure 4. Schematic representation of (a) a thin polymer film supported on an asymmetric support and an (b) asymmetric membrane infiltrated by a polymer solution.[9].

For asymmetric configurations, the polymer's structure and concentration are not the only factors to consider when obtaining a supported film. The choice of the supporting material is crucial to obtaining good coatings.^[75] This could involve modifying the support structure in order to achieve an isotropic distribution of pores, and this could improve polymer coverage and reduce crack formation. Moreover, less starting material is required to form the film and higher gas permeation values can be achieved.^[69] For example, Shah *et al.*^[76] obtained nanoporous carbon membranes by modifying metal supports with low porosity and uniform pore size after incorporating silica nanoparticles into porous stainless steel supports. They demonstrated that the silica particles influence the thickness of the nanoporous carbon layer, resulting in improved Bomax permeability.^[76]

Support modification is, therefore, a method that can be successfully applied to different membrane geometries using different types of fillers to produce nanoporous carbon membranes and achieve flux improvement.^[68,69] Similarly, Liu *et al.*^[28] successfully modified a ceramic support after dip coating with a boehmite solution in order to obtain a supported carbon membrane without cracks. They put the polymer on the outer surface of a tubular α -Al₂O₃ support, and controlled the deposition process, thus avoiding catastrophic cracking. The membranes supported on modified α -Al₂O₃ were mechanically strong at different pressures and temperatures.^[28]

CHARACTERISATION OF CMSMS COVERED IN TUBULAR SUPPORTS

The characterisation of carbon membranes has been fully reported, specifically for unsupported samples. However, most studies of supported tubular-shaped CMSs focus on the final application without considering the transformations of the precursor material into a carbogenic structure, or how the fabrication conditions, the polymer properties and, most importantly, the support affected the final properties.

Gas permeability has been extensively used to characterize CMSMs because the variations in gas permeation rates can be related to the structural characteristics of the porous membrane. Gas permeability studies are commonly coupled with adsorption analysis. However, inconsistent results can be found, as happened with Lua and Su.^[61] Interestingly, they described how the samples with lowest nitrogen uptake gave higher permeance values.

In addition to pore structure and permeation, it is important to observe the nanoporous materials' separation mechanisms; these are molecular sieving, selective adsorption or differences in diffusion rates. In fact, the behaviour of pure gases permeating through membranes can be highly different in the presence of another gas.^[77] In CMS, the main mechanism for gas separation is molecular sieving (Figure 5). This mechanism is strongly dependent on the kinetic diameter of molecules (e.g. He (2.6 Å), H₂ (2.89 Å), CO₂ (3.3 Å), O₂ (3.46 Å), N₂ (3.64 Å)) and the separation is according to the size and shape of the molecules. However, permeation rates and selectivity in gas mixtures are also affected by the competitive adsorption of gas molecules on the pore surface.^[78] Hatori *et al.*^[33] reported that the difference in H₂ selectivities vs gases such as CO and CO₂ was not related to the molecular size of the components in the mixture but rather was related to differences in their predisposition towards adsorption in the micropores. They reported H₂/CO selectivity over 1000. Kim *et al.* studied the molecular sieving mechanism and the surface diffusion mechanism for CMSM. They showed that the mechanisms are not only related to the molecular dimensions but also to the different adsorption behaviors of the gases.^[54] Reid and Thomas^[79] reported that the adsorption kinetics of gases are determined by factors such as the interaction between the adsorptive and the adsorbent surface and the size of the adsorptive species in

relation to the size of the pores in the adsorbent. They highlighted that the main differences in the adsorption kinetic of gases such as oxygen and nitrogen are related to the molecular size and also to the fact that the adsorption process can be influenced by shape factors.^[80] In addition, the same authors^[81] investigated the mechanism of air separation in CMS using adsorption of oxygen, nitrogen and gases with linear structures. In their study, the adsorption of linear molecules was investigated as a way of estimating the contribution of molecular size and shape in the adsorption kinetics of gases on CMSs. They considered a variety of models, such as the linear driving force (LDF), to describe the adsorption in CMSs. They reported differences in adsorption rates between carbon monoxide (2–3 times faster) and nitrogen, despite similarities in their activation energy values and electronic structures. These kinds of studies into unsupported samples can give a better idea of how the adsorber/adsorbent interaction affects the adsorption kinetics of specific mixtures of gases in supported CMSMs.

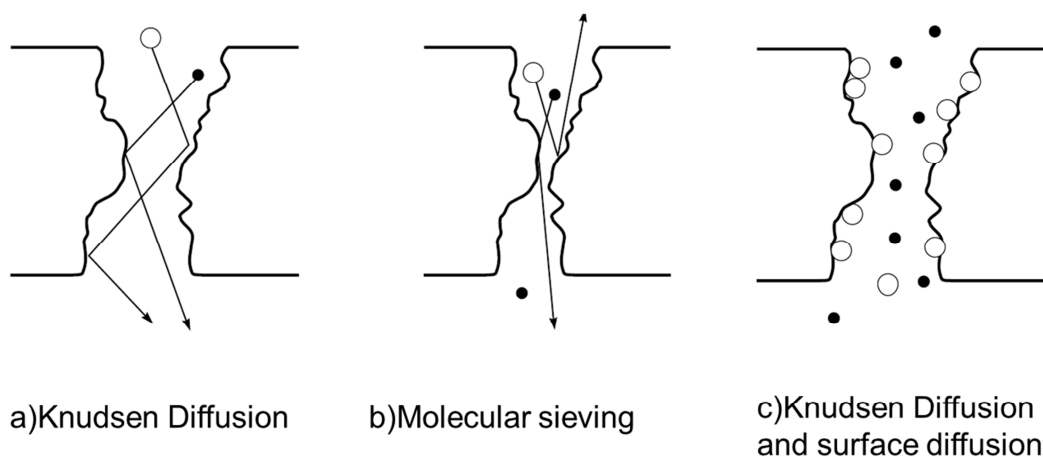


Figure 5. Permeation mechanisms of gas mixtures through finely microporous-membranes.[82].

Desorption kinetic studies are more effective when they monitor the changes in the membrane microstructure during different heat treatments. These studies allow us to determine the relationships between the structure and the properties of carbon membranes, helping in establishing the best conditions for gas separation. Arriagada *et al.*^[83] reported an appropriate carbonisation temperature of around 1000 °C for CH₄ – CO₂ separation. Increasing the carbonisation temperature to 1100 °C blocked the

micropores that were accessible to CO₂, thus decreasing the selectivity. They showed that carbonisation at different temperatures generates materials with different micropore size distributions. They also remarked that the nitrogen adsorption at 77 K is not enough to characterize the micropore structures.

Molecular probing is another powerful technique for characterizing micro- and mesoporosity CMS on the basis of differences in the adsorption kinetics. The molecules must pass through an energy barrier during their diffusion through the selective porosity, and this highlights the differences in the adsorption kinetics of various gases. However, characterizing the selective porosity produced in heterogeneous materials could be difficult and incomplete. David *et al.* described the difficulties of this type of characterization in heterogeneous materials.^[65] In addition, sometimes adsorption analysis requires crunching the sample, thus obtaining partial information regarding the total microporosity of the sample.^[74]

As previously noted, in the case of planar or unsupported CMSMs, there are many publications that correlate CMS structure (the pore distribution, pore size and morphology) to their final performance (gas separation and selectivity), but there is a clear lack of studies dealing with supported CMSMs. Different techniques such as gas adsorption experiments, X-ray diffraction and molecular probes have traditionally been reported; however, in order to understand the material transformation, the formation of micro- and macropores and their relationship to total performance, it is important to analyse the supported carbon membrane on its original support. The influence of the porosity of the support on the overall performance has already been studied,^[29,44] and new studies should focus on establishing the relationships between the structure of the membrane and its performance. The same techniques applied in support characterization can be valid for supported membranes.

During the last decade, different approaches have been presented for characterizing ceramic supports.^[84,85] Otero *et al.*^[86] reported the use of liquid–liquid displacement porosimetry for determining the pore size distribution on ultra-filtration and nanofiltration membranes. Although this technique is still being standardised, it is important to note its non-destructive nature that makes it a potential candidate for

characterizing supported materials. This technique provided a pore size distribution that closely agreed with those recorded using more traditional approaches such as atomic force microscopy (AFM) and salt-retention experiments. This agreement makes liquid–liquid displacement porosimetry a possible alternative to techniques such as microscopy in the characterisation of complete coated membranes in tubular ceramic materials. This is even more valuable given the problems that have been reported in using AFM or scanning probe microscopy (STM) to determine the pore size.[87] AFM problems are related to the intrinsic resolving power of the technique (AFM has only been used for visualizing large mesopores >10 nm), whereas STM problems can be caused by the low conductivity of some nanoporous carbon samples.

Given the questions regarding the mechanical stability of carbon membranes in unsupported configurations, mechanical tests should be considered so as to make them reliable for industrial applications. There are only a few reports dealing with the characterization of the mechanical properties of tubular coated membranes. For this reason, the application of characterization methods used for other materials has been investigated. For example, Huang *et al.* [88] reported five methods for characterizing the adhesion of typical tubular composite palladium membranes in order to distinguish the adhesion between coating and support. These methods are as follows: the cross-cut test, the thermal shock test, the hydrogen embrittling test, the pull-off test and the pressure tolerating test. These studies confirmed that a porous support with a rougher surface and larger pores favours the adhesion of the coating membrane.

Biesheuvel and Verweij[89] reported relationships between the tensile strength and the porous structure of the materials, and different pressures under test conditions. After determining the stress, they described the ceramic supports' sintering temperature and its effect on the homogeneity of the material. They showed that it was large particles in particular that generated defects in the material, which in turn affected the mechanical behavior. All in all, there are not enough studies on mechanical property tests for the author to characterize the differences at a micro-porous level. The techniques usually reported for tubular ceramics can only serve as a guide when characterizing tubular supported materials.

FINAL REMARKS

To summarize, the attempts to develop MRs have directed the research into new materials that are more competitive in performance than the traditional metallic (Pd) and inorganic ceramic membranes. Supported carbon membranes are a promising alternative in reactions where gas separation is needed, especially for high scale applications. However, in contrast with hollow fibre and planar membranes, carbon membranes are not easy to fabricate. It is necessary to understand how factors such as synthesis conditions, precursor selection, type of support, and fabrication method can influence the final structure of the CMSM, the permeation and selectivity of different-sized gases and the competitive adsorption characteristics during the separation of mixtures.

There is a lack of non-destructive techniques for determining the macro- and microporous-structure and for characterizing all the mechanisms involved in the separation process of hybrid structures, this process being finally related to the type of graded structure that includes the membrane and its support. In addition, the asymmetric configuration is promising for all the different kinds of support modifications needed for higher values of flux and yield in MR applications. Finally, even this study has only focused on gas separation; research into CMSM development would bring new responses to other problems in the field of membranes such as water adsorption, separation of biomolecules and liquid/gas mixtures^[90 - 92] where separation can be controlled by grading porosity of supported membranes.

Acknowledgements

The authors are grateful to the Spanish Government for financial support (Project CTQ2005-09182/PPQ). Similarly, authors are grateful to the commission of European Communities Specific OpenTok (Project MTKD-LT-2005-030040).

REFERENCES

- [1] S. Kawatsu. Advanced PEFC developments for fuel cells powered vehicles *J. Power Sources*, **1998**; *71*, 150–155.
- [2] R.K. Ahluwalia, X. Wang. ., Effect of CO impurities performance of direct hydrogen polymer-electrolyte fuel cells, *J. Power Sources*, **2008**; *180*, 122–131.
- [3] S. Ahmed, M. Krumpelt, Hydrogen from hydrocarbon fuel for fuel cells , *Int. J. Hydrogen Energy*, **2001**; *26*, 291–301.

- [4] J. Huang, W.S. Winston Ho. Effects of system parameters on the performance of a CO₂ selective WGS membrane reactor for fuel cells, *J. Chinese Inst. Chem. Eng.*, **2008**; *39*, 129–136.
- [5] A. Brunetti, A. Caravella, G. Barbieri, E. Drioli, Simulation study of water gas shift reaction in a membrane reactor, *J. Memb. Sci.*, **2007**; *306*, 329–340.
- [6] F. Gallucci, S. Tosti, A. Basile, Pd-Ag tubular membrane reactors for methane dry reforming: a reactive method for CO₂ consumption and H₂ production, *J. Memb. Sci.*, **2007**; *317*, 96–105.
- [7] G. Centi, R. Dittmeyer, S. Perathoner, M. Reif. Tubular Inorganic catalytic membrane reactors: advantages and performance in multiphase hydrogenation reactions, *Catal. Today*, **2003**; *79-80*, 139–149.
- [8] A.L.Y. Tonkovich, J.L. Zilka, D.M. Jimenez, G.L. Roberts, J.L. Cox. Experimental investigations of organic membrane factors: a distributed feed approach for partial oxidation reactions, *Chem. Eng. Sci.*, **1996**; *51(5)*, 789–806.
- [9] A. Julbe, D. Farrusseng, C.H. Guizard, Porous ceramic membranes for catalytic reactors_overview and new ideas, *J. Memb. Sci.*, **2001**; *181*, 3–20.
- [10] T. Tsuru, T. Morita, H. Shintani, T. Yoshioka, M. Asaeda, Membrane reactor performance of steam reforming of methane using hydrogen-permselective catalytic SiO₂ membranes, *J. Memb. Sci.*, **2008**; *316*, 53–62.
- [11] H. Cong, M. Radosz, B.F. Towler, Y. Shen. Polymeric-Inorganic nanocomposite membranes for gas separation, *Sep. Purif. Technol.*, **2007**; *55*, 281–291.
- [12] G.Q. Lu, J.C. Diniz da Costa, M. Duke, S. Giessler, R. Socolow, R.H. Williams, T. Kreutz, Inorganic membranes for hydrogen production and purification: A critical review and perspective, *J. Colloid Interface Sci.*, **2007**; *314*, 589–603.
- [13] H.A. Meinema, R.W.J. Dirrix, H.W. Brinkman, R.A. Terpstra, J. Jekerle, P.H. Kusters. Ceramic membranes for gas separation-recent developments and state of the art *Inter Ceram*, **2005**; *54*, 86–91.
- [14] F. Gallucci, A. Basile, S. Tosti, A. Iulianelli, E. Drioli. Methanol steam reforming and ethanol steam reforming in membrane reactors: an experimental study, *Int.J. Hydrogen Energy*, **2007**; *32*, 1201–1210.
- [15] E. Kikuchi, Membrane reactor application to hydrogen production, *Catal. Today*, **2000**; *56*, 97–101.
- [16] X. Yin, L. Hong, Z.-L. Liu. Asymmetric Tubular Oxygen-Permeable Ceramic Membrane Reactor for Partial Oxidation of Methane, *J. Phys. Chem. C*, **2007**; *111*, 9194–9202.
- [17] H. Weyten, J. Luyten, K. Keizer, L. Willems, R. Leysen. Membrane performance: the key issues for hydrogenation reactions in a catalytic membrane reactor, *Catal. Today*, **2000**; *65*, 3–11.
- [18] S. Tosti, L. Bettinali, V. Violant, Rolled thin Pd and Pd-Ag membranes for hydrogen separation and production, *Int. J. Hydrogen Energy*, **2000**; *25*, 319–325.
- [19] J. Coronas, J. Santamaria, Catalytic reactors based on porous ceramic membranes, *Catal. Today*, **1999**; *51*, 377–389.
- [20] D.-W. Lee, S.-J. Park, C.h.-Y. Yu, S.-K. Ihm, K.-H. Lee., Study on methanol reforming-inorganic membrane reactors combined with water-gas shift reactions and relationship between membrane performance and methanol conversion, *J. Memb. Sci.*, **2008**; *316*, 63–72.
- [21] N. Itoh, K. Haraya, A carbon membrane reactor, *Catal. Today*, **2000**; *56*, 103–111.
- [22] Y. Kusuki, H. Shimazaki, N. Tanihara, S. Nakanishi, T. Yoshinaga, Gas permeation properties and characterization of asymmetric carbon membranes prepared by pyrolysing asymmetric hollow fiber membrane, *J. Memb. Sci.*, **1997**; *134*, 245–253.
- [23] J.N. Barsema, N.F.A. Van der Vegt, G.H. Koops, M. Wessling, Carbon molecular sieve membranes prepared from porous fiber precursor, *J. Memb. Sci.*, **2002**; *205*, 239–246.
- [24] M.B. Shiflett, J.F. Pedrick, S.R. McLean, S. Subramoney, Characterization of Supported Nanoporous Carbon Membranes, H.C. Foley. *Adv. Mater.*, **2000**; *12(1)*, 21–25.
- [25] O.M. Ekiner, G. Vassilatos, Polyaramide hollow fibers for H₂/CH₄ separation II. Spinning and properties, *J. Memb. Sci.*, **2001**; *186*, 71–84.
- [26] J. Won, H.C.h. Park, U.Y. Kim, Y.S. Kang, S.D.H. Yoo, J.Y. Jho, The effect of dope solution characteristics on the membrane morphology and gas transport properties: PES/g-BL/NMP system, *J. Memb. Sci.*, **1999**; *162*, 247–255.
- [27] N. Peng, T.-S. Chung, K.Y. Wang, Macrovoid evolution and critical factors to form macrovoid-free hollow fiber membranes, *J. Memb. Sci.*, **2008**; *318*, 363–372.
- [28] B.S. Liu, N. Wang, F. He, J.X. Chu, Separation Performance of Nanoporous Carbon membranes fabricated by catalytic decomposition of CH₄ using Ni/polyamide templates. *Ind. Eng. Chem. Res.*, **2008**; *47(6)*, 1896–1902.
- [29] D. Lee, L. Zhang, S.T. Oyama, S. Niu, R.F. Saraf, Synthesis, characterization, and gas permeation properties of a hydrogen permeable silica membrane supported on porous alumina *J. Memb. Sci.*, **2004**; *231*, 117–126.

- [30] C.W. Jones, W. Koros, Carbon molecular sieves gas separation membranes I: Preparation and Characterization based on polyimide precursors, *Carbon*, **1994**; 32(8), 1419–1425.
- [31] J.E. Koresch, A. Soffer. Mechanism of Permeation through Molecular-sieve Carbon Membrane, *J. Chem. Soc., Faraday Trans. 1*, **1986**; 82, 2057–2063.
- [32] V. Ley, A.P. Kruzic, R.B. Timmons, Permeation rates of low molecular weight gases through a plasma synthesized allyl alcohol membrane, *J. Memb. Sci.*, **2003**; 226, 213–226.
- [33] H. Hatori, H. Takagi, Y. Yamada, Gas separation properties of molecular sieving carbon membranes with nanopore channels, *Carbon*, **2004**; 42, 1169–1173.
- [34] D. Grainger, M.B. Hägg, Evaluation of cellulose-derived carbon molecular sieve membranes for hydrogen separation from light hydrocarbon, *J. Memb. Sci.*, **2007**; 306, 307–317.
- [35] H. Foley, Review_ carbogenic Molecular Sieves: Synthesis, properties and applications, *Microporous Mater.*, **1995**; 4, 407–433.
- [36] Z. Lai, G. Bonilla, I. Diaz, G. Nery, K. Sujaoti, M. Amat, E. Kokkoli, O. Terasaki, R. Thompson, M. Tsapatsis, D. Vlachos, Microstructural optimization of a zeolite membrane for organic vapor separation, *Science*, **2003**; 300(5618), 456–460.
- [37] R.M. De Vos, H. Verweij, High-Selectivity, High-Flux Silica Membranes for Gas Separation, *Science*, **1998**; 279, 1710–1711.
- [38] A.A. Lapkin, S.R. Tennison, W.J. Thomas, A porous carbon membrane reactor for the homogeneous catalytic hydration of propene, *Chem. Eng. Sci.*, **2002**; 57, 2357–2369.
- [39] B. Fayyaz, A. Harale, B.-G.i. Park, P.K.T. Liu, M. Sahimi, T.T. Tsotsis, Design aspects of hybrid adsorbents-membrane reactors for hydrogen production, *Ind. Eng. Chem. Res.*, **2005**; 44, 9398–9408.
- [40] A. Harale, H.T. Hwang, P.K.T. Liu, M. Sahimi, T.T. Tsotsis, Experimental studies of a hybrid adsorbent-membrane reactor (HAMR) system for hydrogen production, *Chem. Eng. Sci.*, **2007**; 62, 4126–4137.
- [41] S. Lagorsse, F.D. Magalhães, A. Mendes, Aging study of carbon molecular sieve membranes *J. Memb. Sci.*, **2008**; 310, 494–502.
- [42] K. Steel, W. Koros. An investigation of the effect of pyrolysis parameters on gas separation properties of carbon materials, *Carbon*, **2005**; 43, 1843–1856.
- [43] T.A. Centeno, J.L. Vilas, A. Fuertes, Effects of phenolic resin pyrolysis conditions on carbon membrane performance for gas separation, *J. Memb. Sci.*, **2004**; 228, 45–54.
- [44] J. Carretero, J.M. Benito, A. Guerrero-Ruiz, I. Rodriguez- Ramos, M.A. Rodriguez, Infiltrated glassy carbon membranes in γ -Al₂O₃ supports, *J. Memb. Sci.*, **2006**; 281, 500–507.
- [45] S.M. Saufi, A.F. Ismail, Fabrication of carbon membrane for gas separation-a review, *Carbon*, **2004**; 42, 241–259.
- [46] A. Fuertes, T. Centeno, Supported carbon molecular sieve membranes based on phenolic resins, *J. Memb. Sci.*, **1999**; 160, 201–211.
- [47] D. Adinata, W. Mohd, A. Daud, M. Aroua, Production of carbon molecular sieves from palm shell based activated carbon by pore size modification with benzene for methane selective separation, *Fuel Process. Technol.*, **2007**; 88, 599–605.
- [48] P.-S. Tin, T.-S. Chung, S. Kawi, M.D. Guiver, Novel approaches to fabricate CMSM based on chemical modified and solvent treated polyimides, *Macroporous Mesoporous Mater.*, **2004**; 73, 151–160.
- [49] W. Wei, X. Hu, G. Qin, L. You, G. Chen, Pore structure control of phenol-formaldehyde based carbon microfiltration membranes, *Carbon*, **2004**; 42, 667–669.
- [50] L. Shao, T.-S. Chung, G. Wensley, S.-H. Goh, K.-P. Pramoda, Casting solvent effects on morphologies, gas transport properties of novel 6FDA/PMDA-TMMDA copolyimide membrane and its derived carbon membranes, *J. Memb. Sci.*, **2004**; 244, 77–87.
- [51] K. Kusakabe, M. Yamamoto, S. Morooka, Gas permeation and micropore structure of carbon molecular sieving membranes modified by oxidation, *J. Memb. Sci.*, **1998**; 149, 59–67.
- [52] H. Wang, L. Zhang, G.R. Gavalas. *J. Memb. Sci.*, **2000**; 177, 25–31.
- [53] J.-I. Hayashi, H. Mizuta, M. Yamamoto, K. Kusakabe, S. Morooka, Preparation of supported carbon membranes from furfuryl alcohol by vapor deposition polymerization, *J. Memb. Sci.*, **1997**; 124, 243–251.
- [54] Y.K. Kim, H.B. Park, Y.M. Lee, Gas separation properties of carbon molecular sieve membranes derived from polyimide/polyvinylpyrrolidone blends: effect of the molecular weight of polyvinylpyrrolidone, *J. Memb. Sci.*, **2005**; 251, 159–167.
- [55] X. Zhang, H. Hua, Y. Zhua, S. Zhu, Carbon molecular sieve membranes derived from phenol formaldehyde novolac resin blended with poly(ethylene glycol), *J. Memb. Sci.*, **2007**; 289, 86–91.

- [56] L. Shao, T.-S.h. Chung, K.P. Pramoda, The evolution of physicochemical and transport properties of 6FDA-durene towards carbon membranes; from polymer, intermediate to carbon, *Microporous Mesoporous Mater.*, **2005**; *84*, 59–68.
- [57] J.N. Barsema, S.D. Klijnstra, J.H. Balster, N.F.A. Van der Vegt, G.H. Koops, M. Wessling, Intermediate polymer to carbon gas separation membranes based on Matrimid PI, *J. Memb. Sci.*, **2004**; *238*, 93–102.
- [58] C.h.L. Burket, R. Rajagopalan, A.P. Marencic, K. Dronvajjala, H.C. Foley, Genesis of porosity in polyfurfuryl alcohol derived nanoporous carbon, *Carbon*, **2006**; *44*, 2957–2963.
- [59] B. Zhang, T. Wang, S. Liu, S. Zhang, J. Qiu, Z. Chen, H. Cheng, Structure and morphology of microporous carbon membrane materials derived from poly(phthalazinone ether sulfone ketone), *Microporous Mesoporous Mater.*, **2006**; *96*, 79–83.
- [60] H.-J. Lee, M. Yoshimune, H. Suda, K. Haraya Gas permeation properties of poly(2,6-dimethyl-1,4-phenylene oxide) (PPO) derived carbon membranes prepared on a tubular ceramic support, *J. Memb. Sci.*, **2006**; *279*, 372–379.
- [61] A.C.h. Lua, J. Su, Effects of carbonisation on pore evolution and gas permeation properties of carbon membranes from kapton polyimide, *Carbon*, **2006**; *44*, 2964–2972.
- [62] J. Su, A.C.h. Lua Influence of carbonisation parameters on the transport properties of carbon membranes by statistical analysis, *J. Memb. Sci.*, **2006**; *278*, 335–343.
- [63] D. Lozano-Castello, J. Alcaniz-Monge, D. Cazorla-Amoro, A. Linares-Solano, W. Zhu, F. Kapteijn, J.A. Moulijn, Adsorption properties of carbon molecular sieves prepared from activated carbon by pitch pyrolysis, *Carbon*, **2005**; *43*, 1643–1651.
- [64] W.M.A. Wan Daud, M.A. Ahmad, M.K. Aroua. Carbon molecular sieves from palm shell: Effect of the benzene deposition times on gas separation properties, *Sep. Purif. Technol.*, **2007**; *57*, 289–293.
- [65] E. David, A. Talaie, V. Stanciu, A.C. Nicolae, Synthesis of carbon molecular sieves by benzene pyrolysis over microporous carbon materials, *J. Mater. Process. Technol.*, **2004**; *157–158*, 290–296.
- [66] Y.-Y. Li, T. Nomurab, A. Sakoda, M. Suzuki. Fabrication of carbon coated ceramic membranes by pyrolysis of methane using a modified chemical vapor deposition apparatus, *J. Memb. Sci.*, **2002**; *197*, 23–35.
- [67] P.-X. Hou, T. Yamazaki, H. Orikasa, T. Kyotani, An easy method for the synthesis of ordered microporous carbons by the template technique., *Carbon*, **2005**; *43*, 2618–2641.
- [68] M.B. Shiflett, H. Foley, Ultrasonic deposition of high-selectivity nanoporous carbon membranes., *Science*, **1999**; *285*, 1902–1905.
- [69] A. Merritt, R. Rajagopalan, H. Foley, High Performance nanoporous membranes for air separation, *Carbon*, **2007**; *45*, 1267–1278.
- [70] M.B. Shiflett, H. Foley, Reproducible production of nanoporous carbon membranes, *Carbon*, **2001**; *39*, 1421–1446.
- [71] H. Suda, K. Haraya, Gas permeation through micropores of carbon molecular sieve membranes derived from kapton polyimide, *J. Phys. Chem B.*, **1997**; *101*, 3988–3994.
- [72] W. Wei, G. Qin, H. Hu, L. You, G. Chen, Preparation of supported carbon molecular sieve membrane from novolac phenol–formaldehyde resin, *J. Memb. Sci.*, **2007**; *303*, 80–85.
- [73] Y. Huang, R. Dittmeyer, Preparation of thin palladium membranes on a porous support with rough surface, *J. Memb. Sci.*, **2007**; *302*, 160–170.
- [74] M.G. Sedigh, M. Jahangiri, K.T. Paul, M. Sahimi, T. Tsotsis, Structural characterization of polyetherimide based carbon molecular sieve membranes, *AIChE J.*, **2000**; *46*(11), 2245–2255.
- [75] Y.D. Chen, R.T. Chang, Preparation of Carbon Molecular sieves membranes and diffusion of binary mixtures in the membrane, *Ind. Eng. Chem. Res.*, **1994**; *33*, 3146–3153.
- [76] T.N. Shah, H.C. Foley, A.L. Zydney, ., Development and characterization of nanoporous carbon membranes for protein ultrafiltration, *J. Memb. Sci.*, **2007**; *295*, 40–49.
- [77] W. Jia, S. Murad. Molecular dynamics simulations of gas separations using faujasite-type zeolite membranes, *J. Chem. Phys.*, **2004**; *120*(10), 4877–4885.
- [78] S. Lagorsse, F.D. Magalhães, A. Mendes, Carbon molecular sieve membranes Sorption, kinetic and structural characterization, *J. Memb. Sci.*, **2004**; *241*, 275–287.
- [79] C.R. Reid, I.P. O'koye, K.M. Thomas, Adsorption of Gases on Carbon Molecular Sieves Used for Air Separation. Spherical Adsorptives as Probes for Kinetic Selectivity, *Langmuir*, **1998**; *14*, 2415–2425.
- [80] C.R. Reid, K.M. Thomas, Adsorption Kinetics and Size Exclusion Properties of Probe Molecules for the Selective Porosity in a Carbon Molecular Sieve Used for Air Separation, *J. Phys. Chem. B*, **2001**; *105*, 10619–10629.
- [81] C.R. Reid, K.M. Thomas, Adsorption of Gases on a Carbon Molecular Sieve Used for Air Separation: Linear Adsorptives as Probes for Kinetic Selectivity, *Langmuir*, **1999**; *15*, 3206–3218.

- [82] R.W. Baker. *Membrane Technology and Applications* (2nd edition). John Wiley & Sons: England, **2004**; p.78.
- [83] R. Arriagada, G. Bello, R. Garcia, F. Rodríguez-Reinoso, A. Sepulveda-Escribano, Carbon molecular sieves from hardwood carbon pellets. The influence of carbonization temperature in gas separation properties, *Microporous Mesoporous Mater.*, **2005**; *81*, 161–167.
- [84] J.A. Otero, G. Lena, J.M. Colina, P. Pradanos, F. Tejerina, A. Hernandez, Characterisation of nanofiltration membranes Structural analysis by the DSP model and microscopical techniques, *J. Memb. Sci.*, **2006**; *279*, 410–417.
- [85] J.I. Calvo, A. Botino, G. Capanelli, A. Hernandez., Comparison of liquid-liquid displacement porosimetry and scanning electron microscopy image analysis to characterize ultrafiltration track-etched membranes, *J. Memb. Sci.*, **2004**; *239*, 189–197.
- [86] J.A. Otero, O. Mazarrasa, J. Villasante, V. Silva, P. Pradanos, J.I. Calvo, A. Hernandez. *J. Memb. Sci.*, **2008**; *309*, 17–27.
- [87] J.I. Paredes, A. Martinez-Alonso, J.M.D. Tascon, Three independent ways to obtain information on pore size distributions of nanofiltration membranes, *Microporous Mesoporous Mater.*, **2003**; *65*, 93–126.
- [88] Y. Huang, S. Shu, Z. Lu, Y. Fan, Characterization of the adhesion of thin palladium membranes supported on tubular porous ceramics, *Thin Solid Films*, **2007**; *515*, 5233–5240.
- [89] P.M. Biesheuvel, H. Verweij, Design of ceramic membrane supports: permeability, tensile strength and stress, *J. Memb. Sci.*, **1999**; *156*, 141–152.
- [90] S. Al-Asheh, F. Banat, N. Al-Lagtah. Separation of ethanol-water mixtures using molecular sieves and Biobased adsorbents, *Chem. Eng. Res. Des.*, **2004**; *82*, 855–864.
- [91] S. Lagorsse, M.C. Campo, F.D. Magalhaes, A. Mendes, Water adsorption on carbon molecular sieves membranes: Experimental data and isotherm model, *Carbon*, **2005**; *43*, 2769–2779.
- [92] J.M. Kisler, A. Dahler, G.W. Stevens, A.J. O'Connor, Separation of biological molecules using mesoporous molecular sieves, *Microporous Mesoporous Mater.*, **2001**; *44–45*, 769–764.

□

CHAPTER 3:
Carbon Based Membrane Reactors
(Art. 2)

Accepted for publication: Handbook of membrane reactors

Chapter 10: Carbon based membrane reactors

Woodhead Publishing

Carbon Based Membrane Reactors

K. Briceño^a, A. Basile^b, J. Tong^c, K. Haraya^d

^a*Department d'Enginyeria Química, Universitat Rovira i Virgili, Av. Pasos Catalans, 26, 43007, Tarragona, Spain*

^b*ITM-CNR via P. Bucci c/o University of Calabria - Cubo 17/C, Rende (CS) - 87036 – Italy*

^c*Metallurgical & Materials Engineering, Colorado School of Mines, 1500 Illinois Street, Golden, CO 80401, USA*

^d*National Institute of Advanced Industrial Science and Technology (AIST), Tsukuba Central 5, Tsukuba 305-8565, Japan*

List of contents

1. Introduction
2. Carbon membrane materials
3. Carbon membrane classifications
 - 3.1. Classification by transport mechanism
 - 3.2. Classification by configuration
4. Unsupported carbon membranes
 - 4.1. Planar membrane
 - 4.2. Asymmetric hollow fiber membrane
5. Supported carbon membranes
 - 5.1. Polymer precursors
 - 5.2. Porous substrates
 - 5.3. Fabrication techniques
 - 5.4. Technical challenges
6. Carbon-based macro membrane reactors
7. Carbon-based micro membrane reactors
8. Conclusions and future trends
9. Acknowledgements

10. References

List of acronyms

- AAM: α -Alumina asymmetric membrane
- ASCM: Adsorption selective carbon membranes
- CAM: coated alumina membrane
- C-MEMS: Carbon microelectromechanical systems
- CMR: carbon membrane reactor
- CMS: carbon molecular sieves
- CVD: Chemical vapor deposition
- FAME: fatty acid methyl esters
- FBR: fixed bead reactor
- HAMR: Hybrid adsorbent-membrane reactor
- MIMIC: Micro molding in capillaries
- MRs: Membrane reactors
- MSCM: Carbon molecular sieves membranes
- LDH: Layered double hydroxides
- PA: Polyamic acid
- PEMFC: Proton exchange membrane fuel cells
- PSA: Pressure swing adsorption
- Pd: Palladium
- PDMS: Polydimethylsiloxane
- PFR: plug flow reactor
- PTFE: polytetrafluoroethylene
- SRM: Steam reforming of methanol
- XRD: X-ray diffraction
- YSZ: Yttria-stabilized zirconia
- μ TM: Micro transfer molding

Abstract

Membrane reactors research has been focused on new membrane materials to be integrated in a compact configuration. Carbon membranes has been scarcely explored in the past due to mechanical drawbacks. For this reason carbon membranes are recommended to be supported. However, this imply formation of defects which difficult MR applications. This chapter explore the main variables to be consider in development of carbon membranes mainly focused when the carbon material has to be supported. I fact, some applications are revised for macro and micro reactors.

1. Introduction

Membrane reaction processes are systems where the separation and the reaction are carried out simultaneously, and the continuous extraction of one of the products can shift the equilibrium which produce enhancement of yield and selectivity if compared with a traditional system [1]. The development of membrane reactors has been suited to innovations in membrane materials or catalysts. Specifically, in the case of membranes that the same type of materials used to obtain them can also be suited to support different catalysts. To think in the integration of the separation and catalysis functions, the porous membranes with permeance superior to dense membranes are preferred candidates for the application in membrane reactors, which include porous oxide, zeolite, glass, metal, and newly exploited carbon membranes. Although the carbon membranes are still in their infant stage and have some serious challenges such as weak mechanical strength for unsupported membranes and bad controllability and reproducibility of the fabrication for supported membranes, they are believed to be promising candidates for porous membrane based membrane reactors because the easiness for fabrication, low price for both fabrication and raw materials, molecular sieve separation effect, and high permeance [2-7].

Carbon membranes can be fabricated through the pyrolysis of polymer precursors. Their permeance and separation factors are better than those corresponding polymeric membranes from the same polymer precursors. The investigation of carbon membranes have mostly focused on the sheet, capillary, hollow fiber, and composite configurations. However, for large-scale applications the capillary or hollow fiber membranes are more

important due to their high packing density. For this reason, the first attempts to test carbon membrane reactors have been done using hollow fiber membranes for dehydrogenation reactions [8]. In fact, the integration of carbon membranes in membrane reactors took place from the same need to find alternatives to silica and zeolite membranes. However, very few attempts have been reported in the literature due to the infant development state of the carbon membranes. There are still some problems to be overcome, especially when the carbon membranes are supported on a second substrate with different compositions and structures in order to improve their mechanical strength. The crack, hydrothermal and mechanical resistance inevitably are resulted in. Moreover, the properties measured for the carbon membranes cannot be simply transferred to the carbon based membrane reactors like their competitive counterparts. Therefore, the fabrication of high-quality carbon membrane with controllable and reproducible technique and the exploration of the proper chemical reactions for carbon-based membrane reactors are the two key tasks for the development of the promising carbon based membrane reactors [5].

In this chapter, we first give an overview of carbon membrane materials (section 2) and the classification of carbon membranes (section 3). Then, the unsupported carbon membranes are discussed based on planar membranes and asymmetric hollow fiber membranes (section 4). In section 5, the supported carbon molecular sieve membranes (CMSs) membranes are reviewed in details based on the subsections of precursors, supports, fabrications, and problems. In section 6, the carbon-based membrane reactors are discussed in detail based on the topics of dehydrogenation reactions, hydration reactions, hydrogen production reactions, H_2O_2 synthesis, bio-diesel synthesis, and new carbon membranes for carbon membrane reactors (CMRs). In the end, the new concept to use carbon membranes in microscale devices (micro carbon-based membrane reactor) is simply outlined (section 7).

2. Carbon membrane materials

Carbon is normally stabilized in various multi-atomic structures with different molecular configurations called allotropes. The three relatively well-known allotropes of carbon are amorphous carbon, graphite, and diamond. Once considered exotic, fullerenes are nowadays commonly synthesized and used, which include buckyballs, carbon nanotubes, carbon nanobuds and nanofibers. Several other exotic allotropes have

also been discovered, such as lonsdaleite, glassy carbon, carbon nanofoam and linear acetylenic carbon. Although, most the of carbon allotropes can be used as materials for the preparation of carbon membranes, the amorphous carbon and graphite related molecular configurations (as shown in Figure 1) have been most extensively investigated as carbon membrane materials [9].

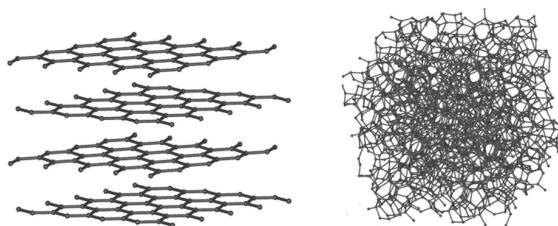


Figure 1 - Molecular configurations of (a) graphite structure and (b) amorphous carbon structure ^[9]

Graphite has a layered, planar structure (**Figure 1a**). In each layer, the carbon atoms are arranged in a hexagonal lattice with separation of 0.142 nm, and the distance between planes is 0.335 nm. The two known forms of graphite, α (hexagonal) and β (rhombohedral), have very similar physical properties (except that the grapheme layers stack slightly differently). The hexagonal graphite may be either flat or buckled. The α form can be converted to the β form through mechanical treatment and the β form reverts to the α form when it is heated above 1300 °C. At normal pressures carbon takes the form of graphite, in which each atom is bonded trigonally to three others in a plane composed of fused hexagonal rings, just like those in aromatic hydrocarbons. The resulting network is 2-dimensional, and the resulting flat sheets are stacked and loosely bonded through weak van der Waals forces. After carbonization, an organic precursor can be converted into a material with higher carbon content. Below 1500 K there is a parallel alignment of molecules even though the structure of each hexagonal layer is not regular, which is favorable for formation of holes.

The amorphous carbon (Figure 1b) is an assortment of carbon atoms in a non-crystalline, irregular, and glassy state, which is essentially graphite but not held in a crystalline macrostructure. As with all glassy materials, some short-range order can be observed. It is the main constituent of substances such as charcoal, lampblack (soot) and

activated carbon. In a crystallographic sense, however, these materials are not truly amorphous, but are polycrystalline or nanocrystalline materials of graphite or diamond within an amorphous carbon matrix.

For the purpose of this chapter we are focusing the carbon membrane materials with a turbostratic structure. This structure was considered in the past as amorphous carbon, which is not completely true. Nowadays, it is considered there are fundamental building blocks of so-called amorphous carbon and microcrystalline domains where hexagonal planes are not aligned but displaced from each other or overlapped, giving a high disorder character. In fact, there is a folding of hexagonal sheets which brings holes of size smaller than 2 nm [10]. The carbon molecular sieves (CMS) are a kind of turbostratic carbon membranes materials with nanoporous structure that allow separation of molecules based on adsorption rate differences given by its size and shape [3]. Similarly, some obvious distinctions exist between CMS and zeolite materials. For example, CMS are mainly amorphous materials, but zeolites are crystallized materials. The structure of zeolites contains water of hydration that limits their application at high temperatures due to possible structure collapse. On the contrary, CMS do not have this characteristic, which makes it possible to apply CMS at high temperatures [3]. Furthermore, comparing with zeolites, CMS have other advantages such as good shape selectivity to planar molecules, high hydrophobicity, electrical neutrality, and synthesis feasibility [5].

CMS can be obtained from controlled pyrolysis of synthetic and natural precursors. In the case of synthetic precursors a large variety of polymers has been employed in the past. Although the high-quality CMS can be easily obtained from synthetic polymer, the cost of these synthetic polymers is very high comparing with the natural polymers, which makes the commercialization more intricate and expensive [3]. For this reason, in the case of air recovery through pressure swing adsorption, the adsorbents of CMS are obtained from cost-effective natural polymers instead of synthetic polymers. However, the advantages originating from pyrolysis of high-quality synthetic polymer, as *e.g.* polyimides, impulse the use of these polymers over supports. Lower quantities of polymer can be used when the polymer is supported than in the case of self-supported membranes. The fabrication process of self-supported membranes, as in the case of hollow fibers, must imply the use of a large quantity of polymer for dope formulation,

which must be extruded for producing the asymmetric membrane (composed by the membrane itself but also by the self-supporting part). From this point of view, the application of CMS to carbon membrane separation and (macro and micro) carbon membrane reactors should be more promising.

3. Carbon membrane classification

Carbon membranes can be obtained after pyrolysis of corresponding polymer precursor membranes. The carbon membrane prepared by Koresh and Sofer et al. [11] is one of the earliest works in this topic. These membranes are important due to the improvement on the trade-off upper limit between permeability and selectivity compared with their polymer precursor membranes. In this sense, Singh-Ghosal and Koros [12] reported the Robeson's plot (O_2/N_2 selectivity versus O_2 permeability) for some carbon membranes and corresponding polymer membranes (**Figure 2**). It is obvious that the performance of carbon membranes is much better than that of corresponding polymer membranes. Moreover, the permeance of the carbon membranes depends on the surface characteristics and the interactions between pores and gas molecules rather than on the bulk properties for the polymer membranes. When carbon membranes separate molecules based on molecular sieving mechanism, the molecules have to overcome an energetic barrier created by the differences between pore dimension and gas molecules.

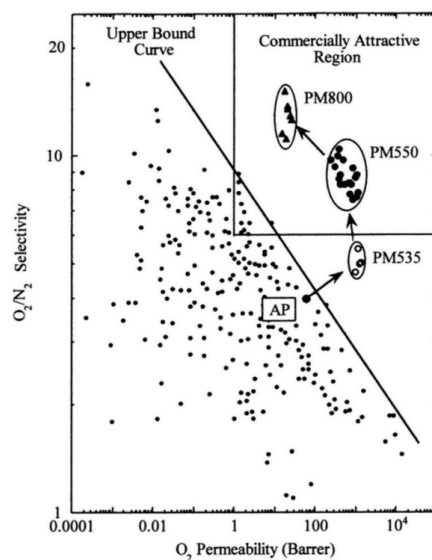


Figure 2 - Robeson's plot: literature data for O_2/N_2 selectivity versus O_2 permeability related to polymeric and carbon membranes. (AP represent polymer precursor of PM carbon membranes) ^[12]

3.1 Classification by transport mechanism

Carbon membranes have been extensively reported for gas separations [5], which can be classified on the basis of the main transport mechanisms. In the case of gas transport depending on the effective sizes of the gas molecules rather than on the adsorption effect, we talk about Molecular Sieves Carbon Membranes (MSCM) with pore sizes in the range of 3-5 Å. When gas permeation is governed by adsorption effects rather than the sizes of the gas molecules, we talk about Adsorption Selective Carbon Membranes (ASCM) with pore sizes in the range of 5-7 Å [13]. On the other hand, depending on both the pore size and the pore population, it is possible to find alternative transport mechanisms such as Knudsen diffusion and adsorption-surface diffusion etc. For Knudsen diffusion, the mean free path of gas molecules is larger than the pore sizes. Gas molecules diffuse through the pores in agreement with the concentration gradient while colliding with the pore walls. The diffusion flux is inversely dependent on the square root of molecular weight. This Knudsen diffusion mechanism occurs more often when pore sizes are in mesoporous range (2-50 nm) or the pore population is between meso- and macro-porosity. As for the adsorption-surface diffusion mechanism, the transport behaviour of gas molecules is mainly dominated by the properties of the pore surface. During transport, gas molecules can be adsorbed on the pore walls and diffuse on the surface, which depends on how strong one or more components are adsorbed on the surface. The adsorbed molecules can plug the pores avoiding the pass of their own molecules but allowing the pass of other species.

3.2 Classification by configuration

An alternative classification of carbon membranes is based on their configurations, which has described in **Figure 3**. It is clear that carbon membranes can be divided into supported and unsupported carbon membranes like most of the other membranes. The unsupported carbon membranes include the configurations of flat, capillary, and hollow fiber etc. The carbon membranes with this three configurations, especially the hollow fiber, sometimes can be fabricated with asymmetric structure with a thin separation layer (small pore size) and thick mechanical support layer (large pore size), which can also be called self-supported carbon membranes. In this chapter, we ascribed this

asymmetric structure to the supported one because at least two type of materials are involved. The unsupported carbon membranes are easy to fabricate and the membrane quality is easy to control and reproduce. However, the intrinsic weak mechanical strength of this kind of membranes greatly limits their practical applications. On the other hand, for the supported carbon membranes, we mainly focus on the configurations with thin top carbon separation layer supported on a porous substrate with strong mechanical strength and non-carbon compositions such as ceramic and glass substrates. The supported carbon membranes can be further divided into macro flat, micro flat, macro tube, and micro tube etc. It is easy to figure out that this kind of configuration can largely improve the mechanical strength and increase the membrane packing volume density. However, the fabrication of this kind of supported membranes still has a lot of challenges. It is difficult to obtain well-controlled and reproducible high-quality carbon membranes on foreign porous substrates.

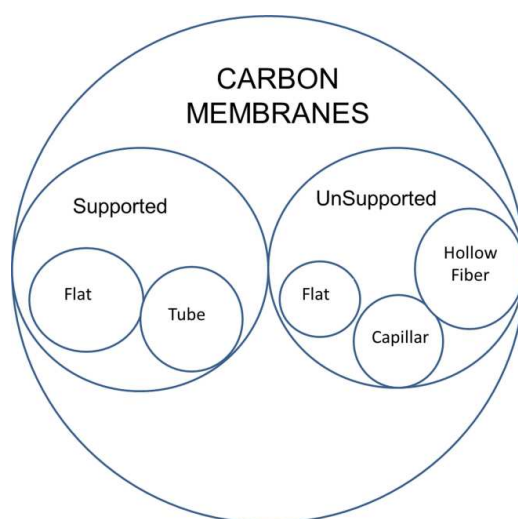


Figure 3 - Classification of Carbon membranes

4. Unsupported carbon membranes

4.1. Symmetric flat carbon membranes

In the case of unsupported flat carbon membranes, Suda and Haraya [14] reported that the pyrolysis of Kapton polyimide at 1273 K can successfully result in high-quality carbon membranes. Kapton is one of the most studied materials for the fabrication of carbon membranes. The flat carbon membranes, obtained by pyrolyzing Kapton at the

temperatures range of 1073-1273 K, showed molecular sieving behaviour. They also observed the global amorphous nature of their carbon membrane and the increasing pyrolysis temperature increased crystalline domains, which was related to the decrease of permeability and the increase of permselectivity. These changes were coupled with the decrease of interplanar spacing (d_{002}). They concluded that the contribution of the decreased interplanar spacing, which decreased amorphous zone, is the main reason for the increased microporosity in their carbon membranes. Suda and Haraya [15] explained the influences of pyrolysis conditions on tailoring the microstructure of their carbon membranes. The experimental parameters of pyrolysis temperature, pyrolysis atmosphere, and heating rate were confirmed to be the main variables for controlling the formation of pore structures. In addition, they also studied the effects of the three experimental variables on the pore population of the carbon membranes. This is another important property to affect the gas separation performance for carbon membranes. In fact, it is possible that a pore population obtained at a specific pyrolysis conditions can benefit to the separation for a couple of gases but not for some different gases with similar effective sizes.

4.2. Asymmetric carbon membranes

Symmetric flat carbon membranes are good prototypes to study the relationship between the experimental conditions and the pore formation behavior and pore property in the carbon membranes. However, they are limited for industrial applications because of the low permeance and volume density, which can be improved by an alternative asymmetric geometry such as asymmetric capillary and hollow fiber membranes. Haraya et al. [2] fabricated asymmetric capillary CMS. They obtained asymmetric structure using phase inversion process through controlled coating polyamic acid (PA) membrane on a polytetrafluoroethylene (PTFE) micro tube. After polymer gelification in several liquid baths, the PTFE micro tube was removed and the PA capillary membrane was left, which was further imidized to Kapton membrane and pyrolyzed at 1223K to form the final capillary carbon membranes. The structures of the resulted membranes were highly dependent on coagulation baths. Therefore, the thickness of dense layer and the pore sizes of membranes can be controlled using different baths. For example, the membranes prepared in methanol bath showed a H_2/N_2 selectivity up to 1080, while the lower H_2/N_2 selectivity of 95.9 was obtained for the membranes

prepared in water bath. However, the phase inversion technique for fabricating capillary carbon membranes showed a relatively low reproducibility. One of the reasons is that it is difficult to control the rapid formation of the dense layer, which is responsible for the separation performance. Moreover, this method allows the formation of large defects, which can decrease the separation performance of the asymmetric membranes. It should also be mentioned that this asymmetric configuration of capillary carbon membranes requires an important consideration of the technical machinery.

5. Supported carbon membranes

As an alternative to unsupported carbon membranes, the carbon separation layer can be supported on flat or tubular substrates to fabricate supported carbon membranes. In the case of supported membrane configuration, we have to consider the influence of the same experimental variables reported in symmetric unsupported flat carbon membranes (pyrolysis temperature, pyrolysis atmosphere, and heating rate). In addition, another experimental parameter of fabrication method have to be considered carefully because it can greatly influence the membrane nanostructure [16]. It is obvious that the supported carbon membranes have very good mechanical stability because the porous substrates of ceramic or metal with high mechanical strength are employed as the substrates. The special structure of the substrate makes membranes suitable for all types of combination of catalysts and carbon separation layers, which can greatly benefit to the application of membrane reactors. This concept is schematically described in **Figure 4**, which includes a microporous top layer and a bimodal catalytic support [17]. Therefore, both gas separation and catalytic reaction functions are combined together to form a membrane reactors. In the following parts we will introduce the most popular supported carbon membranes of CMS membrane on tubular substrates based on polymer precursors.

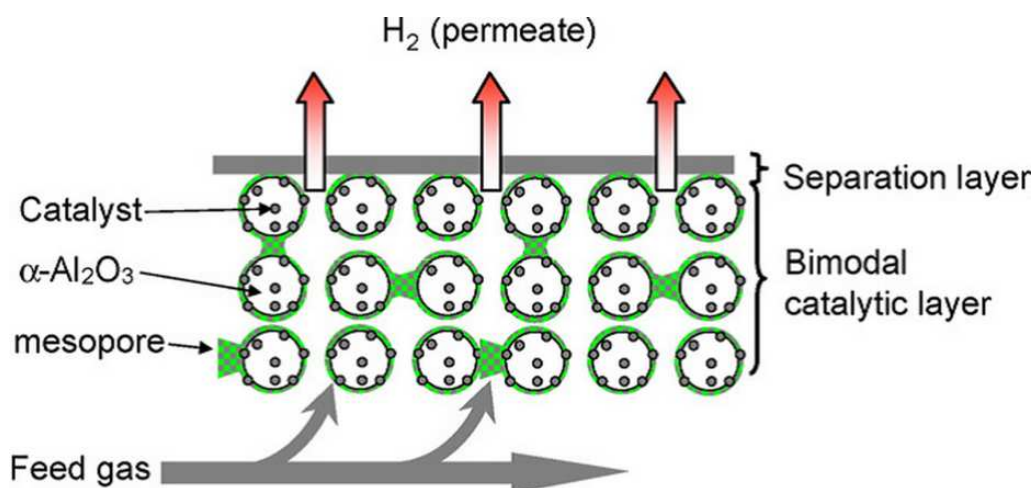


Figure 4 -Schematic concept of a bimodal catalytic membrane (microporous top layer coated on a bimodal catalytic support).^[17]

5.1 Polymer precursors

As mentioned before, the carbon membranes can be fabricated through pyrolyzing the corresponding polymer precursor membrane at high temperature in a controlling atmosphere. For the selection of polymer precursors for the fabrication of carbon membranes, the choices have to be preferred to those polymers that show graphitization behavior. For example, commercial polyimides are chosen as polymer precursor for carbon membrane because they can change into highly crystallized graphite films after carbonization. Concerning to this idea, Shiflett and Foley [18] reported that differences in polymer structures can affect the degree of cross-linking in the char. At higher temperatures, the highly cross-linked polymer will not be suitable for graphitizing. This implies that some amorphous carbon can be available in the graphite domains in the turbostratic carbon structure as represented in **Figure 5** [3]. The control of graphite domains is very important to tailor the pore size distribution of carbon membrane. Moreover, in addition to the polymer structure itself, the organization of the polymer during casting can also affect the final structure of carbon membrane. In this sense, Shao et al. [19] found that the polyimide films coated from polyimide solution with *N,N*-dimethylformamide as solvent has a crystallized structure. On the other hand, those polyimide films coated from polyimide solution with 1-methyl-2-pyrrolidone and

dichloromethane as solvents have an amorphous structure. For carbon membranes obtained from amorphous polymer films after pyrolyzing at 823K, the polymer structure determines the permeance of the resulted carbon membranes. However, at higher pyrolysis temperatures, the permeance of the resulted carbon membrane will be more influenced by pyrolysis conditions.



Figure 5 - Schematic of folded graphite-like layers ^[3]

The most commonly used polymer precursors for carbon membranes have been reported to be polyimides, polyfurfuryl alcohol, phenol formaldehyde resins, and cellulose. Their common characteristic is that they all don't melt during pyrolysis at high temperature, which keeps their original shape and structure during the thermal heating and decomposition process. In this sense, the commercially available Matrimid and Kapton are the fully imidized polyimides with high T_g values. They don't abruptly change their structure during pyrolysis. This important characteristic of these two polyimides has been extensively appreciated by some investigators in the fabrication of CMSM [2,19-21].

As similar to considered in unsupported carbon membranes, pyrolysis temperature also influences the carbon structure of supported carbon membranes. Centeno et al. [22] studied the effect of pyrolysis temperature on permeance of phenolic resins supported on a ceramic tube. They showed how permeance decreases with increase of pyrolysis temperature after 973K. Between 973-1023K the membranes were highly effective for separation of absorbable and non-absorbable species which were considered as ASCM

instead of carbon molecular sieving membranes. Over 1073 K the carbon structure becomes more ordering which implies decrease of pore size causing molecular sieving behavior.

Kusakabe et al. [23] coated a polyamic acid (PA) membrane on the outer surface of a porous alumina tube, which was later pyrolyzed at 873-1173 K and post-oxidized at 673-773 K in series. They showed that the post-oxidation treatment combined with the normal thermal pyrolysis step increased the gas permeance of composite membranes.

Instead of the PA precursors, Hayashi et al. [24] deposited a polyimide film on the outer surface of a porous alumina tube by dip-coating three times. After imidized and pyrolyzed at 973-1073 K, the carbon membranes were fabricated on porous alumina tube. The enhancement of the volume of micropores accessible to smaller molecules has been observed. Hayashi et al. obtained an optimal pyrolysis temperature of 973 K and the maximum permeance was achieved. In order to improve selectivity, a carbon layer was further deposited on the resulted supported carbon membrane by chemical vapor deposition (CVD) of propylene at 923 K. The CVD process favors the deposition of carbon in micropores, which explained the increase of the selectivity of CO₂/N₂ from 47 to 73.

However, polyimide precursors are very expensive. In order to explore alternative cost-effective polymer precursors, Fuertes and Centeno [25] spin-coated a polyetherimide film on a porous carbon disk. They used isopropanol as coagulation bath for the gelification of polyetherimide and obtained a defect-free membrane. After further plasticization by thermal treatment, the polymeric membrane minimally penetrates the porous substrate. The supported carbon membrane obtained through this process showed a molecular sieving behavior. In a successive work, the same investigators [26] started to use polyamic acid in the preparation of coated tubes. In that work, they reported the addition of an intermediate layer to the macroporous substrate in order to improve the substrate surface towards to achieve defect-free carbon membranes. The introduction of this intermediate layer allowed to decrease the pore size in the substrate. After 1-3 times coating all the resulted membranes were able to show ideal selectivity factors over Knudsen theoretical values. Moreover, the permeance also increased with the increasing operational temperature, which indicated all the membrane showed molecular sieving behavior.

5.2. Porous substrates

In the design of the carbon supported membrane, the porous substrates have to be considered too. The most popular commercial porous substrates are porous stainless steel [27] and porous alumina [28]. The selection of substrate depends on the type of tight or connection of the membrane into the module. However, in both cases the macroporous structure can result in large defect on the supported carbon membrane. For this reason, some strategies have been considered to reduce this effect. In this sense, Liu et al. [28] modified the surface morphology of an alumina macroporous substrate by dip-coating in boehmite sol for several times. Merrit et al. [29] incorporated nanofillers into the pores of a porous stainless steel substrate to reduce pore size and much thinner carbon membrane was obtained on the modified substrate. The oxygen permeance increased in some degree without sacrificing selectivity.

5.3. Fabrication techniques

Once the polymer precursor and the porous substrate have been decided, we can go to the most important step of the fabrication of CMSM on the substrate. The fabrication technique must guaranty reproducibility and minimization of defects. The separation carbon layer has to be placed over a defect free substrate, otherwise all substrate defects can be copied to the coated carbon membrane, which in most cases can decrease the selective properties of the composite membrane. In spite of the different strategies that can be considered on minimize defects on substrates, the fabrication techniques can also favor or minimize this problem. **Table 1** resumes the most important methods reported in fabrication of CMSM supported as flat or tubes.

Table 1. Methods for the preparation of supported CMSM

| Method | Support | Coating times | Thickness (μm) | Max. | Membrane position | Reference |
|-----------------------------|---|---------------|-----------------------------|---------------------------|-------------------|-----------|
| | | | | pyrolysis temperature (K) | | |
| Ultrasonic nozzle | SS tube | 3 | 15 ± 2 | 873 | Outside | [18] |
| Dip coating | Carbon support | 1 | 35 | 1073 | Inside | [21] |
| Dip coating + Spinning | Ceramic | | 2 | 973-1273 | Inside | [22] |
| Dip Coating + PP | α -alumina | 3 | | 973 | Outside | [24] |
| Spinning coating | Macroporous carbon disc | 1 or 3 | 2 | 1073 | Outside | [25] |
| Ultrasonic spray + rotation | Sintered SS | 1 -3 | | 723 | | [27] |
| Sponge soaked + Spinning | α -Al ₂ O ₃ modified by bohemite sol | 1 - 3 | 4.7-13.9 | 873-973 | Outside | [28] |
| Vapor deposition | γ -Al ₂ O ₃ / α -Al ₂ O ₃ | 1 - 2 | 6 | 873 | Outside | [30] |

5.4. Technical challenges

One of the common problems in fabrication of supported carbon membranes is related to cracks formation and minimization of defects producing after pyrolysis. **Figure 6** shows a supported carbon membrane obtained from a commercial polyimide Matrimid coated on a porous substrate after pyrolyzing at 973 K with a ramp rate of 2.5 K/min in N₂ atmosphere. The differences of thermal expansion coefficients between substrate and coated polymer film during the heat pyrolysis created a lot of cracks in the resulted carbon membrane. Therefore, the selection of polymer precursor and the optimization of pyrolysis temperature and deposition parameters of polymer layer are believed to very important for avoiding such cracks.

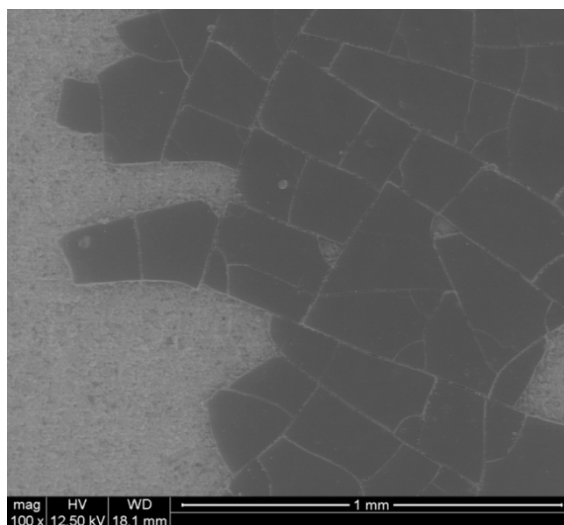


Figure 6 - Crack formation on carbon supported membrane

6. Carbon-based membrane reactors (CMRs)

Due to their molecular-sieving effect, carbon membranes show a high H_2 selectivity and for this aspect they are considered a good candidate for hydrogen production via dehydrogenation reactions in CMR. In fact, CMR is one of the most promising applications of carbon membranes. Nevertheless, despite to the very high potentiality of CMRs, to the best of our knowledge only few works have been published in this specialised and very interesting field.

6.1 Dehydrogenation reactions

In 2000, Itoh and Haraya [8] constructed the first CMR and experimentally examine the performance of a dehydrogenation reaction in their CMR. Asymmetric polyimide hollow fiber were pyrolyzed in a vacuum oven at 1023 K in order to obtain hollow fiber carbon membranes. Their CMR consists of stainless steel in which 20 carbonized hollow fibres (0.295 mm diameter and 128 mm long) and catalyst pellets (0.5 wt.% Pt/ Al_2O_3) were allocated. The reactor, used for cyclohexane dehydrogenation to benzene at 468 K, shows a fair improvement over equilibrium conversions. In details, the temperature dependency of the permeation rates shows that the carbon membrane has micropores with an average diameter close to those of the gas molecules and

therefore the permeation process is molecular-sieving controlled. The ideal H₂/Ar separation factor (i.e. the ratio of permeation rates) shows a value of 53 at 448 K, and decreases with increasing temperature.

Comparing with the traditional reactor, obviously higher cyclohexane to benzene conversion has been observed in the CMR. The conversion of 25-37% at 468K was obtained while keeping the pressure in the permeated side (H₂ side) relatively high. On the other hand, while keeping the pressure in the permeated side relatively low, the conversion as high as 30-70 % was obtained, which was ascribed to the larger amount of H₂ permeated through the carbon membrane. The experimental results were also fitted with a simulated mathematical model, derived on the assumption of ideal flow. This assumption can effectively explain the experimental data within a limited range of the reaction condition. Beyond this range, however, the simulated predications deviated significantly from the experimental results, which probably can be ascribed to the radial concentration polarization of H₂ that reduced the conversion and the possible decrease of the catalyst activity occurred under lower H₂ atmosphere. This preliminary simulated work evidenced that not only a more precise model, but also additional studies on the integration of carbon membrane and catalyst were needed.

The dehydrogenation reaction has also been attempted by Szejner and Sheintuch in 2004 [31]. They constructed a CMR using a molecular-sieve carbon membrane and carried out dehydrogenation reactions. Their CMR was composed of 100 fibers with diameter of 100 μm and thickness of 10 μm, which had a total membrane area of 150 cm². The catalyst pellets were loaded between the tube and the membrane module. In particular, the isobutane dehydrogenation on a chromia alumina catalyst was chosen as a model reaction. Following the simulated results summarized in **Table 2**, the conversions of isobutane in the plug flow reactor (PFR) mode and all the three CMR modes increase gradually with the increasing temperature. At certain temperature, the operation in the counter-current mode showed higher isobutane conversion than the operation in the co-current mode. The conversion values in the vacuum mode are pretty close to those in the counter-current mode.

Table 2. Simulated conversion results at various temperatures and operation modes

| Temp. (K) | PFR (%) | CMR (%) | | |
|-----------|---------|------------|-----------------|--------|
| | | Co-current | Counter-current | Vacuum |
| 723 | 18.6 | 48.7 | 52.1 | 53.9 |
| 773 | 32.4 | 74.1 | 79.9 | 80.8 |
| 623 | 49.6 | 89.7 | 95.1 | 95.1 |

On the other hand, the experimental results for PFR mode and CMR counter-current and vacuum modes are studied at different operation temperatures. The temperature really showed a great effect on the isobutane conversion that almost no reaction occurred at relatively low temperatures. Although the higher temperature showed obvious enhancement of isobutane conversion, the reaction in CMR operation modes were not stable. Furthermore, the effect of feed flux on the isobutane conversion were experimentally studied at 773 K and the results are shown in **Figure 7**.

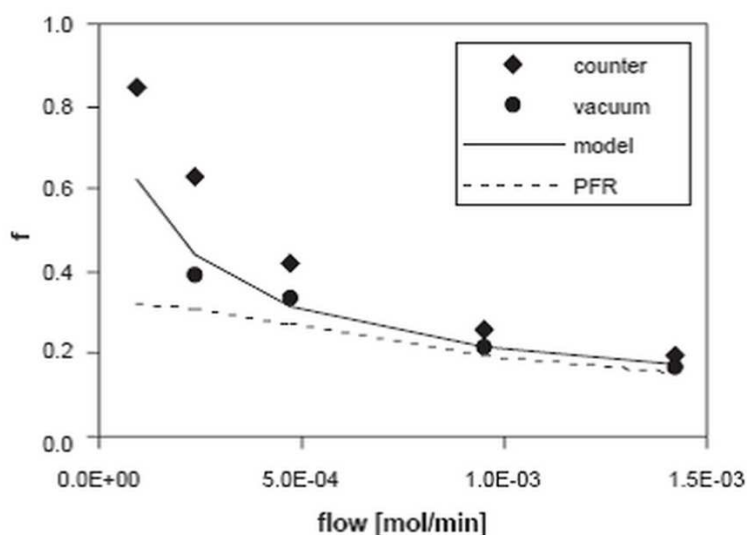


Figure 7 – Results from an experimental study of the effect of feed flux on the isobutane conversion at 773 K ^[31]

For comparison, the simulated results for the CMR counter-current operation mode are also plotted in the same figure. It is evident that all the experimental and simulated conversions decrease gradually with the increasing feed flow, which can be ascribed to the decreasing contact time between the catalyst and the membrane because of the increasing feed flow (space velocity). As expected, the conversion of the PFR (*i.e.* no separation) shows the lowest values for each feed flow studied. The highest isobutane conversion was achieved in the sweep gas counter-current flow mode with a maximum of 85 % at 773 K. In the vacuum mode (no nitrogen transport and dilution effect), the isobutane conversions are lower than those in the sweeping gas mode (but still higher than that of 30% in the PFR) with a maximum of 40 % at 773 K. Nevertheless, in this case, no dilution occurs, so that all the improvement is due only to the H₂ separation. Moreover, the discrepancy between the experimental results and the simulated predictions may result from the experimental factors or the assumed constant transport selectivities in simulation. A much deeper investigation on these aspects is required because, as stressed by the authors, the most important improvement should be in improving and understanding transport selectivity. Following the experimental results, the highly selective and relatively inexpensive molecular-sieve carbon membrane used by the authors can be considered a good candidate to be used in a MR at relatively high temperatures.

Simultaneously, based on the same experimental studies, Sheintuch et al. studied the dehydrogenation of isobutane in CMRs from a modeling point of view [32]. In particular, they considered the separation in a membrane module either by maintaining the shell-side under lower pressure (or under vacuum) or by sweeping it with an inert gas. The main purpose of their work was to derive multi-component transport expressions from thermodynamics of molecular adsorption into and diffusion within the pores of the carbon membranes. Simultaneously, by comparing the simulation results with the experimental ones, the probability analysis of both transport multi-component single-file transport and single-component single-file transport in co- and counter-diffusion modes was applied for the design of CMRs. Furthermore, in order to explain the dramatic change in permeabilities measured in counter-diffusion mode and those measured as single component, the factor of the measured pore size distribution was also included in their simulation work. The analysis was repeated for a family of parallel pores.

Simulated predictions and experiential results showed that good consistence for the the CMR performance obtained for a reaction coupled with separation by sweeping the hydrogen with nitrogen, but large discrepancy for a reaction coupled with vacuum-driven separation. CMR performance in the former mode is better due to excellent transport selectivity, which was attributed to mutual blocking of counter-diffusion by nitrogen and hydrocarbons.

6.2 Hydration reactions

Later, the CMRs were also attempted to carry out homogeneous catalytic reaction e.g. hydration of propene. Lapkin et al. [33] prepared a carbon membrane from a macroporous phenolic resin and constructed a CMR for the hydration reaction. In this gas phase continuous catalytic membrane reactor, the flat carbon membrane was used as a contactor for carrying out reactions at high temperature and pressure. In particular, the hydration of propene, catalysed by an aqueous solution of phosphoric acid, was selected as a suitable model reaction. Olefin and water were fed separately in order to have an additional benefit of an increased alcohol concentration in the product stream due to the absence of steam in the propene feed.

The membrane contactor type of reactor, fabricated from a porous carbon artefact, was used for solving the difficulties associated with the SLP (supported liquid phase) hydration catalyst, without introducing deleterious mass transfer resistances. In fact, the porous contactor is able to provide complete retention of the liquid catalyst, whereas the membrane reactor configuration serves for enabling the retention of catalyst. As it is well known, thermodynamic equilibrium between gas and liquid at the interface is influenced by chemical reaction, diffusion of products from the reaction zone and convective flow on either side of the membrane. In such a contactor-reactor with a porous membrane, an increase in the conversion is expected. In particular, the system was operated in a mass transfer limited regime. Moreover, periodic oscillation of transmembrane pressure reduced mass transfer resistance and improved the overall reactor performance. Another important aspect is related to the possibility to achieve a stable operation of the reactor at high operating pressures by tailoring the porous structure of the carbon membrane and coupling the reactor with an on-line feedback pressure controller.

The flat carbon membranes (diameter 31 mm; thickness 2-4 mm), used for carrying out experiments at 403 K and 2 MPa, were allocated in a stainless steel reactor. The experimental results of both CMR and a conventional SLP reactor were compared using the apparent rate of production (R_p in $\text{kg}_{\text{alcohol}}/\text{m}^3_{\text{membrane pore volume}}\cdot\text{h}$) of propan-2-ol. R_p depends on: the rate of reaction in the liquid phase; the rate of gas-liquid mass-transfer; the mass-transfer within the membrane; and the convective transport in the gas space above the membrane. Therefore, R_p does not directly correspond to the intrinsic rate of reaction. The best experimental measure of R_p was referred to equilibrium, estimated as the percentage of the vapour phase alcohol concentration compared with the equilibrium concentration of alcohol calculated from the reaction model.

In the absence of any mass transfer resistances induced by the porous membrane, the continuous sweep of products in the gaseous phase effects a shift in thermodynamic equilibrium towards formation of alcohol. This was also demonstrated by the authors by introducing a convective mass transfer to the batch reaction model. In fact, a dynamic model of the reactor was also developed and the results of simulations were compared favourably with experiments and the performance of a commercially operated conventional reactor.

Both experimental and simulation results showed that oscillation of transmembrane pressure significantly reduces the liquid phase mass transfer resistance. This aspect is considered to be very important for slow reactions, for which the volume of liquid catalyst is a more important parameter than the gas-liquid interfacial area, as indeed is the case for the hydration of propene.

Feeding reagents separately to the contactor (propene fed as gas and water fed as liquid on the opposite sides of membrane) results in a lower concentration of water in the vapour products, which decreases the cost of downstream product separation.

Among the various advantage of this hybrid configuration (e.g. the rates of alcohol production are satisfactory; the retention of catalyst and separation of product from the reaction mixture are important for industrial-scale operation; the carbon membranes used for the contactor are robust and are unaffected by the presence of a strong acid, such as phosphoric acid catalyst), must be also cited that the membrane preparation and

fabrication techniques can be optimised for reducing the mass transfer resistance in the liquid filled pores and consequently increase the yield of desired product.

For commercial applications, the development of membranes in the form of monoliths or hollow fibre modules with considerably thinner walls than that of flat disk membranes is considered necessary, especially for a better shift in thermodynamic equilibrium.

6.3 Hydrogen production reactions

Zhang et al. [34] carried out the methanol steam reforming reaction, in both a MR and a conventional reactor for hydrogen production. The FBR and CMR consisted of a stainless steel tube and of a tubular carbon membrane, respectively, with the same i.d. of 6 mm. The carbon membrane tube, a pinhole-free carbon composite membrane layer (thickness 20-30 μm), was sealed inside a stainless steel tube (length 30 cm, i.d. 2 cm). In both reactors, 1.05 g of Cu/ZnO/Al₂O₃ catalyst pellets were packed in the reaction zone. Experimental parameters such as temperature, flow rate of carrier gas, and feed ratio were investigated to better understand the separation effect of hydrogen in the CMR on the methanol conversion and the product selectivity. The experimental results confirmed that both the methanol conversion and the H₂ selectivity in the CMR are much better than those in FBR at all the studied experimental conditions. On the other hand, if the overall yields of hydrogen were kept the same in both the reactors, the higher hydrogen purity can be obtained using CMR. The main results are summarized in the following:

- (1) In both the CMR and FBR, the methanol conversion increases gradually with the increase in either the operation temperature or the feed ratio of H₂O/CH₃OH. The methanol conversion in the CMR is always higher than that in the FBR in all the studied temperature range, and the methanol conversion at 523 K in the CMR is as high as 99.9 %.
- (2) An increase in the carrier gas flow rate (only in CMR) increases the methanol conversion up to a plateau.
- (3) With regard to permeation selectivity in the CMR, the hydrogen selectivity is 97 %.

- (4) The CO yield in the CMR is always lower than that in the FBR in the all studied temperature range.

Recently, the research group of Prof. Adelio Mendes (Portugal) [6, 7] studied two types of membranes a CMS and a Pd one for carrying out the methanol steam reforming in a MR. The potential advantages of CMS membranes over the palladium membranes to conduct the methanol steam reforming are related to very high permeabilities and hydrogen recovery; whereas Pd membranes are more expensive but exhibit much higher selectivity towards hydrogen. The authors' main objective was to analyze in which conditions each of the membranes perform better than the other and also how both membranes can be integrated simultaneously in the same reactor in order to get a synergy. For these purposes, a 1-D comprehensive mathematical model of a packed-bed membrane reactor was developed for determining the effect of various parameters, such as the Da number, the reaction temperature and so on, on the methanol conversion, the carbon monoxide concentration in the hydrogen rich stream and the hydrogen recovery. The goal was to maximize the methanol conversion and the hydrogen recovery, while keeping the CO concentration at the permeate side below 10 ppm. The authors emphasized that carbon membrane allows the permeation of water depending on pressures and residence time while Pd membrane does allow this under any conditions. Depending on hydrogen pressure in retentate and membrane permeance, the water depletion can affect the final methanol conversion. In addition, they noticed that different properties of the carbon membranes can affect the hydrogen purity based on the different reaction rates. For example, if the reaction rates of the reactants in the retentate side are slow, the consumption of reactants can be affected by increasing water partial pressure. They did the analysis in the Da number and affirmed that it is possible to have an excess of steam and shift the steam reforming and water gas shift reactions towards to the production of hydrogen and to consumption of carbon monoxide for high hydrogen selectivity. Moreover, it was also established that, depending on Da numbers, the reaction rates could be too high to change the gas mixture composition at the reaction side due to the increasing of methanol conversion. They also mentioned a particular case that the reverse water gas shift reaction, producing carbon monoxide and decreasing hydrogen selectivity were determined by contact time and characteristics of the carbon membranes. The H_2/CO reaction selectivity increases for the Pd-MR,

whereas an opposite effect for the CMS-MR is observed. Hydrogen recovery increases with and Da numbers for both MR, although the effect is almost unnoticeable for the Pd-MR and for low Da numbers. The CMS-MR presents higher hydrogen recovery than the Pd-MR at high hydrogen concentrations, and the Pd-MR proved to be more advantageous for lower hydrogen production rates. Finally, the Pd-MR performance is enhanced by high retentate pressures and low permeate pressures, while the CMS-MR performance is enhanced for intermediate values. Concerning the combination of “CMS+Pd membrane reactor”, it shows some advantages towards the CMS-MR; specifically, higher hydrogen recovery is achieved, keeping the CO concentration at the permeate side below 10ppm. In comparison to the Pd-MR, this membrane combination allows the use of smaller membranes and higher feed flow rates, without prejudice of the membrane reactor performance.

The reaction of methanol steam reforming was studied in a CMR over a commercial CuO/ZnO/Al₂O₃ catalyst by Sá et al [7]. A commercial CMSM was allocated in a CMR, which was operated at atmospheric pressure and with vacuum (15mbar) at the permeate side, at 473 K. High methanol conversion and hydrogen recovery were obtained with low carbon monoxide permeate concentrations. A sweep gas configuration was simulated with a 1-D model. The experimental mixed-gas permeance values at 473 K were used in a mathematical model that showed a good agreement with the experimental data. The advantages of using water as sweep gas were investigated in what concerns methanol conversion and hydrogen recovery. The concentration of carbon monoxide at the permeate side was under 20 ppm in all simulation runs. These results indicate that the permeate stream can be used to feed a polymer electrolyte membrane fuel cell. A good agreement between the mathematical model and the experimental data was observed. It was found that methanol conversion, hydrogen recovery and hydrogen yield are enhanced by lower feed flow rates due to higher residence times, with the drawback of higher production of carbon monoxide. The simulation study showed that using water as sweep gas brings several advantages. In addition to an increase in both methanol conversion and hydrogen recovery, the production of carbon monoxide decreases drastically. The results presented in this study confirm the potential of using methanol steam reforming in a CMR to produce humidified hydrogen directly usable for PEMFC applications.

Briceño et al. [35] prepared a carbon membrane starting from a polyimide material coated and pyrolyzed under N_2 atmosphere on TiO_2 - ZrO_2 macroporous tubes. The supported carbon membrane was used for both to determine its permeation for low molecular weight gases such as H_2 , CH_4 , CO , N_2 and CO_2 and also for carrying out the methanol steam reforming in MR. As for the steam reforming of methanol, both the H_2 yields and the methanol conversions at different operation temperatures were compared respectively for the reactors of both TR and CMR (**Table 3**). The experimental data obtained in this preliminary study on the methanol steam reforming demonstrates the possible use of this type of carbon membrane in MR applications: both the yield and the methanol conversion of CMR are above those of the TR system.

Table 3. H_2 yield and methanol conversion versus temperature in both TR and CMR for steam reforming of methanol

| Temperature (K) | Reactor | H_2 yield (%) | Methanol conversion (%) |
|-----------------|---------|-----------------|-------------------------|
| 473 | TR | 64 | 43 |
| | CMR | 68 | 48 |
| 498 | TR | 70 | 45 |
| | CMR | 71 | 52 |
| 523 | TR | 72 | 49 |
| | CMR | 75 | 55 |

6.4 H_2O_2 synthesis

The research group coordinated by Prof. Gabriele Centi prepared a series of tubular catalytic membranes (TCMs) and tested in the direct synthesis of H_2O_2 [36-38]. Such TCM's are asymmetric α -alumina mesoporous membranes supported on macroporous γ -alumina, either with a subsequent carbon coating or without, which were respectively named as carbon coated alumina membranes (CAMs) and α -Alumina asymmetric membranes (AAMs). For AAM, a dense Pd film was deposited on such supports by electroless plating deposition. After further thermal treatment in inert atmosphere at 773 K, a surface with well developed large and ordered crystallites was obtained. For CAM, Pd catalyst was introduced by deposition-precipitation technique. The carbon

membrane layer of CAM possesses a high surface area and are micro- to meso-pores. Catalytic tests were carried out in a semi-batch re-circulating mode under very mild conditions. Concentrations as high as 250-300 ppm H_2O_2 were commonly achieved with both carbon membrane deposition and without carbon membrane deposition after 6-7 h on stream. However, the H_2O_2 decomposition rate was particularly high in the presence of H_2 . CAM's catalytic activity depended strongly on the Pd particle size, whereas well developed crystallites was necessary to improve catalytic activity of AAM's. These features seem to indicate that a smooth metallic surface was necessary to improve catalytic activity.

The preparation of a novel catalytic membrane system to be used in multiphase H_2O_2 production have also been discussed in details by Tennison et al. in 2007 [39]. In their review, it was shown that it is possible to produce a membrane system that is potentially suitable to be used in both multiphase and gas phase membrane reactor systems based on a 2-layer ceramic substrate. Moreover, the performance is sensitive to the degree of perfection of the support. The carbon membrane deposited within the nanoporous layer of the substrate has the structure and surface area to enable high dispersions of catalyst metals to be achieved when oxidized in carbon dioxide that have shown good performance in the direct synthesis of H_2O_2 . When prepared under nitrogen, despite the simple production route, the carbon membrane shows excellent gas separation characteristics.

6.5 Bio-diesel synthesis

Dubé et al. [40] studied the production of biodiesel in a semi-batch two-phase CMR using an acid- and a base-catalyzed transesterification of canola oil. Tubular carbon membranes (pore size 0.05 μ m, i.d. 6 mm, o.d. 8 mm, length 1200 mm) are used in the reactor for their stability at high temperatures and resistance to chemical attack. The methanol and sulfuric acid catalyst, after pre-mixing, were charged into the membrane module. The authors demonstrated that CMR is able to alleviate many of the difficulties related to the transesterification of triglycerides to FAME (fatty acid methyl esters). The tests were carried out in the CMR in semi-batch mode at 333, 338 and 343K and at different catalyst concentrations and feed flow rates. Increases in temperature, catalyst

concentration and feedstock (methanol/oil) flow rate significantly increased the conversion of oil to biodiesel. The novel reactor enabled the separation of reaction products (FAME/glycerol in methanol) from the original canola oil feed. The two-phase membrane reactor was particularly useful in removing unreacted canola oil from the FAME product yielding high purity biodiesel and shifting the reaction equilibrium to the product side. In this work was found that maintaining a 2-phase (emulsified) system in the MR inhibits the transfer of triglyceride and non-reacting lipids to the product stream. The production of a triglyceride-free FAME leads to the production of high quality FAME. For this motive, the MR allowing a phase barrier which limits the presence of triglyceride and non-reacting lipids in the product, is highly desirable in maintaining quality assurance in the production of biodiesel.

6.6 Development of new carbon membrane for CMRs

More recently, Countinho et al. [4] prepared carbon membranes by pyrolysis of polyetherimide hollow fibers to be used as a catalyst or catalyst support as well as separation medium, raising reaction yield, selectivity and reducing the need for further separation steps. The authors investigated the pyrolysis process parameters as well as stabilization parameters to find an optimum condition for preparing polyetherimide based carbon membranes. The experimental results permitted the production of thermostable carbon hollow fibers and selection of best treatment conditions. In particular, when at the stabilization temperature > 773 K, an intensive degradation of the fiber was observed. An initial exposure to an oxidizing atmosphere seems to be fundamental in order to control the final membrane properties. In this atmosphere, heating rates as low as $1 \text{ K}\cdot\text{min}^{-1}$ during stabilization reduce cracks in the surface of final membranes.

An excellent review concerning the fabrication of carbon membranes for gas separation as well as for membrane reactors was published by Saufi and Ismail [5]. Among the various aspects, some important key-points are resumed in the following:

- (1) The production of carbon membranes currently involves a very high cost (between one and three orders of magnitude greater than that of a typical

polymeric membrane). Therefore, carbon membranes must achieve a superior performance in order to compensate for their higher cost.

- (2) Optimization of fabrication parameters during the pyrolysis process is arguably the best way to achieve this goal and because of the large number of parameters involved, computer simulation will help in optimizing the pyrolysis process.
- (3) Once, a carbon membrane of high performance is produced, at first it is important to determine the effect of exposure to water vapor because it becomes quite important when the carbon membrane is commercialized.
- (4) Moreover, the humidity found in the ambient atmosphere can also have an adverse effect on carbon membrane performance. Therefore, the study of storage conditions for carbon membranes is also another important aspect to be considered.

7. Micro carbon-based membrane reactors

As mentioned in the previous sections, the porous carbon membrane materials can be supported on different substrates to form a supported carbon membrane, which can be used for gas separation or construction of membrane reactors for the improvement of reaction performance. The pyrolysis of the polymer precursor membrane with specific characteristics of graphitization and tunable pore size distributions for the fabrication of the carbon membranes can also be used in other important applications such as the carbon-based microporous devices. De Jong et al. [41] posed the need to find alternative materials for the fabrication of the porous microfluidic devices, which should provide the rapid screening of toxic or dangerous reactions in microscale. Moreover, the micro devices can save high-valued reactants because of the high compactness of the device. Therefore, in following parts of this section, we are going to give a simple overview on the carbon-based micro membrane reactors, a kind of micro devices.

The micro devices with microchannels consisting of ceramic, polymer, and silicon etc. have been extensively fabricated to provide spaces (the walls of microchannels) for the contact of the reactant and product. However, for further intensifying the reactor, the integration of separation function through the channel walls are believed to be very attractive. Therefore, we think that, by controlling the same experimental variables for the fabrication of the supported carbon membranes, it is also possible to design

microporous layers as the walls of the microchannels in micro devices for some specific applications. De Jong et al. also pointed the application of porous materials in membrane-based-gas-liquid contacting and porous channel emulsification for production of mono-dispersed droplets. In fact, Splinter et al. [42] have explored the fabrication of a porous silicon membrane doped with palladium for conversion of CO to CO₂ at 140 °C as component in gas sensor devices as shown in **Figure 8**, which is very good example of the integration of the porous membrane into the microreactors.

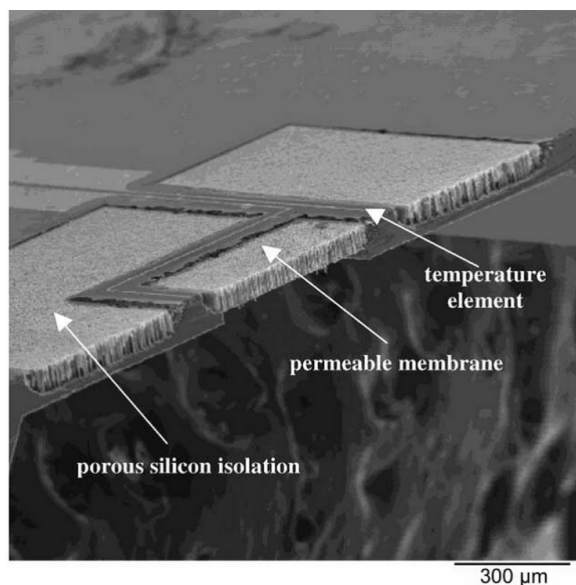


Figure 8 - SEM cross-section of porous membrane reactor [42]

In the case of carbon-based micro membrane reactors, the fabrication of the glassy carbon films has been reported by Schueller et al. [43] through molding a furfuryl alcohol modified resin. They put polymer precursor of polydimethylsiloxane (PDMS) in contact with a substrate with defined cavities or microchannels. Two techniques of MIMIC (micro molding in capillaries) and μ TM (micro transfer molding) have been used for this fabrication. After a drop of polymer was added to one these structures, the fluid filled the channels. In both techniques, the polymer was cured with temperature and PDMS peeled off from the substrates leaving the tridimensional feature. After further treatments, the resin was converted to glassy carbon while keeping the shape. Moreover, these authors also reported that the use of the reactive ion etching technique to generate patterns on a glassy carbon surface. **Figures 9** and **10** show a schematic view of the process and some details of the microstructure. These methods allow the

fabrication of microstructures of large area and high aspect ratio in short periods of time.

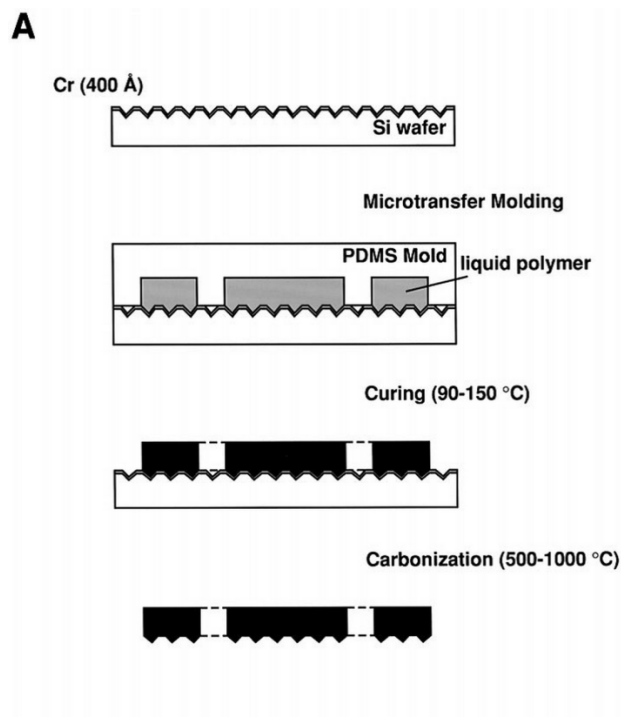


Figure 9 - Schematic describing the preparation of a glassy carbon microstructure using a PDMS mold ^[43]

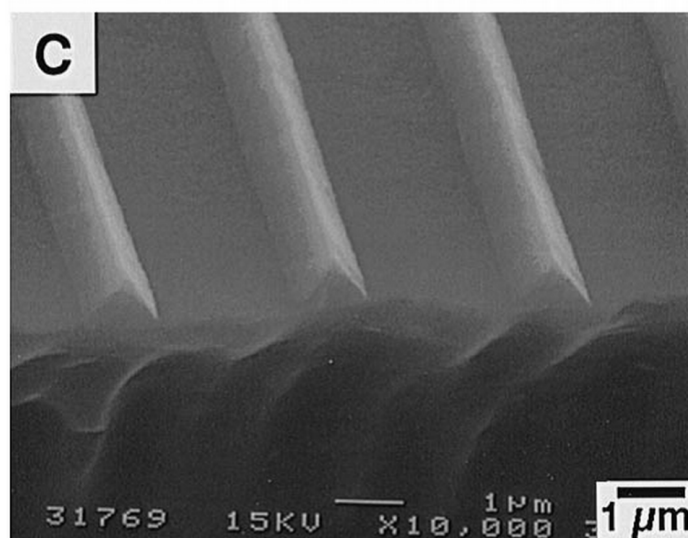


Figure 10 - Close up of glassy carbon surface ^[43]

Fabrication of carbonaceous microstructures has been reported also by Malladi et al. [44] by spin-coating a SU-8 photoresist material on a Si wafer. The photoresist material is coated on a Si wafer under the UV mask that transfer the pattern, which undergoes pyrolysis at 900°C in N₂ atmosphere. This process allows the fabrication of suspended carbon microelectromechanical systems (C-MEMS), which are highly appreciated on sensor applications.

To the best knowledge of these authors, there is not any micro device integrating carbon glassy carbon membranes. The nearest idea in membrane fabrication is the fabrication of a composite material proposed in the past by Carretero et al. [45]. They fabricated a microporous glassy carbon membrane infiltrated inside a mesoporous Al₂O₃ support. After dip-coating of a phenolic resin on the inner face of Al₂O₃ tubes, the composite membrane was cured in air at 170 °C, and later at 700 °C under N₂ atmosphere to obtain the microporous structure. XRD pattern evidenced formation of graphite and graphite layer stacked in a disorder structure in unsupported samples of the pyrolyzed resin. The obtained membrane showed a decrease of permeability with molecular size of gases tested (H₂, CO₂, O₂, N₂) with values of $5 \cdot 10^{-7}$ - $10 \cdot 10^{-7}$ mol/m²·s·Pa

8. Conclusions and future trends

Although the carbon membranes are still in their infant stage and have some serious challenges such as weak mechanical strength for unsupported membranes and bad controllability and reproducibility of the fabrication for supported membranes, they are believed to be promising candidates for porous membrane based membrane reactors because the easiness for fabrication, low price for both fabrication and raw materials, molecular sieve separation effect, and high permeance.

A turbostratic carbonaceous structure allows obtaining carbon membranes suitable for gas separation and membrane reactor. The pore size distribution and porosity of this kind of carbon membrane materials can be easily tailored by controlling the fabrication variables. There is an extended work developed on non-supported carbon membrane such as planar and asymmetric hollow fiber configurations. However, in order to consider the practical industrial applications they have to face the mechanical stability problem. In this sense, the fabrication of carbon thin films can be developed over substrates that bring them higher mechanical stability. However, the goal to achieve

supported carbon membranes has to face the problem of crack-formation. During the pyrolysis, the resulted carbon membrane from its polymer precursor has to achieve the turbostratic structure without cracks or defects. For example, for membrane fabrication the selection of the carbon membrane material has to consider the graphitization behaviour. Pyrolysis conditions as temperature and heating rate will determine the pore structure. It is also very important to consider the type of substrate because defects from the substrate's surface can be transmitted to the supported polymer and later carbon membrane. On minimization of defects, the modification of the support and several coating steps are strategies to follow.

The most important application for carbon membrane is to construct a carbon-based membrane reactor to carry out some special chemical reactions. The dehydrogenation reactions, hydration reactions, and hydrogen production reactions were commonly carried out in CMRs. The concept of separation of hydrogen, one of the products, in dehydrogenation and hydrogen production reactions, really shifted the reaction equilibrium to the product side by increasing the conversions. However, the certainly the hydrogen selectivity and membrane stability needs further improvement to meet the reactions' demand. Moreover, the simulated work was also tried and more rigorous new model needs to developed to described these membrane reactions process. The flat carbon membrane was also used as a contactor for carrying out hydration of propene. The carbon membrane contactor has the following advantages. The rates of alcohol production are satisfactory; the retention of catalyst and separation of product from the reaction mixture are important for industrial-scale operation; the carbon membranes used for the contactor are robust and are unaffected by the presence of a strong acid, such as phosphoric acid catalyst. For commercial applications, the development of carbon membranes in the form of monoliths or hollow fibre modules with considerably thinner walls than that of flat disk membranes is considered necessary, especially for a better shift in thermodynamic equilibrium. Furthermore, the reactions of H_2O_2 and bio-diesel synthesis were also tried in the CMRs and exciting preliminary results have been obtained. Certainly more work needs to be done this research area. Simultaneously, the research about how to improve the fabrication of carbon membranes and make them suitable for application in CMRs were also tried and summarized.

Finally, the flexibility supported carbon membranes can present for membrane reactors in a high scale can be transfer to a micro scale. For this reason, as similar to silica materials, it is possible to achieve carbonaceous microstructures applying traditional microfabrication techniques reported using other materials. It is possible to achieve integration of carbonaceous microporous structures in small chips for micro reactions. Using PDMS moulding allows casting polymeric materials towards defined structures using mask that allow features with dimensions over 20 μ m.

9. Acknowledgements

The Authors wish to thank Prof. Naotsugu ITOH (Utsunomiya University, Japan) for his help in reviewing the draft of the chapter.

10. References

- [1] J. Zaman, A. Chakma, Inorganic membrane reactor, *J. Membrane. Sci.*, **1994**, 92, 1-28.
- [2] K. Haraya, H. Suda, H. Yanagishita, S. Matsuda, Asymmetric capillary membrane of a carbon molecular sieve, *J. Chem. Soc., Chem. Commun.*, **1995**, 1781-1782.
- [3] H.C. Foley, Carbogenic molecular sieves: synthesis, properties and applications, *Microporous Materials*, **1995**, 4, 407-433.
- [4] M.B. Coutinho, V.M.M. Salim, C.P. Borgees, Preparation of carbon hollow fiber membranes by pyrolysis of polyetherimide, *Carbon*, **2003**, 41, 1707-1714.
- [5] S.M. Saufi, A.F. Ismail, Fabrication of carbon membranes for gas separation—a review, *Carbon*, **2004**, 42, 241-259.
- [6] S. Sá, H. Silva, J. M. Sousa, A. Mendes, Hydrogen production by methanol steam reforming in a membrane reactor: Palladium vs carbon molecular sieve membranes, *J. Membrane Sci.*, **2009**, 339, 160-170.
- [7] S. Sá, J. M. Sousa, A. Mendes, Steam reforming of methanol over a CuO/ZnO/Al₂O₃ catalyst part II: a carbon membrane reactor, *Chem. Eng. Sci.*, **2011**, 66, 5523-5530.
- [8] N. Itoh, K. Haraya, A carbon membrane reactor, *Catalysis Today*, 2000, **56**, 103-111.
- [9] http://en.wikipedia.org/wiki/File:Eight_Allotropes_of_Carbon.png
- [10] José Miguel Martín Martínez, Adsorción física de gases y vapores por carbonos, Universidad de Alicante, ISBN: 84-86809-33-9.
- [11] J.E. Koresh, A. Sofer, *Separ. Sci. and Technol.*, **1983**, 18, 723-734.

- [12] A. Singh-Ghosal, W.J. Koros, Air separation properties of flat sheet homogeneous pyrolytic carbon membranes, *J. Membrane Sci.*, **2000**, 174, 177-188.
- [13] A.B. Fuertes, Adsorption-selective carbon membrane for gas separation, *J. Membrane Sci.*, 2000, 177, 9-16.
- [14] H. Suda, K. Haraya, Molecular Sieving Effect of Carbonized Kapton Polyimide Membrane, *J. Chem. Soc. Chem. Commun.*, 1995, 1179-1180
- [15] H. Suda, K. Haraya, Gas permeation through micropores of carbon molecular sieve membranes derived from Kapton polyimide, *J. Phys. Chem. B*, **1997**, 101, 3988-3994.
- [16] M.S. Strano, A.L. Zydney, H. Barth, G. Wooler, H. Agarwal, H.C. Foley, Ultrafiltration membrane synthesis by nanoscale templating of porous carbon, *J. Membrane Sci.*, **2002**, 198, 173-186.
- [17] T. Tsuru, T. Morita, H. Shintani, T. Yoshioka, M. Asaeda, Membrane reactor performance of steam reforming of methane using hydrogen-permselective catalytic SiO₂ membranes, *J. Membrane Sci.*, **2008**, 316, 53-62
- [18] M.B. Shiflett, H.C. Foley, Ultrasonic deposition of high-selectivity nanoporous carbon membranes, *Science*, **1999**, 285, 1902-1905.
- [19] L. Shao, T.S. Chung, G. Wensley, S.H. Goh, K.P. Pramoda, Casting solvent effects on morphologies, gas transport properties of a novel 6FDA/PMDA-TMMDA copolyimide membrane and its derived carbon membranes, *J. Membrane Sci.*, **2004**, 244, 77-87.
- [20] K.M. Steel, W.J. Koros, Investigation of porosity of carbon materials and related effects on gas separation properties, *Carbon*, **2003**, 41, 253-266.
- [21] W. Wei, G. Qin, H. Hu, L. You, G. Chen, Preparation of supported carbon molecular sieve membrane from novolac phenol-formaldehyde resin, *J. Membrane Sci.*, **2007**, 303, 80-85.
- [22] T.A. Centeno, J.L. Vilas, A.B. Fuertes, Effects of phenolic resin pyrolysis conditions on carbon membrane performance for gas separation, *J. Membrane Sci.*, **2004**, 228, 45-54.
- [23] K. Kusakabe, M. Yamamoto, S. Morooka, Gas permeation and micropore structure of carbon molecular sieving membranes modified by oxidation, *J. Membrane Sci.*, **1998**, 149, 59-67.
- [24] J. Hayashi, H. Mizuta, M. Yamamoto, K. Kusakabe, Sh. Morooka, Pore size control of carbonized BPDA-pp' ODA polyimide membrane by chemical vapor deposition of carbon, *J. Membrane Sci.*, **1997**, 124, 243-251.
- [25] A.B. Fuertes, T.A. Centeno, Carbon molecular sieve membranes from polyetherimide, *Micropor. Mesopor Mat.*, **1998**, 26, 23-26.
- [26] A.B. Fuertes, T.A. Centeno, Preparation of supported carbon molecular sieves membranes, *Carbon*, **1999**, 37, 679-684.

- [27] M.B. Shiflett, H.C. Foley, Reproducible production of nanoporous carbon membranes, *Carbon*, **2001**, 39, 1421-1446.
- [28] B. S. Liu, N. Wang, F. He, and J. X. Chu, Separation performance of nanoporous carbon membranes fabricated by catalytic decomposition of CH₄ using Ni/polyamideimide templates, *Ind. Eng. Chem. Res.*, **2008**, 47, 1896-1902.
- [29] A. Merritt, R. Rajagopalan, H.C. Foley, High performance nanoporous carbon membranes for air separation, *Carbon*, **2007**, 45, 1267-1278.
- [30] H. Wang, L. Zhang, G. R. Gavalas, Preparation of supported carbon membranes from furfuryl alcohol by vapor deposition polymerization, *Journal of Membrane Science* 177 (2000) 25–31
- [31] G. Szejner, M. Sheintuch, Application of a carbon membrane reactor for dehydrogenation reactions, *Chem. Eng. Sci.*, **2004**, 59, 2013-2021.
- [32] M. Sheintuch, I. Efremenko, Analysis of a carbon membrane reactor: from atomistic simulations of single-file diffusion to reactor design, *Chem. Eng. Sci.*, **2004**, 59, 4739-4746.
- [33] A. A. Lapkin, S. R. Tennison, W. J. Thomas, A porous carbon membrane reactor for the homogeneous catalytic hydration of propene, *Chem. Eng. Sci.*, **2002**, 57, 2357-2369.
- [34] X. Zhang, H. Hu, Y. Zhu, S. Zhu, Methanol steam reforming to hydrogen in a carbon membrane reactor system, *Ind. Eng. Chem. Res.*, **2006**, 45, 7997-8001.
- [35] K. Briceño, A. Iulianelli, D. Montané, R. Garcia-Valls, A. Basile, Carbon molecular sieve membranes supported on non-modified ceramic tubes for hydrogen separation in membrane reactors, *Int.J.Hydrogen Energy.*, **2012**, Accepted
- [36] S. Abate, G. Centi, S. Melada, S. Perathoner, F. Pinna, G. Strukul, Preparation, performances and reaction mechanism for the synthesis of H₂O₂ from H₂ and O₂ based on palladium membranes, *Catal. Tod.*, **2005**, 104(2-4), 323-328.
- [37] S. Melada, F. Pinna, G. Strukul, S. Perathoner, G. Centi, Direct synthesis of H₂O₂ on monometallic and bimetallic catalytic membranes using methanol as reaction medium, *J. Catal.*, **2006**, 237, 213- 219.
- [38] S. Melata, F. Pinna, G. Strukul, S. Perathoner, G. Centi, Palladium-modified catalytic membranes for the direct synthesis of H₂O₂: preparation and performance in aqueous solution, *J. Catal.*, **2005**, 235, 241-248.
- [39] S. R. Tennison, K. Arnott, H. Richter, Carbon ceramic composite membranes for catalytic membrane reactor applications, *Kinetics & Catalysis*, 2007, 48(6) 864-876.
- [40] M.A. Dubé, A.Y. Tremblay, J. Liu, Biodiesel production using a membrane reactor, *Bioresource Technol.*, **2007**, 98, 639-647.
- [41] J. de Jong, B. Ankone, R. G. H. Lammertink, M. Wessling, New replication technique for the fabrication of thin polymeric microfluidic devices with tunable porosity, *Lab. Chip*, **2005**, 5, 1240-1247.

- [42] A. Splinter, J. Stürman, O. Bartels, W. Benecke, Micro membrane reactor: a flow a through-membrane for gas pre-combustion, *Sensor Actuat. B-Chem.*, 2002, 83, 169-174
- [43] O.J.A. Schueller, S.T. Brittain, G.M. Whitesides, Fabrication of glassy carbon microstructures by soft lithography, *Sensor Actuat. B-Phys.*, 1999, 72, 125-139.
- [44] K. Malladi, C. Wang, M. Madou, Fabrication of suspended carbon microstructures by e-beam writer and pyrolysis, *Carbon*, 2006, 44, 2602-2607.
- [45] J. Carretero, J.M. Benito, A. Guerrero-Ruiz, I. Rodriguez-Ramos, M.A. Rodriguez, Infiltrated glassy carbon membranes in γ -Al₂O₃ supports, *J. Membrane Sci.*, 2006, 281, 500-507.

CHAPTER 4:

Fabrication Variables Affecting the Structure and Properties of Supported Carbon Molecular Sieve Membranes for Hydrogen Separation

(Art. 3)

Available on line: Journal of Membrane Science 2012.

DOI: 10.1016/j.memsci.2012.05.015

Fabrication Variables Affecting the Structure and Properties of Supported Carbon Molecular Sieve Membranes for Hydrogen Separation

Kelly Briceño^{a}, Daniel Montané^b, Ricard Garcia-Valls^a, Adolfo Iuianelli^c, Angelo Basile^c*

^aDepartment d'Enginyeria Química, Universitat Rovira i Virgili, Av. Països Catalans, 26, 43007, Tarragona, Spain

^bCatalonia Institute for Energy Research (IREC). Bioenergy and Biofuels Area. C/ Marcel·lí Domingo 2, Building N5, Universitat Rovira i Virgili. 43007, Tarragona, Spain

^cITM-CNR via P. Bucci c/o University of Calabria - Cubo 17/C, Rende (CS) - 87036 – Italy,

**Corresponding author e-mail: kelly.briceno@urv.cat*

Tel: + 34 977 558506

KEYWORD: Carbon supported membranes, gas separation, hydrogen separation, Matrimid membranes, polyimide membranes, fabrication variables, ceramic tubular support, materials for membrane reactors.

Abstract

A high molecular weight polyimide (Matrimid) was used as a precursor for fabricating supported carbon molecular sieve membranes without crack formation at 550-700 °C pyrolysis temperature. A one-step polymer (polyimide) coating method as precursor of carbon layer was used without needing a prior modification of a TiO₂ macroporous support. The following fabrication variables were optimized and studied to determine their effect on the carbon structure: polymeric solution concentration, solvent extraction, heating rate and pyrolysis temperature. Two techniques (Thermogravimetric analysis and Raman spectroscopy) were used to determine these effects on final carbon structure. Likewise, the effect of the support was also reported as an additional and important variable in the design of supported carbon membranes. Atomic force microscopy and

differential scanning calorimetry quantified the degree of influence. Pure gas permeation tests were performed using CH₄, CO, CO₂ and H₂. The presence of a molecular sieving mechanism was confirmed after defects were plugged with PDMS solution at 12 wt%. Gas selectivities higher than Knudsen theoretical values were reached with membranes obtained over 650 °C, showing as best values 4.46, 4.70 and 10.62 for H₂/N₂, H₂/CO and H₂/CH₄ ratio, respectively. Permeance values were over $9.82 \cdot 10^{-9}$ mol/m²·Pa·s during pure hydrogen permeation tests.

1. Introduction

The separation of gas mixtures represents a huge field in membrane technology. Natural gas processing, syngas production and conversion, CO₂ separation and hydrogen purification are just a few of the industrial applications in which membranes are playing a growing role. In particular, the field of hydrogen purification requires membranes with high selectivity for separating hydrogen from other gas molecules. Different materials have been used for membranes manufacture in hydrogen separation area and particular attention has been paid for silica- and palladium-based membranes^[1]. Silica membranes require many fabrication steps and careful control of dust conditions in clean room facilities, while palladium membranes are too expensive for large-scale applications. However, molecular sieve zeolite membranes have been also developed as an alternative for separating hydrogen from gas mixtures, but they are complex to fabricate and this limits their applicability. Carbon-based membranes are an interesting option for gas separation. The turbostratic structure of carbon molecular sieve membranes has been reported to provide good separation selectivity for permanent gases and among them, membranes obtained by the controlled pyrolysis of polyimides are the most promising^[2,3]. Fully imidized polyimides with high glass transition temperatures (*T_g*), such as Matrimid and Kapton, are suitable polymer precursors because their structure gradually changes during carbonization; this is a key characteristic for obtaining defect-free Carbon Molecular Sieve Membranes (CMSM)^[4-6].

Carbon membranes can be tailored to accommodate the characteristics of the mixture to be processed. Mixtures of large hydrocarbons are better dealt with using adsorption-selective carbon membranes having pore structures in the range of 5-7 Å^[7], whereas small gases such as H₂, N₂, CO₂, and CH₄ require membranes with molecular sieving

mechanisms, which means that the pore size of the membrane has to be below 4 Å. Different studies have shown how it is possible to tailor the pore size of the carbon membranes by manipulating the pyrolysis conditions ^[7], in particular the temperature and pyrolysis rate. Other studies have addressed the influence of the polymeric precursor's preparation conditions and thermal history on the distribution of pore sizes in the carbon material ^[8]. Most of these studies investigated non-supported flat membranes or hollow fibers, but different studies focused on supported membranes in which the influence of the supporting material plays a significant role and may lead to the formation of defects and cracks in the selective carbon-based layer ^[6].

Fabrication of supported membranes is important for applications needing the combination of a highly hydrogen selective and permeable material with enhanced mechanical stability. Supported membranes offer more flexibility because both these requirements can be developed using different and optimized materials and/or technologies for the structural support and the selective layer ^[9]. This is the case, for instance, of catalytic membrane reactors ^[10], where highly selective supported membranes in tubular configuration are used to achieve optimal integration of the membrane and the catalyst ^[11].

Several methods have been considered for the fabrication of supported tubular carbon membranes, which are a type of asymmetric membranes ^[12-15]. These methods require multiple coating steps or carbonization cycles that increase the fabrication cost. Different strategies have been used to modify the support before applying the polymer precursor in order to achieve a defect-free membrane. Ceramic supports such as Al₂O₃ have been modified with boehmite ^[12]; stainless-steel supports have been modified with nanofillers ^[16]. However, despite these strategies, particles may still be included and causing defects. This means that, in practice, both repeated coatings and clean room facilities are needed, as in the case of silica membranes ^[17].

The technique of directly depositing a film of polymer to be used as a carbon precursor on the porous support is fraught with the same problems regarding most of other methods for fabricating composite membranes in which polymer concentration is essential for achieving defect-free membranes ^[18]. Determining how the fabrication variables affect the final structure of the membrane is important for pore tailoring,

especially when the membranes are intended for separating gases with similar kinetic diameters.

The characterization of the obtained carbon material is also a key issue because it is not always straightforward to analyze real samples of supported carbon membranes. Some studies [6, 15] have investigated the relationships between the structure and the properties of supported carbon membranes in a configuration like to non-supported samples undergoing the same thermal treatment but without the support stage. However, the potential modifications made on the porous structure by the support, although presumably minimal, may be important if the membranes are used for separating gases whose kinetic diameters differ by only one tenth of a nanometer.

The purpose of this paper is to describe a method for fabricating ceramic-supported CMSM for hydrogen separation/purification. Imidized Matrimid is deposited as the carbon precursor in a one-step coating method in a normal laboratory environment (*i.e.* without white-room facilities) and using unmodified inorganic supports. The influence of the main fabrication parameters on the structure of the supported carbon layer is investigated and discussed. The results support the potentiality of this simple and relatively fast procedure, which offers new ways of designing and directly characterizing supported carbon membranes for the separation of hydrogen mixtures.

2. Materials and Methods

2.1 Polymer Characterization

Different polymer solutions were prepared as carbon precursors. Matrimid (3, 3', 4, 4'-benzophenonetetracarboxylic dianhydride and diamino-phenylindane) from Huntsman Advanced Materials was used as the polyimide and 1-methyl-2-pyrrolidone (NMP) 99.5% from Sigma-Aldrich was used as the solvent. Solutions of 2-20 wt% Matrimid/NMP were obtained. The viscosities of the polymer solutions were measured in a Hakke viscosimeter.

The molecular weight of the polymer was determined by Gel Permeation Chromatography using a PL MIXED-C column (Polymer Labs, UK). Tetrahydrofuran (THF) at a flow rate of 1.0 mL/min was used as a solvent. The analyses were performed at room temperature in a Series 1200 Agilent HPLC chromatograph, in a multi-angle-

light scattering detector from DAWN EOS Wyatt Tech, USA (wave length 658 nm) and in a RI detector ETA-2020 from Bures (DE, wave length 620 nm). The samples were analyzed at a concentration of 1 mg/mL.

2.2 Fabrication of the carbon membrane precursor: polymer films

Tubular ceramic membranes with a nominal cut-off of 1 kD (TAMI) were used as supports for the fabrication of the CMSM. The segments have length of 4 cm (o.d. 10 mm, i.d. 5.6 mm) were made by TiO₂ (4.5-5.5 μm) with a coating of ZrO₂ (2-3 nm) on the inner surface. The porosity of the ceramic material was 20-28% according to the supplier's specifications. The supports were ultrasonicated in methanol (99.8% from Fluka) and distilled water at 50:50 concentration in order to eliminate impurities from storage. To carry out the spinning coating process, the supports were mounted on a homemade coating device, rotated from 500 to 700 rpm. Approximately 3 g of polymer solution were loaded into a glass pipette and applied to the outer face of the ceramic element under rotation. Once the polymer layer was gelified, the rotation was stopped and the supports were placed in a vertical position for 24 h to allow a slow evaporation of the solvent. Different concentrations of polymeric solution were applied using an FEI Quanta 600 Environmental Scanning Electronic Microscope (ESEM) in order to study how these concentrations affected the thickness of the polymeric film.

To determine the physical properties of the polymer without the support influence, around 2 g of 13 wt% polymer solution were loaded into a watch glass to prepare non-supported polymer samples. Supported and non-supported films were placed in an air oven at 110 °C for 24 hrs. The remaining solvent was extracted by washing in methanol for 48 h at room temperature. Methanol traces were finally eliminated after 3 h at 110 °C.

Thermogravimetric analysis (TGA) was performed to determine the effect of the methanol immersion on the carbon structure of the non-supported polymer samples. TGA was performed under a constant flux of N₂ at a heating rate of 10 °C/min up to a final temperature of 900 °C. The influence of methanol and the aging temperature in the range of 300-350 °C on the structure of the carbon membranes was also monitored. Owing to the low crystallinity of the produced amorphous carbon materials, it was necessary to characterize the carbon structure using Raman analysis in order to

determine the I_d and I_g peaks and, thus, finding the relationships between amorphous and graphite regions. Raman spectroscopy was performed using the 785 nm line of the diode laser of an INVIA microscope. The spectra were recorded in the range of 300-2000 cm^{-1} . The ratio of intensities within I_d (1350 cm^{-1}) and I_g (1580 cm^{-1}) signals was determined and related to the disordered and graphite regions of the carbon material. The I_d/I_g ratio was thought to be the reason for the changes in structure towards amorphous and graphite regions.

2.3 Fabrication of the supported carbon membranes

Once the polymer concentration has been optimized, the pyrolysis-supported polymer films were placed in an oven under N_2 atmosphere (500 mL/min) at 2.5 $^\circ\text{C}/\text{min}$ to determine the critical temperature for crack formation. The effect of methanol washing on the reduction of cracks formation was also studied. However, reproducibility was too low at the 2.5 $^\circ\text{C}/\text{min}$ heating rate. Therefore, it was necessary to optimize this variable by using lower heating rates. Once the heating rate was optimized, the effect of the final pyrolysis temperature was studied. Supported carbon membranes were obtained at 550, 650 and 700 $^\circ\text{C}$. To eliminate the existence of possible pinholes, the supported carbon membranes were dip-coated in PDMS solutions (Sylgard 184 silicone from Dow Corning) at 12 % w/w in n-hexane (99% from J.T Baker) at room temperature. After 20 h immersion, the membranes were placed at 60 $^\circ\text{C}$ in air for 30 min to encourage PDMS crosslinking and blocking of the pinholes. An FEI Quanta 600 Environmental Scanning Electron Microscope (ESEM) was used in backscattering mode to characterize the membrane morphology.

2.4 Characterization of supported and non-supported carbon membranes.

Supported and non-supported samples were characterized for analyzing the influence of the porous support on the structure of the carbon membrane. Polymer films were evaluated to determine the differences in their physical properties. Differential scanning calorimetry tests were carried out by using a Mettler-Toledo DSC821 with a heating rate of 10 $^\circ\text{C}/\text{min}$ to evaluate T_g of the supported and non-supported polymer films. In most of cases, no transitions were observed during the first heating run; then, the glass-transition temperatures were measured after a second run at 10 $^\circ\text{C}/\text{min}$.

A multimode atomic force microscope (AFM) with a nanoscope V controller (Bruker ASX, USA) was used to obtain images of the supported and non-supported samples. The images were recorded in tapping mode, at 1 Hz in air at room temperature. Silicon nitride cantilevers (NP-S, Bruker) with a nominal spring constant of 0.12 Nm^{-1} and a resonant frequency of 23 kHz were used. The AFM images were processed using the WSxM program ^[19]. The gold-coated back sides were cleaned in ethanol and acetone before use.

2.5 Gas permeation tests

The supported membranes were placed in a stainless steel module with Viton o-rings to carry out the gas permeation experiments. The polymer supported and carbon supported membranes were housed in a tubular shaped module (4 cm as a length, i.d. 1.10 cm and 3 cm o.d.). A pure gas was supplied in the annulus of the membrane module at room temperature. The composition of the gaseous mixtures coming out from the membrane module was measured by a mass spectrometer (see Fig. 1).

Mass flow controllers were used and supplied by Bronkhorst (0-100 NmL/min). Pure Ar, H₂, CH₄, CO₂ and CO were supplied by the Air Liquid company and used to feed the membrane module from port 2 (see Fig. 1), while the retentate was directed to port 3 and, then, into the atmosphere. A back pressure regulator at the retentate side was used to control the transmembrane pressure, keeping constant the permeate pressure between 1.0-3.0 bar. A pressure test was performed for each specimen to reject those that had large defects. Ar was used as a sweep gas to fix the calibration curves of each single gas permeance before the permeation tests. Thus, each gas composition in the permeate stream was determined according to the previously established calibration curves. Permeance was measured at room temperature and 1.0 bar of transmembrane pressure difference and it was calculated as the ratio between pure gas permeating flux and the transmembrane pressure difference. The error of measurement was in the order of 0.2 %. Ideal selectivity was calculated as the ratio between the permeances of the pure gases.

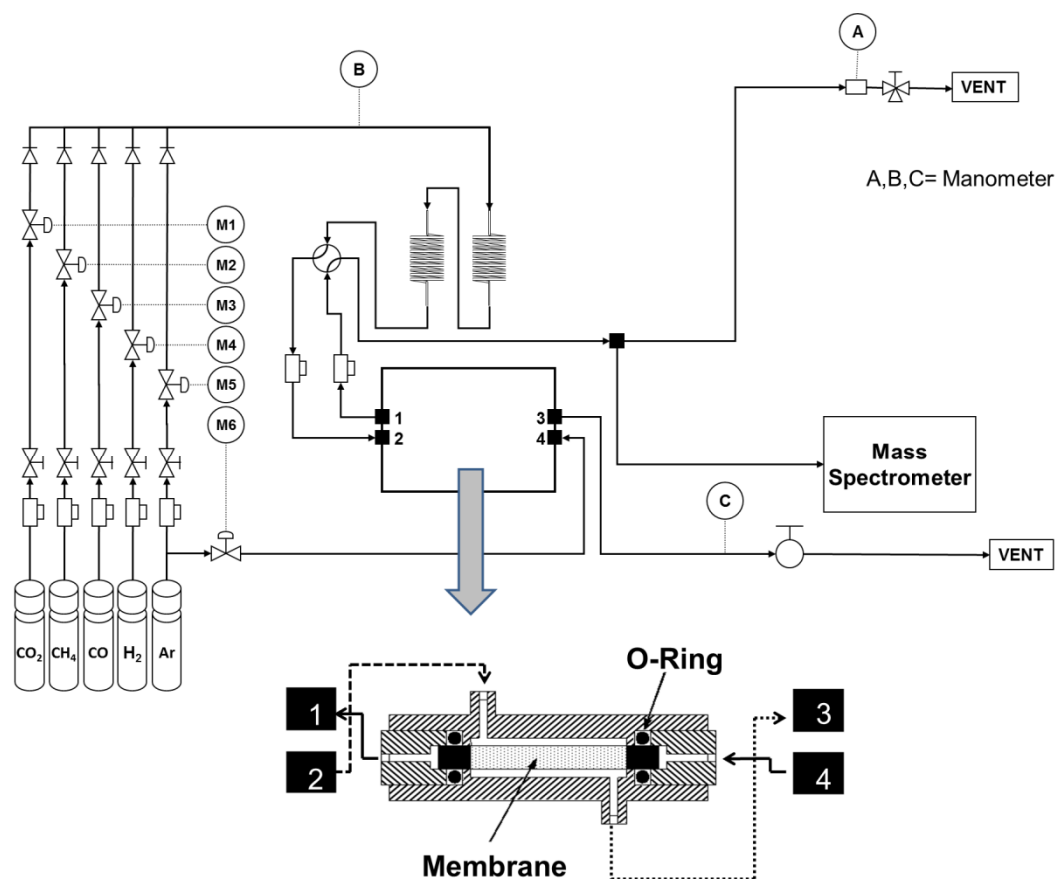


Fig. 1 Experimental setup for gas permeation experiments

2.6 Carbon structure characterization

Having in mind to observe the influence of the pyrolysis temperature on pore structure, carbon membranes were scratched from the support and analyzed by Wide angle X-Ray Diffraction (WXRd), using a Bruker-AXS D8-Discover diffractometer. The X-ray diffractometer was operated at 40 kV and 40 mA to generate $\text{Cu}_{k\alpha}$ radiation. Interplanar d distance was determined with the help of software integrated into the equipment. In addition, adsorption-desorption analysis was also used to record changes in the carbon material. Isotherms were determined at different temperatures CO_2 (273 K), CH_4 (273 K), H_2 (77 K) using a home-made instrument. Before starting, the run samples were simultaneously heated and outgassed at 250 °C for 4 hours.

3. Results and Discussion

3.1 Characterization of the Matrimid solutions

Gel permeation chromatography (GPC) analysis carried out with a light scattering detector determined a weight-average molecular weight (M_w) of 97800 g/mol and a polydispersity (M_w/M_n) of 1.64. Both values indicate a high molecular weight polymer and the presence of a fraction of a low molecular weight material in the commercial polyimide. In the specialized literature, it has been reported that materials with a M_w below 20000 g/mol are not useful for forming defect-free membranes ^[18]. The high molecular weight of this polymer makes it suitable for forming defect-free membranes after just one spin coating. The molecular weight of the polymer and its interaction with the solvent determine the hydrodynamic volume of the solvated polymer molecules. When polymer molecules have small solvated diameters or the polymer has a wide molecular weight distribution, capillary forces tend to pull the thin polymer solution into the pores of the support, thus disrupting the coating layer ^[18].

The high molecular weight of Matrimid gives high viscosity solutions at low polymer/solvent ratios. As shown in Table 1, the viscosity of the polymer solutions (3-13 wt%) was in the range of 16 - 700 mPa·s.

Table 1. Viscosity Matrimid/NMP polymeric solutions

| Concentration | Viscosity |
|----------------------|------------------|
| w.t% | mPa·s |
| 3 | 16 |
| 10 | 230 |
| 13 | 700 |
| 16 | * |
| 20 | * |

*Not possible to determine a value.

Small variations in the polymer/solvent ratio produce large variations in the viscosity of the polymer solution, which is related to changes in the entanglement of the polymer chains during the deposition of the polymer on the ceramic support and its penetration into the porous structure.

3.2 Influence of polymer concentration

To encourage the formation of a stable layer of polymer on the ceramic support, the ceramic tube was mounted on an axis that rotated at a constant speed. This ensured that a film of regular thickness may be formed during the gelification of the polymeric solution. Firstly, the concentration of the polymer solution was investigated because this parameter controls the thickness of the film and, thus, influences crack formation ^[20]. It was observed that 3 and 10 wt % solutions infiltrated inside the porous of the ceramic support prevented the formation of a regular polymeric film. On the contrary, a concentration of 13 wt% obtained a film of regular thickness and smooth surface after gelification. By increasing the concentration to 16-20 wt %, polymeric films with fringes and an irregular surface during rotation and gelification were obtained, which in turn caused the formation of defects during pyrolysis, similar to the *striations* reported in the spin coating of polymeric films on planar supports ^[21]. Fig. 2 shows the formation of the polymeric film over the ceramic support for 3, 13 and 20 wt%. Fig. 2.A shows a transversal view of the ceramic support without polymer solution, while Fig. 2.B provides a transversal view of the polymer deposited with a 3 wt% solution. Figs. 2.C and 2.D show homogeneous polymeric films having thickness between 30 and 80 μm and formed with polymer solutions of 13 and 20 wt%, respectively.

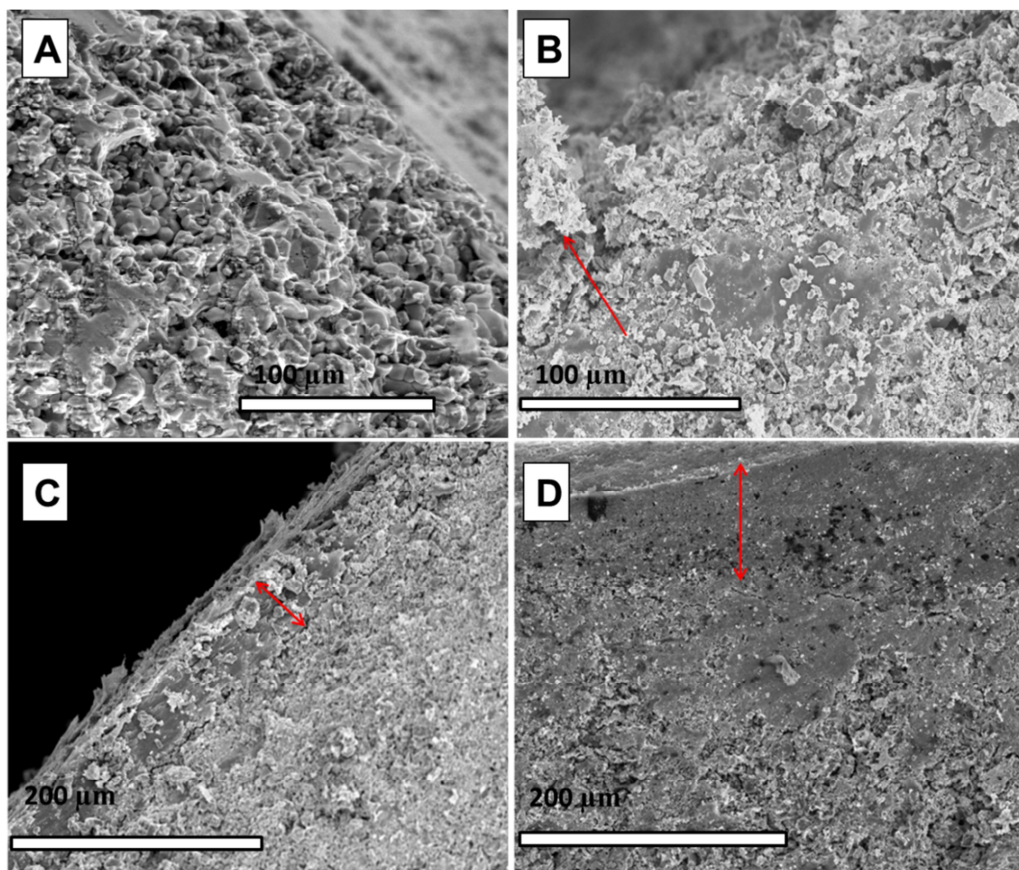


Fig. 2. Transversal photomicrography of the polymer films deposited on the ceramic support at different polymer concentrations (A untreated ceramic; B 3 wt%, C 13 wt%, and D 20 wt%)

Figs. 3.B and 3.C show the surface of the films deposited using 13 wt% and 20 wt% solutions. These solutions cover the ceramic structure completely, whereas the porous ceramic structure is still visible after the deposition of the 3 wt% solution (Fig. 3A). In conclusion, the regularity and thickness of the polymeric film can be controlled by adjusting the concentration of the polymer solution, as it is the case for the procedures based on dip-coating ^[20].

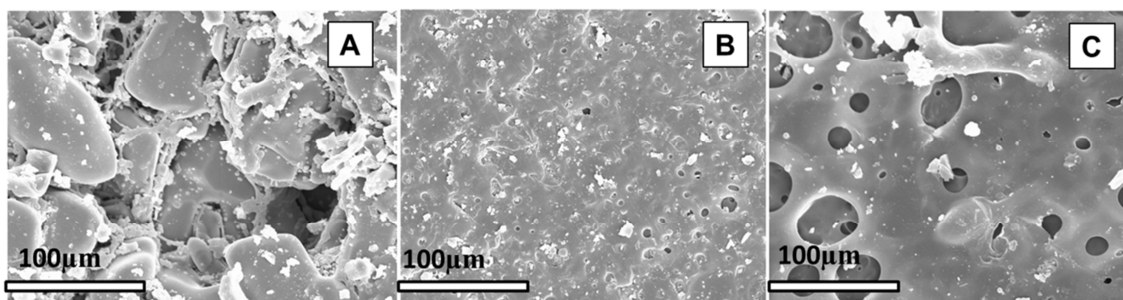


Fig. 3 Surface photomicrography of the polymer films deposited on the ceramic support at different polymer concentrations (A = 3 wt%, B = 13 wt%, and C = 20 wt%)

It is important to consider the relationship between the polymer concentration and the dimensions of the pores on the support (between 1-0.7 μm). Low concentrations created a low viscosity solution, which was thus better able to penetrate the large pores of the support. Otherwise, if the concentration was higher, the solution's increased viscosity prevented it from penetrating the porous structure. The extent of the polymer penetration can be estimated by comparing the theoretical thickness of the polymeric film [22] with the real thickness observed by ESEM. The theoretical thickness was calculated using Equation 1, where W and S are the weight and the surface of the coated (cm) and non-coated membrane (nm), respectively, and ρ_p is the Matrimid density. This provides a theoretical thickness of 70 μm for the 13 wt% film. The observed thickness was between 30 and 40 μm , which indicates a high degree of polymer penetration.

$$t = \frac{(W_{cm} / S_{cm}) - (W_{nm} / S_{nm})}{\rho_p} \quad (1)$$

Differences in the concentration of the polymer deposited on the ceramic support induce differences in the structure of the carbon membranes obtained after pyrolysis [23] and this affects the permeation properties of the latter. As it has been established for non-supported membranes [24], the degree of solvent elimination can influence the final structure of the membrane. The polymer concentration creates differences in thickness

and affects the rate of solvent evaporation. The impact of this variable is discussed in the following analysis of both supported and non-supported membranes.

Polymer concentration is also important in the formation of cracks. After pyrolysis at 550 °C, the 13 wt% films showed fewer cracks than the 16 and 20 wt% films. The samples obtained above 16 wt% showed cracks after pyrolysis along the entire length of the ceramic tube, which is probably caused by excessive thickness of the polymeric film. Above 16 wt% the polymeric film is more than 40 µm, the limiting thickness value reported by Shiflett and Foley for crack prevention ^[25]

3.3 Critical temperature for crack formation

To determine the critical temperature for crack formation, pyrolysis of the supported polymer films was performed at several temperatures using a constant heating rate of 2.5 °C/min. Fig. 4 shows how the polymer film was rearranged towards a more regular surface when the aging temperature was increased from 100 to 200 °C. The increase in temperature caused cracks to appear above 420 °C. This is in agreement with the temperature of 450 °C at which low molecular weight gases began to evolve very rapidly during Matrimid carbonization ^[26].

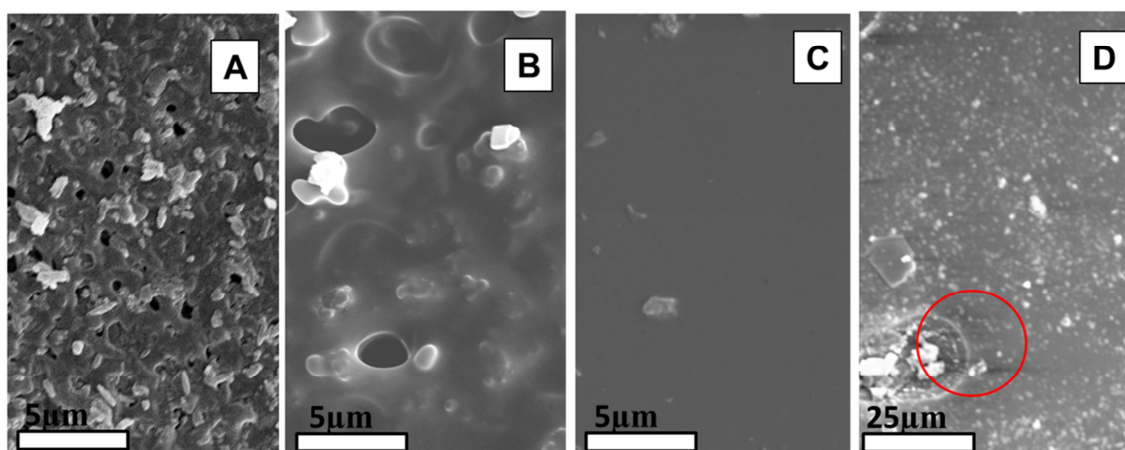


Fig 4. Progressive formation of cracks with pyrolysis temperature increasing at a heating rate of 2.5°C/min. (A: 100°C, B: 220°C, C: 420°C, D: 580°C)

3.4 Influence of methanol washing on crack formation and carbon structure

The formation of cracks appeared to be related to both the gases and the low molecular weight volatiles that were produced during pyrolysis. These were trapped inside the carbonizing polymer and produced fractures in the material when finally released. However, it is also possible that either the low molar mass compounds present in the polymer or the residual solvent trapped in the polymer film also contributed to crack formation upon volatilization. To test this, solvent traces in the polymer film were eliminated by intensive washing with methanol [27] after curing at 110 °C for 24 hrs.

Fig. 5 shows the TGA curves of Matrimid after methanol washing. It can be observed that there is no significant loss of mass between 200 and 550 °C, once the low molar mass compounds and entrapped solvent have been removed by methanol washing.

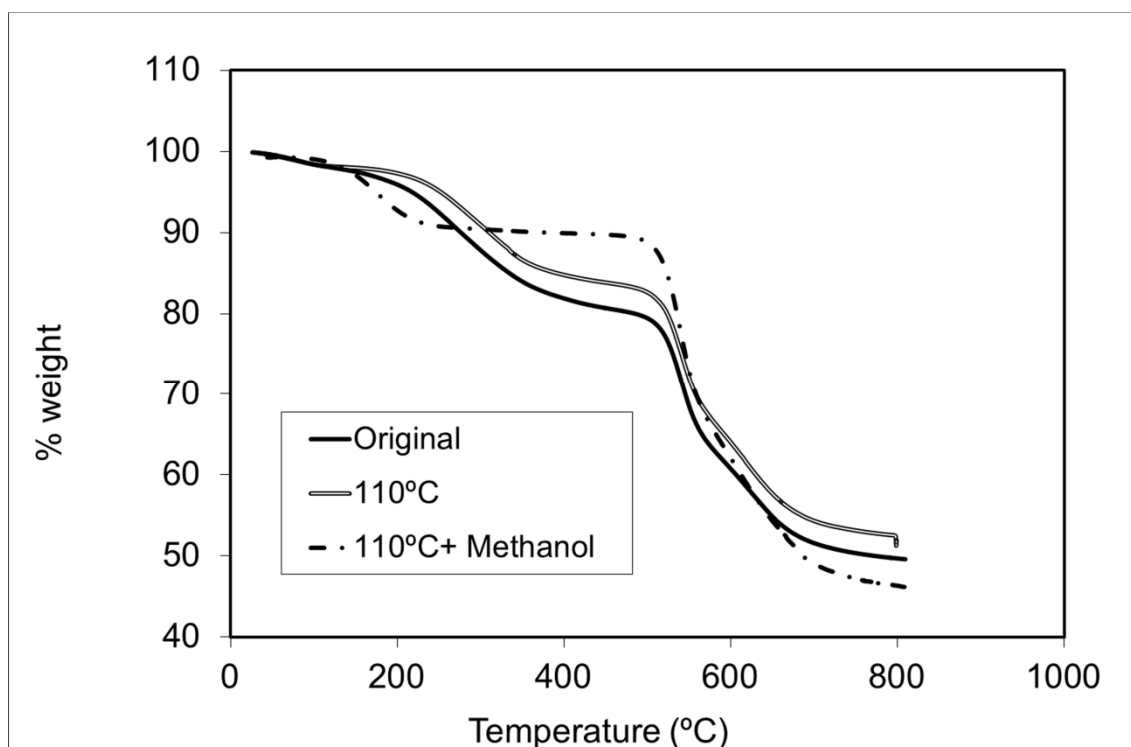


Fig. 5 Thermogravimetric analysis curves of a Matrimid powder (Original), cast membrane after 110 °C, and a casted membrane after 110 °C and methanol bath (110 °C + methanol)

Methanol washing raised the temperature at which cracks were formed. Fig. 6 shows real time ESEM imaging of crack formation on a supported polymer film after methanol washing, where cracks did not appear until 580 °C at a heating rate of 2.5 °C/min.

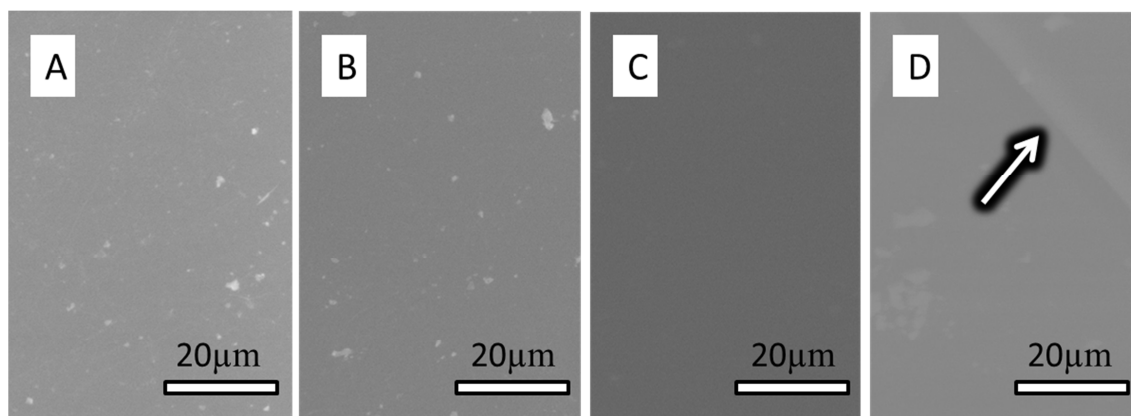


Fig. 6. On-line ESEM imaging of the pyrolysis of a supported polymer film after ethanol washing (A: 100 °C, B: 220 °C, C: 420 °C, D: 580 °C)

However, methanol can also act as a modifier of the polymer structure, thus influencing the final structure of the carbon membrane after pyrolysis^[28,29]. I_d/I_g ratios obtained from Raman spectroscopy were used to determine the ratio between disordered and organized phases of the carbon. Low values of I_d/I_g correspond to graphitized carbons, while high values are for more amorphous carbons. Table 2 shows the influence of methanol on the carbon structure after pyrolysis at 900 °C under nitrogen. Washed samples had higher I_d/I_g ratios (1.76-1.9) than unwashed samples (1.37), suggesting a less organized carbon structure when methanol washing was applied. This may be related with the swelling of the Matrimid in contact with methanol, which seems to promote a less organized polymer pre-carbon structure.

Table 2 also presents the effect of methanol washing when combined with aging at 300 or 350 °C (*i.e.* below and above T_g). The aging temperature did not induce significant differences in I_d/I_g , but a significant effect was observed when methanol washing was performed.

Table 2. I_d/I_g values for carbon samples obtained after different treatments

| Sample nº | Type of Treatment | | | | | I_d/I_g | |
|-----------|-------------------|--------|--------------------|-------------|--------|-----------|------|
| 1 | 24 hrs-25 °C | 110 °C | | | 900 °C | 1.37 | |
| 2 | 24 hrs-25 °C | 110 °C | CH ₃ OH | | 900 °C | 1.9 | |
| 3 | 24 hrs-25 °C | 110 °C | CH ₃ OH | 3hrs-110 °C | 900 °C | 1.72 | |
| 4 | 24 hrs-25 °C | 110 °C | CH ₃ OH | 3hrs-110 °C | 300 °C | 900 °C | 1.79 |
| 5 | 24 hrs-25 °C | 110 °C | CH ₃ OH | 3hrs-110 °C | 350 °C | 900 °C | 1.76 |
| 6 | 24 hrs-25 °C | 110 °C | | 3hrs-110 °C | 300 °C | 900 °C | 1.58 |
| 7 | 24 hrs-25 °C | 110 °C | | 3hrs-110 °C | 350 °C | 900 °C | 1.60 |

3.5 Effect of heating rate and pyrolysis temperature

Once the influence of polymer concentration and methanol washing was established, the heating rate was changed both to diminish crack formation and improve the reproducibility of the supported carbon membranes. A value of 1 °C/min was finally adopted because lower heating rates did not lead to a significant improvement. The pyrolysis temperature was, then, varied to study the influence of temperature on the performance of the carbon membrane. At a heating rate of 1 °C/min, it was possible to obtain supported crack-free carbon membranes at a pyrolysis temperature of up to 700 °C. This is a significant finding considering that other fabrication methods such as solution spray have only provided defect-free membranes below 600 °C [15]. Fig. 7 compares the TiO₂ support and a supported carbon membrane obtained at a heating rate of 1 °C/min and a final temperature of 700 °C. From this figure, it is possible to observe that a carbon layer of 11 µm thickness was successfully formed over a porous inorganic support.

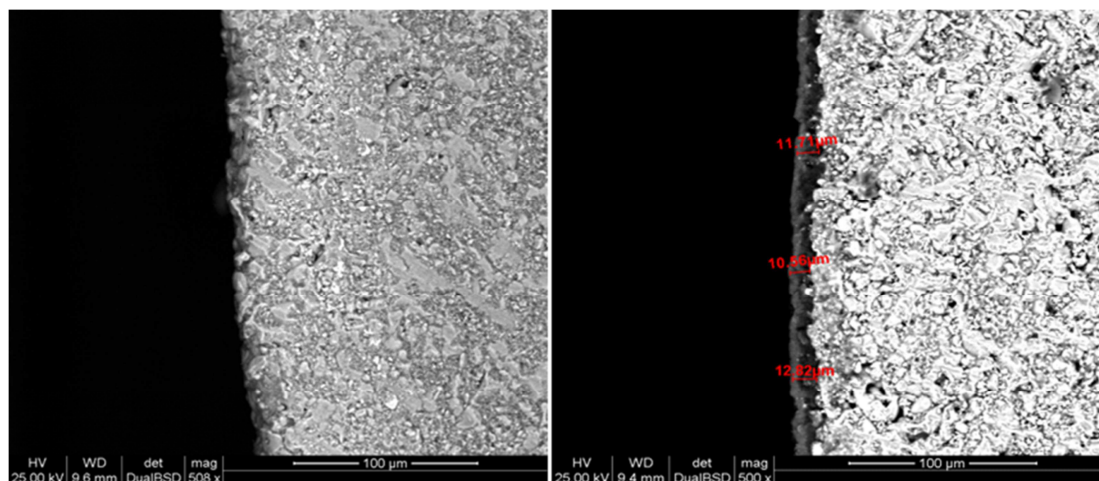


Fig. 7 Back scattering images of the ceramic support and a supported carbon membrane obtained at a heating rate of 1 °C/min and a final temperature

3.6 Influence of the support on the structure of the carbon membrane

The separation of gas mixtures containing H₂, CH₄, CO and CO₂ is a complex problem because of the similarities in molecular diameters. Good knowledge of the mechanisms involved in the development of the porous carbonaceous structure during the thermal decomposition of the polymer is needed in order to control the sizes of the pores in the membrane. A factor that may influence the development of the carbonaceous matrix is the interaction between the polymer and the ceramic support. Therefore, a series of experiments was performed in which samples of Matrimid, both non-supported and supported, were pyrolyzed under identical temperature and heating rate conditions, and the resulting carbon membranes were characterized using AFM and WXRD.

The final structure of the carbon membrane is influenced by the structure of the polymer used as a precursor. Thermal curing of Matrimid below its glass transition temperature encourages the formation of charge transfer complexes that restrict the mobility of the polymer chains. The alternating sequence of the electron-rich donor and electron-deficient acceptor molecules present in polyimides has been reported to depend on the fabrication method^[30]. When the rings of donor and acceptor electrons are close to each other, this creates complexes that reduce chain mobility^[31]. When the polymer is coated over a support, the interfacial stress between polymer and support reduces the *T_g* of the polymer^[32], thus limiting the formation of complexes. Table 3 shows that the *T_g* of the

supported polymer film was lower than that of the non-supported material, thus showing the influence of the support-polymer interactions.

Table 3. Glass transition temperature (T_g) of supported and non-supported Matrimid samples

| Sample | T_g (°C) |
|----------------------|------------------------------|
| Non-supported | 335.41 |
| Supported | 325.58 |

Fabrication conditions may also influence the structure of the polymeric film ^[30]. Differences in thickness between spin-coated and non-supported samples and the time required to evaporate the solvent and for gelification may all influence the formation of charge transfer complexes. The presence of a porous support will favor the formation of thinner polymer layers because the polymer is better able to penetrate the pores of the support. Differences in the formation of a homogeneous polymer surface will create differences in carbon microstructure after pyrolysis. In addition to microporous domains, the carbonaceous structure may present sponge-like porous carbon, thus affecting the pore size distribution and permeability of the carbon membrane ^[23]. Our results suggest that a strong interaction between the polymer and the ceramic support leads to aggregation zones that compete with the formation of charge transfer complexes, thus limiting the arrangement of the polymer chains towards a compact structure, which in turn increases the free volume and decreases T_g . The formation of such domains can be inferred from AFM imaging of supported and non-supported samples (Fig. 8), which shows that the polymer is adapted to the structure of the ceramic support.

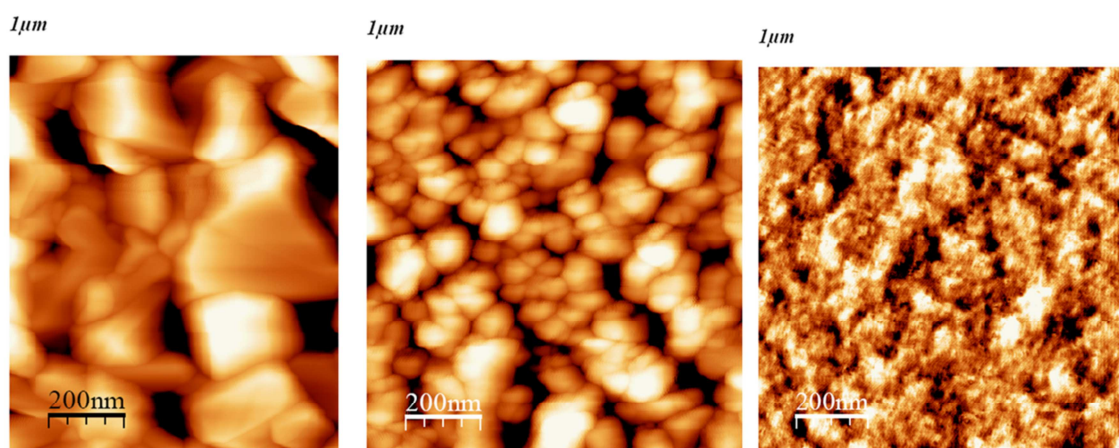


Fig. 8. AFM images of the ceramic support (left), the supported carbon membrane (center) and a non-supported carbon membrane (right).

The structure was further investigated using WXR D and the main results are presented in Figs. 9 and 10. Temperature and support affect the interplanar distance spacing d calculated using Bragg's equation ($\alpha = 2d \sin \theta$, where α is the wavelength of X-rays and θ the diffraction angle). At 550 °C, the broad peak at 22.4 Å shows d spacing of 4.83 Å and 5.03 Å for non-supported and supported carbon membranes, respectively, which reveals a structure that is more compact than that reported by Koros for a dense planar film of Matrimid (5.20 Å) ^[33]. The intensity of the peak is lower for the supported carbon membrane, which indicates that it has a less organized structure than non-supported films ^[34]. The difference in the d spacing of the graphite-like phase becomes smaller at higher pyrolysis temperatures. In fact, after pyrolysis at 850 °C both supported and non-supported samples show similar values of d spacing, which were 3.89 Å and 3.86 Å for non-supported and supported membranes, respectively. This shows that the amorphous phase becomes similar for both types of film regardless of the presence of the support. However, the presence of a graphite peak at $2\theta = 43^\circ$ ($d = 3.35$) ^[35] reveals the presence of organized graphite-like regions in the non-supported membrane that are not observed in its supported counterpart. Pyrolysis temperature decreases d spacing, thus causing narrower pore sizes and increasing selectivity.

Carbon Molecular Sieve Membranes for Gas Separation

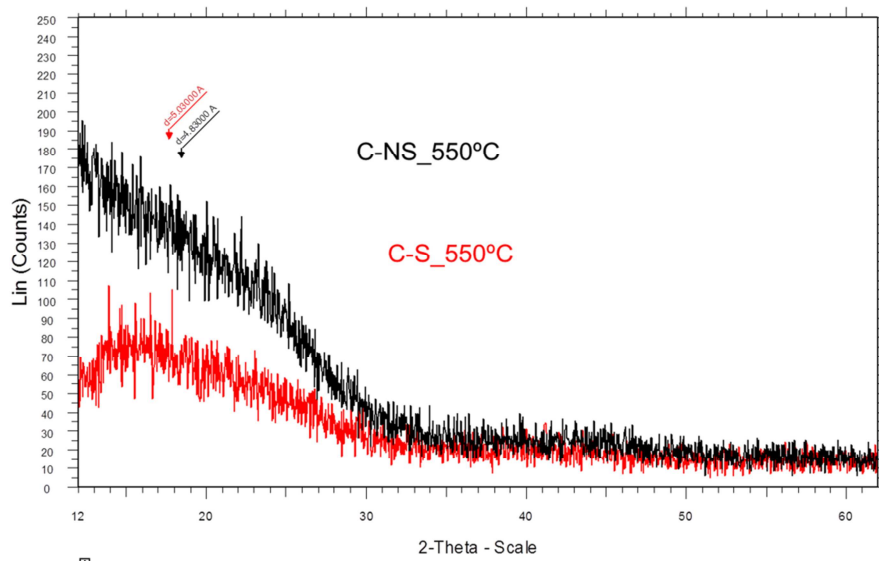


Fig. 9 WXR D for carbon supported (C-S) and non-supported (C-NS) carbon membranes obtained at 550 °C

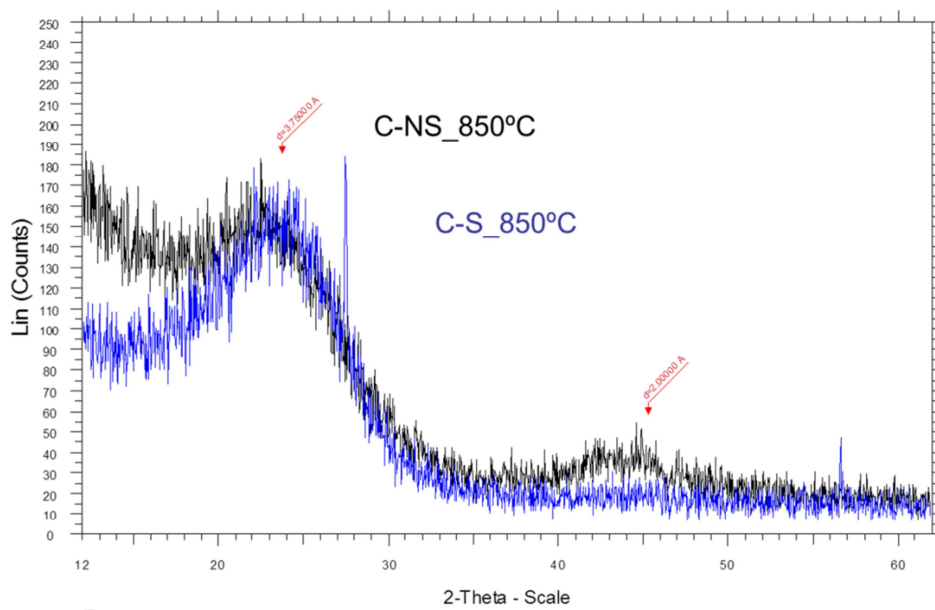


Fig. 10 WXR D for carbon supported (C-S) and non-supported (C-NS) carbon membranes obtained at 850 °C

3.7 Permeance of supported carbon membranes

The supported carbon membranes produced under the optimal fabrication conditions were tested to determine their gas permeances. Even though the membranes were free of observable cracks, there were still defects in the membranes and initial tests with pure gases revealed that the membranes' permeance depended on them, having been fabricated under the correct pressure and with a high viscous flow. Indeed, this was due to the existence of small pinholes and microscopic imperfections that were caused by ambient dust particles during the membrane fabrication/preparation procedure. These particles contaminated the polymer film during deposition. Since clean room facilities were not available to manufacture the membranes, the carbon membranes were coated with PDMS to eliminate imperfections and pinholes ^[36-37].

Fig. 11 shows the permeances of the gases at room temperature for the membranes obtained at different pyrolysis temperatures. In all cases, the permeance decreased in the order 550, 700, 650 °C. Differences in permeance are determined by differences in the carbon microstructure that directly affect the transport mechanism of the membrane ^[38]. The high permeance at 550 °C may be due to the existence of pores wider than those at 650 °C and 700 °C. In fact, differences in pore characteristics make possible the predominance of different transport mechanisms on the membrane. The permeances of membranes pyrolyzed at 650 °C depend on the kinetic diameter of the gases and this in turn confirms the presence of a molecular sieving mechanism in these membranes. However, this does not apply to membranes pyrolyzed at 700 and 550 °C because the permeance of these membranes is not governed solely by the kinetic diameter of the gases. This was demonstrated by the fact that when these membranes were tested for CH₄ permeance they showed a small deviation away from molecular sieving, which indicates that additional transport mechanisms coexist with the molecular sieving ^[37,38].

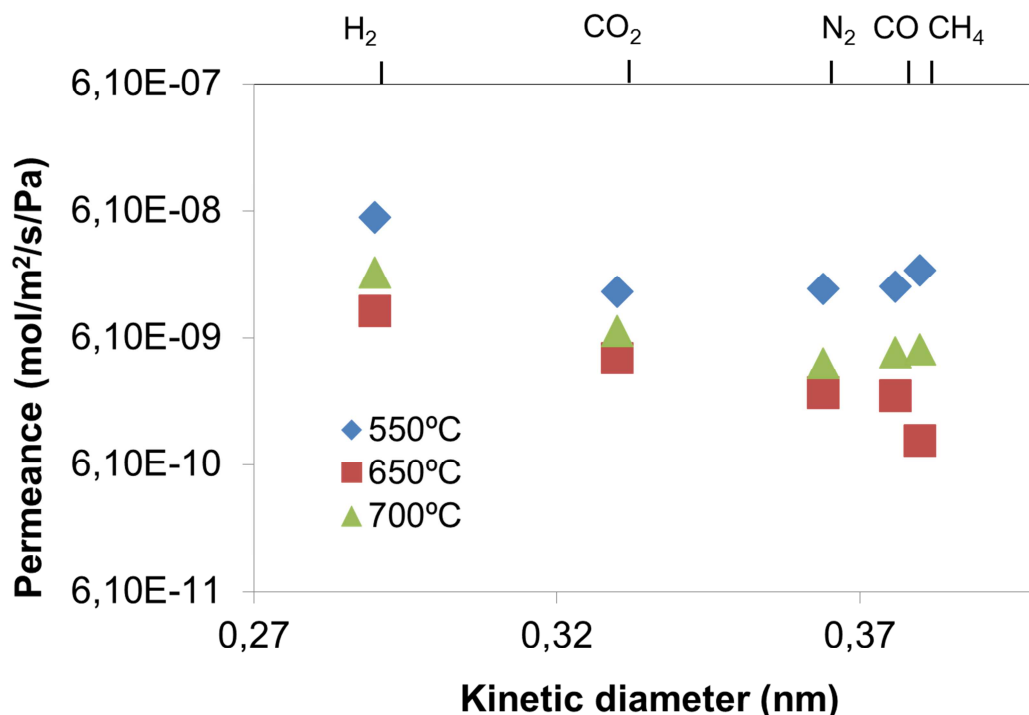


Fig. 11. Permeance values for supported carbon membranes at different pyrolysis temperatures

Above 550 °C, pores become smaller as the increased pyrolysis temperature shrinks the carbon structure. However, between 650 and 700 °C there is a small increase in permeance related to the pyrolysis temperature that can be explained by an increase in pore size, an increase in the number of pores, or both of these factors ^[39]. Changes in the carbon structure were confirmed by adsorption-desorption analysis. Fig. 12 shows a decrease in adsorption for H₂, CO₂, and CH₄ molecules above 550 °C, which in turn indicates pore reduction. The hydrogen permeance values are significant being between $9.82 \cdot 10^{-9}$ mol/m²·Pa·s and $1.97 \cdot 10^{-8}$ mol/m²·Pa·s for membranes obtained at 650 and 700 °C, respectively. These values are comparable to those reported at 40 °C with hollow fiber membranes from Matrimid carbonized at 900 °C using a different gas composition during pyrolysis, in the range of $9.65 \cdot 10^{-10}$ - $6.82 \cdot 10^{-9}$ mol/m²·Pa·s ^[40].

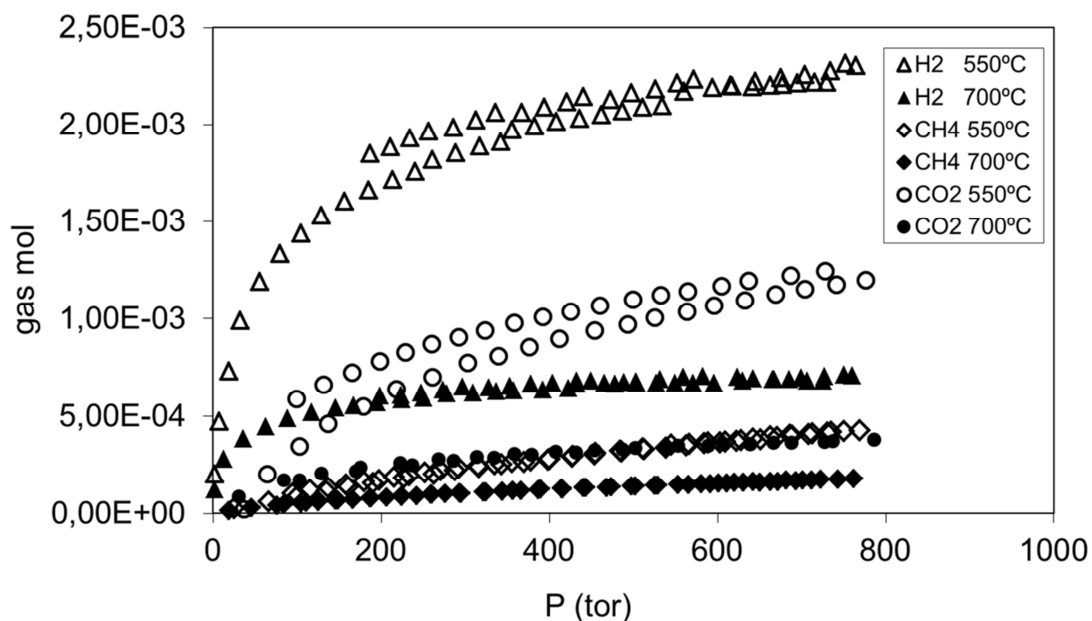


Fig. 12 Adsorption-desorption isotherms for supported carbon membranes at different pyrolysis temperatures

As previously mentioned, differences in the carbon membrane structure cause differences in the transport mechanism and in the gas selectivities of pair analyzed (Fig. 13). For membranes obtained at 550 °C and for all pairs of gases analyzed, ideal selectivities were only slightly below the Knudsen theoretical values, which indicate that the PDMS coating was an effective treatment for plugging small cracks and defects in the carbon layer. Above 650 °C, ideal selectivities were over the Knudsen theoretical values and this suggests that the gases were separated by molecular sieving. This is in agreement with the decrease in porosity and the change in the structure of the carbon membrane observed in the adsorption-desorption isotherms (Fig. 12).

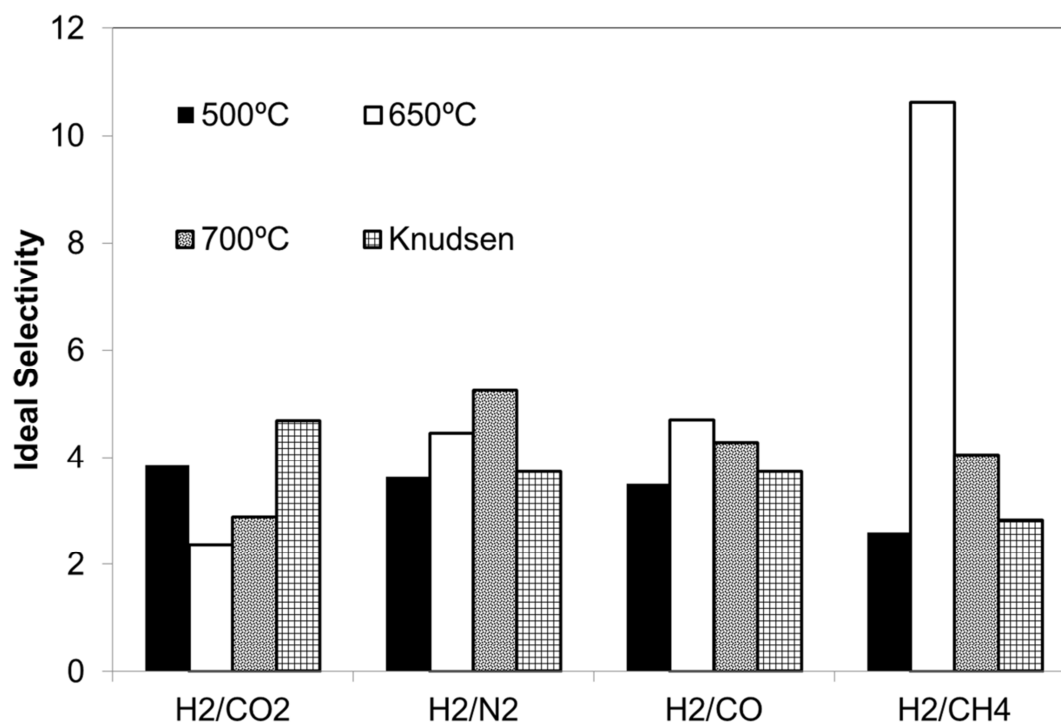


Fig. 13 Ideal selectivity values for supported carbon membranes at different pyrolysis temperatures

With the aim to compare the fabrication method with other reported in the literature, Table 4 reports some permeance and ideal selectivity values. It is clear that an additional research has to be done in order to improve the morphology of the carbon membranes. However, the method presented in this work can be considered promising for achieving competitive membranes for gas separation.

Table 4. References reported in the fabrication of asymmetric/supported carbon membranes.

| Membrane Type | Single gas permeance · 10 ⁻¹⁰ (mol/m ² ·s· Pa) | | | | | | Ideal selectivity | | Reference |
|-----------------------|--|-----------------|----------------|----|-----------------|------|-------------------|---------------------------------|-----------|
| | H ₂ | CO ₂ | N ₂ | CO | CH ₄ | He | He/N ₂ | N ₂ /CO ₂ | |
| Hollow fiber | 9.65-68 | | 0.36-0.904 | | | | | | [40] |
| Supported on tube | 177.7 | | 44.90 | | | | | | [41] |
| | 4460 | | 1100 | | | | | | |
| | 13200 | | 5140 | | | | | | |
| Capillary CMSM | 2.43-277 | | 0.0033-2.01 | | | | | | [37] |
| Disk-shaped supported | | | 64.4 | | | 245 | 3.8 | | [42] |
| | | | 6.9 | | | 72 | 10.5 | | |
| | | | 11.5 | | | 85 | 7.4 | | |
| | | | 0.2 | | | 27 | 136 | | |
| | | | 1.2 | | | 30.4 | 25.3 | | |
| Disk-shaped supported | 80 | 20 | 5 | | 0.23 | | 16 | | [43] |
| Supported on tube | 409 | | 65 | | | 213 | | | [25] |
| | 17.5 | | 0.28 | | | | | | |
| | 332 | | 34 | | | | | | |
| | 6.05 | | 0.183 | | | | | | |
| Supported on tube | | 200 | 80 | | | | 40 | | [15] |
| Supported on tube | 98.2 | 41 | 22 | 21 | 9.31 | | | | This work |

4. Conclusions

A simple one-step polymer coating for formation of the carbon layer has been developed to fabricate ceramic-supported carbon membranes without modifying the macroporous support. The thickness of the polymeric film and hence, the characteristics of the carbon membrane after pyrolysis were controlled by concentrating the polymer solution during deposition. Other parameters that affected the quality of the carbon membranes were washing the polymer film with methanol, aging the polymer after deposition, the heating rate and the final temperature during pyrolysis. Important differences were observed between supported and non-supported membranes and they showed that the polymer-support interactions make an important contribution to the properties of the carbon membrane. A pyrolysis temperature of 650 °C gives a carbon membrane with a pure molecular sieving mechanism at room temperature. Permeance ranges from $9.82 \cdot 10^{-9}$ mol/m²·Pa·s for H₂ to $9.31 \cdot 10^{-10}$ mol/m²·Pa·s for CH₄, representing ideal gas selectivities of 2.37, 4.70 and 10.62 for H₂/CO₂, H₂/CO and H₂/CH₄, respectively.

5. Acknowledgements

The authors are indebted to the Spanish Government for financial support (project CTQ2008-02491, partially funded by the FEDER program of the European Union) and to the commission of European Communities Specific OpenTok Project MTKD-LT-2005-030040. Dr. S. Nunes from the Water Desalination and Reuse Center at the King Abdullah University of Science and Technology (KAUST), Kingdom of Saudi Arabia, is acknowledged for providing the Matrimid polymer. Dr. J. L. Toca from the Department of Naniobiotechnology BOKU-Vienna and Dr. A. Lederer from the Leibniz-Institute of Polymer Research Dresden are acknowledged for their assistance with the AFM and Light Scattering measurements, respectively. Special thanks to Dr. Marta Giamberini and Dr. Jose Antonio Reina from Rovira I Virgili University for their support on realization of experiments.

6. References

- [1] Y. Yoshino; T. Suzuki; B.N. Nair; H. Taguchi; N. Itoh; Development of tubular substrates, silica based membranes and membrane modules for hydrogen separation at high temperature, *J. Membrane Sci.*, 267 (2005) 8–17.
- [2] J.E. Koresh; S. Abrah; The carbon molecular sieve membranes. General properties and permeability of CH₄/H₂ mixture, *Sep. Sci. Techn.*, 22 (1987) 973-982.
- [3] S. Suda; K. Haraya; Gas Permeation through micropores of carbon molecular sieve membranes derived from Kapton polyimide, *J. Phys. Chem. B*, 101 (1997) 3988-3994.
- [4] H. Suda; K. Haraya; Molecular sieving effect of carbonized Kapton polyimide membrane, *J. Chem. Soc. Chem. Commun.*, (1995) 1179.
- [5] K.M. Steel, W.J. Koros; Investigation of porosity of carbon materials and related effects on gas separation properties, *Carbon*, 41 (2003) 253–266
- [6] W. Wei; G. Qin; H. Hu; L. You; G. Chen; Preparation of supported carbon molecular sieve membrane from novolac phenol–formaldehyde resin, *J. Membrane Sci.*, (2007) 80–85.
- [7] T.A. Centeno; J.L. Vilas; A.B. Fuertes; Effects of phenolic resin pyrolysis conditions on carbon membrane performance for gas separation, *J. Membrane Sci.*, 228 (2004) 45–54.
- [8] P.T. Tin; Y. Xiao; T.-Sh. Chung, Polyimide-Carbonized membranes for gas separation: structural, composition and morphological control of precursors, *Sep. Purif. Rev.*, 35 (2006) 285–318.
- [9] I. Pinnau, B. Freeman, Formation and modification of polymeric Membranes: overview. From Membrane formation and modification, ACS Symposium series 744, American Chemical Society. Danvers, MA, 1999.
- [10] A. Julbe; D. Farrusseng; C. Guizard; Porous ceramic membranes for catalytic reactors—overview and new ideas, *J. Membrane Sci.*, 181 (2001) 3–20.
- [11] T. Tsuru; T. Morita; H. Shintani; T. Yoshioka; M. Asaeda; Membrane reactor performance of steam reforming of methane using hydrogen-permselective catalytic SiO₂ membranes, *J. Membrane Sci.*, 316 (2008) 53–62.
- [12] B.S. Liu; N. Wang; F. He; J.X. Chu; Separation performance of nanoporous carbon membranes fabricated by catalytic decomposition of CH₄ using Ni/Polyamideimide templates, *Ind. Eng. Chem. Res.*, 47 (2008) 1896–1902.
- [13] H. Wang; L. Zhang; G.R. Gavalas; Preparation of supported carbon membranes from furfuryl alcohol by vapor deposition polymerization, *J. Membrane Sci.*, 177 (2000) 25–31.
- [14] J.I Hayashi; H. Mizuta; M. Yamamoto; K. Kusakabe; S. Morooka; Pore size control of carbonized BPDA-pp' ODA polyimide membrane by chemical vapor deposition of carbon, *J. Membrane Sci.*, 124 (1997) 243–251.
- [15] C.J. Anderson; S.J. Pas; G. Arora; S.E. Kentish; A.J. Hill; S.I. Sandler; G.W. Stevens, Effect of pyrolysis temperature and operating temperature on the performance of nanoporous carbon membranes, *J. Membrane Sci.*, 322 (2008) 19–27.
- [16] A. Merritt ; R. Rajagopalan; H.C. Foley; High performance nanoporous carbon membranes for air separation, *Carbon*, 45 (2007) 1267–1278.
- [17] R.M. de Vos; H. Verweij; High-Selectivity, high-Flux silica membranes for gas separation, *Science*, 279 (1998) 1710-1711.

- [18] M.E. Rezac; W.J. Koros; Preparation of polymer-ceramic composite membranes with thin defect-free separating layer, *J. App. Polym. Sci.*, 46 (1992) 1927-1938
- [19] I. Horcas, R. Fernandez, J. M. Gomez-Rodriguez, J. Colchero, J. Gomez-Herrero, A. M. Baro, "WSxM: A software for scanning probe microscopy and a tool for nanotechnology, *Rev. Sci. Instrum.*, 2007, 78.
- [20] M.G. Sedigh; M. Jahangiri; P.-K.-T. Liu; M. Sahimi; T.T. Tsotsis, Structural characterization of polyetherimide- based carbon molecular sieve membranes, *AIChE J.*, 46 (2000) 2245-2255.
- [21] D.E. Haas; D.P. Birnie; M.J. Zecchino; J.T. Figueroa, The effect of radial position and spin speed on striation spacing in spin on glass coatings *J. Mater. Sci. Lett.*, (2001) 1763 – 1766.
- [22] I.F.J. Vankelecom, B. Moermans; G. Verschuere; P.A. Jacobs, Intrusion of PDMS top layers in porous supports, *J. Membrane Sci.*, 158 (1999) 289-297.
- [23] T. Miyake; M. Hanaya, Carbon-coated material with bimodal pore-size distribution, *J. Mater. Sci.*, 37 (2002) 907– 910.
- [24] H. Kawakami; M. Mikawa; S. Nagaoka; Formation of surface skin layer of asymmetric polyimide membranes and their gas transport properties, *J. Membrane Sci.*, 137 (1997) 241-251.
- [25] M.B. Shiflett; H.C. Foley; On the preparation of supported nanoporous carbon membranes, *J. Membrane Sci.*, 179 (2000) 275–282.
- [26] J.N. Barsema , S.D. Klijnstra ; J.H. Balster; N.F.A. van der Vegt; G.H. Koops; M. Wessling; Intermediate polymer to carbon gas separation membranes based on Matrimid PI, *J. Membrane Sci.*, 238 (2004) 93–102.
- [27] S. Shishatskiy; C. Nistor; M. Popa; S.P. Nunes, K.V. Peinemann, Polyimide asymmetric membranes for hydrogen separation: influence of formation conditions on gas transport properties, *Adv. Eng. Mater.*, 8 (2006) 390-397.
- [28] P.S. Tin; T.S. Chung; Y. Liu; R. Wang; S.L. Liu; K.P. Pramoda; Effects of cross-linking modification on gas separation performance of Matrimid membranes, *J. Membrane Sci.*, 225 (2003) 77–90.
- [29] P.S. Tin, T.-Ch. Chung, A.J. Hill, Advanced fabrication of carbon molecular sieve membranes by nonsolvent pretreatment of precursor polymers, *Ind. Eng. Chem. Res.*, 43 (2004) 6476-6483.
- [30] H. Kawakami; M. Mikawa; S. Nagaoka, Gas transport properties in thermally cured aromatic polyimide membranes, *J. Membrane Sci.*, 118 (1996) 223-230.
- [31] J.J. Krol; M. Boerrigter; G.H. Koops, Polyimide hollow fiber gas separation membranes: preparation and the suppression of plasticization in propane/propylene environments, *J. Membrane Sci.*, 184 (2001) 275–286.
- [32] H. Wang H; K.S. Siow; IEEE/CPMT, 1997; Electronic Packaging Technology Conference.
- [33] K.M. Steel, W.J. Koros, An investigation of the effects of pyrolysis parameters on gas separation properties of carbon materials, *Carbon*, 43 (2005) 1843–1856.
- [34] M. Yoshimune; I. Fujiwara; K. Haraya; Carbon molecular sieve membranes derived from trimethylsilyl substituted poly(phenylene oxide) for gas separation, *Carbon*, 45 (2007) 553–560.
- [35] A.C. Lua, J. Su, Effects of carbonisation on pore evolution and gas permeation properties of carbon membranes from Kapton_ polyimide, *Carbon*, 44 (2006) 2964–2972.
- [36] B.R. Rowe; B.D. Freeman; D.R. Paul; Physical aging of ultrathin glassy polymer films tracked by gas permeability, *Polymer*, 50 (2009) 5565-5575.

- [37] J. Petersen; M. Matsuda; K. Haraya; Capillary carbon molecular sieve membranes derived from Kapton for high temperature gas separation, *J. Membrane Sci.*, 131 (1997) 85-94.
- [38] K. Briceno, R. Garcia-Valls, D. Montane, State of the art of carbon molecular sieves supported on tubular ceramics for gas separation applications, *Asia Pac. J. Chem. Eng.*, 5 (2010) 169–178.
- [39] J.N. Barsema; N.F.A. van der Vegt; G.H. Koops; M. Wessling; Carbon molecular sieve membranes prepared from porous fiber precursor, *J. Membrane Sci.*, 205 (2002) 239–246.
- [40] E.P. Favvas; G.C. Kapantaidakis; J.W. Nolan; A.Ch. Mitropoulos ; N.J. Kanellopoulos; Preparation, characterization and gas permeation properties of carbon hollow fiber membranes based on Matrimid® 5218 precursor, *J. Mater. Process Techn.*, 186 (2007) 102–110.
- [41] K. Kusakabe, Z. Y Li, H. Maeda, S. Morooka, Preparation of supported composite membrane by pyrolysis of polycarbosilane for gas separation at high temperature, *Journal of Membrane Science* 103 (1995) 175-180
- [42] A. Fuertes, T. Centeno, Preparation of supported carbon molecular sieve membranes, *Carbon* 37, (1999), 679-684.
- [43] T.A Centeno, A.B Fuertes, Supported carbon molecular sieve membranes based on a phenolic resin, *Journal of Membrane Science* 160 (1999) 201-211

CHAPTER 5:

Characterization of Carbon Molecular Sieve Membranes Supported on Ceramic Tubes

(Art. 4)

(In preparation)

Characterization of Carbon Molecular Sieve Membranes Supported on Ceramic Tubes

K. Briceño^a, J. Silvestre-Albero^b, A. Silvestre-Albero^b, J.I Calvo^c, D. Montané^d, R. García-Valls^a, A. Hernández^c, F. Rodríguez-Reinoso^b.

^a *Department d'Enginyeria Química, Universitat Rovira i Virgili, Av. Paisos Catalans, 26, E-43007, Tarragona, Spain*

^b *Laboratorio de Materiales Avanzados, Departamento de Química Inorgánica, Universidad de Alicante, E-03080 Alicante, Spain*

^c *Departamento de Física Aplicada, Facultad Ciencias, Universidad de Valladolid, E-47071 Valladolid, Spain*

^d *Catalonia Institute for Energy Research (IREC), Bioenergy and Biofuels Division, Building N5, C/ Marcel·lí Domingo 2, E-43007, Tarragona, Spain*

Corresponding author e-mail: kelly.briceno@urv.cat

Tel: + 34 977 558506

Abstract

Carbon molecular sieve membranes have been analyzed in supported and unsupported configurations. Adsorption analysis of CO₂, N₂ and CH₄ were performed in order to establish differences between the two types of samples. Experimental results show an important effect of the support, which can be considered as an additional parameter to tailor pore size on these carbon membranes. Immersion calorimetry measurements into liquids of different molecular dimensions ((dichloromethane, benzene, n-hexane, 2,2-dimethyl-butane) were also performed. Similarities were found between adsorption and calorimetric analysis. The pore volume of samples analyzed ranged from 0.016 to 0.263 cm³/g. The effect of the pyrolysis temperature, either 550°C or 700°C, under N₂ atmosphere was also analyzed. Quantification of the pore size distribution of the support was done by LLDP (liquid-liquid displacement porosimetry). The composite membrane was considered for CO₂/CH₄ separation before and after pore plugging was done. The ideal selectivity factors value (4.47) was over Knudsen theoretical factor (0.60) for membrane pyrolyzed at 600°C, thus indicating the potential application of these membranes in separation of low molecular weight gases.

KEYWORDS: Carbon molecular sieve membranes, amorphous carbon characterization,

LLDP, gas separation, composite membranes

1. Introduction

Carbon molecular sieve (CMS) materials have been employed in different gas separation applications ^[1]. Their turbostratic structure consists in an array of narrow constrictions at the entrance of micropores that are interconnected through a system of galleries allowing separation of molecules based on their different shape and/or size. The amorphous character of these materials allows gases to diffuse through the constrictions at different adsorption rate ^[2]. Extended applications of CMS have been reported in industrial separation processes, e.g. N₂ separation from air ^[3, 4]. Their thermal stability and superior inertness when compared with other molecular sieves such as zeolites make them suitable for demanding applications, like those involving temperature and elevated partial pressure of water. Furthermore, synthesis of molecular sieves based on carbon is simpler and cheaper than those based on other materials such as zeolites, whose methods are intricate and require additional post-treatments steps ^[2]. Beyond their use as adsorbents CMS have been explored in the past for membrane applications (CMSM), building on the pioneering works of Rao ^[5] and Koresh ^[6].

CMSM can be produced in different geometries – planar, hollow fiber and supported films – by pyrolysis of polymers at temperatures between 550-1000°C ^[7]. The selection of membrane presentation depends on the final application of the membrane. Supported membranes are asymmetric structures that are preferred over the unsupported due to their superior mechanical properties. However, even when using the same precursor, membrane properties can largely vary depending on the preparation procedure used. For example, in their attempts to reduce the number of coatings, Fuertes and Centeno ^[8] reported differences between supported membranes obtained after 3 carbon-coating cycles and those obtained after deposition of three layers of the same precursor polyimide with a subsequent carbonization step. The latest sample exhibited higher permeation rates but lower selectivity compared to the former one. It is obvious that the way in which the carbon structure is formed depends on the coating procedure, thus producing differences on the properties of the carbon layer. Singh-Goshal and Koros ^[9]

outlined that it is easier to compute entropic selectivity on dense symmetric films than in asymmetric membranes.

Identification of the carbon structure becomes more complex if variables often considered to affect the carbon structure of flat membranes have to be considered on asymmetric configurations. Vu et al. ^[10] confirmed an understandable decrease in the CO₂ permeance values for CMS fibers (asymmetric membranes) after pyrolysis. On the contrary, permeance increased in planar films made from the same polymer (unsupported) following the same pyrolysis conditions. Apparently, when the polymer precursor is pyrolyzed in an asymmetric structure, as is the case of hollow fiber or supported samples, the carbonaceous structure obtained after pyrolysis becomes different from those samples obtained in a planar shape and dense film. It could be hypothesized that the presence of the support could determine differences in carbon structure due to carbon layer differences.

The reasons explaining this difference have been scarcely explored in the past because it is not easy to characterize the changes in pore structure of these materials. In fact, characterization of unsupported carbon films has been used in the past to explain the morphological changes of its supported counterparts ^[8, 11]. However, little evidence has been shown in the past to understand the extent of this extrapolation. In addition, excluding permeance analysis, there are few studies that match the characterization of the overall supported membrane and its isolated carbon supported layer.

The aim of this work is to find structural differences and similarities between carbon samples obtained in supported tubes and those obtained in unsupported planar configuration. The effect of coating layer on modification of a ceramic support has been explored using Liquid-Liquid Displacement Porosimetry (LLDP), a characterization technique that can distinguish active pores, thus contributing to actual flux, from those that do not actually interconnect both sides of the membrane. Although, it is not an objective of this work to propose a mechanism of carbon formation, a correlation has been found between the characteristics of the composite membrane and the structure of the carbon layer obtained.

2. Experimental

2.1 Preparation of asymmetric carbon membranes

The carbon precursor was a polymeric material called Matrimid (3,3',4,4'-benzophenonetetracarboxylic dianhydride and diamino-phenylindane) from Huntsman Advanced Materials. The carbon precursor was dissolved on 1-methyl-2-pyrrolidone (NMP) 99.5% (Sigma-Aldrich) at 13% w/w concentration. The solution was coated once with a pipette on a TiO₂/ZrO₂ macroporous ceramic support (Tami 1 kD membrane of 10 cm length x 4 cm outer radii) under rotation. After controlled drying, polymer-coated supports were placed in an oven at 300°C under air. This coated support was designated as supported (S) polymer (P), S_P300. In order to obtain carbon (C) supported samples two more membranes were prepared by using a higher pyrolysis temperature (550 and 700°C), designated as S_C550 and S_C700, respectively. The pyrolysis treatment was performed under a N₂ atmosphere at a total flow of 500 mL/min using a heating rate of 1°C/min. After carbonization and before any characterization, carbon materials were mechanically extracted from the tube using a manual drill. The samples were immersed in hydrofluoric acid (Sigma-Aldrich 48 wt % in water) at 60°C in order to eliminate TiO₂ particles [12].

To compare supported with unsupported samples, a solution of the same concentration of polymer was casted on a glass support and the resulting film was pyrolyzed under the same experimental conditions described above. The unsupported (NS) samples were designed as NS_C550 and NS_C700 to identify those pyrolyzed at 550 and 700°C. The morphology of the synthesized samples (supported and unsupported) was analyzed by scanning electron microscopy after sputtering with Au.

2.2 Sorption measurements

All materials were characterized by means of adsorption of probe molecules of different dimensions (CO₂, CH₄, and N₂) at different temperatures (77 K for N₂ and 273 K for CO₂ and CH₄). The respective kinetic dimensions diameters of the gases used were N₂ (0.36 nm), CO₂ (0.33 nm) and CH₄ (0.38 nm). Prior to the adsorption experiments, samples were outgassed under vacuum at 523 K for 4 h [13, 14].

2.3 Immersion Calorimetry

Immersion calorimetry measurements were performed at 303K into different liquids (n-hexane (Aldrich, $\geq 97\%$), 2-methylpentane (Fluka, $\geq 99,5\%$) and 2,2 dimethylbutane (Aldrich, 99%)) using a Setaram C80D calorimeter. Previous to each experiment, the sample was outgassed under vacuum (10^{-3} Pa) at 523 K for 4 h in a glass bulb; the bulb was later sealed and placed into the calorimetric unit that contained the immersion liquid. Once thermal equilibrium was reached the bulb was broken allowing the liquid to penetrate into the bulb and be in contact with the sample. The heat released was followed as a function of time.

2.4 Liquid-Liquid Displacement Porosimetry (LLDP)

LLDP porosimetry was performed as shown elsewhere ^[15, 16]. Prior to be placed in the porosimetric cell, supported polymer and carbon membranes were cut into pieces of 4 cm length that were sealed to both ends with a ceramic aspect enamel painting (Titanlux®) 24 hours before the porosimetric test. The liquid mixture used to perform the LLDP measurements was a mixture of Isobutanol/Methanol/Water (15:7:25 w/w). The separated aqueous-rich phase was drained off and used as the wetting liquid and the alcohol-rich phase was used as the displacing liquid. In order to achieve complete wetting of membrane samples, carbon supported membranes were immersed into the LLDP wetting phase for half-an-hour under vacuum (150 mmHg) at room temperature. Pore size was determined after pore depleting (flux-pressure plots). The mean pore size and the pore flow distribution of active pores were obtained from contributions to total flux, using an algorithm described in previous works ^[16]. From this flow distribution, and applying the Hagen-Poiseuille model for convective flow through capillary pores, flow distributions were converted into pore number distributions, which can be used to estimate the cut-off values of the analyzed membranes, as shown elsewhere ^[17].

2.5 Permeance measurements

Pure gases (CO₂ and CH₄) were fed into the module at a transmembrane pressure difference of 1 bar. Ar gas was used as a carrier and the gas composition at the exit was followed using a mass spectrometer. The permeance of supported carbon membranes was determined according to calibration curves previously established. A tubular stainless steel module, 63 mm length, o.d. 30 mm, i.d 12.2 mm containing the tubular

composite membrane was fitted with Viton o-rings that allowed the membrane housing in the module without leakage. In order to plug pinholes or defects in the composite membrane, supported carbon membranes were dip-coated on a 12% wt. polydimethyl siloxane (PDMS, Sylgard® 10:1 precursor:catalyst) solution in n-hexane (Aldrich).

3. Results and discussion

The morphology of carbon membranes was analyzed with scanning electron microscopy. Fig 1 shows photomicrographs of unsupported samples obtained after pyrolysis of the polymer at 550°C and 700°C, respectively. Contrary to observations in supported samples (shown later in Fig 2), the unsupported membranes are very dense. On the contrary, supported samples exhibit a lower density due to the presence of big holes and cavities not observed on the unsupported configuration. Apparently, the supported carbon film keeps similarities with the porous structure of the inorganic support, as it seems to copy the surface structure.

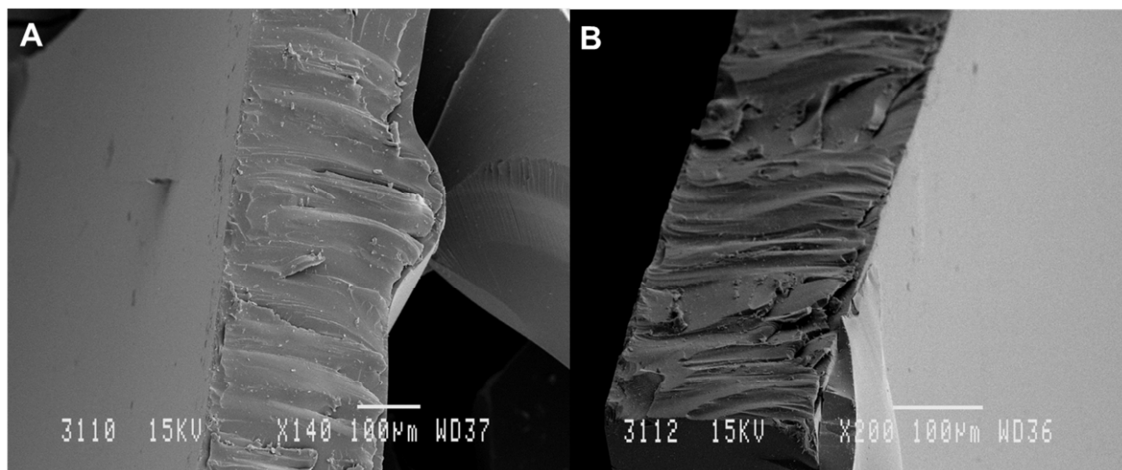


Fig 1 Unsupported carbon obtained at 550°C (A) and 700°C (B)

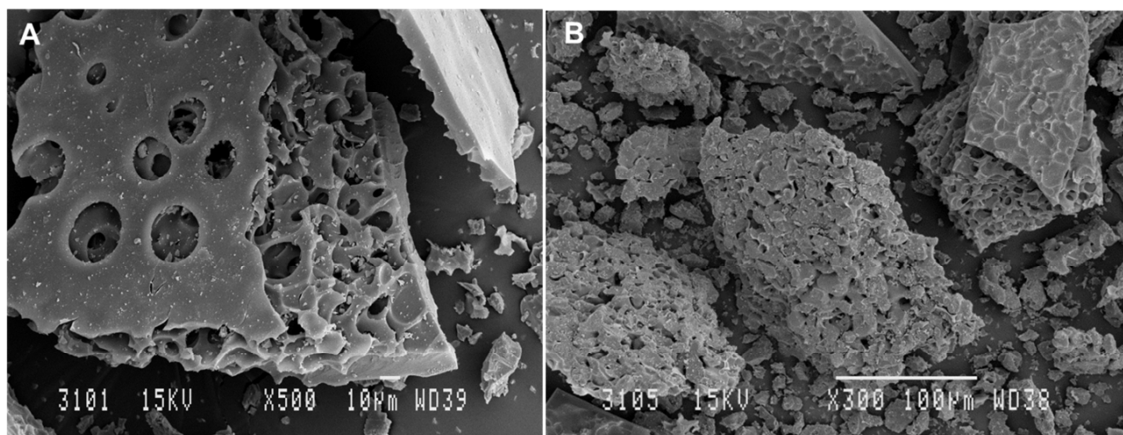


Fig 2 Supported carbon obtained at 550°C (A) and 700°C (B)

3.1 Sorption measurements

Sorption measurements were carried out to study the effect of the porous support on the textural properties of the carbon layer, as well as the effect of the pyrolysis temperature. Adsorption isotherms allow drawing conclusions about the porous structure of the material. The quantity of gas adsorbed by the adsorbent varies depending on the material structure and test conditions (pressure, temperature). The adsorption isotherms in microporous and mesoporous materials are well defined and they can be classified according to the IUPAC recommendation as type I, for purely microporous solids, and a combination of type I and IV for materials exhibiting both micro and mesoporosity^[18]. Eventually, deviations from these trends can be observed when the sample is not homogeneous or there are kinetic restrictions, i.e. cavities of molecular dimensions where probe molecules have problems of accessibility. This would imply that the desorption branch does not follow the path of the adsorption branch. In this sense, the use of different gases such as N₂, CO₂ and CH₄, with differences in kinetic diameters, will allow extracting differences between materials porosity.

N₂ adsorption was null in the synthesized materials, both supported and unsupported, thus suggesting the presence of narrow constrictions inaccessible to nitrogen at cryogenic temperatures (77 K). A similar observation was reported by Favvas et al ^[19]. The dimensions of the pores and constrictions of these carbon molecular sieves must be comparable to the kinetic diameter of the N₂ molecule and, consequently, the diffusion of this gas at cryogenic temperatures (77 K) is limited due to the very low rate of

activated adsorption producing no adsorption in the conventional time of measurement [21]. In fact, the presence of micropores is expected on the analyzed samples.

Figs 3-4 show the adsorption isotherms of CO₂ and CH₄ for supported and unsupported samples at 273 K, respectively. The amount of gas adsorbed, expressed in mmol of gas adsorbed per gram of adsorbent, is plotted as function of equilibrium pressure. As expected, the adsorption capacity is larger in all samples for a smaller molecule such as CO₂ compared to CH₄, with a larger kinetic diameter. The adsorption of these two gases at 273K shows that the adsorption of N₂ at 77K was kinetically restricted because of the low adsorption temperature, since the nitrogen molecule is smaller than methane. Furthermore, the isotherms for non-supported samples (Figure 3) are not reversible, exhibiting hysteresis, and this means that equilibrium is difficult to reach even at the high adsorption temperature of 273K, as expected in molecular sieves. When comparing supported and unsupported samples, the adsorption capacity is always lower in supported samples when using the same pyrolysis temperature, i.e. the presence of the support becomes detrimental for the final textural properties of the membrane. Finally, an increase in the pyrolysis temperature on supported samples (Fig 3) gives rise to a decrease in the total adsorption capacity for CO₂ and CH₄, whereas the opposite trend is observed for the unsupported configuration (fig 4). These results clearly suggest that i) the porous structure of the synthesized membranes highly depends on the presence of the underlying support, i.e. the presence of the support gives rise to a shrinkage of the porosity and, ii) the stability of these membranes towards an increase in the pyrolysis temperature is also highly sensible to the final conformation.

The different effect of the pyrolysis temperature on the textural properties of supported and unsupported samples can be explained based on their morphological differences. SEM analysis described above showed that supported samples copied somehow the structure of the underlying support in contrast to the unsupported samples. Most probably, the asymmetric structure of the supported membrane also affects the narrow microporosity on the denser membrane, i.e. narrower micropores, compared to the unsupported configuration, i.e. differences not only in the morphology but also in the pore size distribution for each type of samples.

In unsupported samples the adsorption capacity increases with pyrolysis temperature this implying an increase in the pore size and volume. For the same type of polyimide, Steel and Koros et al ^[22] reported an increase in the volume fraction of pores between $0.4 < x < 0.68$ nm when the final pyrolysis temperature was increased from 550 to 800°C. In fact, they reported an increase of the integral pore volume from 0.08 cm³/g at 550°C to 0.10 cm³/g at 800°C and outlined the differences in pore size distribution for both types of temperatures. They also remarked pore volume values as the determinant factor on equilibrium sorption. Also in the analysis done with unsupported Kapton, Suda and Haraya ^[23] reported micropore volumes using sorption isotherms of probe molecules with different kinetic diameters. They observed a decrease in pore volume and pore size with an increase in the pyrolysis temperature. The pore volume changed from 0.22 cm³/g to 0.15 cm³/g when temperature changed from 600 to 1000°C. The effect of pyrolysis temperature can differ even when considering the same type of polymer. For example, Lua and Su ^[24] reported an increase in CO₂ uptake with pyrolysis temperature for Kapton polyimide membranes obtained between 550-1000°C. In fact, they remarked that up to 600°C, a large portion of micropores and mesopores are created but between 600-800°C large pores shrink in parallel with formation of new micropores due to H₂ evolution during this stage of pyrolysis.

In the case of supported samples it is more common than reported for unsupported samples to find a maximum pyrolysis temperature for permeance increase. In the case of supported samples it is common to find an intermediate pyrolysis temperature that maximizes permeance. Above that pyrolysis temperature permeance and adsorption capacity decrease again implying a decrease in pore volume due to pore shrinkage. In this sense, Hayashi et al ^[25] reported an increase in permeance of CO₂ for a supported film of polyimide BPDA-ODA (3,3',4,4'-biphenyltetracarboxylic dianhydride- 4,4'-oxydianiline) membrane after pyrolysis between 500-900°C. Permeance reached a maximum at 650-700 °C, and the maximum micropore volume was near 800°C, with decreasing values above that temperature.

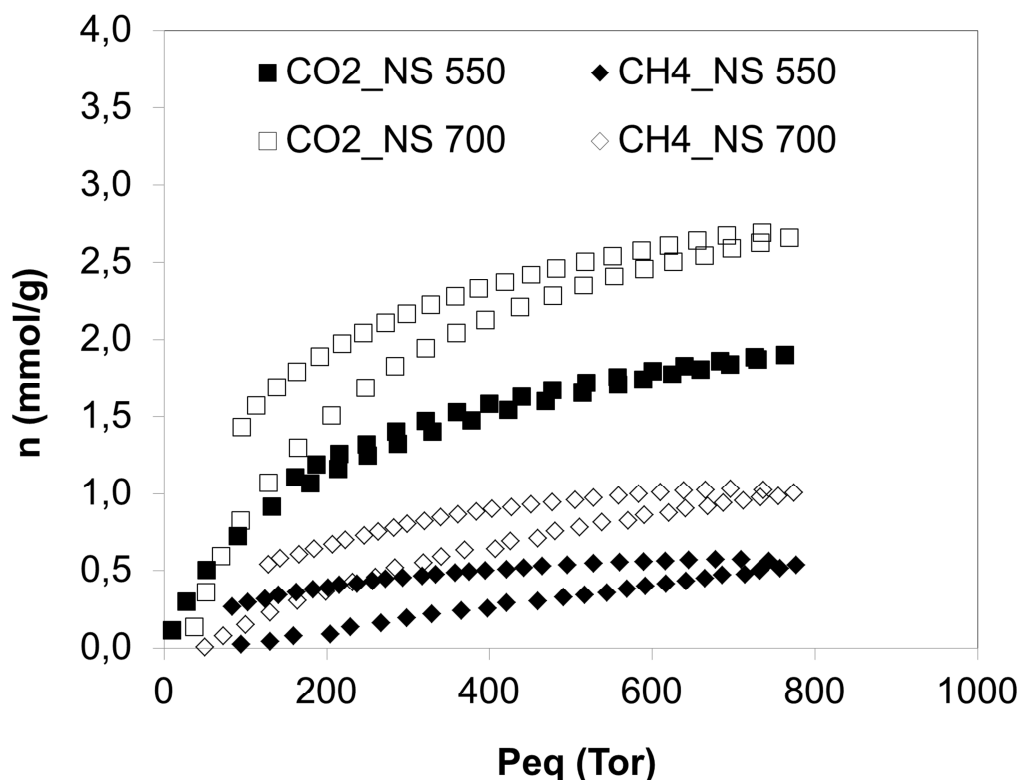


Fig 3 CH₄ and CO₂ adsorption–desorption isotherms for the different carbon non-supported membranes obtained at 550°C and 700 °C pyrolysis temperatures.

Similarly, Centeno et al ^[26] reported the development of pores near 500°C and their subsequent enlargement between 700-800°C when a phenolic resin was supported on a ceramic tubular porous support of 20 nm pore size diameter. Afterwards, pores suffered shrinkage and complete collapse near 1000°C. Those results support the existence of an optimal temperature to maximize pore volume development, after which shrinkage or enlargements probably occurs.

Differences on both types of membranes (supported vs. unsupported samples) can be observed in this work in close agreement with the literature. Moreover, these differences are more difficult to establish because they depend on the type of precursor. Suda and Haraya ^[23] already outlined that polyimide membranes could present a higher presence of amorphous regions or larger pores that could bring different structure and eventually different properties. Most probably unsupported samples must exhibit larger amorphous regions than supported samples. This effect is more important when pyrolysis temperature is also present. In both types of samples, the presence of hysteresis in the

adsorption isotherms reflects the presence of a heterogeneous porous structure with narrow constrictions, i.e. kinetic restrictions. A delay on desorption isotherms implies problems of equilibrium on the adsorption branch due to the presence of small pores/constrictions where the gas molecule has accessibility problems, the desorption branch requiring lower pressures. The reason that explains the differences between the two types of samples could be that for each system different pore size distributions determine the final adsorption-desorption capacities. Steel and Koros^[27] mentioned that there could be a tail of ultramicroporous pores in the size distribution that would determine the quantity of pores available for smallest molecules while rejecting those with higher dimensions.

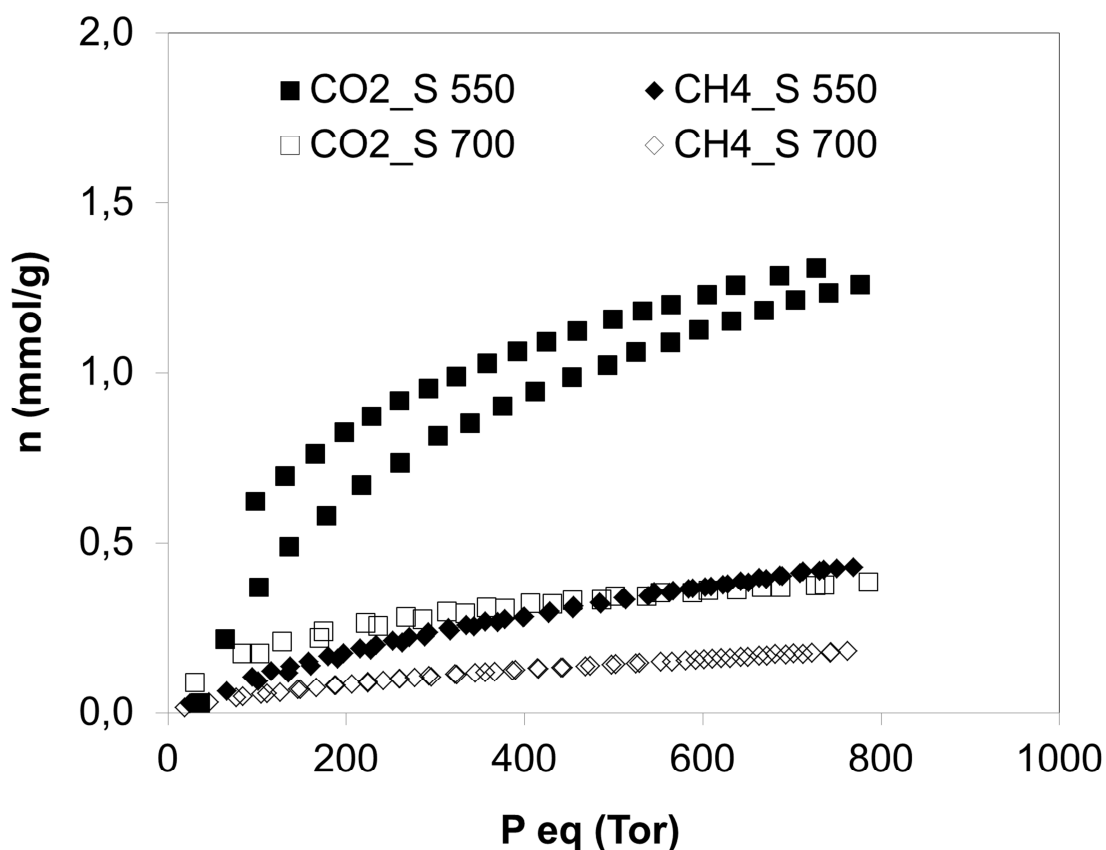


Fig 4 CH₄ and CO₂ adsorption-desorption isotherms for the different carbon supported membranes obtained at 550°C and 700°C pyrolysis temperature.

3.2 Immersion Calorimetry

In order to achieve a detailed pore size characterization immersion calorimetry was performed into liquids of different molecular dimensions as DCM (0.33 nm); Bz (0.37 nm), n-hx (0.43 nm) and 2-2 DMB (0.56 nm) [28]. As described in the previous section, molecular accessibility seems to be limited by the pore mouth on these carbon materials; an idea of the pore size, shape and pore volume can be extracted after calorimetric screening with several molecules of different molecular dimensions.

Fig 5 shows that both unsupported and supported carbon samples exhibit micropores around or below 0.33 nm, which is reflected in a large heat of immersion into a small molecule such as dichloromethane. Increasing probe molecular size gives rise to a drastic decrease in the heat of immersion, i.e. a limited accessibility. In this sense, non-supported samples do not have microporosity above 0.43 nm due the low or null heat of immersion of these samples when using n-hexane as a probe molecule. On the contrary supported samples present some heat of immersion even for n-hexane, this meaning that the pore size of supported membranes is slightly wider than for the unsupported ones. For all types of samples studied the limiting pore size value is determined to be below 0.56 due the small heat of immersion when using DMB in all the samples.

Furthermore, it is interesting to highlight the nice agreement between the adsorption results when using small molecules such as CO₂, with a kinetic diameter of 0.33 nm, and immersion calorimetry measurements using a molecule with similar dimensions as dichloromethane (0.33 nm). Taking into account that immersion calorimetric measurements are free of kinetic restrictions, the similarity between both measurements validates the adsorption results described above.

For supported samples, an increase in the pyrolysis temperature gives rise to a decrease in the heat of interaction with DCM, in close agreement with CO₂ adsorption results. On the other hand, when samples are unsupported an increase in the pyrolysis temperature produces an increase on the heat of interaction in the same way as the adsorption capacity does.

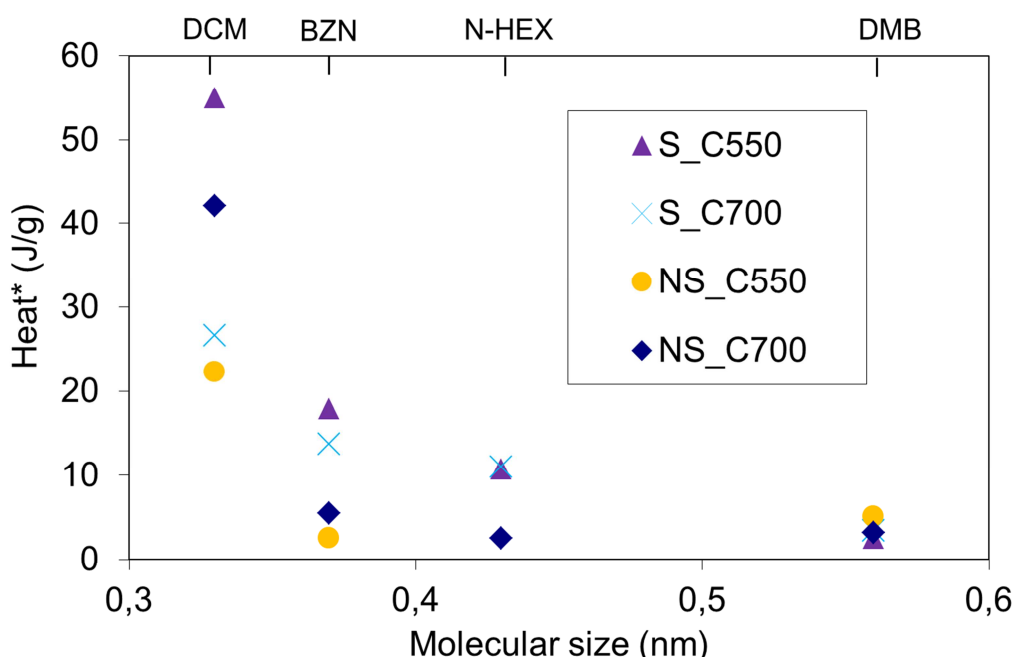


Fig. 5 Enthalpy of immersion (J/g) for the different supported and unsupported samples into liquids of different molecular dimensions (dichloromethane (DCM), benzene (BZN), n-hexane (N-HEX), 2,2-dimethyl-butane(DMB))

It is important to outline that carbon materials usually exhibit slit-shape micropores. In this sense, immersion calorimetry into benzene can be used as an extra tool to discern the shape of the microporosity (either cylindrical or slit-shape). According to Fig 5, carbon materials, e.g. NS_C550, exhibit a gradual decrease in the heat of immersion from DCM (0.33 nm) to DMB (0.56 nm) passing through Bz (0.37 nm) but not through n-hex (0.43 nm). This behavior is due to the planar configuration of benzene when accessing the micropores in these carbon materials (benzene, a disc-shaped molecule has 0.37 nm in thickness and 0.57 nm in diameter), i.e. this is a confirmation of the slit-shape configuration on these membranes (at least the supported membranes). For the unsupported samples this behavior was not identified distinctly although we would expect a similar shape.

From the heat of immersion into DCM and after the appropriate calibration using a standard non-porous carbon, the accessible surface area for a given liquid can be calculated. Table 1 shows the values of the accessible surface area for DCM in all

carbon samples studied. As observed in adsorption analysis, the influence of pyrolysis temperature is not the same in both types of supported and unsupported samples. Table 1 also reports micropore pore volume obtained after the CO₂ isotherms using the DR model. Micropore volume decreases for supported samples volume after increasing pyrolysis temperature. On the contrary, it increases after an increase of pyrolysis temperature for unsupported samples. This would explain why adsorption capacity increases with pyrolysis temperature. On the contrary, supported samples decrease just slightly the pore volume after an increase of pyrolysis temperature; this should explain the decrease in adsorption capacity observed on the adsorption-isotherms curves. Supported samples exhibit a decrease in the accessible surface area after an increase of the pyrolysis conditions. Once again these results match with those observed by adsorption isotherms and calorimetry.

Table 1 Area and pore volume of carbon samples determined by immersion calorimetry.

| Sample | Area (m ² /g) | Micropore Volume (cm ³ /g) |
|---------|-----------------------------|--|
| S_C550 | 488 | 0.017 |
| S_C700 | 236 | 0.016 |
| NS_C550 | 197 | 0.102 |
| NS_C700 | 374 | 0.263 |

3.3 Modification and characterization of the macroporous structure

In the last section the microporous character of the membranes was investigated by an analysis of the microporosity, which is the main parameter related to selectivity of carbon molecular sieve membranes. However, the support can affect the optimal performance of composite membranes. For example, when membranes are considered for membrane reactors application equilibrium between selectivity and permeance can be significant in terms of production and gas recovery [29].

CMSM have to be supported on ceramic or metallic supports to provide mechanical stability thus making them suitable for scaling-up. When a CMSM is pyrolyzed over porous supports, however, it is important to determine how the support influences the deposition of the polymer film and the resulting carbon layer. Depending on permeance it would be possible to manipulate the support during the fabrication process. However, few techniques allow a non-destructive characterization of composite membranes during fabrication due to limitations in their detection ranges. Liquid-liquid displacement porosimetry (LLDP) has been successfully used for characterization of tubular composite membranes ^[15] and it is a technique that allows a non-destructive characterization of planar or tubular supports. For this reason we considered this technique to observe the most important changes the ceramic TiO₂ support suffers when polymer or carbon layers are added. The technique is based on applying increasing pressures of a displacing fluid which should be able to displace the wetting immiscible one from increasingly smaller pores. The relation between applied pressures, P , and radius of the pores successively being emptied, r , on each step pressure is given by the Cantor equation, which requires knowledge of the interfacial tension, γ , between wetting and displacing liquids.

$$P = \frac{2\gamma}{r} \quad (1)$$

Figure 6 presents the distribution of permeabilities versus pore size, which corresponds to the contribution (in percentage) of each pore size to the total permeability. It is possible to observe that for the uncoated support the total flux is mainly governed by pore sizes in the range 2.5-4 nm. After application of the polymer layer aged at 300°C the larger pores of the support are closed and a new population of pores in the range 2.1-2.5 nm governs the flow. After pyrolysis of the supported polymer membrane the flux decreases further, thus indicating that it is governed by the pores with smallest sizes. These results agree with those reported by Sedigh et al ^[11] in the modification of an inorganic support with a carbon layer. They reported the decrease of pore sizes in the mesoporous region of the support from $5.4 \cdot 10^{-9}$ m to $3.6 \cdot 10^{-10}$ m after carbon layer coating as obtained by using N₂ adsorption. Figure 6 shows that the decrease of the largest micropores depends on the pyrolysis temperature, in agreement with the results reported for unsupported carbon membranes ^[25]. Samples pyrolyzed at 550 °C (2.3-2.6

nm) seems to present bigger micropores than those pyrolyzed at 700 °C (1.7-2 nm). Even if this technique does not allow determination of ultramicropores, it is considered useful to determine the modification of the porosity of the support with polymer coating and carbon formation.

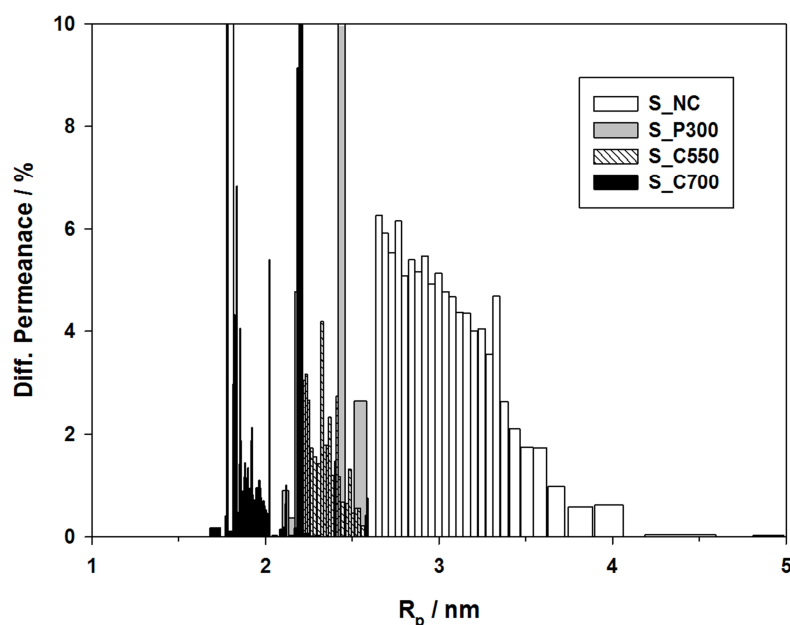


Fig 6 Permeability distribution for a Tami Support non coated (S_NC) coated with polymer (S_P300), coated with carbon pyrolyzed at 550° (S_C550) and 700°C (S_C700).

Figure 7 shows the molecular weight cut-off (MWCO) estimation of an original support and a composite membrane at different stages (polymer and carbon). The MWCO of the TiO₂ support was near 1600 Da, the difference with the nominal value reported by the manufacturer (1 kDa) attributable to the use of different measuring techniques. However the relative differences between the uncoated ceramic support and the coated elements were quantified. Once a polymer layer is applied, MWCO decreased because the larger pores in the support were blocked by the polymer. A new porosity is thus created on the ceramic support depending on the pyrolysis temperature, as already explained in terms of the pore size distributions. To summarize, the LLDP technique allows detection of the rearrangements in the structure of the support-coat ensemble due to the effect of pyrolysis temperature, and the consequent changes on porosity ^[26].

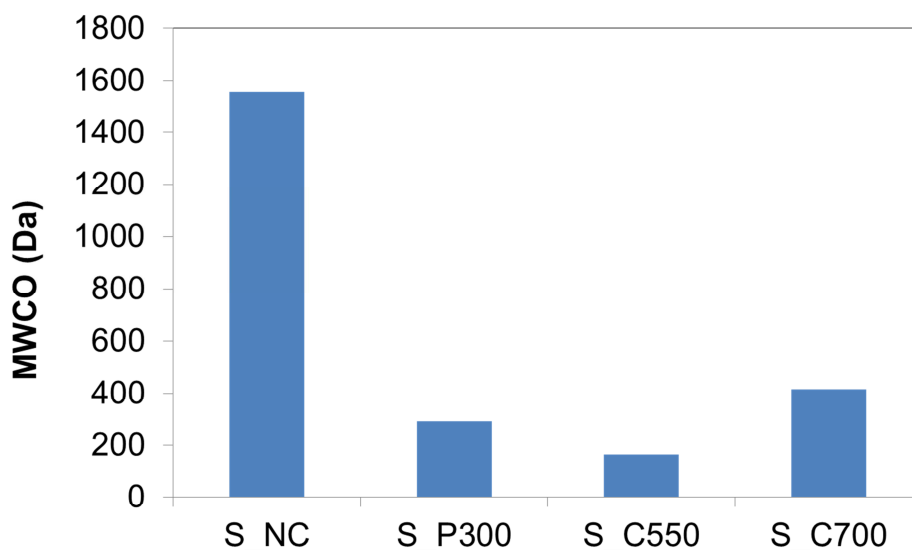


Figure 7 Molecular cut-off for TiO₂ support (S_NC), polymer supported membrane (S_P300), carbon supported membrane obtained at 550 and 700 °C (S_C550, S_C700).

3.4 Permeance and selectivity of carbon supported membranes

LLDP quantifies pores on the mesoporous and microporous ranges. However, to observe potential application on gas separation it is necessary to plug big pores or possible defects that avoid effective CO₂ and CH₄ separation. Fig 8 shows permeance and selectivity values of two different types of supported carbon membranes with and without support interactions. In the case of supported carbon membranes obtained at 550°C, permeances of CO₂ and CH₄ were $3.84 \cdot 10^{-8}$ and $6.15 \cdot 10^{-8}$ mol/m²·Pa·s respectively. This corresponds to an ideal selectivity factor of 0.62, slightly above the theoretical Knudsen selectivity value (0.60). High permeance and low selectivity suggest presence of defects in the composite membrane. For this reason, Polydimethylsiloxane (PDMS) coating was applied onto the composite membranes.

After pinholes or defect plugging with PDMS polymer, CO₂ and CH₄ permeance values decreased to $1.4 \cdot 10^{-8}$ and $2.06 \cdot 10^{-8}$ mol/m²·Pa·s respectively, with a small increase of the ideal selectivity factor to 0.68. The reason of this behavior is that PDMS only plugs big defects leaving those pores with dimensions close those of CO₂ and CH₄ molecules

unaffected. However, at 550° microporosity formation is low while increasing temperature of pyrolysis increases microporosity. At 600°C, PDMS plugging still produces low permeance values of $4.16 \cdot 10^{-9}$ and $9.31 \cdot 10^{-10}$ mol/m²·Pa·s for CO₂ and CH₄ respectively but a marked increase of the ideal selectivity factor to 4.47. Further increase of pyrolysis temperature would increase even more microporosity. However, at 700°C both permeance and ideal selectivity factor decrease compared with those for the 650°C sample. This was attributed to pore collapse, as established by the characterization of supported carbon samples by adsorption isotherms and calorimetry.

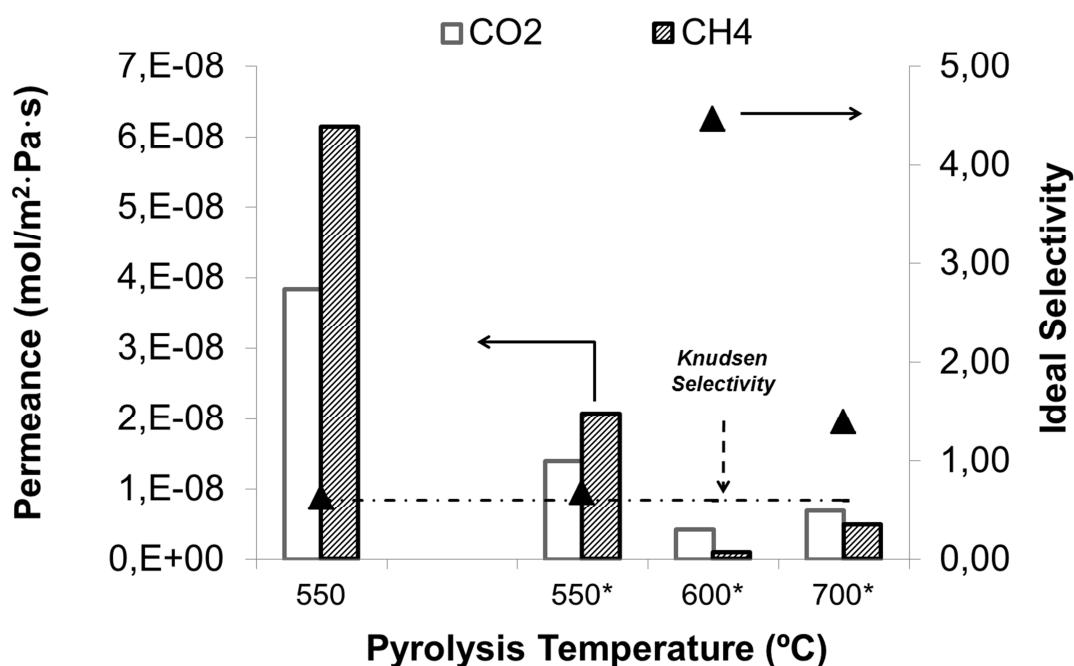


Fig 8 CO₂ and CH₄ permeance (bars) and ideal selectivity factors (▲) for supported carbon samples obtained at 550°C 600°C and 700°C. * denotes samples with an additional PDMS coating. Values measured at 23°C and 1 bar.

4. Conclusions

Unsupported carbon membranes were produced at 550°C and 700°C. Adsorption-desorption show that pore size increases with pyrolysis temperature. On the contrary, when the same polymer was coated on porous ceramic supports the pore and volume size decreased with pyrolysis temperature. Membranes on a porous support were prone to have an asymmetric structure that allowed a pore formation process differing from that obtained for dense membranes. The effect of these differences in the fabrication of

composite carbon supported membranes was monitored by LLDP as a non-destructible and fast characterization technique allowing a detailed characterization of the supports used. This information was completed with a not less detailed characterization of the pores of the carbon layer. In this case, immersion calorimetry allowed differentiation between supported and unsupported samples. There was an heterogeneous nature of the samples evidenced by different pore size distributions. The hysteresis found in both type of samples matched with the differences of heat of adsorption. Both temperature and the interactions with the support determined those differences.

The carbon structure obtained on porous ceramic support at 500°C was still incipient, and contained pinholes and defects that caused small separation factors. After pore plugging the effect of the defects was eliminated, and CO₂/CH₄ ideal separation selectivity rose above the theoretical values of a pure Knudsen-controlled transport.

5. Acknowledgements

The authors are indebted to the Spanish Government for financial support (project CTQ2008-02491, partially funded by the FEDER program of the European Union) and to the commission of European Communities Specific OpenTok Project MTKD-LT-2005-030040. Special thanks to Mr. Enrique Gadea from University of Alicante for his support on realization of experiments.

6. References

- [1] A.F. Ismail, L.I.B. David, A review on the latest development of carbon membranes for gas separation, *Journal of membrane science* 193 (2001), 1-18
- [2] H.C. Foley; Carbogenic molecular sieves: synthesis, properties and applications, *Microporous Materials* 4 (1995) 407-433
- [3] H.K. Chagger, F. E. Ndaji, M.L. Sykes, M. Thomas, Kinetics of adsorption and diffusional characteristics of carbon molecular sieves, *Carbon* Vol. 33, No. 10, (1995) 1405-1411.
- [4] A. I. Shirley, N. Lemcoff, High-Purity Nitrogen by Pressure-Swing Adsorption, *AIChE Journal*, 43, (1997), 419-424
- [5] M.B. Rao, S. Sircar, Performance and pore characterization of nanoporous carbon membranes for gas separation, *Journal of Membrane Science* 110 (1996) 109-118
- [6] J.E. Koresh, A. Soffer, The carbon molecular sieve membranes. General properties of permeability of CH₄/H₂ mixture, *Separation Science and Technology* 22 (1987), 973-982
- [7] S.M. Saufi, A.F. Ismail, Fabrication of carbon membranes for gas separation—a review, *Carbon* 42

Carbon Molecular Sieve Membranes for Gas Separation

- (2004) 241–259
- [8] A.B Fuertes, T.A Centeno, Preparation of supported carbon molecular sieve membranes, *Carbon* 37 (1999), 679-684
- [9] A. Singh-Ghosal, W.J. Koros, Air separation properties of flat sheet homogeneous pyrolytic carbon membranes, *Journal of Membrane Science* 174 (2000) 177–188
- [10] De Q. Vu, W. J. Koros, Stephen J. Miller, High Pressure CO₂/CH₄ Separation Using Carbon Molecular Sieve Hollow Fiber Membranes, *Ind. Eng. Chem. Res.* 2002, 41, 367-380
- [11] M.G. Sedigh, M. Jahangiri, P. K. T. Liu, M. Sahimi, T. T. Tsotsis, Structural Characterization of Polyetherimide-Based Carbon Molecular Sieve Membranes, *AIChE Journal* November 2000 Vol. 46, No. 11
- [12] S.Shimada, M. Yoshimatsu, M. Inagaki, S. Otani, Formation and characterization of carbon at the ZrC/ZrO interface by oxidation of ZrC single crystal, *Carbon* 36, (1998), 1125-1131.
- [13] K. Briceño, R. Garcia-Valls, D. Montane, State of the art of carbon molecular sieves supported on tubular ceramics for gas separation applications, *Asia-Pac. J. Chem. Eng.* 2010; 5: 169–178
- [14] A. B. Fuertes, Adsorption-selective carbon membrane for gas separation, *Journal of Membrane Science* 177 (2000) 9–16
- [15] J.I. Calvo, A. Bottino, G. Capannelli, A. Hernández; Pore size distribution of ceramic UF membranes by liquid–liquid displacement porosimetry, *Journal of Membrane Science* 310 (2008) 531–538
- [16] R. I. Peinador, J.I. Calvo, P. Prádanos, L. Palacio, A. Hernández; Characterisation of polymeric UF membranes by liquid–liquid displacement porosimetry; *Journal of Membrane Science* 348 (2010) 238–244
- [17] J.I. Calvo, R.I. Peinador, P. Prádanos, L. Palacio, A. Bottino, G. Capannelli, A. Hernández; Liquid–liquid displacement porometry to estimate the molecular weight cut-off of ultrafiltration membranes; *Desalination* 268 (2011) 174–181
- [18] K. S. W. Sing; D. H. Everett; R. A. W. Haul; L. Moscou; R. A. Pierotti; J. Rouquerol; T. Siemieniewska; Reporting physisorption data for gas/solid systems with special reference to the determination of surface area and porosity, *Pure & App. Chem.*, Vol. 57, No. 4, pp. 603–619, 1985.
- [19] E. P. Favvas E. P. Kouvelos G. E. Romanos G. I. Pilatos A. Ch. Mitropoulos N. K. Kanellopoulos, Characterization of highly selective microporous carbon hollow fiber membranes prepared from a commercial co-polyimide precursor, *J Porous Mater*, 186 (2007) 102–110
- [20] R.V.R.A Rios, J. Silvestre-Albero, A. Sepulveda-Escribano, M. Molina-Sabio, F. Rodriguez-Reinoso, *J. Phys Chem C* 111, 3803-3808 (2007);
- [21] F. Rodriguez-Reinoso, J. de D. Lopez-Gonzalez, C. Berenguer, Activated carbons from almond shells— I: Preparation and characterization by nitrogen adsorption, *Carbon* 20, 513 (1982)
- [22] K.M. Steel, W. J. Koros, Investigation of porosity of carbon materials and related effects on gas separation properties, *Carbon* 41 (2003) 253–266
- [23] H. Suda, K. Haraya, Gas Permeation through Micropores of Carbon Molecular Sieve Membranes Derived from Kapton Polyimide, *J. Phys. Chem. B* 1997, 101, 3988-3994
- [24] A. C. Lua, J. Su, Effects of carbonisation on pore evolution and gas permeation properties of carbon membranes from Kapton_ polyimide, *Carbon* 44 (2006) 2964–2972
- [25] J. Hayashi, M. Yamamoto, K. Kusakabe, S. Morooka, Simultaneous Improvement of Permeance and Permselectivity of 3,3',4,4'-Biphenyltetracarboxylic Dianhydride-4,4'-Oxydianiline Polyimide Membrane by Carbonization, *Ind. Eng. Chem. Res.* 1995,34, 4364-4370

- [26] T.A. Centeno, J.L. Vilas, A.B. Fuertes, Effects of phenolic resin pyrolysis conditions on carbon membrane performance for gas separation, *Journal of Membrane Science* 228 (2004) 45–54
- [27] K.M. Steel, W. J. Koros, An investigation of the effects of pyrolysis parameters on gas separation properties of carbon materials, *Carbon* 43 (2005) 1843–1856
- [28] J. Silvestre-Albero, C. Gomez de Salazar, A. Sepulveda-Escribano, F. Rodriguez-Reinoso, Characterization of microporous solids by immersion Calorimetry, *Colloids and Surfaces, A: Physicochemical and Engineering Aspects* 187–188 (2001) 151–165
- [29] D.W Lee, S.J Park, C.Y Yu, S.K Ihm, K.H Lee, Study on methanol reforming–inorganic membrane reactors combined with water–gas shift reaction and relationship between membrane performance and methanol conversion, *Journal of Membrane Science*, (2008), 63–72

CHAPTER 6:

Carbon Molecular Sieve Membranes Supported on Non-modified Ceramic Tubes for Hydrogen Separation in Membrane Reactors

(Art. 5)

International Journal of Hydrogen Energy

(Accepted 2012)

Carbon Molecular Sieve Membranes Supported on Non-modified Ceramic Tubes for Hydrogen Separation in Membrane Reactors

Kelly Briceño^{a*}, Adolfo Iulianelli^c, Daniel Montané^b, Ricard Garcia-Valls^a, Angelo Basile^c

^a *Department d'Enginyeria Química, Universitat Rovira i Virgili, Av. Pasos Catalans, 26, 43007, Tarragona, Spain*

^b *Catalonia Institute for Energy Research (IREC). Bioenergy and Biofuels Area. Building N5. Universitat Rovira i Virgili. C/ Marcel·lí domingo, 2. 43007, Tarragona, Spain*

^c *ITM-CNR via P. Bucci c/o University of Calabria - Cubo 17/C, Rende (CS) - 87036 – Italy,*

* *Corresponding author e-mail: kelly.briceno@urv.cat*

Tel: + 34 977 558506

Abstract

Supported carbon membranes have been regarded as more competitive than traditional gas separation materials due to the versatile combination of different pyrolyzable polymers and supports which in turn leads to high separation factors and mechanical stability. In order to determine the extent to which supported carbon membranes are more competitive, the transport mechanism of supported carbon membranes was investigated in the range 32-150 °C and 1-2.5 bar. Polyimide (Matrimid 5218) material was coated and pyrolyzed under N₂ atmosphere on TiO₂-ZrO₂ macroporous tubes (Tami) that had not been structurally modified in any way. The supported carbon membrane was studied to determine its permeation for low molecular weight gases such as H₂, CH₄, CO, N₂ and CO₂. For these gases, the permeance of the composite supported carbon membranes obtained after pyrolysis at 550 °C increased with inverse square root of molecular weight. The temperature dependence of the permeance was described using an Arrhenius law with the negative activation energies for hydrogen, carbon dioxide and nitrogen providing evidence of a non-activated process. The ideal separation selectivity computed from single gas measurements leads to values slightly lower than the Knudsen because of the influence of viscous flow. The coexistence of more than one transport mechanism in the composite membrane was confirmed. After plugging the possible defects with Polydimethylsiloxane (PDMS), the supported carbon

membranes obtained at a pyrolysis temperature of 650 °C showed evidence of a molecular sieving mechanism. This paper shows the separation properties of a crack-free supported carbon membrane obtained using a simple fabrication method that does not require modification of the mesoporous support. The permeance and selectivity values were compared with those of other hydrogen selective materials. Finally, the membranes were applied to methanol steam reforming (MSR).

KEYWORDS: Supported carbon membranes, gas separation, hydrogen separation, molecular sieve membranes, Knudsen diffusion, membrane reactors

1. Introduction

A significant part of the scientific community is engaged in finding alternative solutions to the current energy and environmental problems. Hydrogen has been proposed as the main vector for achieving clean energy. It can be obtained by separating syngas in a coal-fired integrated gasification combined cycle (IGCC)^[1]. Integrating membranes into gasification systems in order to separate hydrogen and CO₂ uses less energy than traditional hydrogen purification technologies do. This system has a lot of hydrogen purification units; therefore, membrane separation units can be used strategically at different points of the cycle ^[2]. One of these, for example, is the water gas shift reaction (WGS), which can be coupled to traditional process units or more modern membrane reactors (MR). Membranes can be integrated into a membrane reactor (MR) after the retentate space has been packed with catalyst or being the membrane catalytic by itself ^[3]. This configuration shifts the thermodynamic equilibrium towards the products whilst increasing conversion. Furthermore, obtaining membranes on an inorganic tube is useful for scaling-up applications. This forms a tubular composite membrane with an enhanced surface/area ratio of reaction due to the compact configuration.

However, placing hydrogen separation membranes on inorganic supports is not a simple task because of the potential formation of defects. Hennis and Tripodi ^[4] demonstrated that is rather difficult to achieve an adequate thin skin without pinholes when coating a porous support. They highlighted the advantages of using thicker coatings over highly porous substrates to avoid the fabrication problems that occur with thinner layers. The effective separation in a resistant model (RM) membrane is determined principally by

the substrate and not by the coating, provided that porosity of the support is sufficiently high to allow a thick coating layer. This means that the performance of the composite membrane depends on the coating thickness matching the porosity of the support. By varying the thickness of the coating layer, differences in flux can be obtained on the same support. This is achieved by controlling the formation of the separation layers. Different structures and different transport mechanisms can be obtained that will define the separation properties and performance of the composite membrane. Moreover, membranes with similar compositions may have different capabilities depending on the final application.

For example, Park et al. ^[5] have reported using stainless steel supported Knudsen membranes in a dimethyl ether (DME) reforming membrane reactor to produce hydrogen after modifying the stainless steel porous support with colloidal silica sol containing 1 nm sized silica spheres. They also modified the same type of support using boehmite and polymeric silica sol to obtain different membrane structures for methanol steam reforming (MSR) combined with WGS reaction ^[6]. They showed that the microporous structure does not favor high hydrogen recovery. Also, mesoporous and macroporous membranes do not favour efficient removal of CO because of their low separation properties. This suggests that controlling the membrane structure is very important because this determines the membrane's corresponding transport mechanism. The types of transport mechanism for porous membranes are molecular diffusion and viscous flow (macropores and mesopores), Knudsen diffusion (mesopores), surface diffusion (mesopores and micropores) and activated diffusion (micropores) ^[3]. In order to choose the most suitable transport mechanism for a specific application, the structure-properties relationship of the composite membrane must be fully determined. However, most research on the use of membranes in MRs has studied membrane materials in terms of the selective layer and does not take into account the influence of the support ^[7]. A proper balance between selectivity and permeation has to be found for each type of gas separation application.

Different materials have been considered for fabricating MRs and include metal ^[8], alumina ^[6] and zeolites ^[9]. However, some of these membranes are expensive (e.g. Pd^[10]), require several fabrication steps in controlled conditions (e.g. alumina ^[11]) or are difficult to synthesize (e.g. zeolites ^[12-13]). These drawbacks are especially evident when these materials have to be used in MR applications ^[12] because they need to be

supported in order to be mechanically stable. Consequently alternative materials must be obtained that enable good gas separation properties from simple fabrication methods.

Carbon molecular sieve membranes (CMSM) obtained after polymer precursor pyrolysis have been extensively reported in gas separation applications ^[14-18]. The excellent characteristics of these membranes in unsupported form can be maintained by controlling fabrication conditions such as pyrolysis temperature ^[16] and heating rate ^[18]. Fabrication variables create different pore sizes and populations which direct different transport mechanisms such as molecular sieving, selective surface flow and the Knudsen mechanism ^[19-20]. Moreover, the fabrication method also influences the carbon structure, thereby affecting the membranes' transport mechanism ^[15].

Despite the advantages reported for unsupported and supported CMSM in gases separation, they are not mechanically stable. They must be supported in order to overcome their mechanical instability and being suitable for industrial applications. Although, fabrication of supported membranes is not a simple matter, few examples successfully report their use in MR ^[21-22]. There are still some limitations to increase their applicability at high scale, as their hydrothermal stability at high temperatures. However, the development of a membrane combined with low temperature catalyst has opened up new opportunities for their use in MR configurations ^[6,23]. Moreover, fabricating carbon membranes over tubular supports for use in MR applications deals with the problem of how to obtain a membrane with no cracks or defects after polymer pyrolysis. This problem, which has been encountered when coating porous surfaces with inorganic layers ^[3], becomes critical in the case of gas separation, and strategies have been developed to solve it that involve using multiple coatings ^[24] or reducing the pore size of the mesoporous support with colloidal sol ^[25]. However, these strategies increase the cost of the membrane and its fabrication time.

The main objective of this paper is to determine the permeation and selectivity properties of carbon molecular sieve membranes supported on macroporous tubular ceramics that are intended for hydrogen separation applications. In order to achieve high permeance values, the fabrication method presented here does not take into account any previous modification of the mesoporous support, which is a different approach from the traditional fabrication methods reported in bibliography. The transport mechanisms of pure gases frequently found in syngas mixture is related to the structure of the

composite membrane. The membrane performance includes the influence of the support before and after its defects have been plugged. This study aims to find a competitive way of applying carbon membrane supported membranes in a field traditionally dominated by alumina membranes ^[5,6,26]. The study also presents an application of MRs in methanol steam reforming.

2. Experimental

2.1 Preparation of the polymer solution and ceramic tube coating

Matrimid solutions were prepared by dissolving 13 wt% of Matrimid in 1-methyl-2-pyrrolidone (NMP) from Sigma-Aldrich for 4 hours with mechanical stirring. The mixture was maintained under a controlled vacuum to remove all air bubbles from the solution. Polymer supported membranes were prepared by distributing a uniform layer of the polymeric solution over the external surface of a tubular ceramic support (1 kD membrane of 4 cm in length x 10 cm outer radii; Tami). The ceramic tube consisted of a TiO₂ structure that supported a ZrO₂ membrane located on the inner part of the tube. Table 1 shows the dimensions of the support's pores and its internal layer. The support was mounted horizontally and rotated at constant speed during the deposition of the polymer solution. Around 3 g of polymeric solution were deposited with a pipette. The membranes were then aged at 110 °C for 24 h, washed with methanol and then placed at 300 °C for 2 h in air atmosphere to allow slow removal of the solvent.

Table 1. Parameters of the TiO₂ ceramic support

| Pore diameter (ZrO ₂) (nm) | Pore diameter (TiO ₂) (µm) | Porosity (ZrO ₂ /TiO ₂) |
|--|--|---|
| 2-3 | 4.5-5.5 | 20-28% |

2.2 Preparation of supported carbon membrane

The supported carbon membranes were prepared after the polymer supported membranes had been placed inside a tube furnace. The polymer pyrolysis was performed following a temperature program up to 550, 650 and 700 °C at a constant heating rate of 1°C/min under a flow rate of 500 ml/min of nitrogen.

2.3 PDMS Coating of tubular ceramic supports

Due to the high permeance of the original tubular supports, it was not possible to measure single gas permeance. For this reason the PDMS coating was optimized in order to obtain lower fluxes. A 12% wt polydimethyl siloxane (PDMS) (Sylgard@ 10:1 precursor:catalyst) in n-heptane was applied to the raw ceramic tubes. Later this coating was applied to the supported carbon membranes in order to study the gas transport mechanism without support influence.

2.4 Permeance measurements at room temperature

Pure H_2 , N_2 , CO , CO_2 , CH_4 , were fed into the module at a transmembrane pressure difference of between 0.5 and 3 bar. Ar gas was used as a carrier to feed the sample to a mass spectrometer. The permeance of supported carbon membranes was determined according to previously established calibration curves. A tubular stainless steel module of 63 mm in length, o.d. 30 mm and i.d. 12.2 mm was used to contain the tubular composite membrane (Fig. 1). The membrane was fitted with Viton o-rings that allowed the membrane to be housed in the module without leakages.

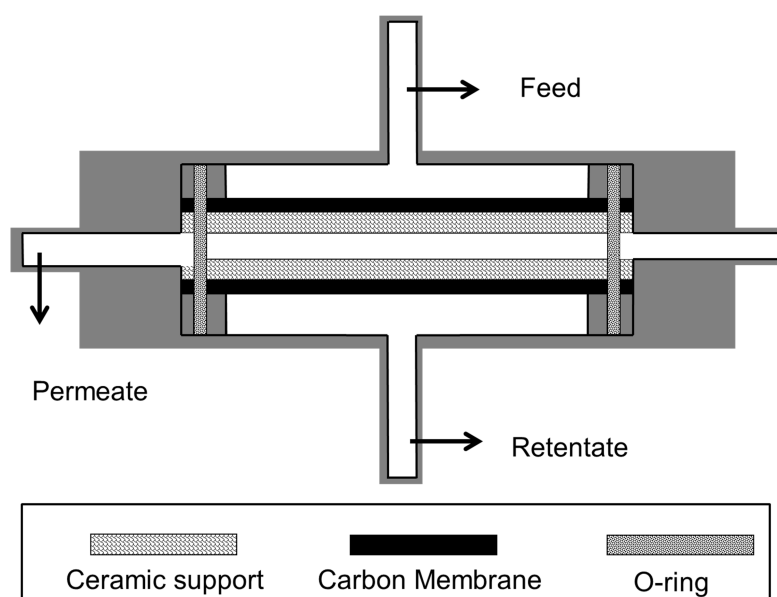


Fig. 1. Schematic view of carbon supported membrane in the permeation module

2.5 Permeance of supported carbon membranes at different temperatures

Single gas permeation of a supported carbon membrane without PDMS coating was measured with pure H₂, N₂, CH₄, CO, CO₂ gases in the range of 26-150 °C. The membrane was housed in the same module used in section 2.4. A single gas test was conducted using the pressure variation method, which involved controlling the pressure of the retentate after creating a pressure difference with the permeate side. The transmembrane pressure was varied in the range of 1-2.5 bar and the flux of the permeated gases was measured using a soap film flow-meter. The ideal selectivity of the membrane was defined as the ratio of hydrogen permeance to another pure gas permeance measured at the same transmembrane pressure and temperature.

2.6 Membrane reactor tests

The supported carbon membrane obtained after pyrolysis at 550°C was inserted into the same MR module used in the gas permeation experiments (section 2.4). The tubular supported membrane was plugged from one side and reactants were fed by means of a stainless steel tube (o.d. 1/16 in., i.d. 1/40 in.) placed outside the membrane lumen.

For the methanol steam reforming, membrane reactor catalyst pellets were carefully packed between the outer radii of the membrane and the inner radii of the reactor. 1 g of an ICI 83-3 (51% CuO, 31% ZnO, 18% Al₂O₃) catalyst purchased from Syntex (UK) was used in the methanol steam reforming experiments. The experiments were carried out in a reaction temperature range of 200-250 °C and using a H₂O/MeOH mixture with a molar ratio of 3, at a liquid feed flow rate of 0.03 mL/min. The H₂O/MeOH mixture was evaporated in a preheating line. No sweep gas was used. The pressure difference was 2 bar. Gas chromatography was used to analyze the concentrations of products and reactants in the retentate and permeate sides. Methanol conversion, hydrogen purity, yield and hydrogen selectivity in the membrane reactor were calculated according to equations (1) to (3). To calculate hydrogen yield, the molar flow rate of hydrogen produced was related to the maximum stoichiometric yield attainable by steam reforming (equation 4).

$$\text{Conversion to gas (\%)} = \frac{(\text{CO} + \text{CO}_2)_{\text{out}}}{\text{CH}_3\text{OH}_{\text{in}}} \cdot 100 \quad (1)$$

$$\text{Permeate purity}_{\text{H}_2} (\%) = \frac{\text{H}_{2, \text{permeate}}}{(\text{H}_2 + \text{CO} + \text{CO}_2)_{\text{permeate}}} \cdot 100 \quad (2)$$

$$\text{yield}_{\text{H}_2\text{-TOT}} (\%) = \frac{\text{H}_{2, \text{out}}}{3\text{CH}_3\text{OH}_{\text{in}}} \cdot 100 \quad (3)$$



The subscript “OUT” indicates the total outlet flow rate (for both the retentate and permeate sides) of each species while “IN” refers to the feed stream.

In the case of the traditional reactor (TR), the permeate side of the MR was closed and the reaction was carried out under the same conditions of space velocity, pressure and temperature.

The subscript “OUT” indicates the total outlet flow rate (for both the retentate and permeate sides) of each species while “IN” refers to the feed stream.

In the case of the traditional reactor (TR), the permeate side of the MR was closed and the reaction was carried out under the same conditions of space velocity, pressure and temperature.

3. Results and discussion

3.1 Membrane permeance and selectivity of supported carbon membranes obtained at 550°C

The permeance of supported carbon membranes obtained at 550°C was evaluated for H₂, CH₄, CO, N₂ and CO₂ in order to determine their transport mechanism. Fig. 2 shows that the single gas permeance increases with the average pressure difference at 150 °C.

In the literature, the fact that permeance increases with the pressure difference has been reported as evidence of viscous flow^[27]. This behaviour is also observed in inorganic

membranes as a consequence of defects or pinholes that occur during fabrication [28].

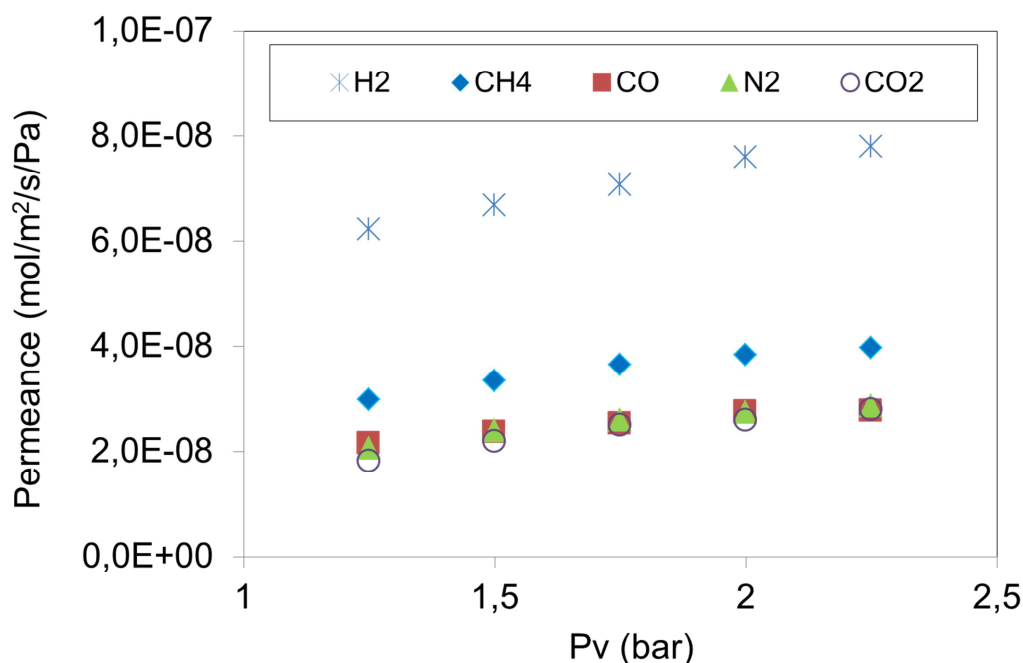


Fig 2 Permeance vs average pressure for a supported carbon membrane (150 °C)

Fig. 3 shows that permeance depends on the square root of the molecular weight of gases. A good fit to linear regression was obtained ($r^2=0,9779-0,9895$), thus indicating the presence of the Knudsen diffusion mechanism. The Knudsen mechanism is therefore the main transport mechanism of the supported carbon membranes reported in this study. However, it is well known that Knudsen diffusion does not depend on temperature [29]. On the contrary, temperature influence is thought to cause a deviation from a pure Knudsen diffusion, especially at low temperatures, due to a possible adsorption effect at the pore walls [30]. Consequently, a more detailed analysis was carried out. The results of this analysis can be seen in Fig. 4, which shows permeance versus the inverse of square root of temperature. In this case, even though the fitting parameters are lower ($r^2=0,8547-0,9063$) than the previous ones, the influence of temperature on the whole transport mechanism of the membrane is still evident.

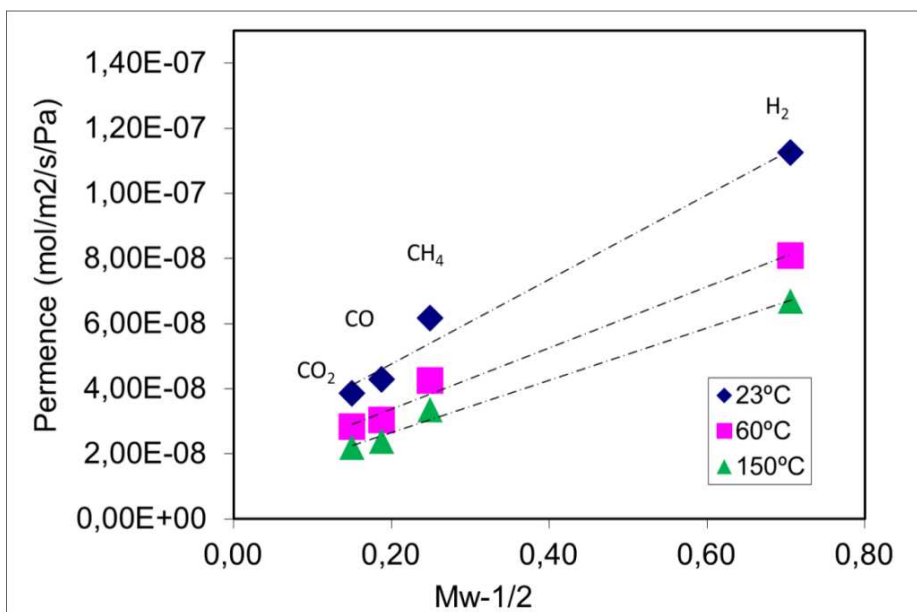


Fig 3 Gas permeance vs $1/\sqrt{M_w}$ for carbon supported membrane at different permeation temperatures ($\Delta P= 1$ bar).

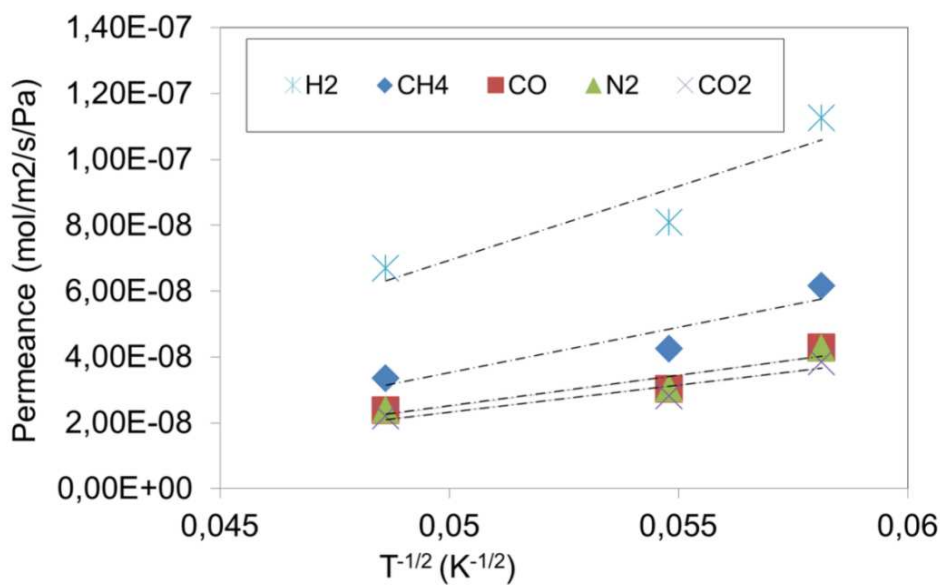


Fig 4 Gas permeance vs $1/\sqrt{T}$ for a carbon membrane for different gases ($\Delta P= 1$ bar)

Temperature influence on permeance can be described using Arrhenius type dependency, as in equation (5)

$$Q = Q_0 \exp\left(\frac{-E_a}{RT}\right) \quad (5)$$

where Q is the gas permeance, Q_0 the pre-exponential factor ($\text{mol/m}^2 \cdot \text{s} \cdot \text{Pa}$), E_a the activation energy ($\text{J/mol} \cdot \text{K}$), R the gas constant and T the absolute temperature (K).

In supported carbon membranes with molecular sieving behaviour, the activation energy parameter for the gases is positive because of the activated diffusion transport mechanism^[31]. However, for the same group of gases, the activation energy can become negative if the interactions between gas molecules and pore walls are altered by changes in surface polarity, pore size dimension or pore population. Table 2 shows the pre-exponential term and negative activation energy calculated for H_2 , CH_4 , CO , N_2 and CO_2 . These data are compatible with non-activated transport mechanisms^[28] and are comparable to those reported by Kusakabe^[32] regarding a surface diffusion mechanism for carbonized polycarbosilane supported on alumina membranes, and those reported by Richard et al.^[28] for a microporous silica membrane with a predominant Knudsen mechanism.

Table 2. Arrhenius coefficient for a supported carbon membrane at $\Delta P = 1$ bar

| Gas | Pre-exponential factor ($\text{mol/m}^2 \cdot \text{s} \cdot \text{Pa}$) | Activation energy (E_a) kJ/mol |
|---------------|---|---------------------------------------|
| H_2 | 2.03E-08 | - 4.07 |
| CH_4 | 8.30E-09 | - 4.78 |
| CO | 6.10E-09 | - 4.66 |
| N_2 | 6.41E-09 | - 4.54 |
| CO_2 | 6.08E-09 | - 4.43 |

From the previous data we may conclude that at least three transport mechanisms coexisted in the supported carbon membranes reported in this study, these being:

Knudsen, viscous flow and surface diffusion. The coexistence of more than one transport mechanism has been reported, for example, in asymmetric hollow fiber membranes [33,34]. Knudsen and viscous flows are related to the mesoporous part of the structure, while surface diffusion is closely related to the effect of temperature on the microporous domain. Depending on the size of the gas molecules and the size of the membrane pores, this effect can involve activated or non-activated diffusion. In the present study, Fig. 4 shows a change of slope at $T^{-1/2} = 0.054 \text{ K}^{-1/2}$ which corresponds to $60 \text{ }^\circ\text{C}$. Liu et al. [35] reported 50°C as a limiting temperature where both gas adsorption and diffusion coexist, with adsorption being predominant at the lowest temperature.

The effect of permeance temperature on the transport mechanism of supported carbon membranes became more evident when the ideal selectivity factors are analyzed. Fig. 5 shows how the ideal selectivity factor for different pairs of gases depended on temperature. Ideal selectivity factors computed from single gas permeation values were similar for most of the pairs of gases analyzed, with exception of the H_2/CO_2 pair. This is due to the marked surface adsorption of CO_2 at low temperatures.

The influence of pressure on the transport mechanism of this type of membrane was also studied. A comparison of Fig. 5 and Fig. 6 shows small fluctuations from ideal selectivity values below $60 \text{ }^\circ\text{C}$ for H_2/CH_4 , H_2/CO , and H_2/N_2 . Surface diffusion effects for highly condensable gases such as CH_4 and CO_2 are to be expected. Therefore, it is important to outline the small contribution made by surface diffusion to the overall transport mechanism of the membrane. The transport mechanisms for the different types of gas are highly influenced by the pore size.

We compared the single gas permeance values of supported carbon membranes measured at 150°C in the present study with those obtained by Fuertes and Centeno [24] after they had made an initial coating of a carbon layer over a macroporous carbon support modified with an intermediate carbon layer. They reported values of $1.19 \cdot 10^{-8}$ and $8.2 \cdot 10^{-9} \text{ mol/m}^2 \cdot \text{Pa} \cdot \text{s}$ for CO_2 and CH_4 respectively and an Ideal Selectivity Factor (ISF) of $\text{CO}_2/\text{CH}_4 = 1.45$. In the present study, the support was not modified and these gases show higher permeance values of $1.26 \cdot 10^{-8}$ and $1.86 \cdot 10^{-8} \text{ mol/m}^2 \cdot \text{Pa} \cdot \text{s}$ and a lower ISF of 0.68, which is still above the Knudsen theoretical value of 0.60. We also compared the single permeance values for H_2 and N_2 reported by Shiflett and Foley [36].

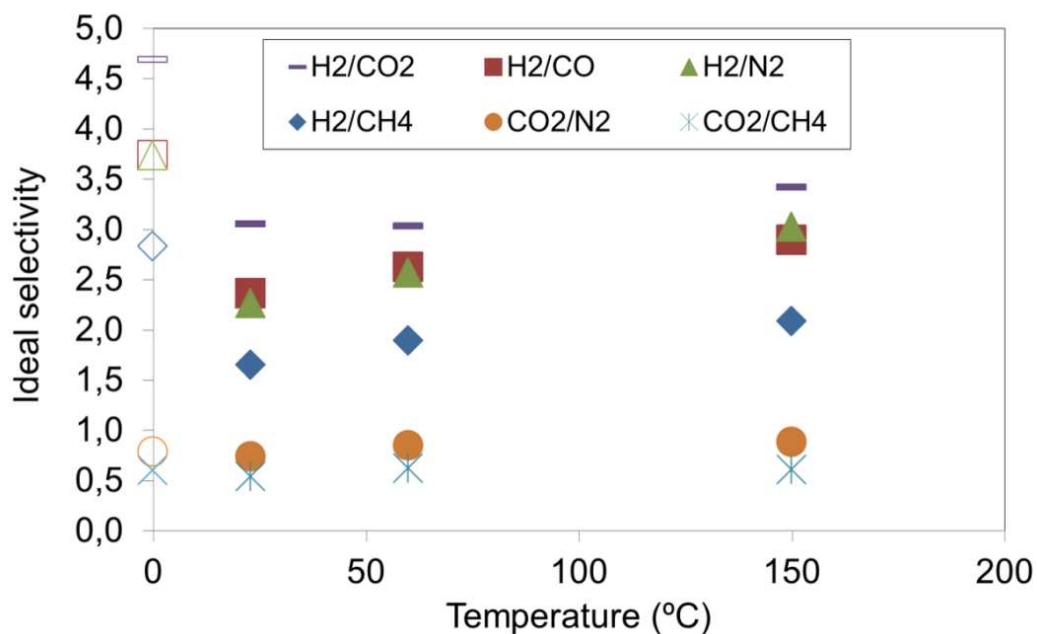


Fig. 5 Ideal selectivity factor vs permeation temperature for different pair of gases at $\Delta P = 0.5$ bar (empty symbols= Ideal Knudsen theoretical values)

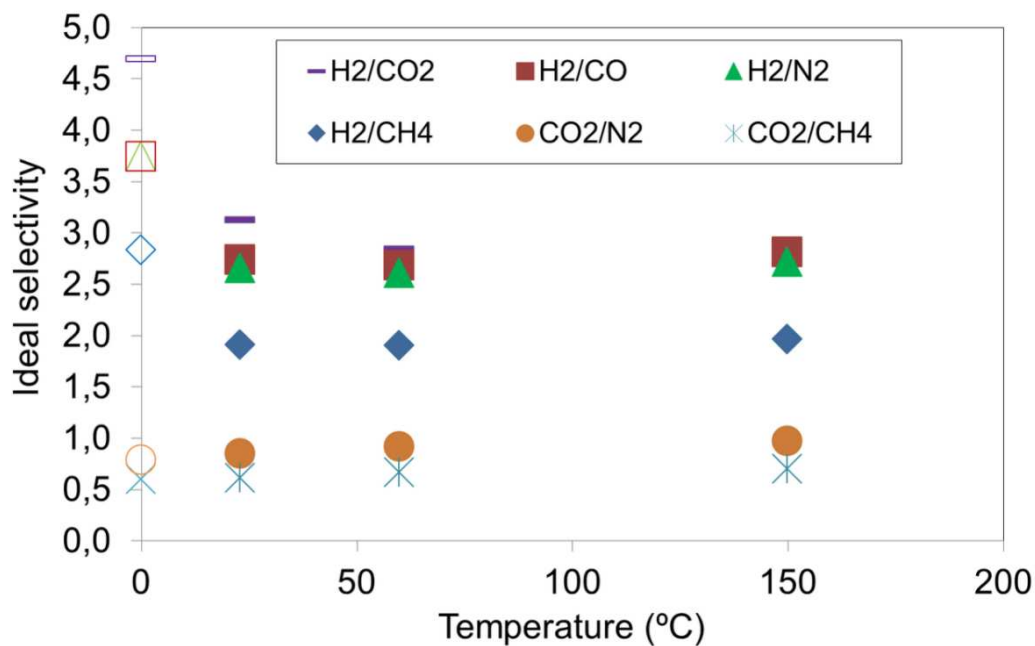


Fig. 6 Ideal selectivity factor vs permeation temperature for different couples of gases at $\Delta P = 2.5$ bar (empty symbols= Ideal Knudsen theoretical values)

They reported values of $4.09 \cdot 10^{-8}$ and $6.5 \cdot 10^{-9}$ mol/m²·Pa·s and an ISF of 6.3 for a supported carbon membrane placed over a stainless steel tube by ultrasonic deposition of the polymer solution. In contrast, we obtained a permeance of $6.25 \cdot 10^{-8}$ mol/m²·Pa·s for H₂ and $2.37 \cdot 10^{-8}$ mol/m²·Pa·s for N₂ and an ISF of 2.64, which was slightly lower than the Knudsen theoretical value of 2.65. These results are important because there is no report in the literature of any modification of the macroporous support or simple fabrication method that achieves comparable results. In addition, it is important to mention that the membrane compared with those studies was obtained at a pyrolysis temperature of 550°C. As the next section will show, these values can be improved by using a different pyrolysis temperature and an alternative strategy to reduce the influence of defects.

3.2 Molecular sieving behavior of supported carbon membranes after PDMS coating

In order to observe which type of transport mechanism was present in the raw support when there was no influence from pinhole defects, a 12% wt PDMS coating was optimized in original ceramic tubes and then applied to the supported carbon membranes obtained at different pyrolysis temperatures. PDMS is a rubber material with low selectivity and high permeability due to the high flexibility of its siloxane linkages^[37]. The effect of the PDMS coating on reducing convective flow caused by defects has also been investigated in the literature by other authors^[38,39]. Indeed, the application of PDMS to carbon membranes can reduce the effect of viscous flow. This hypothesis was confirmed after applying a PDMS solution. Fig. 7 shows the room-temperature permeance of supported carbon membranes pyrolyzed at 550 °C with or without PDMS coating. After coating with PDMS the viscous flow and Knudsen diffusion in supported carbon membranes decreased. However, the CH₄ permeance values increase with pressure difference, which means the PDMS did not fully plug the pores. On the contrary, the permeance of CO₂ keeps constant with pressure. It seems that a PDMS coating plugs pores similar in size to CO₂ but does not plug pores larger than CO₂ kinetic diameter (0.33 nm) because it allows the permeance of larger species as in the case of CH₄ with a kinetic diameter of 0.38 nm.

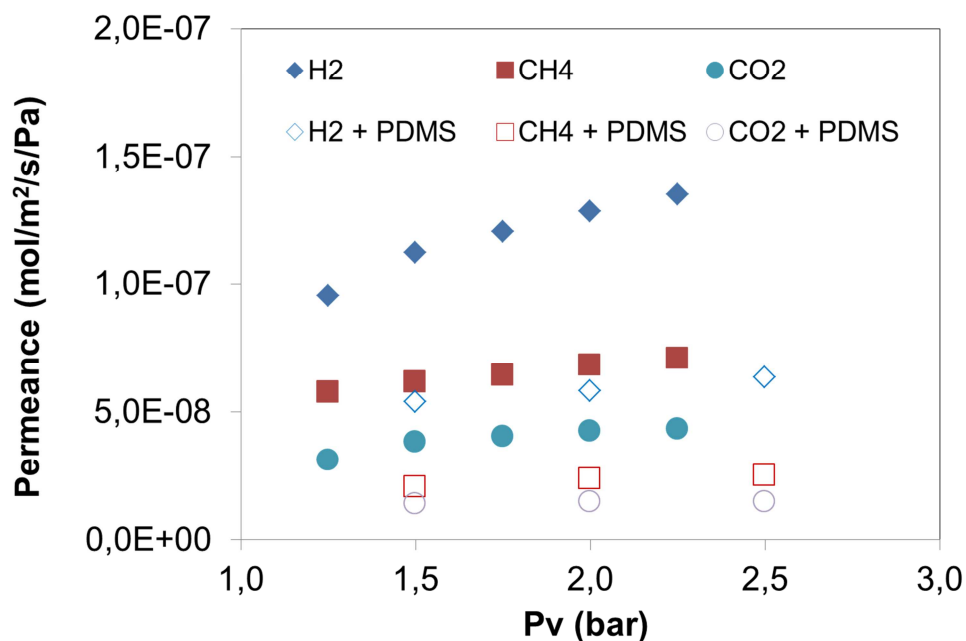


Fig. 7 Permeance versus average pressure in supported carbon membranes with and without PDMS coating.

3.3 Effect of pyrolysis temperature on molecular sieving behavior of supported carbon membranes

The defects were plugged in order to determine the transport mechanism in membranes obtained at different pyrolysis temperatures. By visual inspection crack-free supported carbon membranes were obtained at 550, 650 and 700 °C. As shown in the previous section, smallest defects or pinholes, which were not detected under visual inspection, were reduced by PDMS coating. The influence of support as pinhole promoter was minimized which allowed exploring the transport mechanism of the carbon membrane outside the viscous flow regime. Fig. 8 shows the permeance versus kinetic diameter of supported carbon membranes at different pyrolysis temperatures. Membranes obtained at 650 °C show molecular sieving behavior because the permeance decreases in line with the kinetic diameter of the gas molecules analyzed. This behavior corresponds to molecular sieve transport mechanisms reported by other researchers in carbon membranes^[40]. However, the same trend was not observed at 550 and 700 °C. These differences in permeation and selectivity properties resulting from different pyrolysis temperatures have been reported by several researchers^[16,18] as one of the main variables that affects the carbon structure. Indeed, controlling the pyrolysis temperature

allows the pore size distribution to be fine tuned to include meso and micro pores, which in turn results in different fluxes and separation factors. The same figure shows that permeance decreases at pyrolysis temperatures over 550 °C as a result of the pores shrinking. According to Steel and Koros^[41], an increase in pyrolysis temperature for the same Matrimid polymer in the range of 550 - 800 °C decreases permeation and increases the ideal selectivity for a pair of gases as a result of changes in the pore volume fraction.

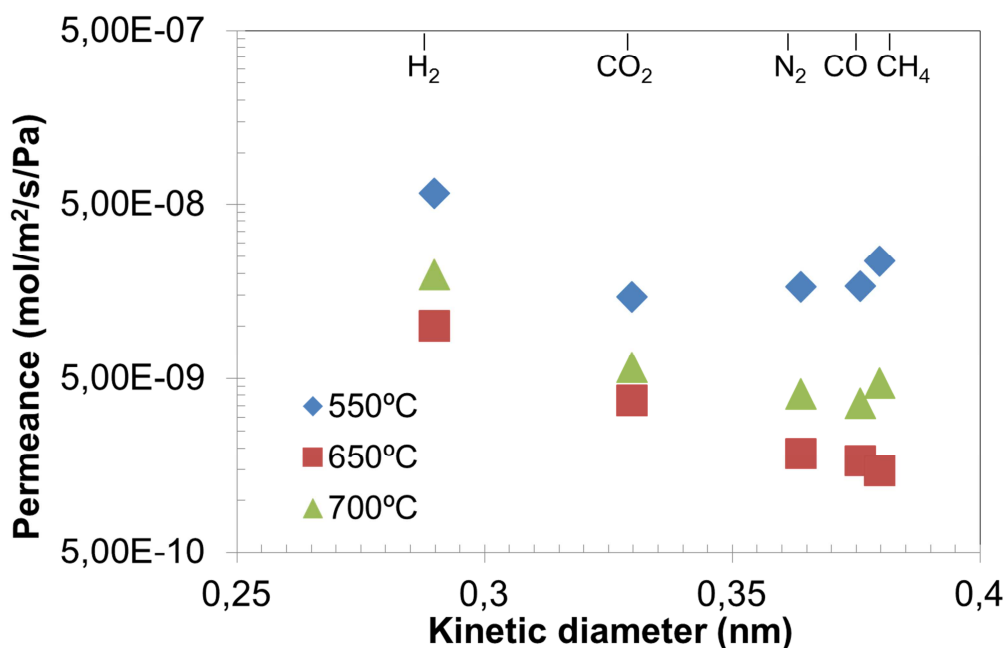


Fig. 8 Permeance versus kinetic diameter for carbon supported membrane after PDMS coating evaluated at room temperature ($\Delta P = 2$ bar)

Fig. 9 shows changes in the ideal selectivity factors for small gas molecules in membranes produced in a range of pyrolysis temperatures between 550-700 °C. All of the H₂ gas pair's selectivities are over the Knudsen theoretical factor for all the pyrolysis temperatures reported with the exception of the H₂/CO₂ pair. This could be because the pore size distribution is not sufficient to allow separation of these two molecules whose kinetic diameter difference is 0.41 Å. In contrast, the H₂/N₂, H₂/CH₄, H₂/CO gas pair series have higher kinetic diameter difference of 0.75, 0.91, 1.41 Å, respectively. The kinetic diameter analysis does not fully explain the ideal selectivity values of CO₂/CH₄ and CO₂/N₂, which have kinetic diameter difference of 0.5 and 0.34 respectively. These

pairs of gases reported permeances above the theoretical Knudsen value. In these cases, adsorption effects also come into play, in addition to the role played by the molecular size of gases.

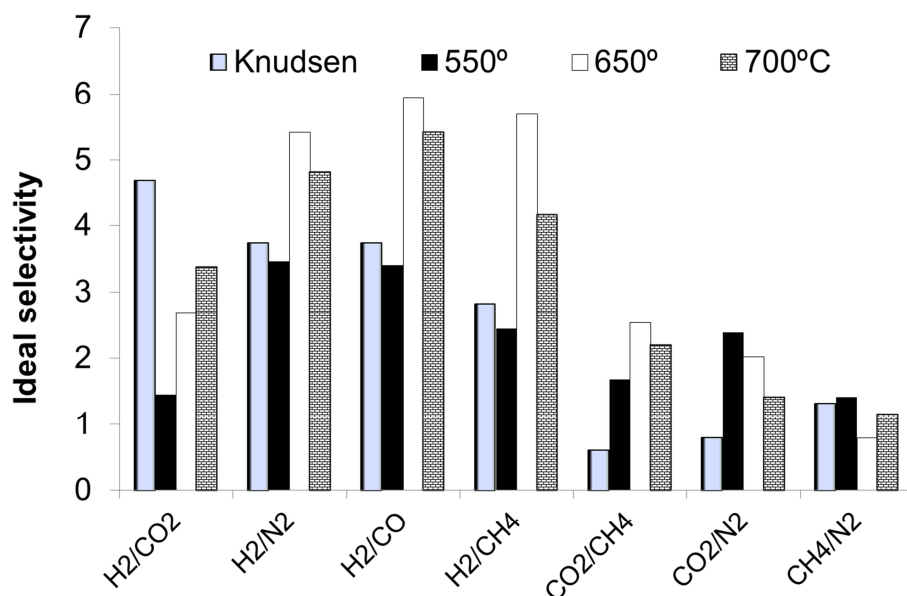


Fig. 9 Ideal selectivity for different pair of gases for carbon supported membrane after PDMS evaluated at room temperature. ($\Delta P = 2$ bar)

It should be noted that permeance was not measured at high temperatures where the sorption effect can be reduced by increased gas diffusion^[15]. Lua and Su^[42] outlined the presence of different pore size populations in the microporous structure of a carbon membrane derived from Kapton pyrolysis in the range of 550 - 1000 °C. They found that not only did pores shrink at higher a pyrolysis temperature, but also that new pores were produced which coexisted with larger depleted or shrunken pores. This could also explain the changes in ideal selectivity in the range 650-700 °C, where a difference of just 50°C can modify the pore size distribution of the carbon.

3.4 Carbon membrane used in methanol steam reforming

As mentioned previously, a carbon membrane pyrolyzed at 550°C achieved results comparable to those of supported carbon membranes reported in the literature. To explore the competitive applications of the former, they must also be compared with

membranes used in MR applications. The selectivity values of the carbon membranes obtained in the present study are comparable to those reported by Lee et al ^[6] for mesoporous γ -alumina and stainless steel supports. The γ -alumina support had H_2 and N_2 permeances in the range of $2.8\text{-}3.8\cdot 10^{-8}$ and N_2 $0.8\text{-}1.1\cdot 10^{-8}$ $\text{mol/m}^2\cdot\text{Pa}\cdot\text{s}$ respectively, and a H_2/N_2 ISF of 3.3-3.4. The stainless steel support had H_2 and N_2 permeances of $2.0\text{-}5.1\cdot 10^{-4}$ and N_2 $0.8\text{-}2.4\cdot 10^{-4}$ $\text{mol/m}^2\cdot\text{Pa}\cdot\text{s}$ respectively, and a H_2/N_2 ISF of 2.1-2.5. This meant that similar hydrogen recovery and conversion values could be expected for our carbon membrane, which indeed reported H_2 and N_2 permeances in the range of $1.29\cdot 10^{-7}\text{-}9.38\cdot 10^{-8}$ and $2.74\text{-}4.82 \cdot 10^{-8}$ $\text{mol/m}^2\cdot\text{Pa}\cdot\text{s}$ respectively and a H_2/N_2 ISF of 2.67-2.77 at 2 bar pressure difference in the range of 23-150°C.

Fig. 10 and Fig. 11 show the behavior of both the total yield and the CH_3OH conversion of the reaction in the MR and TR configurations. There is little difference between both configurations; however, the total yield and methanol conversion are higher in MR, which validates the use of the carbon membrane for this application. Methanol conversion is higher in the MR due to the shifting of products. A methanol conversion of around 48% is achieved at 200 °C in the MR, while a similar value of 49% is achieved in the TR at 250°C. This means that higher conversions are achieved in the MR than in the TR. This is one of the main advantages of using MR instead of TR when the reaction is limited by thermodynamic equilibrium. It should also be emphasized that TR and MR have exactly the same geometry and that the only difference is the presence of the membrane. In other words, the geometry of the reactor, the catalysis load and type, and the operative conditions are the same for both systems. Therefore, the higher values observed in the experimental results are caused by the membrane alone. The results are comparable with a mesoporous inorganic membrane described by Lee et al ^[6] who reported methanol conversion of 55% at 200°C.

Methanol conversion is related to the permeance characteristics of the membrane. As pointed out in section 3.1 the membrane permeance decreases as the temperature rises but the conversion of methanol which is related to these permeation capabilities does not follow the same trend. The same behavior is reported by Lee et al ^[6] using a stainless steel support. Despite the reduced permeance, the membrane permeance in the MR configuration is still sufficiently high to allow the equilibrium to be continuously shifted to the products.

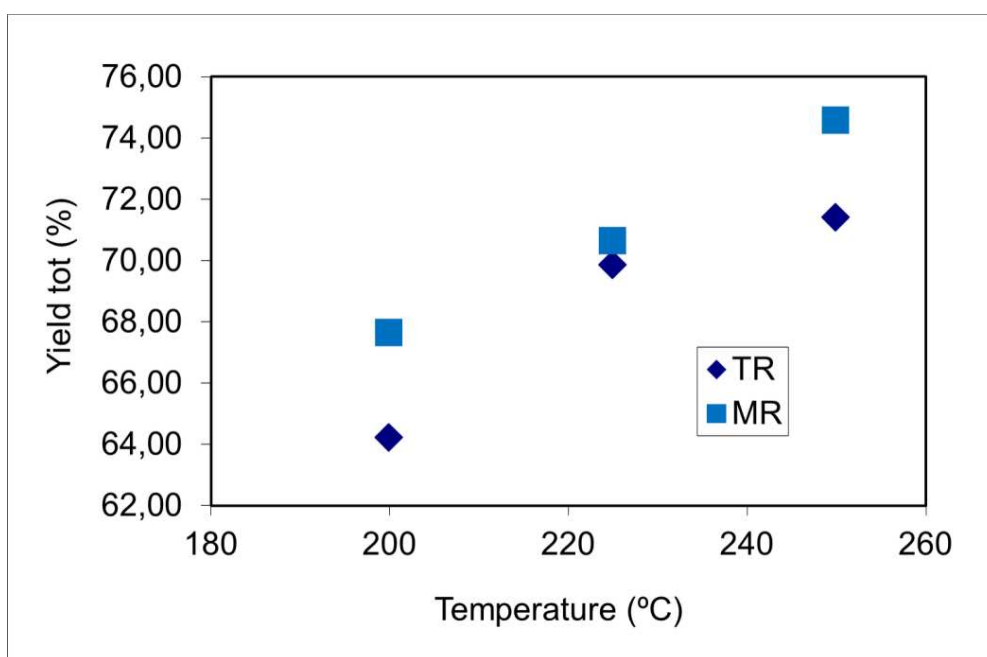


Fig 10. Yield versus temperature of a TR and a carbon membrane reactor for SRM

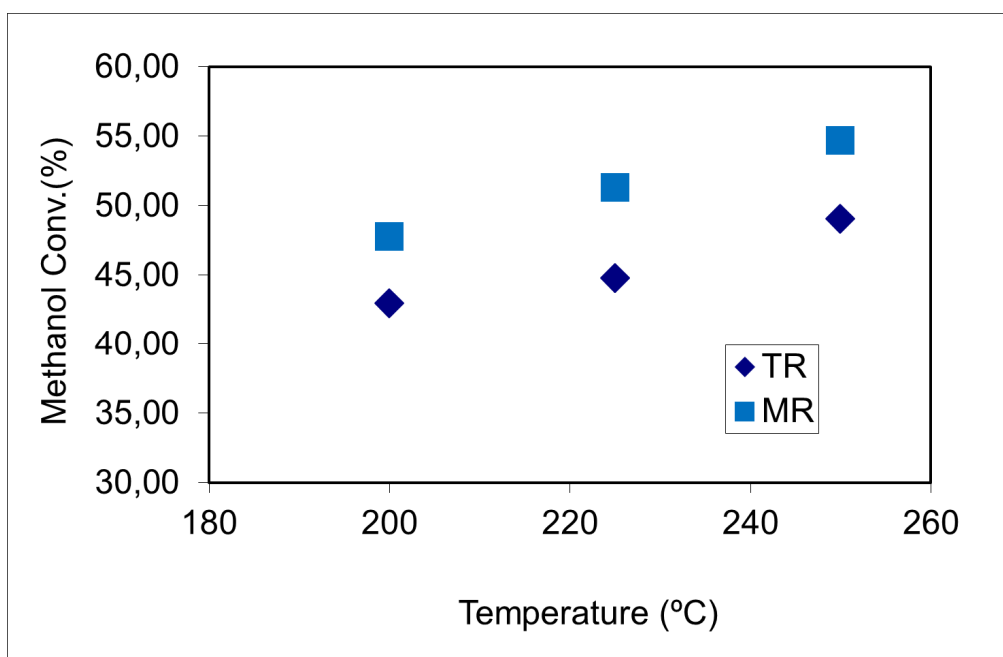


Fig 11 Methanol conversion versus temperature of a TR and a carbon membrane reactor.

Park et al. ^[5] reported the performance of a stainless-steel Knudsen-supported composite membrane for dimethyl ether (DME) steam reforming. They found that a membrane with a H₂/N₂ selectivity in the range 3-3.5 and a H₂ permeation between $(6.7-8.2) \cdot 10^{-6}$ mol/m²·s·Pa showed an increased conversion at temperature that was similar to the

carbon membrane reported in the present study. They also reported hydrogen recovery between 19.8-20.8% at 200-250°C and hydrogen permeate purity increasing with temperature. Table 3 shows that hydrogen purity stays more or less constant in the range of 200-250°C. The difference in both results could be because the hydrogen purity is related to differences in selective properties of the membrane and the type of reaction performed. However, the values of hydrogen purity are comparable for those obtained by Lee et al.^[6] with a mesoporous γ -alumina membrane that after integration with water gas shift reaction achieving 83.1-87.3% hydrogen purity on the permeate side. In addition, it is important to say that the results displayed in the present study are related to one type of carbon membrane obtained after pyrolysis at 550°C. The preparation of membranes must be improved to take into account the synthesis of membranes at higher pyrolysis temperatures and effect of pore plugging after PDMS coating. In addition, reactor variables must be studied. For example, Sa et al.^[43] reported that contact time influenced the hydrogen purity achieved with a carbon molecular sieve membrane (CMSM).

Table 3. Hydrogen purity in a carbon membrane reactor

| Temperature [°C] | 200 | 225 | 250 |
|-------------------------------------|------|------|------|
| Permeate Purity H ₂ % | 79.4 | 77.7 | 79.2 |

The structure of the membrane is linked to the final application. It should always be remembered that the best material for use in MR applications is the one that provides the most selective membrane and high permeance values. As shown by Lee et al.^[6] there is a balance between permeation and selectivity and the same principal can be applied to the continuing developments in carbon membrane reactor analysis. In our next study, we aim to investigate how the integration of the WGS reaction and the addition of sweep gas might improve the performance of the supported carbon membranes. Given that no cracks were observed after two months, this material could be a future alternative for MR applications in IGCC.

4.-Conclusions

Carbon molecular sieve membranes have been obtained after a Matrimid@ polymer layer was applied in one-step and pyrolyzed at 550 °C. No previous modification of the macroporous support was performed, which meant that a composite membrane was produced that had a large viscous flow and a predominant Knudsen diffusion transport mechanism. This is better than the permeance properties reported for more graded structure supports, and thus removes the need for lengthy deposition steps.

Consequently, at 550° C we can see the influence of mesoporous support pinholes and defects on viscous flow and the typical Knudsen diffusion mechanism. However, these are not the only factors to exert an influence because the permeation temperature may also affect the surface diffusion mechanism.

PDMS coating is a useful technique for determining the how the smallest pores in a supported carbon membrane really function without interference from larger pores or defects that occur when coating a porous support. In this regard, it was possible to observe the molecular sieving mechanism of supported carbon membranes pyrolyzed till 700°C temperature. A wide range of permeance values and selectivities were presented with the same type of supported carbon material. Before PDMS coating, the high permeance values were comparable to those of metallic and silica modified membranes used in MR applications. The carbon molecular sieve membranes reported in this paper are comparable to the inorganic membranes reported in the literature. For this reason, they were applied to methanol steam reforming. A preliminary study demonstrated the possible use of this type of membrane in MR applications, given that the MR yields were above those of the traditional reactor system. In order to demonstrate microporous structure were obtained, after PDMS coating the composite membranes pyrolyzed at 650° shown molecular sieving behavior and ideal selectivity factors over Knudsen theoretical values.

5. Acknowledgements

The authors are indebted to the Spanish Government for financial support (project CTQ2008-02491, partially funded by the FEDER program of the European Union) and to the commission of European Communities Specific OpenTok Project MTKD-LT-

2005-030040. Special thanks to Dr. Tiziana Longo and Dr. Simona Liguori from University of Calabria for their support on realization of experiments.

6. References

- [1] A. Bose; Inorganic membranes for energy and fuel applications, Springer, New York, USA.
- [2] J. J. Marano, J.P. Ciferino, Integration of Gas Separation Membranes with IGCC Identifying the right membrane for the right job, *Energy Procedia* 1 (2009) 361-368
- [3] A. Julbe ; D. Farrusseng ; Ch. Guizard ; Porous ceramic membranes for catalytic reactors—overview and new ideas, *J. Membrane Sci.* 181 (2001) 3–20
- [4] J.M.S Henis ; M.K Tripodi , Composite hollow fiber membranes for gas separation: the resistance model approach, *J. Membrane Sci.* 8 (1981)
- [5] S-J. Park; D-W. Lee; Ch-Y. Yu; K.Y Lee; K-H Lee ; Hydrogen production from a DME reforming-membrane reactor using stainless steel-supported Knudsen membranes with high permeability, *J. Membrane Sci.* 318 (2008) 123–128
- [6] D.W Lee , S.J Park; Ch-Y Yu , S-K Ihmb , K-H Lee ; Study on methanol reforming–inorganic membrane reactors combined with water–gas shift reaction and relationship between membrane performance and methanol conversion, *J. Membrane Sci.* 316 (2008) 63-72
- [7] E. Kikuchi, Membrane reactor application to hydrogen production, *Catal. Today* 56 (2000) 97–101
- [8] Basile A; Paturzo L; Laganà F; The partial oxidation of methane to syngas in a palladium membrane reactor: simulation and experimental studies, *Catal. Today* 67 (2001) 65–75
- [9] U. Illgen ; R. Schäfer; M. Noak; P. Kölsch P; A. Kühnle ; J. Caro; Membrane supported catalytic dehydrogenation of iso-butane using an MFI zeolite membrane reactor, *Catal. Commun.* 2 (2001) 339-345
- [10] M.D Dolan; R. Donelson; N.C Dave ; Performance and economics of a Pd-based planar WGS membrane reactor for coal gasification, *Int. J. Hydrogen Ener* 35 (2010) 10994-11003
- [11] R de Vos , H. Verweij ; High-Selectivity, High-Flux Silica Membranes for Gas Separation, *Science* , 279, (1998), 1710-1711
- [12] A.J Burggraaf ; Z.A.E.P Vroon , K. Keizer ; H Verweij; Permeation of single gases in thin zeolite MFI membranes , *J. Membrane Sci.* 144 (1998) 77-86.
- [13] C. Covarrubias , R. García, R. Arriagada ; J. Yanez ; H. Ramanan ; Z. Lai ; M. Tsapatsis ; Removal of trivalent chromium contaminant from aqueous media using FAU-type zeolite membranes, *J. Membrane Sci.* 312 (2008) 163–173
- [14] S.M Saufi , A.F Ismail F; Fabrication of carbon membranes for gas separation—a review, *Carbon* 42 (2004) 241–259
- [15] D.Q Vu ; W.J Koros ; S.J Miller ; High Pressure CO₂/CH₄ Separation Using Carbon Molecular Sieve Hollow Fiber Membranes, *Ind. Eng. Chem. Res.* 2002, 41, 367-380
- [16] K.M Steel ; W.J Koros ; An investigation of the effects of pyrolysis parameters on gas separation properties of carbon materials, *Carbon* 43 (2005) 1843–1856
- [17] J.C.D Da Costa ; G.Q Lu ; H.Y Zhu ; V Rudolph ; *J. Porous Mat.* 6, (1999) 143-151
- [18] T.A. Centeno, J.L. Vilas, A.B. Fuertes, Effects of phenolic resin pyrolysis conditions on carbon membrane performance for gas separation, *J. Membrane Sci.* 228 (2004) 45–54
- [19] J. Gilron ; A. Soffer; Knudsen diffusion in microporous carbon membranes with molecular sieving character, *J. Membrane Sci.* 209 (2002) 339–352
- [20] M.B Rao ; S. Sircar ; Performance and pore characterization of nanoporous carbon membranes for gas separation, *J. Membrane Sci.* 110 (1996) 109-118
- [21] A. Harale ; H.T Hwang ; P.K.T Liu ; M. Sahimi ; T.T Tsotsis ; Experimental studies of a hybrid adsorbent-membrane reactor (HAMR) system for hydrogen production, *Chem. Eng. Sci.* 62 (2007) 4126 – 4137
- [22] N Itoh; K. Haraya ; A carbon membrane reactor, *Catalysis Today* 56 (2000) 103–111
- [23] B. Fayyaz ; A. Harale ; B-G Park ; P.K.T Liu ; M Sahimi ; T.Y Tsotsis ; Design Aspects of Hybrid Adsorbent–Membrane Reactors for Hydrogen Production, *Ind. Eng. Chem.*

- Res., 2005, 44 (25), 9398-9408
- [24] A.B Fuertes, T.A Centeno ; Preparation of supported carbon molecular sieve membranes, *Carbon* 37 (1999), 679-684
- [25] A. Merritt ; R. Rajagopalan ;H.C Foley ; High performance nanoporous carbon membranes for air separation, *Carbon* 45 (2007) 1267–1278
- [26] A. Brunetti ;G.Barbieri ; E. Drioli ; K.H Lee ; B. Sea; D.W Lee, WGS reaction in a membrane reactor using a porous stainless steel supported silica membrane, *Chem. Eng. Process.* 46 (2007) 119–126
- [27] A.J. Burggraaf, in: A.J. Burggraaf, L. Cot (Eds.), *Fundamentals of Inorganic Membrane Science and Technology*, Elsevier, Amsterdam, 1996, pp. 331–4 (Chapter 9).
- [28] V. Richard; E. Favre ; D. Tondeur; A. Nijmeijer ; Experimental study of hydrogen, carbon dioxide and nitrogen permeation through a microporous silica membrane, *Chem. Eng. J.* 84 (2001) 593–598
- [29] X. Pages; V. Rouessac; D. Cot; G. Nabias; J. Durand ; Gas permeation of PECVD membranes inside alumina substrate tubes, *Sep. Purif. Technol.* 25 (2001) 399–406
- [30] D. Lee ; L. Zhang ; S.T Oyama ; S. Niu ; R.F Saraf; Synthesis, characterization, and gas permeation properties of a hydrogen permeable silica membrane supported on porous alumina, *J. Membrane Sci.* 231 (2004) 117–126
- [31] H.C Foley; Carbogenic molecular sieves: synthesis, properties and applications, *Microporous Mat.* 4 (1995) 407 43
- [32] K. Kusakabe; Z. Yan Li; H. Maeda; S. Morooka ; Preparation of supported composite membrane by pyrolysis of polycarbosilane for gas separation at high temperature, *J. Membrane Sci.* 103 (1995) 175-180
- [33] K. Haraya ; K. Obata ; T. Hakuta ; H. Yoshitome ; The permeation of gases through asymmetric cellulose acetate membranes, *J. Chem. Eng. Japan*, 19, (1986) 431-436
- [34] D. Wang ; W.K Teo; K. Li; Permeation of H₂, N₂, CH₄, C₂H₆, and C₃H₈ Through Asymmetric Polyetherimide Hollow-Fiber Membranes, *J. Appl. Polym. Sci.* 86, (2002) 698–702
- [35] B.S Liu; N. Wang; F. He; J.X Chu; Separation Performance of Nanoporous Carbon Membranes Fabricated by Catalytic Decomposition of CH₄ Using Ni/Polyamideimide Templates, *Ind.Eng.Chem.Res.* 47 (6), (2008), 1896-1902.
- [36] M.B Shiflett, Foley H.C, On the preparation of supported nanoporous carbon membranes, *J. Membrane Sci.* 179 (2000) 275–282
- [37] P. Pandey; R.S Chauchan ; Membranes for gas separation, *Prog. Polym.Sci* 26, (2001), 853-893
- [38] B.R Rowe ; B.D Freeman ; D.R Paul ; Physical aging of ultrathin glassy polymer films tracked by gas permeability, *Polymer* 50 (2009) 5565-5575
- [39] J. Petersen; M. Matsuda; K. Haraya; Capillary carbon molecular sieve membranes derived from Kapton for high temperature gas separation, *J. Membrane Sci.* 131 (1997) 85-94.
- [40] J.N Barsema , N.F.A van der Vegt , G.H Koops , M. Wessling , Carbon molecular sieve membranes prepared from porous fiber precursor, *J. Membrane Sci.* 205 (2002) 239–246
- [41] K. Steel K; W.J Koros ; Investigation of porosity of carbon materials and related effects on gas separation properties, *Carbon* 41, (2003), 253-266
- [42] A.Ch. Lua ; J. Su ; Effects of carbonisation on pore evolution and gas permeation properties of carbon membranes from Kapton_ polyimide, *Carbon* 44 (2006) 2964–2972
- [43] S. Sá ; H. Silva; J.M Sousa; A. Mendes; Hydrogen production by methanol steam reforming in a membrane reactor: Palladium vs carbon molecular sieve membranes, *J. Membrane Sci.* 339 (2009) 160–170

CHAPTER 7:

Exploring New Variables in the Fabrication of Supported Carbon Molecular Sieves Membranes for Gas Separation

(Art. 6)

(Article in preparation)

Exploring New Variables in the Fabrication of Supported Carbon Molecular Sieves Membranes for Gas Separation

Kelly Briceño^{a}, Daniel Montané^b, Ricard Garcia-Valls^a, Nadine Kalterborn^c, Ingolf Voigt^d*

^a*Department d'Enginyeria Química, Universitat Rovira i Virgili, Av. Països Catalans, 26, 43007, Tarragona, Spain*

^b*Catalonia Institute for Energy Research (IREC). Bioenergy and Biofuels Area. C/ Marcel·lí Domingo 2, Building N5, Universitat Rovira i Virgili. 43007, Tarragona, Spain*

^c*Nadine Kaltenborn, Energy Technologies, Forschungszentrum Jülich GmbH, 52425, Jülich, Germany*

^d*Fraunhofer Institute for Ceramic Technologies and Systems IKTS, Marie-Curie-Str. 17, 07629 Hermsdorf, Germany*

**Corresponding author e-mail: kelly.briceno@urv.cat*

Tel: + 34 977 558506

Abstract

Supported carbon molecular sieve membranes have been fabricated using a modified Al₂O₃ support. Matrimid® polymer was used as a precursor of carbon membranes after optimization of polymeric solution composition and pyrolysis temperature range of 550-800°C. Optimized carbon membranes were obtained at 6 wt% polymer solution when pyrolyzed at 650°C for H₂/Propane (Pa) separation. However, the optimal pyrolysis and fabrication conditions can be for other couple of gases. The single gas permeance of H₂, He, CO₂, O₂, N₂, CH₄, Propane, n-butane, 1-butene and SF₆ ranged between (0.05-11)·10⁻⁷ mol/(m²·Pa·s) at 150°C. The decrease of permeance with the kinetic diameter of gases and ideal selectivities over Knudsen values confirmed molecular sieving behaviour. The reliability and reproducibility of the fabrication method presented in this work allowed to determine the effect of different fabrication variables on permeance and selectivity of the carbon membranes. Influence of methanol washing, type of support and aging treatment (below and over *T_g*) were identified as important variables to be considered for the screening membrane properties. The molecular sieving

character remained on the carbon membranes after oxidative atmosphere at 250°C and hydrothermal conditions at high and low pressure.

1. Introduction

Gas separation membranes are highly demanded in the current market because they are being used as upgrades of some more traditional gas separation technologies (e.g. in liquid adsorption or pressure swing adsorption processes). Besides polymer, metal, zeolites or silica membranes, carbon membranes have gained importance as alternative gas separation materials due their high permeance and selectivity properties. Since Koresh and Sofer^[1] showed the first gas separation properties of carbon molecular sieve membranes (CMSM), numerous advances have turned them into competitive industrial applications. After polymer pyrolysis it is possible to obtain a turbostratic carbon material under inert atmospheres as N₂, Ar, He, CO₂^[2]. Saufi and Ismail^[2] have been reported to require an accurate control of a set of variables affecting the pore size of carbon membranes, like the type of precursor, pyrolysis temperature, heating rate, soaking time, among others. On the other side, there are alternative variables less reported on carbon membrane fabrication that requires also attention as pore size modifiers^[3]

Despite of the highly efficient separation properties of CMSM, their fragility limits their application at industrial scale. Since they are mechanically unstable, they must be supported on inorganic materials. Fabricating supported membranes implies to overcome crack formation caused by differences on the thermal coefficient between the polymer and the inorganic support during pyrolysis. For smoothing the surface of support materials different strategies have already tested. Merrit et al^[4] incorporated silica nanoparticles on porous stainless steel supports for reducing their porosity prior to coating the carbon precursor material. Liu et al^[5] reduced the pore diameter (0.8-1µm) of Al₂O₃ supports after repeated dip-coating in boehmite prior to CMSM fabrication from polyamideimide. Fuertes and Centeno^[6] deposited graphite particles between the support (1 µm pore diameter) and the selective carbon layer for reducing defect formation prior to CMSM preparation from polyimide coating. However, even when such modifying strategies for the support have been implemented there is a risk of defects or pinholes formation on the carbon layer. As evidence, ideal selectivity values remain under Knudsen ideal selectivity values. For this reason during the fabrication

process sometimes requires to include additional coating steps in order to plug those defects.

Fabricating supported carbon membranes also requires a specific control of the variables involved on the preparation of the membranes ^[7-9]. As an example, Centeno et al ^[7] reported the influence of pyrolysis temperature, carbonization rate on final properties of CMSM obtained from phenolic resin-carbon membranes. Such studies have led to a common observation; the increase of permeance increases with pyrolysis temperature to a maximum. The permeance decrease after such value can be a consequence of the collapse of pores or enlargement of micropores formed at lower pyrolysis temperature. The temperature at which this phenomenon occurs depends on fabrication conditions and the type of precursor employed on CMSM fabrication.

The pore size tailoring process could also depend on other variables that have been reported on unsupported samples but scarcely reported in supported carbon membranes. As an example, Barsema et al ^[10] reported the influence of pre-treatment before and after *T_g* on unsupported carbon membranes derived from Matrimid. Tin et al ^[11] reported the influence of several non-solvents on the final structure of unsupported polyimide samples. None of these variables have been reported for supported samples. As pointed before, the fabrication of supported samples is not simple and frequently requires several coating steps to obtain a defect free membrane.

The first publications on supported membranes considered polyimide membranes as excellent materials for the fabrication of high selective carbon membranes. Yamamoto et al ^[12] obtained carbon membranes after pyrolysis of a polyimide layer previously prepared with a polyamic acid precursor ^[12]. However, in order to eliminate polyamic acid solution preparation, commercial polyamide has been employed on CMSM fabrication ^[13]. In fact, Kapton®, and Matrimid® have been extensively reported for unsupported CMSM preparation ^[2,14]. However, to our knowledge, there are few reports of the use of Matrimid in the fabrication of supported carbon membranes ^[3]

It is clear that CMSMs gain stability when supported on inorganic materials, but it must be considered that studies aiming to develop a reliable and fast method for fabricating supported membrane would allow exploring on detail the tailoring pore size process towards specific separation of gases. It is for this reason that the fabrication method must be considered as another variable to optimize. Shiflet and Foley ^[15] for example,

determined that ultrasonic deposition method allowed exploring different conditions on the fabrication of supported carbon membranes.

Fabricating CMSMs exhibiting enough mechanical stability using a highly reproducible fabrication method is only part of the challenge. Hydrothermal stability of the membranes must also be considered at either high humidity ^[16] or oxidative atmospheres ^[17]. In fact, the low hydrothermal stability has limited their commercial applications.

The objective of this study has been to measure fabrication variables on supported samples for which Matrimid® was the precursor of the carbon structure: support influence, polymer concentration, swelling in non-solvent, pyrolysis temperature, pre-thermal treatment, and stability under oxidation and humidity atmospheres.

The method reported in this article allowed fabrication of supported CMSM after one coating step of the polymer layer over the inorganic support with a high reproducibility.

2. Experimental Part

2.1 Membrane fabrication: polymer coating

Different polymer solutions were prepared as carbon precursors. In all of them, Matrimid (3, 3', 4, 4'-benzophenonetetracarboxylic dianhydride and diamino-phenylindane) from Huntsman Advanced Materials was used as polyimide while 1-methyl-2-pyrrolidone (NMP) 99,5% from Sigma-Aldrich was used as solvent. The different polymeric solutions used on coating of ceramic supports are reported on table 1. The table also includes one membrane that was immersed in methanol after polymer coating by 24 hrs (3*) and a mixture of solvents (10**).

Different Al₂O₃ tubular supports were prepared under IKTS (Hermsdorf-Germany) fabrication standards (Protected by patent) in order to obtain a defect-free support for carbon membranes fabrication. The ends of the tubes were sealed with a 15-mm glass each. The supports were based on α -Al₂O₃ with asymmetric sequence of δ -Al₂O₃ layer of different pore sizes (0.2-5 nm) through the transversal section of the tube. The tubes have an outer diameter of 10 mm and inner diameter of 7 mm and a length of 125 mm.

Table 1. Polymer solutions used on coating of ceramic supports.

| Nomenclature | Polymer concentration | | Solvent | Comments |
|--------------|-----------------------|--|------------------------|--|
| | wt.% | | | |
| 3 | 3 | | NMP | |
| 3* | 3 | | NMP | After coating, immersion in CH ₃ OH |
| 6 | 6 | | NMP | |
| 10** | 10 | | NMP:CH ₃ OH | 50:50 |

After N₂ flux test (see description below), each tubular support was dipped into a polymer solution, by one end, after that the polymer solution was sucked into the tube by applying vacuum in the inner side and keeping the solution in contact with the inner walls of the support for one minute. Afterwards, the vacuum was replaced by N₂ flux for pulling the solution out of the tube. The coated supports were placed for drying overnight in a clean room environment (class 100, humidity 50%, 21.5 °C).

2.2 Aging procedure

Polymer supported membranes were considered for aging before pyrolysis and compared with membranes with a similar polymer history. In this sense, three membranes were placed in an oven at atmospheric pressure. The thermal treatment began at room temperature until reach 250,300, 350°C (at 2.29 °K/min) by one hour.

Pyrolysis process was applied under N₂ atmosphere, starting the heating at room temperature until reaching 380°C at a heating rate of 0.5 K/min, then increasing until 550 °C at 0.6 K/min, and later reaching higher temperatures at (550°C, 600°C, 700°C, 800°C) at 1 K/min. The cooling stage was performed at 5 K/min.

2.3 N₂ flux test at room temperature

As a quality control procedure the flux of the inorganic supports before polymer/carbon coating was tested on stainless steel permeation cells for which the tubes were embedded using Viton O-rings. The measurements were set at P feed= 2 bar and P permeate= 1 bar. The N₂ flux was recorded when the pressure difference was 1 bar

between feed and permeate. When passing the N₂ permeance test, those supports that reached N₂ permeance values below 100 m³/(m²·Pa·s) were chosen as suitable supports for fabrication of carbon membranes. On the contrary, those supports that exceeded this value were rejected and sent for an additional coating of inorganic Al₂O₃ layer

2.4 Single gas permeance measurements

The supported carbon membranes were tested in a standard pressure rise type cell where the membranes were pressurized on the feed side, while the permeate side was maintained at vacuum. The permeation flux was calculated using the ideal gas law by measuring the pressure rise in a standard volume on the permeate side of the membrane after switching off the vacuum. For ensuring a complete removal of adsorbed molecules, the membranes were heated in a vacuum oven at 150°C for at least 15 min before measuring permeation. The gases H₂, He, CO₂, O₂, N₂, CH₄, propane, n-butane, 1-butene, SF₆ were supplied by Linde, Hermsdorf, at a high purity (> 99,9 %).

2.5 Bubble-Point

For measuring bubble point, membranes were firstly passed through propanol with vacuum until there were no more bubbles (5-10 minutes, depending on the membrane, until getting the membranes wet). After this step, the membranes were placed in a special fixture immersed in ethanol and applying pressurized air on feed side. The pressure further on feed was increased (step by step) until bubbles appeared. This pressure was registered (that is the bubble point of the biggest pore or defect) and the pressure further increases until 5 bar. Simultaneously the gas diffusion was measured at each pressure step. At 5 bar the procedure was stopped and the pressure measurement was registered. For displacing the ethanol from the pores a certain pressure difference between the feed and permeate side was necessary. Such pressure difference depended on the pore diameter of the membrane. By converting the Washburn equation, (Equation 1) the pore dimension could be calculated by:

$$\Delta p = 4 \sigma \cdot \cos \theta / D \quad (\text{Eq.1})$$

Δp = pressure difference in bar (Pascal)

σ = surface tension of the liquid in N/m (for example water=72,75mN/m; 2-Propanol 21.7 mN/m)

θ = contact angle

D = pore diameter (m)

2.6 Oxidation test

Membranes were placed in an oven Nabertherm L9/SH at 250°C for 6 hours.

2.7 Humidity test: low pressure

Membranes were placed in a tubular oven in N₂ atmosphere with a humidity of 2.5 vol% of water at 250°C for 24 hrs.

2.8 Humidity test: high pressure

Membranes were placed in an autoclave at 30 bar and 180°C for 24 hrs.

3. Results and Discussion

3.1 System reproducibility

For observing the reliability of the fabrication method, Carbon molecular sieve membranes (CMSM) were tested in order to observe the permeance reproducibility values. Fig. 1 shows the main permeance values of different CMSM obtained at 650°C pyrolysis temperature using 6 wt%. dispersion of permeance values for all CMSM samples depended on type of gas analysed. These differences can be observed in detail on table number 2. For gases with smallest kinetic diameter as H₂, He, CO₂, O₂, N₂, CH₄ and propane the standard deviation is one order of magnitude lower than the measurement which indicates the high reproducibility of the method. For those gases with larger kinetic diameter the standard deviation is comparable with the low permeance values of those gases. This suggest the pore size distribution of these membranes is too small for the group with kinetic diameters over 4.3 Å. Steel and Koros^[14] reported that the microporosity of Matrimid films was lower than 6.8 Å. They also reported a multimodal distribution that decreases with pyrolysis temperature. Table 2 also shows the effect of multimodal distribution on ideal selectivity factors for different pairs of gases. The micropores of the membranes easily exclude the passage of large molecules in front of smaller molecules as in the case of H₂ and propane, but this effect is reduced when gases are similar in size comparable to the constrictions of the carbon pores.

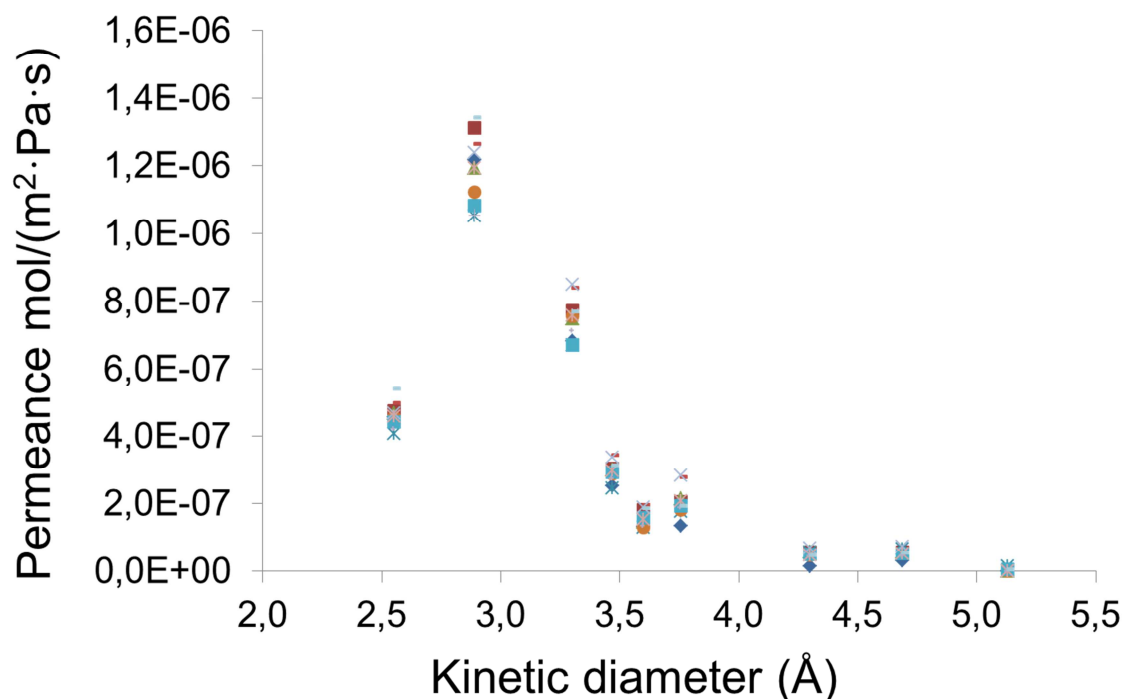


Fig 1 Permeance membranes pyrolyzed at 650°C

Table 2. Permeance and Ideal selectivity of CMSM obtained at the same conditions

| | Permeance ($\times 10^{-7}$) mol/(m ² ·Pa·s) | | | | | | | | | | Ideal selectivity | | | |
|----------------------|---|----------------|-----------------|----------------|----------------|-----------------|--------------|----------|----------|-----------------|--------------------|---------------------------------|----------------------------------|--------------------------------|
| | He | H ₂ | CO ₂ | O ₂ | N ₂ | CH ₄ | Propane (Pa) | n-Butane | 1-Butene | SF ₆ | H ₂ /Pa | H ₂ /CH ₄ | CO ₂ /CH ₄ | O ₂ /N ₂ |
| Kinetic Diameter (Å) | 2.55 | 2.89 | 3.30 | 3.47 | 3.60 | 3.758 | 4.30 | 4.69 | 5.1 | 5.13 | | | | |
| Average | 4.53 | 11.6 | 7.50 | 2.95 | 1.62 | 2.21 | 0.74 | 0.72 | 1.62 | 0.049 | 24.05 | 5.70 | 3.58 | 1.85 |
| Std.Dev | 0.688 | 1.89 | 1.87 | 0.73 | 0.55 | 1.02 | 0.88 | 0.72 | 1.20 | 0.093 | 15.354 | 1.312 | 0.60 | 0.16 |

3.2 Effect of polymer solution concentration

The effect of polymer concentration on membrane permeance values was studied for carbon membranes, with a concentration range of 3-10 wt% and varied compositions, prepared after pyrolysis at 650°C. Figure 2 shows permeance values of diverse gases (H₂, He, CO₂, O₂, N₂, CH₄, n-butane, 1-butene, propane (Pa), SF₆) measured at 150 °C versus the molecular kinetic diameter for MCSM. For each gas analysed, its permeance decrease with molecular kinetic diameter (i.e., the higher the diameter the lower the gas

permeance). This agrees with molecular sieving behaviour and indicates that the coating process and pyrolyzing steps led to the formation of a microporous carbon membrane.

In order to determine the influence of non-solvent immersion on carbon membranes, a supported polymer membranes coated at 3%wt was immersed 24 hrs in methanol and compared with a non-treated methanol sample. From fig 2 it is not possible to conclude about a real influence of immersion of methanol as pretreatment of polymer on the final permeance of CMSM. In a previous work we suggested the influence of methanol as modifier of carbon structure ^[15]. From figure 2 the permeance of H₂ changed from $2.47 \cdot 10^{-6}$ to $2.27 \cdot 10^{-6}$ mol/ m²·Pa·s after methanol immersion which is in the range of standard deviation of the measurement. Similarly, ideal selectivity computed for both types of systems does not allow concluding about the influence of methanol immersion of final properties of carbon membranes. It is important to follow several repetitions in order to conclude about a real effect of methanol immersion as pore modifier ^[18].

From figure 2 it is possible to observe the effect of different polymer compositions of permeance of carbon membranes. It is possible to tailor the pore size of carbon membranes adjusting this parameter. In fact, the variations are out of the range of standard deviation of the measurements. Similarly, from table 3 it is possible to conclude the influence of polymer concentration has on ideal selectivity of CMSM.

For the purpose of this research we identified the best polymer concentration for fabricating CMSM, a 6 wt% polymer concentration. Fig 3. shows 6 wt% as the best polymer solution concentration to prepare carbon membranes for ideal H₂/Propane separation. Such results are promising if the current carbon membrane is compared against molecular sieve membranes obtained over a similar support. Schafer et al ^[19] reported H₂/Propane values around 25 at 150°C, for supported zeolite membranes, which is lower than the value of 77.5 obtained with our membrane after only one polymer coating and pyrolysis step.

As an additional test, a 10 wt.% polymer solution, composed by a mixture of 50:50 NMP and CH₃OH solvent, yielded inferior results to those in which the polymer concentration for separation of H₂ and Pa was at 6% wt. It is clear that both the concentration and composition of polymer solution influence the final properties of the carbon membrane. Such influence can vary according to gas pair considered for the analysis.

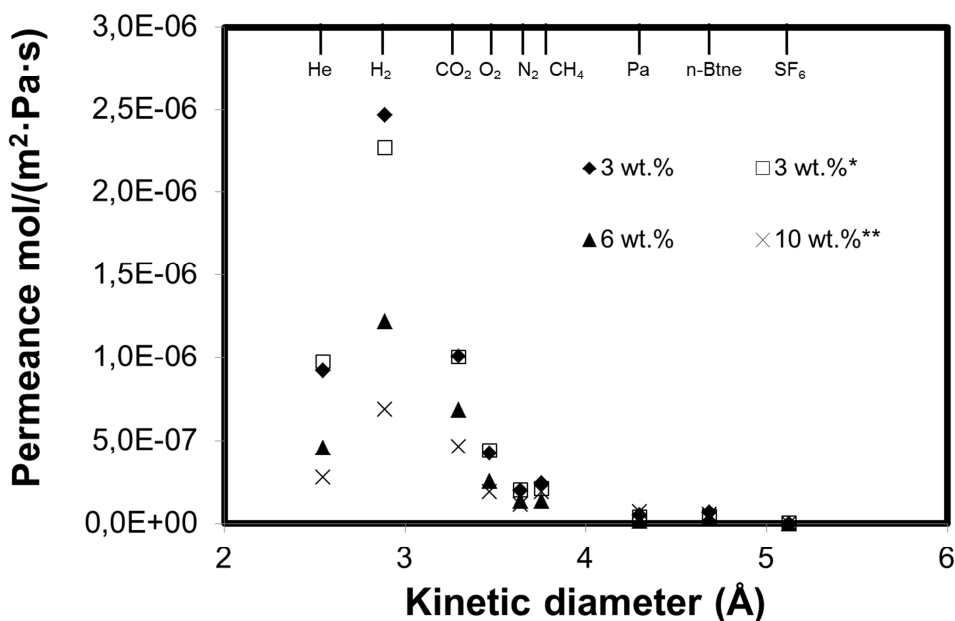


Fig 2 Single gas permeance performed at 150°C of Matrimid carbon supported membrane at different formulations

Table 3 Ideal selectivity of carbon membranes tested at 150°C at different polymer concentrations.

| %wt | Type of Solvent | Membrane Immersion | H ₂ /Pa | H ₂ /CH ₄ | CO ₂ /CH ₄ | O ₂ /N ₂ |
|-------|-------------------------------------|--------------------|--------------------|---------------------------------|----------------------------------|--------------------------------|
| 3 | NMP | - | 49.03 | 10.22 | 4.17 | 2.12 |
| 3 * | NMP | CH ₃ OH | 61.40 | 10.82 | 4.76 | 2.17 |
| 6 | NMP | - | 77.52 | 9.05 | 5.09 | 1.89 |
| 10 ** | NMP:CH ₃ OH 50:50 w/w | - | 9.55 | 3.63 | 2.45 | 1.71 |

3.3 Influence of Methanol at low pyrolysis temperature

In previous section it was explored the influence that methanol can have in the formation of the carbon structure of for a carbon membrane obtained from a supported polymer membrane of 3 wt% polymer composition and pyrolyzed at 650°C. However, it was not possible to conclude a real influence of methanol as pore modifier on CMSM. In order to observe the influence of methanol in a different system, a carbon membrane obtained at 550° pyrolysis temperature and 6% wt polymer solution was considered as a comparative sample.

Fig 3 shows permeance values vs kinetic diameter of gases for a carbon membrane obtained after pyrolysis of membranes immersed and not immersed in methanol. It is expected, the lowest pyrolysis temperatures produce an preliminary microporosity that must be sensible to methanol immersion. From Figure 2 is not possible to observe higher differences between permeance values. If we consider Table 2 the change in permeance is on the limit of the standard deviation of permeance of these carbon membranes. However, the real effect on microporosity can be observed on figure because the change on ideal selectivity is over the standard deviation of the measurement. From this figure H_2/Pa ideal selectivity decreased from 81.55 to 15.74 after methanol immersion. But in the case of O_2/N_2 ideal selectivity increased after methanol immersion from 2.63 to 4.36. These results confirm there is an effect clear trend how methanol affects the microporosity of the carbon. Additional experiments have to be performed to confirm these hypotheses.

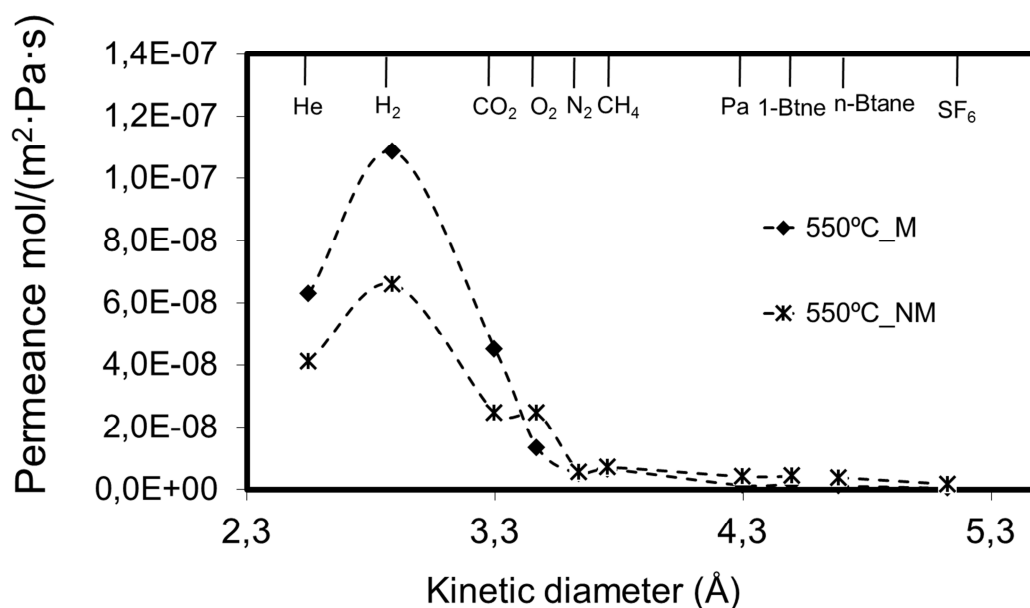


Fig 3 Single gas permeance of carbon supported membranes pyrolyzed at 550°C measured at 150°C.

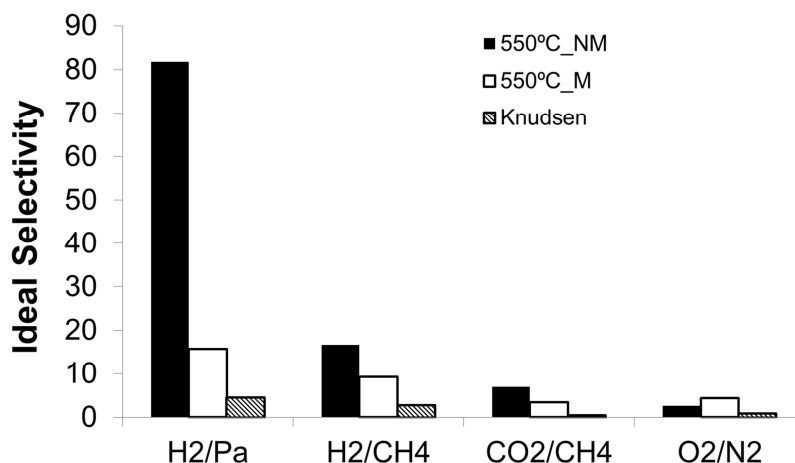


Fig 4 Ideal selectivity of carbon supported membranes pyrolyzed at 550°C

3.4 Influence of pre-treatment.

Fig 5-6 show the effect of thermal treatment in permeance of carbon membranes pyrolyzed at 650°C. It is possible to observe that, when the membranes have the same conditions before pyrolysis, their final permeance values are the same. On the contrary, when the membranes are pre-treated before and after glass transition temperature (T_g) their permeance values are also different and increase as pre-treatment temperature is increased. The scope of this fine influence on porosity is more evident in Fig 5-6.

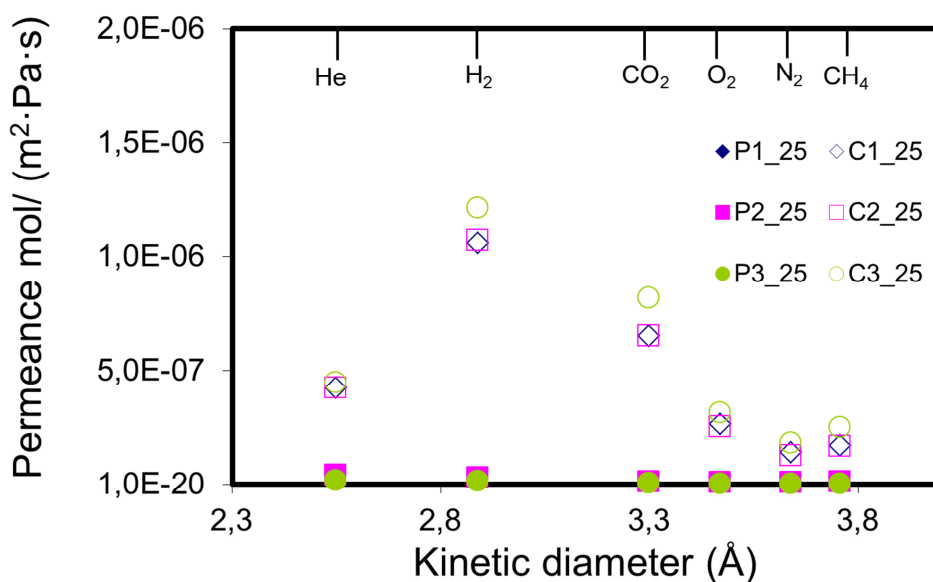


Fig 5. Permeance values for CMSM vs kinetic diameter obtained for samples with the same thermal history before (polymer) and after (carbon) pyrolysis at 650°C.

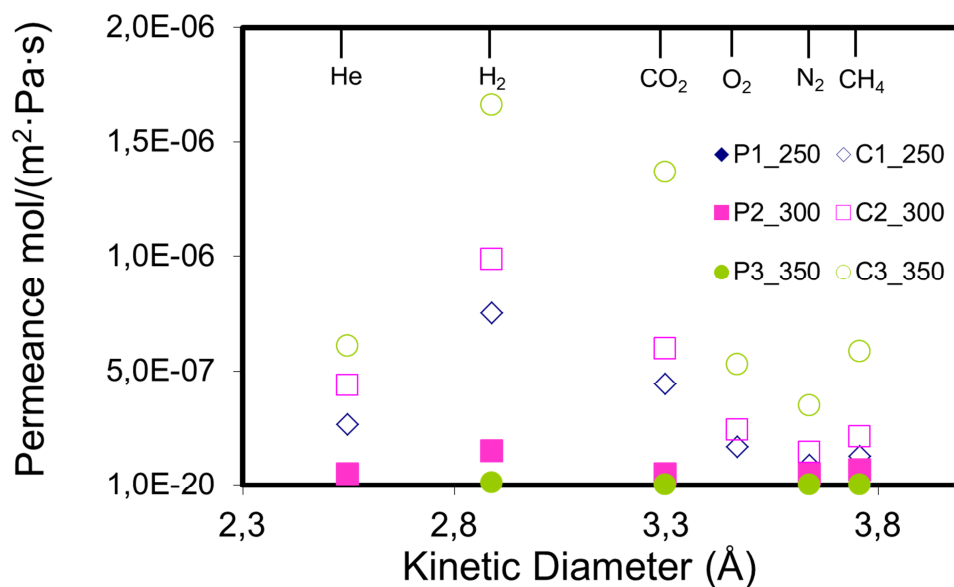


Fig 6. Permeance values for CMSM vs kinetic diameter obtained for samples with different thermal history (pre-treatment at 250°, 300°, 350°C) before (polymer) and after (carbon) pyrolysis at 650°C.

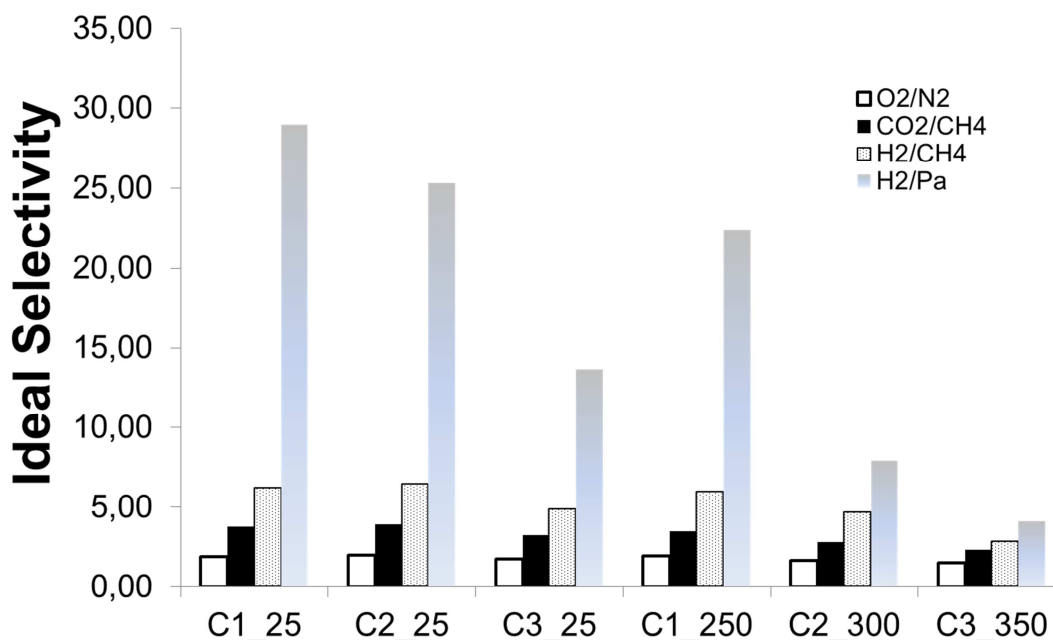


Fig 7. Ideal selectivity values for CMSM vs kinetic diameter obtained for samples with the same and different thermal history after pyrolysis at 650°C.

3.5 Support influence

In a previous publication ^[3] we found an effect of the support on the textural properties of carbon membranes. However, there is a need to investigate the influence of this parameter on final permeance and selectivity properties of carbon membranes.

If a support is highly mesoporous, defect formation is favoured on the coating layer, for instance the permeance values in the supported membrane can increase and ideal selectivity decrease. Fig 8 show the effect of support on permeance of Matrimid pyrolyzed supported membranes. For those membranes pyrolyzed at 550°C using the TiO₂ support the permeance values are about 100 times higher than those obtained over Al₂O₃ supports. The TiO₂ support show lower permeance values when big pores or defects are plugged with PDMS coating . On the contrary, Al₂O₃ shown the lowest permeance values due to the multilayer structure devoted to reduce defect formation for coating.

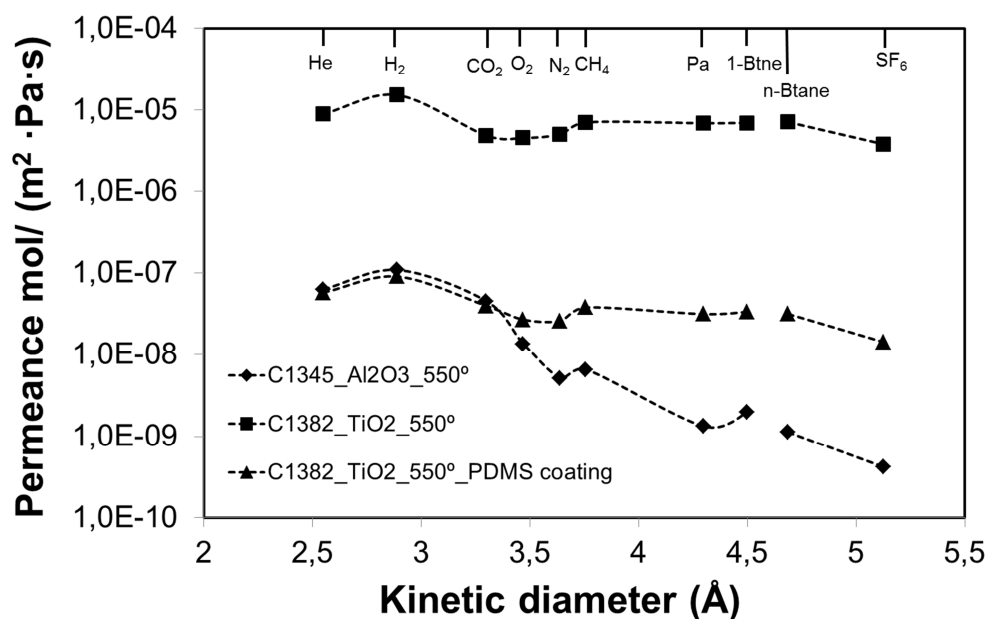


Fig 8. Permeance values of carbon membranes obtained on TiO₂ and Al₂O₃ supports at 550°C.

Table 4 show that membranes obtained over TiO₂ supports have ideal selectivity factors still below Knudsen values, including that one coated with PDMS. In the latter case, it is possible the pore plugging with PDMS was incomplete or the microporosity for both type membranes was not developed enough at 550°C moreover, bubble point analysis

were done for TiO₂ supports without coating detecting defects in the order to 1-3µm. On the contrary, membranes obtained over Al₂O₃ supports did not report defects in the range of bubble point measurements. The molecular sieving behaviour for carbon membranes coated on Al₂O₃ supports was confirmed due to permeance dependence of kinetic diameter and ideal selectivity factors over Knudsen theoretical values. We confirm, the multilayer structure of the support prevent defects formation, favours carbon molecular sieve membrane formation but imply a lower permeance values than those obtained with mesoporous support without a graded microporosity.

Table 4. Ideal selectivity values of carbon membranes obtained on TiO₂ (C1382) and Al₂O₃ (C1345) supports at 550°C.

| Membrane | H ₂ /Pa | H ₂ /CH ₄ | CO ₂ /CH ₄ | O ₂ /N ₂ |
|--------------|--------------------|---------------------------------|----------------------------------|--------------------------------|
| C1382 | 2.21 | 2.16 | 0.69 | 0.90 |
| C1382 (PDMS) | 2.88 | 2.39 | 1.04 | 1.03 |
| C1345 | 81.85 | 16.68 | 6.91 | 2.63 |
| Knudsen | 4.69 | 2.82 | 0.60 | 0.93 |

3.4 Influence of pyrolysis temperature

Figure 9 shows the single-gas permeance of supported carbon membranes obtained at 550-800°C were measured at 150°C. For these tests, there's also evidence of molecular sieving behaviour as the permeance of a gas decreases with its kinetic diameter. The permeance of each gas increases as the temperature at which each membrane was obtained in this order: 550°C, 800°C, 650°C and 700°C. Such trend is not linear and it is due to the different pore size distributions formed at each pyrolysis temperature.

There was found a marked effect of carbonization temperature on microstructure of carbon membrane. Centeno et al ^[7] reported the development of pores near 500°C and found that at 700-800°C the pores are enlarged before shrinking at higher temperatures. This latter may produce differences on separation performances. Similarly, we have observed the same effect of high pyrolysis temperatures in our carbon membranes. Gas permeance increases until pyrolysis temperatures in the range of 650-700°C, but it starts to decrease at 800°C. The differences on permeance evolution with temperature are due to reduction of pores and creation of new micropores during the pyrolysis treatment. Such process depend on precursor type, pyrolysis conditions and gases tested. For a membrane obtained at pyrolysis temperature of 700°C Centeno et al ^[7] reported lower

permeance $1.028 \cdot 10^{-7}$ mol/ (m²·Pa·s) and $2.319 \cdot 10^{-7}$ mol/ (m²·Pa·s) for N₂ and CH₄ respectively than our membranes with $2.09 \cdot 10^{-7}$ mol/(m²·Pa·s) and $2.87 \cdot 10^{-7}$ mol/(m²·Pa·s) for the same gases. However, they obtained higher ideal selectivity factors for CH₄/N₂ and n-butane/N₂ of, respectively, 2.3 and 1.8 (See figure 10) compared to ours of 1.37 and 0.56 for CH₄/N₂ and n-butane/N₂ respectively.

Fuertes and Centeno ^[6] achieved He permeance in the order of $2.45 \cdot 10^{-8}$ - $3.04 \cdot 10^{-9}$ mol/(m²·Pa·s) measured at 150°C which is comparable with our membranes with permeance measured at 150°C ranged between $6.3 \cdot 10^{-8}$ - $1 \cdot 10^{-7}$ at pyrolysis temperature between 550°-800°C. We obtained higher permeance values using only one coating step over a multilayer support but lower ideal selectivity factors. For example, for CO₂/CH₄ pair we obtained the 9.23 as the best ideal selectivity factor (obtained at 800°C pyrolysis temperature) meanwhile Fuertes and Centeno reported 17.

Lee et al ^[20] also reported the effect on temperature in permeance. An increase of permeance was observed with an increase of temperature from 500°C to 700°C. After this value the permeance decreases at 800°C. For a membrane obtained after pyrolysis at 800°C the CH₄ permeance was $2.6 \cdot 10^{-10}$ mol/(m²·Pa·s), which is lower than the permeance reported by our membrane ($2.2 \cdot 10^{-8}$ (mol/ m²·Pa·s)) at the same pyrolysis temperature. In addition, they reported a decrease of CO₂/CH₄ ideal selectivity from 33 to 14; for membranes pyrolyzed at 700°C and 800°C respectively. Our membranes increased CO₂/CH₄ ideal selectivity factor from 3.45 to 9.23.

Differences found between bibliography ^[6,7,20] and our work evidence the complex and heterogeneous nature of the carbon. Moreover, ideal selectivity factors for each pair of gases depend on pore size distribution that includes both micropores and ultramicropores, that favour either diffusion or adsorption of some molecules over others ^[14]. This imply, to find an appropriated pyrolysis temperature depends on the type of precursor and the final application.

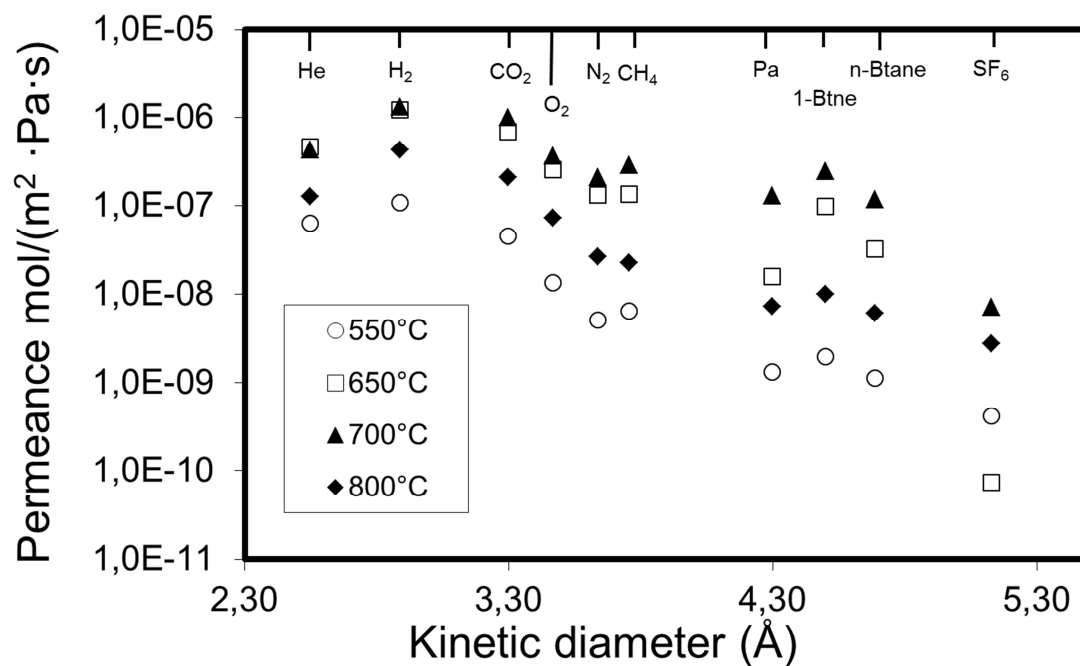


Fig 9. Permeance values for CMSM vs kinetic diameter obtained at different pyrolysis temperatures.

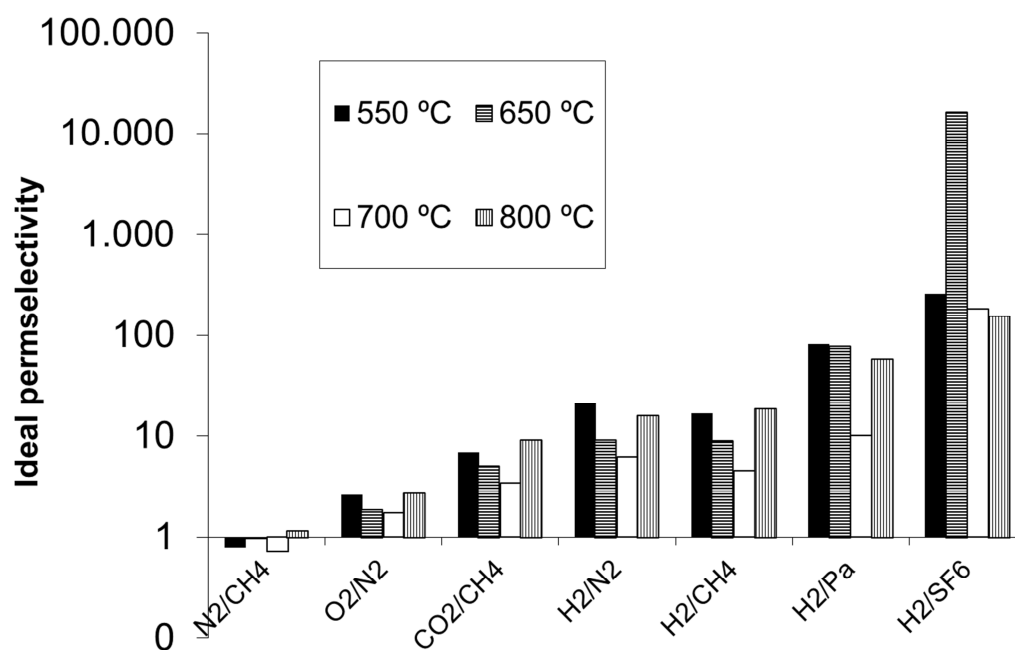


Fig10. Ideal selectivity values for CMSM vs kinetic diameter obtained at different pyrolysis temperatures.

3.5 Stability of carbon membranes

3.5.1 Oxidation test

Fig 11-12 show the effects of oxidation on the permeance of carbon supported membranes obtained at 650°C pyrolysis temperature. In figure 11 it can be seen that there is an increase of permeance after 0.5 h oxidation. However, if oxidation is performed during 6 hr the permeance decrease, which is the opposite to observed at 0.5 hr test. The analysis of ideal selectivity factors of H₂/CH₄, CO₂/CH₄, O₂/N₂, and H₂/Pa (Fig 13) decreased after 0.5 hr. However, the same ratio increased when samples were exposed at 6 hr. Fuertes ^[17] reported an increase of permeance after oxidation during 0.5 hr and at 400°C for a membrane carbonized at 700°C. Fuertes also reported a non-dependence of permeance on the kinetic diameter of membranes oxidized at these conditions. As a consequence, they reported that the original molecular sieve mechanism was lost and replaced by adsorption-desorption mechanism. This was also confirmed by an increase of selectivity for pairs of gases composed by highly adsorbed and weak adsorbed gases as in the case of Pa and N₂.

At 0.5 hr of oxidation our membranes kept a dependence of permeance on the kinetic diameter and reported a decrease of ideal selectivity (Fig 13) for different pairs of gases. As a consequence, we conclude that the membranes kept the molecular sieving mechanism. In the case of the membranes oxidized 6 hr, permeance decreased but there is no clear trend for ideal selectivity. Figure 13 shows a decrease of ideal selectivity for CO₃ sample, but not for CO₄ sample. This could indicate that the 6-hour oxidation process yielded a different carbon structure than that obtained with 0.5 hr. It is probably a different pore size distribution would promote adsorption of some gases as Pa.

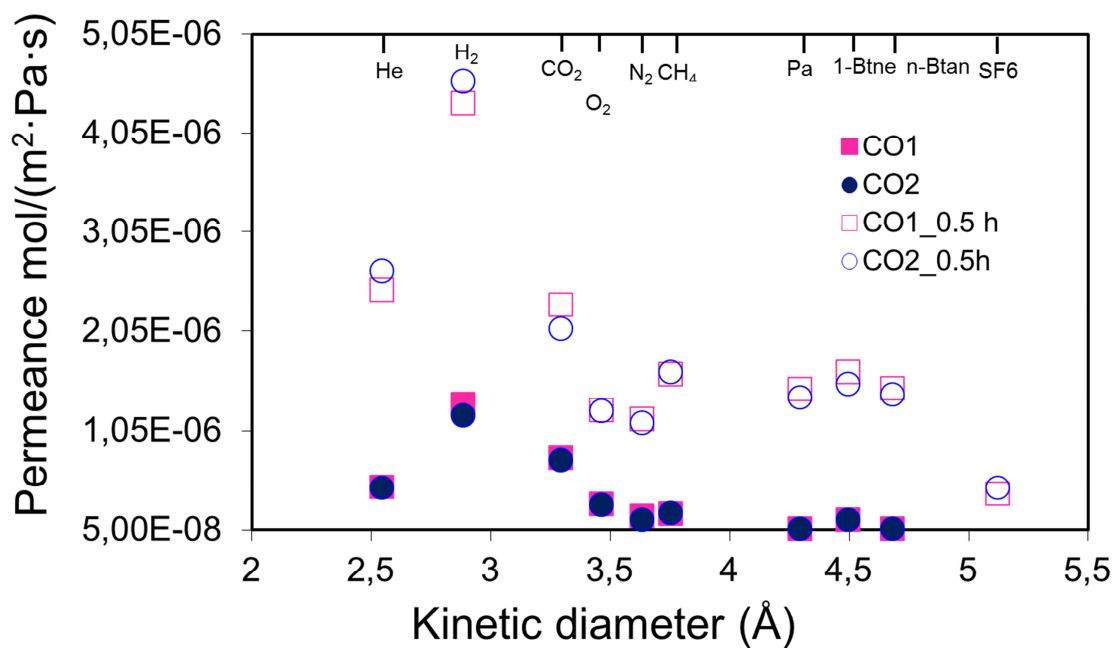


Fig 11 Permeance vs. Kinetic diameter of carbon molecular sieve membrane obtained at 650°C pyrolysis temperature after oxidation treatment at 350°C at 0.5 hrs

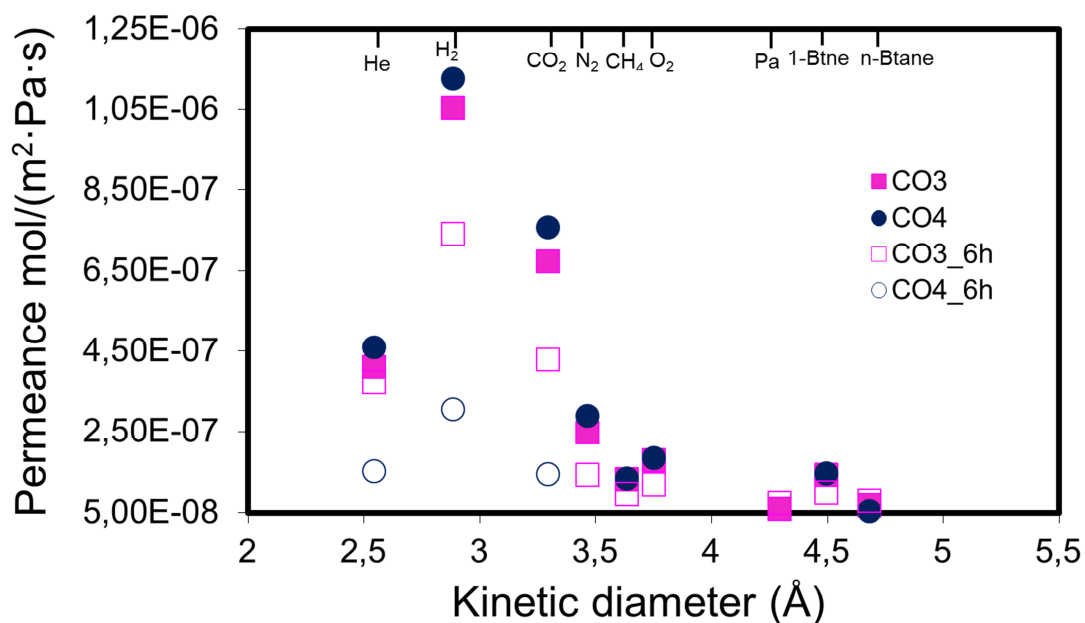


Fig 12 Permeance vs. Kinetic diameter of carbon molecular sieve membrane obtained at 650°C pyrolysis temperature after oxidation treatment at 350°C at 6hrs.

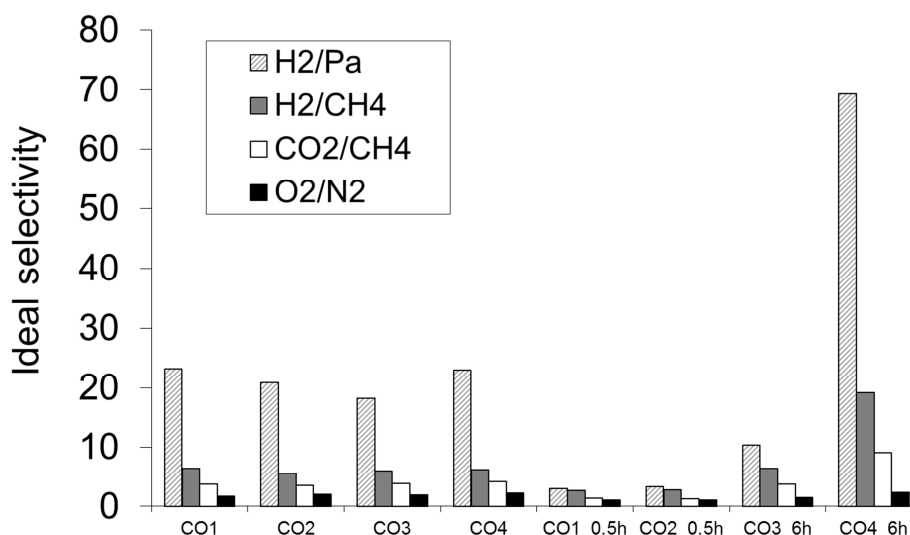


Fig 13 Ideal selectivity factors of carbon molecular sieve membrane obtained at 650°C pyrolysis temperature after oxidation treatment at 350°C at 0.5 and 6hrs.

3.5.2 Humidity Test

Fig 14 shows the effect of low-pressure humidity exposure on the permeance of carbon molecular sieve membranes obtained after pyrolysis at 650°C. All these samples showed a slight decrease in their permeance and a slight increase in their ideal selectivity when compared to their original samples. However, for both samples tested permeance decrease with kinetic values of gases and ideal selectivity factors remain over Knudsen values (Fig 15), which is an evidence of carbon membranes keep the molecular sieving mechanism.

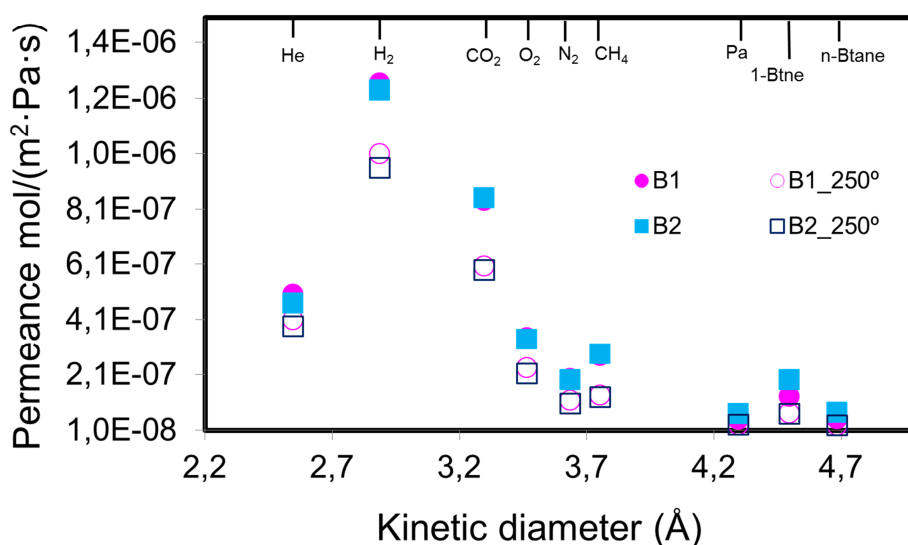


Fig 14 Permeance vs. kinetic diameter of carbon molecular sieve membrane obtained at 650°C pyrolysis temperature at 250°C and low pressure.

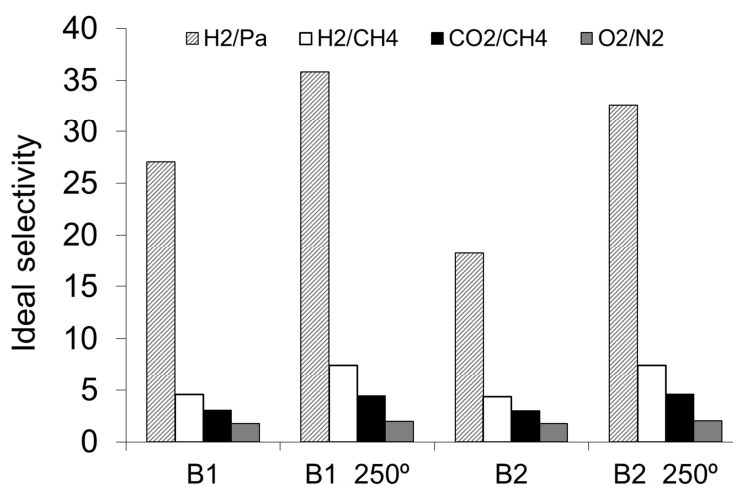


Fig 15 Ideal selectivity factor of carbon molecular sieve membrane obtained at 650°C pyrolysis temperature at 250°C and low pressure.

Humidity and pressure tests were also performed for one membranes obtained at 650°C by having it at high pressure in an autoclave at 180°C for 24 hr. In general, the membrane, identified A suffered a permeance decrease after the first and second exposure (Fig 16). The resulting behaviour coincides with experimental results by Lagorsse et. al. ^[19] in which the decrease of permeance values after exposure to humidity conditions was reported to be a consequence of pore blocking. However, the

impact of these variables is more evident on ideal selectivity (Fig. 17). The dependence of permeance on kinetic diameter allow to conclude the molecular sieving character remain on carbon membranes after humidity test.

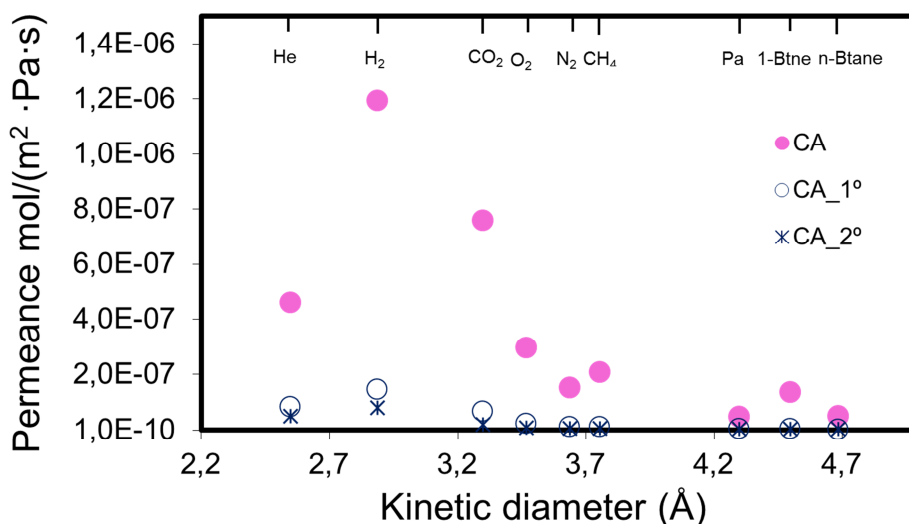


Fig 16 Permeance vs Kinetic diameter of carbon molecular sieve membrane CA_1 obtained at 650°C pyrolysis temperature after autoclave test at 180°C, 30 bar and 24 hr (one exposure and repetition)

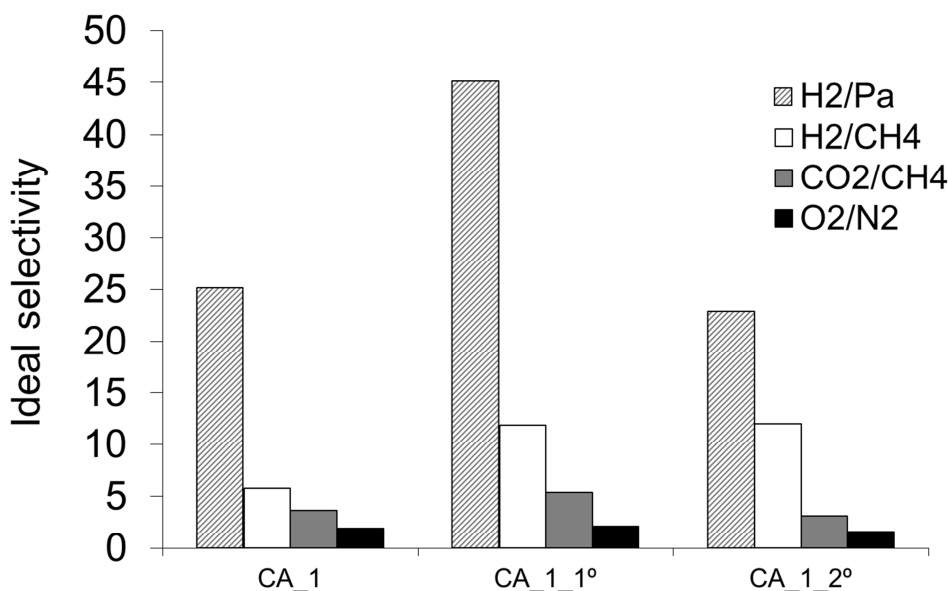


Fig 17 Ideal selectivity of carbon molecular sieve membrane CA_1 obtained at 650°C pyrolysis temperature after autoclave test at 180°C, 30 bar and 24 hr (one exposure and repetition)

4. Conclusions

Supported CMSM were obtained after pyrolysis of polymer membranes at pyrolysis temperature of 550-800°C. The coating of polymer layer was done under controlled conditions of humidity and temperature (Clean room facilities) on highly mesoporous support that were obtained after multistep coating of a macroporous Al₂O₃ substrate. N₂ permeance test allowed to control the quality of limit of the support. The quality control allowed the one step preparation of a carbon membrane free of defects and pinholes. The high reproducibility and reliability of this fabrication method allowed determining the effect polymer solution, pyrolysis temperature, methanol immersion of the polymer membrane, its thermal pre-treatment, and support quality on the final permeance and selectivity properties of the membranes. Pyrolysis temperature and thermal pre-treatment represent the most important variable. The complex influence of methanol immersion as a pre-treatment of the polymer membrane undergoing pyrolysis was not confirmed, for this reason further research is required to quantify the impact of this influence. Similarly, support quality is a determinant parameter to achieve higher or lower permeance values. The influence of this parameter is highlighted in defects formation. Moreover, it is possible that it can also influence the type of carbon layer that is formed over the support. This implies that textural characterization techniques must be included on analysis of CMSM properties. Finally, the membranes were exposed to different oxidation, and humidity conditions. For all type of conditions tested the membranes preserved their molecular sieving behaviour.

5. Acknowledgements

The authors are indebted to the Spanish Government for financial support (project CTQ2008-02491, partially funded by the FEDER program of the European Union) and to the commission of European Communities Specific OpenTok Project MTKD-LT-2005-030040. Special thanks to Mr. Steffen Woehner, Mrs. Petra Puhlfürß, Mrs. Christine Rabenstein, Mrs. Anke Schindler-Fischer, Mrs. Annett Heyer, Mrs. Anke Ihl from the department of Environmental Engineering and Bioenergy, Fraunhofer Institute for Ceramic Technologies and Systems IKTS (Hermsdorf) for his support on realization of experiments.

6. References

- [1] J.A Koresh, A. Soffer, The carbon molecular sieve membranes. General properties and the permeability of CH₄/H₂ mixture, *Separation science and technology*, 22, 973-982 (1987)
- [2] S.M. Saufi, A.F. Ismail, Fabrication of carbon membranes for gas separation—a review, *Carbon* 42 (2004) 241–259
- [3] K. Briceño, D. Montané, R.Garcia-Valls, A. Iuianelli, A. Basile, Fabrication Variables Affecting the Structure and Properties of Supported Carbon Molecular Sieve Membranes for Hydrogen Separation, *Journal of membrane Science*, Available *on-line*, (2012)
- [4] A. Merritt, R. Rajagopalan, H.C. Foley, High performance nanoporous carbon membranes for air separation, *Carbon* 45 (2007) 1267–1278
- [5] B. S. Liu, N. Wang, F. He, J. X. Chu, Separation Performance of Nanoporous Carbon Membranes Fabricated by Catalytic Decomposition of CH₄ Using Ni/Polyamideimide Templates, *Ind. Eng. Chem. Res.*, 2008; 47(6), 1896–1902.
- [6] A.B Fuertes, T.A Centeno, Preparation of supported carbon molecular sieve membranes, *Carbon* 37 (1999), 679-684
- [7] T.A. Centeno, J.L. Vilas, A.B. Fuertes, Effects of phenolic resin pyrolysis conditions on carbon membrane performance for gas separation, *Journal of Membrane Science* 228 (2004) 45–54
- [8] H. Wang, L. Zhang, G. R. Gavalas, Preparation of supported carbon membranes from furfuryl alcohol by vapor deposition polymerization, *Journal of Membrane Science* 177 (2000) 25–31
- [9] K. Kusakabe, M. Yamamoto, S. Morooka, K. Kusakabe, Gas permeation and micropore structure of carbon molecular sieving membranes modified by oxidation, *Journal of Membrane Science* 149 (1998) 59-67
- [10] J.N. Barsema, S.D. Klijnstra, J.H. Balster, N.F.A. van der Vegt, G.H. Koops, M. Wessling, Intermediate polymer to carbon gas separation membranes based on Matrimid PI, *Journal of Membrane Science* 238 (2004) 93–102
- [11] P. S Tin, T.Sh. Chung, A. J. Hill, Advanced Fabrication of Carbon Molecular Sieve Membranes by Nonsolvent Pretreatment of Precursor Polymers, *Ind. Eng. Chem. Res.* 2004, 43, 6476-6483
- [12] M. Yamamoto, K. Kusakabe, J. Hayashi, S. Morooka, Carbon molecular sieve membrane formed by oxidative carbonization of a copolyimide film coated on a porous support tube, *Journal of Membrane Science* 133 (1997) 195-205
- [13] H. Suda, K. Haraya, Molecular Sieving Effect of Carbonized Kapton Polyimide Membrane, *J. Chem. Soc., Chem. Commun.* (1995), 1179-1180
- [14] K. M. Steel, W. J. Koros, Investigation of porosity of carbon materials and related effects on gas separation properties, *Carbon* 41 (2003) 253–266
- [15] M. B. Shiflett, H.C. Foley, On the preparation of supported nanoporous carbon membranes, *Journal of Membrane Science* 179 (2000) 275–282
- [16] Ch. W. Jones, W. J. Koros, Characterization of Ultramicroporous Carbon Membranes with Humidified Feeds, *Ind. Eng. Chem. Res.* (1995), 34, 158-163
- [17] A. B. Fuertes, Adsorption-selective carbon membrane for gas separation, *Journal*

of Membrane Science 177 (2000) 9–16

- [18] P.S Tin, T-Sh. Chung, A. J. Hill, Advanced Fabrication of Carbon Molecular Sieve Membranes by Nonsolvent Pretreatment of Precursor Polymers, *Ind. Eng. Chem. Res.* (2004), 43, 6476-6483
- [19] S. Lagorsse, F.D. Magalhães, A. Mendes, Aging study of carbon molecular sieve membranes, *Journal of Membrane Science* 310 (2008) 494–502

CHAPTER 8

General Conclusions and Future Work

GENERAL CONCLUSIONS

The present PhD presents an alternative fabrication method to obtain supported carbon molecular sieve membranes for gas separation. In order to achieve this goal a detailed revision of the bibliography was done in order to identify the weak points associated to the research devoted to obtain defect free carbon membranes for industrial applications. The method was evaluated including the influence of fabrication variables on the carbon structure. The main conclusions of this research work can be summarized as follow:

1. Controlling the viscosity of the polymer solution it is possible to obtain a simple one-step polymer coating method for the formation of the ceramic-supported carbon membranes. The combination of spinning and optimization of the viscosity allow the formation of polymer and then carbon membrane without modifying the macroporous support. In order to obtain a reproducible fabrication method, a detailed control of each fabrication variable was performed. This allowed identifying other parameters that affected the quality of the carbon membranes as washing of the polymer film with methanol, aging the polymer after deposition, the heating rate and the final temperature during pyrolysis. A pyrolysis temperature of 650 °C gives a carbon membrane with a pure molecular sieving mechanism at room temperature. Permeance ranges from $9.82 \cdot 10^{-9}$ mol/m²·Pa·s for H₂ to $9.31 \cdot 10^{-10}$ mol/m²·Pa·s for CH₄, representing ideal gas selectivities of 2.37, 4.70 and 10.62 for H₂/CO₂, H₂/CO and H₂/CH₄, respectively.

2. From a detailed characterization of the carbon material it was possible to observe the influence of the fabrication variables on carbon membrane structure. In this sense, it was possible to observe differences between the type of coated material when is considered for supported and non-supported samples. Polymer-support interactions make an important contribution to the structure of the carbon membrane because affects the formation and organization of the alternative charge transfer complex in polyimides. When the same polymer was coated on porous ceramic supports the pore and volume size decreased with pyrolysis temperature on opposite way to reported when the sample is non-supported. A detailed characterization of the pores of the carbon layer by adsorption-desorption isotherms and immersion calorimetry confirmed these differences. There was an heterogeneous nature of the samples evidenced by different pore size distributions. The hysteresis found in both type of samples matched with the

differences of heat of adsorption. The effects of the temperature and support influence were highlighted. The carbon structure obtained on porous ceramic support at 500°C was still incipient, and contained pinholes and defects that caused small separation factors. After pore plugging the effect of the defects was eliminated, and CO₂/CH₄ ideal separation selectivity rose above the theoretical values of a pure Knudsen-controlled transport.

3. The supported carbon membranes obtained by the method developed in this work can present different gas separation mechanism. In this sense, after polymer pyrolysis the carbon membrane has a Knudsen-like transport mechanism. The reason why it is not pure Knudsen is due the effect of adsorption on the pores of the membrane. The presence of pinholes reduces the possibility to obtain higher separation factors. Moreover, a plug strategy was successfully performed after polydimethylsiloxane (PDMS) coating. The addition of this polymer allowed to increase the separation factor of the carbon membranes obtained reducing the permeance. Until this point, it is possible to conclude than from the same fabrication method it was possible to obtain a range of permeance and selectivity values for hydrogen separation.

4. PDMS coating is a useful technique for determining the how the smallest pores in a supported carbon membrane really function without interference from larger pores or defects that occur when coating a porous support. It was possible to observe the molecular sieving mechanism of supported carbon membranes pyrolyzed till 700°C temperature for those membranes obtained by spinning-coating method.

5. Membranes obtained by spinning-coating method shown optimal carbonization temperature at 650°C. The same temperature was considered as optimal for those membranes obtained in IKTS (dip-coating method in clean room).

6. Carbon molecular sieve membranes were obtained in clean room conditions (dip-coating method) at different pyrolysis temperature ranged from 550-800°C. Polymer composition and pyrolysis temperature were optimized to obtain different permeance and selectivity values. The best combination for H₂/Pa separation was 6%wt Matrimid/NMP solution pyrolyzed at 650°C. However, depending on the pair of gas these conditions can be different.

6. Alternative to pyrolysis temperature and polymer concentration, other variables were found to influence final carbon structure of the carbon membrane. In this sense, it is concluded from this work the high influence aging (polymer pretreatment), type of supports have on carbon membrane. It was not clear the influence of methanol immersion.

7. Carbon membranes obtained after Matrimid@ pyrolysis showed a good oxidation and thermal stability after exposure to high and lowest pressure. For all membrane test, the molecular sieving behavior remain as the main transport mechanism of these membranes.

8. As common idea, the fabrication process presented in this thesis avoid several polymer coating and pyrolysis steps, which is a competitive advantage to previous research done by other researchers. Moreover the key point of this method outlines the influence of the ceramic support in to achieve defect free membranes. Depending on the final requirement the permeance mechanism of carbon membranes derived from Matrimid@ ranges between Knudsen-like diffusion and molecular sieve.

9. The permeance and selectivity properties of carbon membranes place them in a competitive position as materials for gas separation. Since the last two decades the main fabrication variables to be considered on the fabrication of carbon membranes were identified as synthesis conditions, selection of the precursor, and the type of fabrication method for an specific separation problem. Moreover, the influence of these variables has been extensively reported considering characterization techniques such as adsorption-desorption isotherms, AFM, and electronic microscopy. However, there is a problem associated to the mechanical stability of carbon membranes that requires them to be supported on supports to overcome this limitation. Important research work has been developed by several researchers to obtain supported carbon membranes. Most of the methods reported outline dip-coating or ultrasonic deposition as effective methods to achieve the supported material. In spite of this advances, there are still problems as crack formation and pin-holes presence on the composite membrane. There is a need to obtain carbon membranes in a simple method but also identify the characterization techniques that allow to integrate the changes of the carbon material when is integrated

with the support. This work attempt to solve this problem and bring alternative point of view towards find new solutions.

FUTURE WORK

1. The original idea of supported carbon membranes for gas separation can be extended in many fields of chemical engineering. As reported in several publications, it is possible to tailor the porous structure of the carbon in order to obtain different separation factors, this work stated that it is possible to obtain different separation factors controlling the integration of the carbon material and its support. It is possible for instance to obtain different properties of the composite membrane and apply them in membrane reactors at high scale or in small microreactors. Few attempts have been reported in the past from experiences derived from electronic or microfabrication. For this reason, the same fabrication techniques can be applied to obtain new application of the carbon membranes in dehydrogenation reactions, hydration reactions or hydrogen production reactions. The flexibility supported carbon membranes can present for membrane reactors in a high scale can be transferred to a micro scale. It is possible to achieve integration of carbonaceous microporous structures in small chips for micro reactions.

2. The spinning-coating fabrication method proposed in this thesis can be used with other polymers or mixtures of polymers in order to study the influence of the precursor on the carbon structure. This study can include the characterization techniques presented in this thesis.

3. An extensive study of permeance can include the influence of different porous support with different porosity values and their performance on steam reforming of methanol. A characterization of the LLDP technique can be related to the permeance values of these membranes.

4. It must be considered the automatization of the fabrication method of spinning-coating in order to increase the reproducibility and avoid problems associated to manual coating of the polymer layer. The automatic device must deliver the polymer solution under controlled speed rotation in order to allow minimal thickness variations and longer depositions areas over the inorganic support.

5. It is proposed an experimental design to study the influence of immersion of polymer membranes previous to carbonization and the combined effect with pretreatment.

6. As shown in this work the permeance and selectivity properties of carbon membrane obtained by spinning coating were comparable to those of metallic and silica modified membranes used in MR applications. The carbon molecular sieve membranes reported in this paper are comparable to the inorganic membranes reported in the literature. For this reason, they were applied to methanol steam reforming. A preliminary study demonstrated the possible use of this type of membrane in MR applications, given that the MR yields were above those of the traditional reactor system